Stability and Performance Analysis of Polynomial Fuzzy-Model-Based Control Systems and Interval Type-2 Fuzzy Logic Systems

Xiao, Bo

Awarding institution:
King's College London

A thesis submitted for the degree of
Doctor of Philosophy

Stability and Performance Analysis of Polynomial Fuzzy-Model-Based Control Systems and Interval Type-2 Fuzzy Logic Systems

Author : Bo Xiao
Student Number : 1315358
First Supervisor : Dr. Hak-Keung Lam
Second Supervisor : Dr. Hongbin Liu

20/09/2017

Ph.D. in Robotics
Department of Informatics
Faculty of Natural & Mathematical Sciences
King's College London

Acknowledgment

By only myself, the PhD thesis would not seen possible to be completed. It is my pleasure to acknowledge the people who helped me complete the thesis.

My deep gratitude goes first to Dr. Hak-keung Lam, who guided me through my PhD life with patience and offered me more than I could expect. I have learned a lot from him during the 4-year PhD study, such as how to do research independently, how to write well, how to present my work concisely, etc. Dr. Lam is one of the few people who can keep surprising us by his insight and talents during the research. Studying and working with Dr. Lam as a PhD student, I have gradually become an independent and serious scholar/researcher. Also, his unwavering enthusiasm for research keeps encouraging me to carry on in my academic life.

I would like to thank Dr. Jie Chen from Brunel University London and Dr. Vasile Palade from Coventry University, who are the examiners for my PhD viva. Their advice and comments are of great help to me to further improve my thesis.

My appreciation also extends to my colleagues in the laboratory for working together and my friends for accompanying me.

I would also like to thank the Kings-China Scholarship Council PhD Scholarship Program for the financial support.

Last but not least, I have always been grateful for my parents and my sisters for supporting me on no conditions.

Abstract

The main research objective in this thesis is to investigate the stability and performance of the interval type-2 (IT2) polynomial-fuzzy-model-based (PFMB) control system. PFMB control scheme has been developed recently around 2009 and demonstrates more potential than the traditional Takagi-Sugeno fuzzy-model-based (T-S FMB) control approach to represent the nonlinearities in the plant. Meanwhile, the IT2 fuzzy logic has also been proposed to incorporate uncertainties of the nonlinear systems into the membership functions directly. Through the IT2 PFMB control design approach, both the nonlinearity and the uncertainty in the system can be handled well. The control performance and the relaxation of stability conditions of IT2 PFMB control systems are studied and investigated in the thesis. The main contribution of the thesis is summarized in three tasks and presented as following:

In the first task in Chapter 3, the stability conditions of the PFMB systems equipped with mismatched IT2 membership functions are investigated. Unlike the membership-function-independent (MFI) methods, the information and properties of IT2 membership functions are considered in the stability analysis and contained in the stability conditions in terms of sum-of-squares (SOS) based on the Lyapunov stability theory. Three methods, demonstrating their own merits, are proposed to conduct the stability analysis for the IT2 PFMB control systems and all of the methods can achieve feasible control results. All the three approaches are well-explained, which offers the reader systematic ways to include the information of the membership functions into the analysis. In addition, all the approaches are compared and the pros and cons are presented to help the reader choose the most appropriate approach in the applications.

In the second task presented in Chapter 4, the membership-functions-dependent (MFD) methods have been proceeded to the tracking control problems and the output feedback tracking issues of IT2 PFMB fuzzy control systems are investigated. The output-feedback IT2 polynomial fuzzy controller connected with the nonlinear plant in a closed loop drives the system states of the nonlinear plant to track those of the stable reference model. The system stability is investigated based on the Lyapunov stability theory under the SOS-based analysis approach and the SOS-based stability conditions are derived subject to a prescribed H_∞ performance. Like in the first work, the information of membership functions is also included in the

analysis to facilitate the analysis and help improve the tracking performance in terms of H_∞ performance.

Considering the implementation of the mentioned control schemes on digital computers, the sampled-data control systems are investigated as the last work in the thesis, which is presented in Chapter 5. In this task, the IT2 PFMB tracking control system is extended to the sampled-data based one. Through using the sampled output of both the control system and the reference system, an IT2 polynomial sampled-data based output feedback fuzzy controller can be designed to fulfill the tracking control task, the stability conditions can be obtained in terms of SOS and the tracking error is attenuated by the H_∞ performance index. As did in the previous two works, the information of the IT2 membership functions is used to relax the stability conditions and improve the tracking performance.

The approaches proposed in the thesis to relax the stability conditions as well as to improve the tracking performance of the IT2 PFMB control systems are proved through the Lyapunov based stability theory. Meanwhile, simulation examples are provided to demonstrate and verify the theoretical analysis.

Contents

Author's Publications

[1] **Bo Xiao**, H.K. Lam and Hongyi Li, "Stabilization of interval type-2 polynomial-fuzzy-model-based control systems," *IEEE Transactions on Fuzzy Systems*, vol. 25, no. 1, pp. 205-217, Feb. 2017.

[2] **Bo Xiao**, H.K. Lam, Ge Song and Hongyi Li, "Output-feedback tracking control for interval type-2 polynomial fuzzy-model-based control systems," *Neurocomputing*, vol. 242, pp. 83-95, 2017.

[3] **Bo Xiao**, H.K. Lam, Yan Yu and Yuandi Li, "Sampled-data output-feedback tracking control for interval type-2 polynomial fuzzy-model-based control systems,"*IEEE Transactions on Fuzzy Systems*(under review).

[4] **Bo Xiao**, H.K. Lam, Xiaozhan Yang, Yan Yu, Hongliang Ren, "Tracking control design of interval type-2 polynomial-fuzzy-model-based systems with time-varying delay,"*Engineering Applications of Artificial Intelligence* (under review).

[5] H.K. Lam, **Bo Xiao**, Yan Yu, Xunhe Yin, Hugang Han, Shun-Hung Tsai and Chin-Sheng Chen, "Membership-function-dependent stability analysis and control synthesis of guaranteed cost fuzzy-model-based control systems," *International Journal of Fuzzy Systems*, vol. 18, no. 4, pp. 537-549, 2016.

[6] Hugo Araujo, **Bo Xiao**, Chuang Liu, Yanbin Zhao and H.K. Lam, "Design of type-1 and interval type-2 fuzzy PID control for anesthesia using genetic algorithms," *Journal of Intelligent Learning Systems and Applications*, vol. 6, no. 2, pp. 70-93, May 2014.

[7] H.K. Lam, Udeme Ekong, Hongbin Liu, **Bo Xiao**, Hugo Araujo, Sai Ho Ling and Kit Yan Chan, "A study of neural-network-based classifiers for material classification," *Neurocomputing*, vol. 144, no. 20, pp. 367-377, Nov. 2014.

[8] H.K. Lam, Udeme Ekong, **Bo Xiao**, Gaoxian Ouyang, Hongbin Liu, Kit Yan Chan and S.H. Ling, "Variable weight neural networks and their applications on material surface and epilepsy seizure phase classifications," *Neurocomputing*, vol. 149, part C, pp. 1177-1187, Feb. 2015.

[9] Udeme Ekong, H.K. Lam, **Bo Xiao**, Gaoxiang Ouyang, Hongbin Liu, Kit Yan Chan and Sai Ho Ling, "Classification of epilepsy seizure phase using interval type-2 fuzzy support vector machines," *Neurocomputing*, 199 (2016): 66-76.

[10] Khurram I. Qazi, H.K. Lam, **Bo Xiao**, Gaoxiang Ouyang, Xunhe Yin, "Classification of epilepsy using computational intelligence techniques," *CAAI Transactions on Intelligence Technology*, vol. 1, no. 2, pp. 137-149, 2016.

[11] Yanbin Zhao, **Bo Xiao**, Chuang Liu, Hongyi Li and H.K. Lam, "Relaxed LMI-based stability conditions for fuzzy-model-based control systems under imperfect premise matching: approximated membership function approach," in Proc. of *The 11th World Congress on Intelligent Control and Automation (WCICA 2014)*, 29 June - 4 July, 2014, Shenyang, China.

List of Figures

List of Tables

Acronyms

FMB	Fuzzy-model-based
FOU	footprint of uncertainty
IT2	Interval type-2
LMI	Linear matrix inequality
MFD	Membership-function-dependent
MFI	Membership-function-independent
PDC	Parallel distributed compensation
PFMB	Polynomial fuzzy-model-based
SDOF	Sampled-data output feedback
SOS	Sum of squares
T-S	Takagi-Sugeno
ZOH	Zero-order hold

Chapter 1

Introduction

1.1 Overview of Fuzzy Control

Control of nonlinear systems is essential to guarantee the stability and to improve the performance of domestic and industrial applications. With the high-speed development of control technology and theory, control techniques have been applied to a wide range of applications from domestic products to industrial machines. As most real-world systems are nonlinear in nature, linear control techniques may not be capable of providing satisfactory performance or even stabilizing the systems working in a large operating domain. Therefore, nonlinear control techniques play an important role to achieve specific control objectives. However, nonlinear systems is often difficult and problematic to deal with due to their complexities. Fuzzy control is one of the nonlinear control techniques offering an effective and systematic approach for both stability analysis and control synthesis for complex and ill-defined nonlinear systems.

In 1965, Lotfi A. Zadeh of the University of California at Berkeley mixed the classic set theory with the concept of multiple-value and proposed a brand-new fuzzy set theory. Then, he proposed the concept of fuzzy algorithms, fuzzy decision, fuzzy sequencing in 1968, 1970 and 1971, respectively [2]. He elaborated on his ideas in his paper published in 1973 [3] that introduced the concept of "linguistic variables", which laid the theoretic basis of fuzzy control. Although the history of fuzzy-model-based (FMB) control cannot be deemed very long, but given that FMB control approach has been shown to be an effective control approach for nonlinear plants due to its superior inference and stabilization abilities on handling highly nonlinear and complex systems, the applications of fuzzy-model-based control have experienced a sharp development in the past decades [4–6].

The first fuzzy logic control system was developed by Mamdani and Assilian [5], where control of a small steam engine was considered. The fuzzy control algorithm consists of a set of heuristic control rules, and fuzzy sets and fuzzy logic are used, respectively, to represent linguistic terms and to evaluate the rules. Since then,

fuzzy logic control has attracted great attention from both academic and industrial communities. Many people have devoted a great deal of time and efforts to both theoretical research and application techniques of fuzzy logic controllers. There are many applications of conventional fuzzy control, including robotics, stirred tank reactor, traffic junction, and so on. In addition, fuzzy control has also been widely used in various consumer electronic devices, such as video cameras, washing machines, TV, and sound systems [5].

It is commonly known that system stability and performance are essential issues to be considered in control systems. The nonlinearities and uncertainties of the plants make the system analysis and design difficult. Therefore, traditional linear control analysis and design tools may fail to work with the systems operating in nonlinear regions. As a useful method which has the potential to address the nonlinear problems, fuzzy control approaches have shown that they are capable of dealing with the nonlinear plants systematically and effectively.

In this thesis, the stability and performance issues of the FMB cotnrol systems, especially the interval type-2 fuzzy systems, are the main research target and related works have been done to further relax the stability conditions and improve the performance.

1.2 Fuzzy Models

In this section, the related works in the literature will be reviewed. The Takagi-Sugeno (T-S) fuzzy model and the parallel distributed compensation (PDC) approach will be discussed firstly, and then the linear matrix inequality (LMI) based stability analysis. After that, the polynomial fuzzy model and sum of squares (SOS) based stability conditions will be reviewed, which is one of the main topics in the thesis. At last, the interval type-2 (IT2) fuzzy logic and IT2 T-S/Polynomial FMB control system will be introduced.

1.2.1 T-S Fuzzy model and PDC approach

As one of the most effective fuzzy control approaches, it is well-known that T-S fuzzy model [7] plays an important role in the FMB control systems for its capability of providing general modeling frameworks for nonlinear systems. Besides, thanks to its rigorous mathematical structure, there are systematic ways to carry out stability analysis and control synthesis [5, 7–10], which are considered as the most important issues to be addressed in the FMB control systems.

Stability analysis is one of the most important parts of control design and the Lyapunov stability theory is one of the most popular methods to investigate the stability of T-S FMB control systems. According to the Lyapunov approach, if there exists a common solution to all of the Lyapunov inequalities in terms of LMIs,

the T-S FMB control system is guaranteed to be asymptotically stable [11]. When considering the feedback control, the most popular design method is the PDC [11], which was developed based on the idea that both the plant and controller share the same premise fuzzy rules set. There are a lot of works managed to further relax the stability conditions of the PDC approaches [7–10,12,13] and generalized by applying Pólya's Theorem [14].

1.2.2 LMI Based Stability Conditions

For the T-S FMB control systems, one of the most important techniques to investigate the stability is the LMI based approach. Through Lyapunov stability theory, the stability conditions of the T-S FMB control systems can be obtained in terms of LMIs and the LMI approach has shown its power in the analysis and synthesis of T-S FMB control systems. In the stability analysis of the T-S FMB control system, the stability conditions can be summarized as a set of LMIs, which can be further solved by some numerical software, for example, the LMI toolbox in MATLAB®. According to the Lyapunov approach, if there exists a common solution to all Lyapunov inequalities in terms of LMIs, the T-S FMB control system is guaranteed to be asymptotically stable [11]. Thanks to the merits of the LMI approach, there is a lot of research results on T-S FMB control systems based on LMI approach. Just name a few, there are works on relaxation of the stability conditions of the T-S FMB control systems through LMI approach in [7–10, 12–14], the works on H_∞ control design adopting LMI approach can be found in [15–18], the works on time-delay control problems using LMI techniques in [19–35].

1.2.3 Polynomial Fuzzy Model and SOS based Stability Conditions

As an extension of the T-S fuzzy model, the polynomial fuzzy model has been proposed recently to represent the nonlinear dynamics of the plant [36]. Instead of only considering linear terms in the consequent part in the T-S fuzzy model, the polynomial fuzzy model adopts also polynomial terms. When all the polynomial terms are zero-th order polynomials, the polynomial fuzzy model is reduced to the T-S fuzzy model. Therefore, the polynomial fuzzy model has more potential to precisely represent nonlinear systems over the T-S fuzzy model. However, due to the introduction of polynomial terms, the LMI approach used for the T-S FMB fuzzy control can no longer be used to conduct the stability analysis. Instead, the SOS approach is widely used in the stability analysis of polynomial-fuzzy-model-based (PFMB) control systems. Based on polynomial Lyapunov functions that contain quadratic Lyapunov functions as a special case, the stability conditions are derived in form of SOS, which can be solved efficiently through a third party

MATLAB® toolbox SOSTOOLS and more details about the toolbox can be found in the manual in [37]. Comparing with the T-S FMB control systems, results for SOS-based stability analysis are relatively fewer but can also be found such as in [1, 36, 38–43]. In [36], SOS techniques were first adopted in PFMB control system to achieve stability conditions. The SOS techniques are also applied in the stability analysis in [39] through a Taylor series based approach.

1.2.4 T-S/Polynomial Fuzzy Model with IT2 Fuzzy Logic

Type-1 fuzzy set is able to deal with the nonlinearities in control systems but lacks the capability to directly handle the uncertainties since the membership functions do not contain any uncertain information [44, 45]. Quite often, there are lots of inevitable uncertainties, which can be found during the construction of the rules in FMB control systems. In general, the uncertainties can be classified into two types, namely, the linguistic uncertainties and random uncertainties [44]. In order to include the uncertainties into the type-1 membership functions, the concept of footprint of uncertainty (FOU) has been introduced into the type-1 membership functions, which render type-1 fuzzy systems into type-2 fuzzy systems [44].

In terms of type-2 membership functions, there are huge complexities embedded in the FOU, which results in difficult stability analysis and high computational burden on the numerical simulations. Therefore the widely used type-2 fuzzy systems are based on interval type-2 (IT2) membership functions instead of the general type-2 membership functions. It is worth mentioning that the type-2 fuzzy sets can be also considered as the generalization of interval valued fuzzy sets [46], and interval-valued fuzzy sets are a particular case of the interval type-2 fuzzy sets [47]. Regarding the IT2 membership functions, all membership grades of the secondary membership functions are constants instead of functions of premise variables. Although the compromise on complexity and performance has been made, by adopting IT2 membership functions, we can not only handle the uncertainties directly but also reduce the computational burden [44, 48–50].

By considering the IT2 fuzzy logic in the membership functions of the fuzzy model, the IT2 T-S/Polynomial FMB system can be achieved. In the IT2 T-S/polynomial FMB system, the IT2 fuzzy logic handles the uncertainty in the T-S/Polynomial fuzzy model directly while the T-S/Polynomial fuzzy model is used to represent the nonlinear dynamics. Given that the IT2 T-S/Polynomial FMB system is able to handle both the uncertainty and the nonlinearity in the plant well, it is worth putting the research effects on the IT2 T-S/Polynomial FMB system. Recently, there are lots of research that has been conducted on the T-S FMB control system based on the framework of IT2 fuzzy systems [45, 51–56]. However, the IT2 PFMB system receives less attention. In this thesis, the stability and performance of the IT2 PFMB system are the main research topics.

1.3 Relaxation of the Stability Conditions

Encouraged by the merits of the FMB control systems, many researchers dedicate a great deal of energy and time to the relaxation of the stability conditions.

An FMB control system, which is formed by connecting fuzzy model and fuzzy controller in a feedback loop, is in the form of a weighted sum of local linear sub-control systems. In general, stability analysis is mainly based on the Lyapunov stability theory and the analysis can be classified into two categories, namely the membership-function-independent (MFI) and the membership-function-dependent (MFD) approaches.

MFI Approaches: In MFI approaches, the stability conditions are developed without anything involved with membership functions and the followings are the introduction of the MFI approach.

1) *Dimensions of Fuzzy Summation:* One of the reason why the stability analysis is conservative is the fuzzy summation of the grades of the membership functions. Adopting different properties in the analysis helps reduce the conservativeness, for example, the works in [7–10, 12] utilized the symmetry property to relax the stability conditions, the works in [13,14] extended the fuzzy summation to higher dimension of the fuzzy summation to relax the stability conditions. It is worth mentioning that through applying Pólya's Theorem in [14], the asymptotically necessary and sufficient conditions for stability and performance in fuzzy control can be achieved. The work in [14] generalized the previous works [9, 13], which means the theorems obtained in the previous works can be treated as special cases by applying Pólya's Theorem. After the work reported in [14], the approach regarding the fuzzy summation has been well-studied.

2) *Form of Lyapunov Functions:* Apart from the first source above, the choice made on choosing different Laypunov functions also have its effect on the conservativeness. The quadratic Lyapunov function and its first order derivative are commonly investigated in the stability analysis [11]. To relax the stability conditions, more general types of Lyapunov function candidates have been employed such as piecewise linear Lyapunov function [57, 58], switching Lyapunov function [59], fuzzy Lyapunov function [60–62] and polynomial Lyapunov function [59].

MFD Approaches: For MFD approaches, the information of the membership functions will be incorporated in the stability conditions and it helps to relax the stability conditions. Since the information of the specific membership functions is introduced to the stability conditions, the stability conditions are no longer valid unnecessarily for any kind of membership function, then the stability conditions are more relaxed under the specific membership functions.

Given that the controller is required to share the same rules set with the plant in the PDC approach, in general, the design flexibility is reduced and the implementation cost is also increased. In order to render the system flexibly and lower the implementation cost, it makes sense to consider the case that the fuzzy model and fuzzy controller do not share the same premise fuzzy rule set, which results in imperfectly matched membership functions [63, 64]. It should be noted that when the requirement of the same rule set is removed, the results of stability analysis can be very conservative as the permutations of membership functions used in the PDC design approach cannot be applied due to the imperfectly matched membership functions. Also, in most of the related works, the shapes of membership functions have not been considered during the analysis, which means the stability conditions are valid unnecessarily for any arbitrary membership functions and hence results in conservativeness. As the stability conditions only need to be valid under the specific membership functions used in the investigated fuzzy plant and fuzzy controller, bringing the information of membership functions into the analysis contributes to the relaxation of stability conditions. In [1, 63, 64], the local/global boundary information of membership functions were employed to relax the stability conditions. In [65], staircase-shape functions were adopted to approximate the original membership functions in the stability analysis of FMB control systems, which allows adding the approximated membership functions into the stability conditions to make them membership function dependent, which leads to more relaxed stability analysis results. Along this line, piecewise-linear membership functions (PLMFs) [41] and Taylor-series membership functions (TSMFs) [43] were proposed to carry more information to facilitate the stability analysis.

1.4 Extension of FMB Control Strategy

Besides obtaining the stability condition of the regular FMB control systems, various application of the FMB control strategy can be considered to solve the nonlinear control problems. For example, the sampled-data based control systems, the output feedback control systems, the tracking control systems, the time-delay networked control systems and so on. In the thesis, the sampled-data based control systems, the output-feedback control systems and the tracking control systems will be studied and investigated. The time-delay related control systems will be considered as one of the future research objective.

1.4.1 Tracking Control

In the fuzzy tracking control design, a fuzzy controller is employed to drive the system states of the nonlinear plant to follow a reference or the system states of a stable reference model. Fuzzy tracking control problems are generally considered

as more challenging than stabilization problems [66]. T-S fuzzy model, which plays an important role in the FMB control system thanks to its capability to provide general modeling frameworks for nonlinear systems. Inspired by the success of the FMB control approach on stabilization problems [7–14, 67], the work in [66] introduced a fuzzy tracking control technique where H_∞ performance is considered to attenuate the tracking error to a prescribed level. Further work regarding fuzzy tracking control can be found in [68, 69]. The fuzzy tracking control concept was then combined with output-feedback control method, resulting in output-feedback fuzzy tracking control strategy [15, 70–78], which requires only the system output for feedback compensation. Also, with the consideration of sampled-data concept, sampled-data output feedback (SDOF) fuzzy tracking control strategy was introduced in [79]. Followed by the introduction of the polynomial fuzzy model [36], the above control strategy has been extended to polynomial fuzzy-model-based (PFMB) control systems [42, 80].

1.4.2 Sampled-Data Based Control System

Owing to the rapid development of digital technology, it is possible to implement the controller with a microcontroller or a digital computer at low costs. However, the closed-loop control system becomes a sampled-data control system. As a result of zero-order hold (ZOH), the sampled states or outputs are of staircase signal that it causes discontinuity in the control signal which makes the system dynamic complicated for system analysis and control design. To deal with the hybrid system dynamics in the context of FMB/PFMB control systems, the input-delay approach [28, 42, 81–87], equivalent jump system [88], discretization approach [89], digital redesign [90–94] and the exact discrete-time design approach [95] can be used for stability analysis and control design. Among these approaches, input-delay approach regards the sampled-data input measurements into time-varying delay input, and then the problem will be converted into the continuous-time one, therefore, continuous-time stability analysis can be adopted in the sampled-data control systems. Within the FMB control frame, fruitful results were obtained [28, 42, 82, 84, 96–101] for full-state feedback, fuzzy observer, dynamic output feedback cases.

1.5 Research Motivations and Objectives

The research topics of the IT2 PFMB controls systems in the thesis are mainly formed by two parts: the relaxation of the stability conditions part and improving the control performance part. The motivations and objectives are as follows:

1) For an application of a control system, the first thing needed to be considered is the stability of the system. When the system is not a stable one, the states and/or

the outputs of the system may go to infinity and this causes lots of problems and even put the control systems into dangerous situations. Considering the importance of the stability, in this thesis, the stability conditions of the IT2 PFMB control systems will be developed and relaxed through the Laypunov approach.

2) Apart from the stability of the control systems, another important issue to consider in a control system is the performance. The control performance specifications include stability conditions, relaxed stability conditions, decay rate conditions, constrains on control input and output, and disturbance rejection for both continuous and discrete fuzzy control systems [7,10,102,103]. In this thesis, the performance of the tracking control systems will be indicated and improved through adopting an H_∞ based performance index.

3) In addition, to facilitate digital implementation of the control scheme, the sampled-data based control systems will also be discussed in this thesis, the output feedback sampled-data tracking control system will be investigated, the stability conditions of the PFMB control systems will be developed in terms of SOS and the performance of the tracking control system will be evaluated and improved according to the H_∞ performance index.

1.6 Organization of the Thesis

- In Chapter 2, preliminaries on the construction of a fuzzy model, the Lyapunov based stability theory, the H_∞ performance and some useful lemmas will be given.

- In Chapter 3, the stability conditions of the IT2 PFMB control systems is investigated and the stability conditions summarized in terms of SOS are further relaxed by utilizing the information of the IT2 membership functions.

- In Chapter 4, the tracking control issues based on the IT2 FPBM control systems are investigated, the stability conditions are also summarized as SOS and the stability conditions are relaxed through the information of membership functions. In addition, the tracking performance is evaluated and improved according to the H_∞ performance index.

- In Chapter 5, the tracking control issues in Chapter 4 is expanded to the sampled-data case for the purpose of digital application. As did in Chapters 3 and 4, the stability conditions are obtained as SOS and then further relaxed through using the information of membership functions. The tracking performance is also evaluated and improved according to the H_∞ performance index.

- In Chapter 6, the conclusion of the thesis will be drawn and the future work plan will be discussed as well.

1.7 Contributions of the Thesis

The contributions of the thesis are summarized as follows:

1. The stability conditions of the IT2 PFMB control system are obtained for the first time based on the MFI approach and further relaxed through the MFD approach. The results have been published in "Stabilization of interval type-2 polynomial-fuzzy-model-based control systems," *IEEE Transactions on Fuzzy Systems*, vol. 25, no. 1, pp. 205-217, Feb. 2017.

2. The tracking control of the IT2 PFMB is designed successfully while the tracking performance is improved according to the H_∞ performance index. Also, the stability conditions for the tracking control are relaxed through MFD approach. The results have been published in "Output-feedback tracking control for interval type-2 polynomial fuzzy-model-based control systems," *Neurocomputing*, vol. 242, pp. 83-95, 2017.

3. The sampled-data output feedback tracking control extension of the IT2 PFMB control system is investigated for the first time. The stability conditions are derived in terms of SOS. The tracking control performance is also evaluated by the H_∞ performance index and improved. The results have been submitted to *IEEE Transactions on Fuzzy Systems* as a regular paper "Sampled-data output-feedback tracking control for interval type-2 polynomial fuzzy-model-based control systems".

Chapter 2

Preliminaries

In this chapter, the preliminaries for the main research objectives will be introduced. Firstly, the construction of models will be introduced. In the construction part, the concept of sector nonlinearity, Taylor series approach, polynomial fuzzy modeling and the IT2 membership function construction will be discussed. Secondly, the IT2 PFMB control system formed by IT2 polynomial fuzzy model and IT2 polynomial fuzzy controller will be introduced. Thirdly, the Lyapunov approach to investigate the stability conditions will be introduced and different kinds of Lyapunov function candidates will be discussed in detail. Fourthly, the details of H_∞ norm and the H_∞ performance techniques will be given. Lastly, the useful lemmas going to be used in this thesis are presented.

2.1 Construction of Fuzzy Models

The fuzzy model is described by fuzzy IF-THEN rules which represent local input-output relations of a nonlinear system. The basic procedure to model the T-S/Polynomial fuzzy model can be viewed in Fig. 2.1. It is known that the fuzzy model to represent the nonlinear systems is the essential part in the FMB control system. There are generally two approaches [10] for constructing the fuzzy model.

1) Identification (fuzzy modeling) using input-output data,

2) Derivation from given nonlinear system dynamic equations.

In this thesis, the second approach will be adopted to obtain the fuzzy model and the concept of sector nonlinearity will be utilized to represent the nonlinearity terms in the system, which is an important step to construct the fuzzy models. Let us discuss the concept of sector nonlinearity in the next subsection.

2.1.1 Sector Nonlinearity

Consider a nonlinear system $\dot{\mathbf{x}}(t) = f(\mathbf{x}(t))$, where x(t) is the system state, $\dot{\mathbf{x}}(t)$ is the dynamic of $\mathbf{x}(t)$, $f(\mathbf{x}(t))$ is the nonlinear term and $f(\mathbf{0}) = \mathbf{0}$. The aim of

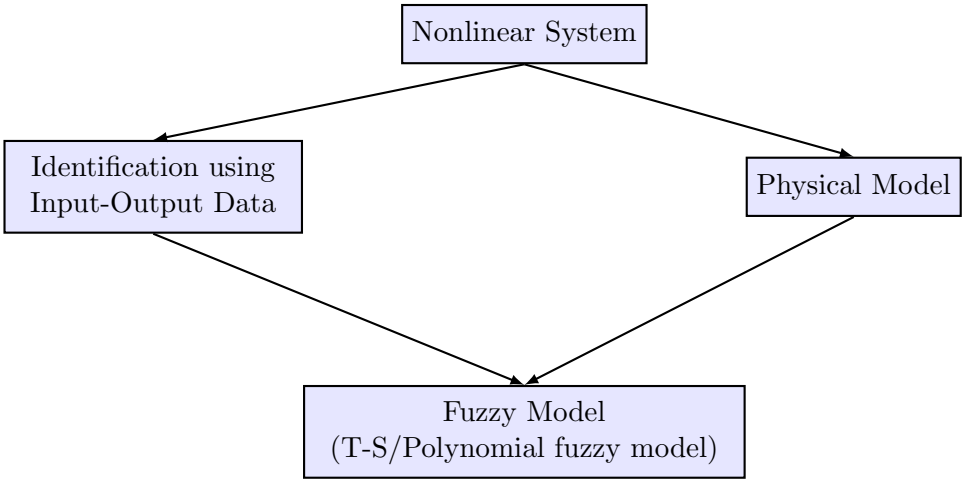

Figure 2.1: Construction of T-S/Polynomial fuzzy models.

the sector nonlinearity approach is to find the global sector such that the nonlinear terms can be represented as the combination of two linear functions of $x(t)$, that is $\dot{\mathbf{x}}(t) = f(\mathbf{x}(t)) \in [a_1\mathbf{x}(t) \quad a_2\mathbf{x}(t)]$. After obtaining the proper constants a_1 and a_2, the nonlinear term $f(\mathbf{x})$ can be represented by weighted sum of $a_1\mathbf{x}(t)$ and $a_2\mathbf{x}(t)$. As we will further see in the polynomial modeling section, the weights are the membership functions. Fig. 2.2 illustrates the global sector nonlinearity approach for $\mathbf{x}(t)$ in one dimensional case, it demonstrates that prober $a_1\mathbf{x}(t)$ and $a_2x(t)$ can ensure that $a_2\mathbf{x}(t) \leq f(\mathbf{x}(t)) \leq a_1\mathbf{x}(t)$.

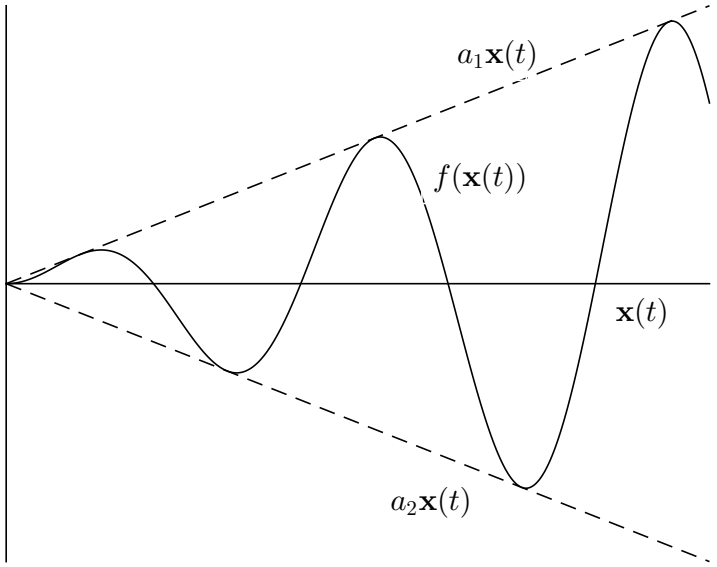

Figure 2.2: Demonstration of global sector nonlinearity.

For more complex cases, it can be difficult to find the global sectors to represent the nonlinear term. In this case, the local sector nonlinearity approach can be considered. As the one dimensional demonstration shown in Fig. 2.3, for $0 \leq \mathbf{x}(t) \leq d$, the two lines $a_1\mathbf{x}(t)$ and $a_2\mathbf{x}(t)$ become local sectors under $0 \leq \mathbf{x}(t) \leq d$. The fuzzy model exactly represents the nonlinear system in the local region associated with the membership functions.

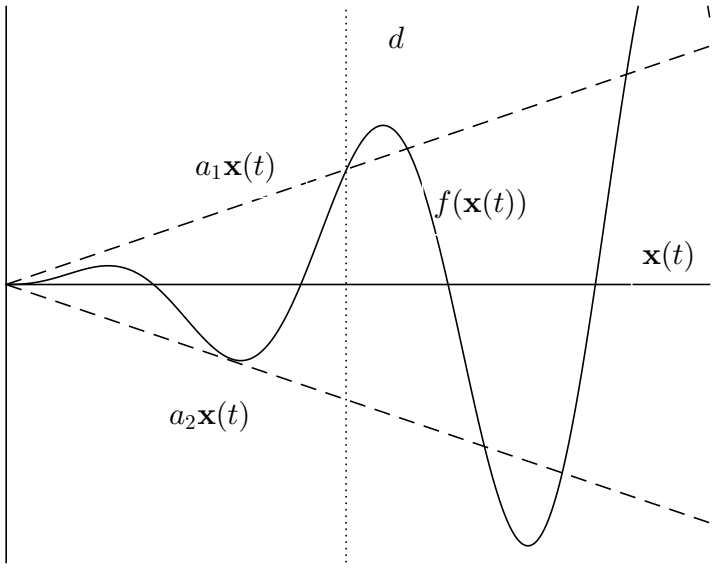

Figure 2.3: Demonstration of local sector nonlinearity.

By considering different local regions, the nonlinear terms in the model can be represented by the weighted sum of two linear functions. To generalize the linear functions of $\mathbf{x}(t)$ in this section, the Taylor series approach based on polynomial functions of $\mathbf{x}(t)$ will be introduced in the following section.

2.1.2 Taylor Series Approach

With the introduction of the PFMB control system, the polynomial terms can be processed by SOS based software. Afterwards, the Taylor series approach to build the polynomial fuzzy model is reported first in [39]. In the Taylor series approach, the sector-nonlinearity approach is extended to polynomial case and generalized polynomial fuzzy models can be obtained. In this way, the sector-nonlinearity approach in Section 2.1.1 can be treated particular case of the Taylor series approach.

Like the sector-nonlinearity approach, the nonlinear system $\dot{\mathbf{x}}(t) = f(\mathbf{x}(t))$, where $f(\mathbf{0}) = \mathbf{0}$ is considered. The aim is to find the global sector such that $\dot{\mathbf{x}}(t) = f(\mathbf{x}(t)) \in [\underline{f}(\mathbf{x}(t)) \quad \overline{f}(\mathbf{x}(t))]$. $\underline{f}(\mathbf{x}(t))$ and $\overline{f}(\mathbf{x}(t))$ are of the polynomial forms of $\mathbf{x}(t)$. After obtaining the $\underline{f}(\mathbf{x}(t))$ and $\overline{f}(\mathbf{x}(t))$ through the Taylor series approach, the nonlinear term $f(\mathbf{x})$ can be represented by $\underline{f}(\mathbf{x}(t))$ and $\overline{f}(\mathbf{x}(t))$. Fig.

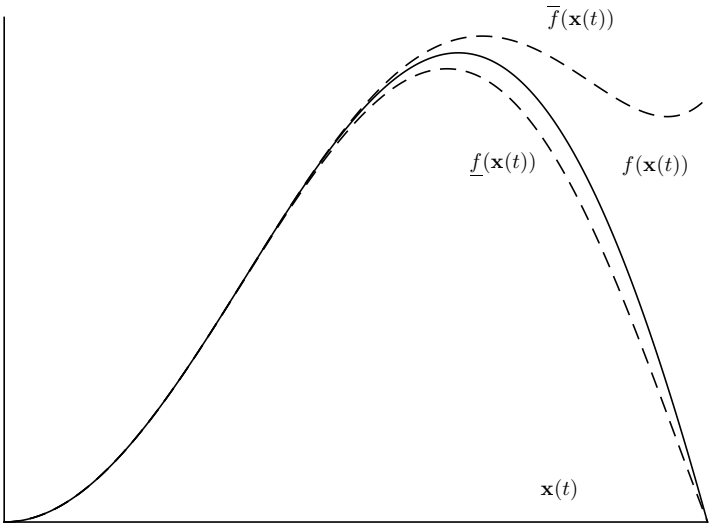

Figure 2.4: Demonstration of the Taylor series approach.

2.4 illustrates the Taylor series approach, in the figure, $\underline{f}(\mathbf{x}(t))$ and $\overline{f}(\mathbf{x}(t))$ are in the 6-th order polynomial form.

It should be noted that by the Taylor series approach, the nonlinear terms in the model can be represented by the polynomial functions of $\mathbf{x}(t)$. Therefore, this approach is to build a polynomial fuzzy model for the nonlinear system which will be discussed in the following section.

It is also worth mentioning that when the order of the polynomial function in the Taylor series approach is reduced to zero, the Taylor series approach will be the same with the sector nonlinearity approach and a T-S fuzzy model will be built.

2.1.3 Polynomial Fuzzy Modeling

In this section, the way to build polynomial fuzzy model from the nonlinear state equation is presented. Since the T-S fuzzy model can be considered as polynomial fuzzy model with the order of all the polynomial terms is zero, the polynomial fuzzy modeling approach can be applied to build a T-S fuzzy model as well.

The general nonlinear system investigated in this thesis is the autonomous input-affine system in the following state-space form:

$$\dot{\mathbf{x}}(t) = \mathbf{A}(\mathbf{x}(t))\hat{\mathbf{x}}(t) + \mathbf{B}(\mathbf{x}(t))\mathbf{u}(t), \tag{2.1}$$

where t is the continuous time in seconds; $\mathbf{x}(t)$ is the system state vector; $\mathbf{A}(\mathbf{x}(t))$ is the nonlinear system matrix; $\mathbf{B}(\mathbf{x}(t))$ is the nonlinear input matrix; $\hat{\mathbf{x}}(t)$ is the monomials of $\mathbf{x}(t)$ and $\mathbf{u}(\mathbf{t})$ is control input.

The Taylor series approach presented previous will be adopted in the polyno-

mial fuzzy modeling process [39]. Through the Taylor series based approach, the polynomial terms can be employed to represent each nonlinear term in $\mathbf{A}(\mathbf{x}(t))$ and $\mathbf{B}(\mathbf{x}(t))$.

For example (time t is omitted in this example), if the nonlinear term is chosen to be $f_1(\mathbf{x})$, we obtained the upper and lower bounds $\overline{f}_1(\mathbf{x})$ and $\underline{f}_1(\mathbf{x})$ by the Taylor series approach discussed previous, both of them are in the form of polynomials of $\mathbf{x}$. Conceptually, we use following fuzzy rules to interpret the modeling process:

$$\begin{aligned}
&\text{Rule 1 : IF } f_1(\mathbf{x}) \text{ is around } \underline{f}_1(\mathbf{x}),\\
&\qquad\qquad \text{THEN } f_1(\mathbf{x}) = \underline{f}_1(\mathbf{x}),\\
&\text{Rule 2 : IF } f_1(\mathbf{x}) \text{ is around } \overline{f}_1(\mathbf{x}),\\
&\qquad\qquad \text{THEN } f_1(\mathbf{x}) = \overline{f}_1(\mathbf{x}).
\end{aligned}$$

The membership functions are exploited to combine the fuzzy rules. To calculate the grades of membership, we employ the following relations:

$$\begin{aligned}
&f_1(\mathbf{x}) = \mu_{M_1^1}(\mathbf{x})\underline{f}_1(\mathbf{x}) + \mu_{M_1^2}(\mathbf{x})\overline{f}_1(\mathbf{x}),\\
&\mu_{M_1^1}(\mathbf{x}) + \mu_{M_1^2}(\mathbf{x}) = 1,
\end{aligned}$$

where $\mu_{M_1^1}(\mathbf{x})$ and $\mu_{M_1^2}(\mathbf{x})$ are the grades of membership corresponding to the fuzzy terms M_1^1 and M_1^2, respectively. In this case, the fuzzy terms M_1^1 and M_1^2 are "around $\underline{f}_1(\mathbf{x})$" and "around $\overline{f}_1(\mathbf{x})$", respectively. Therefore, we can obtain

$$\mu_{M_1^1}(\mathbf{x}) = \frac{f_1(\mathbf{x}) - \overline{f}_1(\mathbf{x})}{\underline{f}_1(\mathbf{x}) - \overline{f}_1(\mathbf{x})}, \mu_{M_1^2}(\mathbf{x}) = 1 - \mu_{M_1^1}(\mathbf{x}).$$

By representing each nonlinear term in the nonlinear system by polynomial terms, a polynomial fuzzy model is eventually established. It is worth mentioning that when the order of the polynomial terms reduced to 1, the polynomial fuzzy model will turn out to be a T-S fuzzy model, which demonstrates that the polynomial fuzzy model has more potential to represent the nonlinearity in the system than the T-S fuzzy model does. The overall form of the fuzzy model will be introduced in the following sections.

2.1.4 IT2 Membership Functions

Considering the uncertainty in the nonlinear system to be modeled, the grade of the membership function will turn out to be an interval value. In the previous discussion, it is known that:

$$\mu_{M_1^1}(\mathbf{x}) = \frac{f_1(\mathbf{x}) - \overline{f}_1(\mathbf{x})}{\underline{f}_1(\mathbf{x}) - \overline{f}_1(\mathbf{x})}, \mu_{M_1^2}(\mathbf{x}) = 1 - \mu_{M_1^1}(\mathbf{x}).$$

When there is uncertainty in $f_1(\mathbf{x})$ to make $f_1(\mathbf{x}) \in [f_1^L(\mathbf{x}) \quad f_1^U(\mathbf{x})]$, by the equation above, $\mu_{M_1^1}(\mathbf{x})$ and $\mu_{M_1^2}(\mathbf{x})$ used above will be rendered to interval sets as $\tilde{\mu}_{M_1^1}(\mathbf{x})$ and $\tilde{\mu}_{M_1^2}(\mathbf{x})$:

$$\tilde{\mu}_{M_1^1}(\mathbf{x}) \in [\underline{\mu}_{M_1^1}(\mathbf{x}) \quad \overline{\mu}_{M_1^1}(\mathbf{x})],$$
$$\tilde{\mu}_{M_1^2}(\mathbf{x}) \in [\underline{\mu}_{M_1^2}(\mathbf{x}) \quad \overline{\mu}_{M_1^2}(\mathbf{x})].$$

Combing the IT2 membership functions with the polynomial fuzzy model, the uncertainty and the nonlinearity can be captured well in the IT2 PFMB control system. For this reason, the IT2 PFMB control system is the main research objective in this thesis.

2.2 IT2 PFMB Control System

In this section, the PFMB control system is presented as the extension the T-S FMB control system. The PFMB control system is basically formed by the IT2 polynomial fuzzy model and the IT2 polynomial fuzzy controller.

2.2.1 IT2 polynomial Fuzzy Model

An IT2 polynomial fuzzy model with p rules, extended from [45,55], is employed to describe the dynamics of the nonlinear plant. The rules are of the following format where the antecedents are IT2 fuzzy sets and the consequent is a linear dynamic system:

$$\begin{aligned}\text{Rule } i : \text{IF } f_1(\mathbf{x}(t)) \text{ is } \tilde{M}_1^i \text{ AND } \cdots \text{ AND } f_\Psi(\mathbf{x}(t)) \text{ is } \tilde{M}_\Psi^i \\ \text{THEN } \dot{\mathbf{x}}(t) = \mathbf{A}_i(\mathbf{x}(t))\hat{\mathbf{x}}(\mathbf{x}(t)) + \mathbf{B}_i(\mathbf{x}(t))\mathbf{u}(t), \\ \mathbf{y}(t) = \mathbf{C}\hat{\mathbf{x}}(\mathbf{x}(t)),\end{aligned} \tag{2.2}$$

where $\tilde{M}_\alpha^i$ is a fuzzy term of rule i corresponding to the known function $f_\alpha(\mathbf{x}(t))$, $\alpha = 1, 2, \ldots, \Psi$ and $i = 1, 2, \ldots, p$; Ψ is a positive integer; $\mathbf{A}_i(\mathbf{x}(t)) \in \Re^{n\times N}$ and $\mathbf{B}_i(\mathbf{x}(t)) \in \Re^{n\times m}$ are known polynomial system and input matrices; $\mathbf{x}(t) \in \Re^n$ is the system-state vector, $\hat{\mathbf{x}}(\mathbf{x}(t)) \in \Re^N$ is a vector of monomials in $\mathbf{x}(t)$, $\mathbf{u}(t) \in \Re^m$ is the control input vector and $\mathbf{C} \in \Re^{q\times N}$ is the constant output matrix, $\mathbf{y}(t) \in \Re^q$ is the system output vector. The firing strength of the i-th rule is within the following interval sets:

$$\tilde{w}_i(\mathbf{x}(t)) \in [w_i^L(\mathbf{x}(t)), w_i^U(\mathbf{x}(t))], \quad i = 1, 2, \ldots, p, \tag{2.3}$$

where

$$w_i^L(\mathbf{x}(t)) = \prod_{l=1}^{\Psi} \underline{\mu}_{\tilde{M}_l^i}(f_l(\mathbf{x}(t))), \tag{2.4}$$

$$w_i^U(\mathbf{x}(t)) = \prod_{l=1}^{\Psi} \overline{\mu}_{\tilde{M}_l^i}(f_l(\mathbf{x}(t))), \tag{2.5}$$

in which

$$0 \leq \overline{\mu}_{\tilde{M}_\alpha^i}(f_\alpha(\mathbf{x}(t))) \leq 1, \tag{2.6}$$

$$0 \leq \underline{\mu}_{\tilde{M}_\alpha^i}(f_\alpha(\mathbf{x}(t))) \leq 1 \tag{2.7}$$

denote the lower and upper grades of membership governed by their lower and upper membership functions, respectively. By the definition of IT2 membership functions, the property $0 \leq \underline{\mu}_{\tilde{M}_\alpha^i}(f_\alpha(\mathbf{x}(t))) \leq \overline{\mu}_{\tilde{M}_\alpha^i}(f_\alpha(\mathbf{x}(t))) \leq 1$ holds, which further leads to $0 \leq w_i^L(\mathbf{x}(t)) \leq w_i^U(\mathbf{x}(t)) \leq 1$ for all i.

We define $\tilde{w}_i(\mathbf{x}(t))$ as

$$\tilde{w}_i(\mathbf{x}(t)) = \underline{\lambda}_i(\mathbf{x}(t))w_i^L(\mathbf{x}(t)) + \overline{\lambda}_i(\mathbf{x}(t))w_i^U(\mathbf{x}(t), \tag{2.8}$$

in which

$$0 \leq \underline{\lambda}_i(\mathbf{x}(t)) \leq 1, \tag{2.9}$$

$$0 \leq \overline{\lambda}_i(\mathbf{x}(t)) \leq 1, \tag{2.10}$$

$$\underline{\lambda}_i(\mathbf{x}(t)) + \overline{\lambda}_i(\mathbf{x}(t)) = 1, \forall\, i, \tag{2.11}$$

in which $\underline{\lambda}_i(\mathbf{x}(t))$ and $\overline{\lambda}_i(\mathbf{x}(t))$ are nonlinear functions to be determined.

The IT2 polynomial fuzzy model is described by

$$\dot{\mathbf{x}}(t) = \sum_{i=1}^{p} \tilde{w}_i(\mathbf{x}(t))(\mathbf{A}_i(\mathbf{x}(t))\hat{\mathbf{x}}(t) + \mathbf{B}_i(\mathbf{x}(t))\mathbf{u}(t)), \tag{2.12}$$

where

$$\sum_{i=1}^{p} \tilde{w}_i(\mathbf{x}(t)) = 1, \tilde{w}_i(\mathbf{x}(t)) \geq 0,\ \forall\, i. \tag{2.13}$$

2.2.2 IT2 Polynomial Fuzzy Controller

An IT2 polynomial fuzzy controller with c rules is employed to stabilize the plant represented by the IT2 polynomial fuzzy model (2.12). The format of the IT2 polynomial fuzzy controller is as follows:

$$\begin{aligned} &\text{Rule } j : \text{IF } g_1(\mathbf{x}(t)) \text{ is } \tilde{N}_1^j \text{ AND } \cdots \text{ AND } g_\Omega(\mathbf{x}(t)) \text{ is } \tilde{N}_\Omega^j \\ &\qquad \text{THEN } \mathbf{u}(t) = \mathbf{G}_j(\mathbf{x}(t))\hat{\mathbf{x}}(\mathbf{x}(t)), \end{aligned} \tag{2.14}$$

where $\tilde{N}_\beta^j$ is an IT2 fuzzy term of rule j corresponding to function $g_\beta(\mathbf{x}(t))$, where $\beta = 1, 2, \ldots, \Omega$ and $j = 1, 2, \ldots, c$, Ω is a positive integer and $\mathbf{G}_j(\mathbf{x}(t)) \in \Re^{m\times N}$, $j = 1, 2, \ldots, c$, is the polynomial feedback gain to be determined. The firing strength of the j-th rule is within the following interval sets:

$$\tilde{m}_j(\mathbf{x}(t)) \in [m_j^L(\mathbf{x}(t)), m_j^U(\mathbf{x}(t))], \quad j = 1, 2, \ldots, c, \tag{2.15}$$

where

$$m_j^L(\mathbf{x}(t)) = \prod_{l=1}^{\Omega} \underline{\mu}_{\tilde{N}_l^j}(g_l(\mathbf{x}(t))), \tag{2.16}$$

$$m_j^U(\mathbf{x}(t)) = \prod_{l=1}^{\Omega} \overline{\mu}_{\tilde{N}_l^j}(g_l(\mathbf{x}(t))), \tag{2.17}$$

in which

$$0 \leq \overline{\mu}_{\tilde{N}_\beta^j}(g_\beta(\mathbf{x}(t))) \leq 1, \tag{2.18}$$

$$0 \leq \underline{\mu}_{\tilde{N}_\beta^i}(g_\beta(\mathbf{x}(t))) \leq 1 \tag{2.19}$$

denote the lower and upper grades of membership governed by the lower and upper membership functions, respectively. By the definition of IT2 membership functions, the property $0 \leq \underline{\mu}_{\tilde{N}_\beta^j}(g_\beta(\mathbf{x}(t))) \leq \overline{\mu}_{\tilde{N}_\beta^j}(g_\beta(\mathbf{x}(t))) \leq 1$ holds and further leads to the $0 \leq m_j^L(\mathbf{x}(t)) \leq m_j^U(\mathbf{x}(t)) \leq 1$ valid for all j.

Inspired by [55], $\tilde{m}_j(\mathbf{x}(t))$ is defined as follows:

$$0 \leq \tilde{m}_j(\mathbf{x}(t)) = \frac{\underline{\kappa}_j(\mathbf{x}(t))m_j^L(\mathbf{x}(t)) + \overline{\kappa}_j(\mathbf{x}(t))m_j^U(\mathbf{x}(t))}{\sum_{k=1}^{c}\left(\underline{\kappa}_k(\mathbf{x}(t))m_k^L(\mathbf{x}(t)) + \overline{\kappa}_k(\mathbf{x}(t))m_k^U(\mathbf{x}(t))\right)} \tag{2.20}$$

where

$$m_j^L(\mathbf{x}(t)) = \prod_{l=1}^{\Omega} \underline{\mu}_{\tilde{N}_l^j}(g_l(\mathbf{x}(t))), \tag{2.21}$$

$$m_j^U(\mathbf{x}(t)) = \prod_{l=1}^{\Omega} \overline{\mu}_{\tilde{N}_l^j}(g_l(\mathbf{x}(t))), \tag{2.22}$$

in which

$$0 \leq \overline{\mu}_{\tilde{N}_\beta^j}(g_\beta(\mathbf{x}(t))) \leq 1, \tag{2.23}$$

$$0 \leq \underline{\mu}_{\tilde{N}_\beta^i}(g_\beta(\mathbf{x}(t))) \leq 1 \tag{2.24}$$

denote the upper and lower grades of membership governed by the lower and upper membership functions, respectively. By the definition of IT2 membership functions,

the property $0 \leq \underline{\mu}_{\tilde{N}_\beta^j}(g_\beta(\mathbf{x}(t))) \leq \overline{\mu}_{\tilde{N}_\beta^j}(g_\beta(\mathbf{x}(t))) \leq 1$ holds and further leads to the $0 \leq m_j^L(\mathbf{x}(t)) \leq m_j^U(\mathbf{x}(t)) \leq 1$ valid for all j.

$$0 \leq \underline{\kappa}_j(\mathbf{x}(t)) \leq 1, \tag{2.25}$$

$$0 \leq \overline{\kappa}_j(\mathbf{x}(t)) \leq 1, \tag{2.26}$$

$$\underline{\kappa}_j(\mathbf{x}(t)) + \overline{\kappa}_j(\mathbf{x}(t)) = 1, \forall j. \tag{2.27}$$

$\underline{\kappa}_j(\mathbf{x}(t))$ and $\overline{\kappa}_j(\mathbf{x}(t))$ are nonlinear functions to be determined.

The IT2 polynomial fuzzy controller is described by

$$\mathbf{u}(t) = \sum_{i=1}^{c} \tilde{m}_j(\mathbf{x}(t))\mathbf{G}_j(\mathbf{x}(t))\hat{\mathbf{x}}(\mathbf{x}(t)), \tag{2.28}$$

where

$$\sum_{i=1}^{c} \tilde{m}_j(\mathbf{x}(t)) = 1, \tilde{m}_j(\mathbf{x}(t)) \geq 0, \ \forall \ j. \tag{2.29}$$

2.3 Lyapunov Method

Lyapunov method is the most popular vehicle to investigate the stability of FMB/PFMB control systems. Based on the Lyapunov stability theory, stability/stabilization and control synthesis problems can be described by a set of LMI/SOS [36,37,104] of which a feasible solution can be found numerically using convex programming techniques. A Lyapunov function candidate plays an essential role in the stability analysis affecting the conservativeness of analysis results and the complexity of analysis.

In general, there are three types of Lyapunov function candidates can be found in the literature. The first type is of common quadratic Lyapunov function candidate. The FMB/PFMB control system is guaranteed to be asymptomatically stable if there exists a common solution to a set of LMI/SOS [11, 36, 105]. Under the parallel distributed compensation (PDC) design concept [11, 105], relaxed LMI-based stability conditions were achieved in [8, 12–14, 67, 106, 107] with the consideration of the permutations of membership functions and the introduction of slack matrices. Under the PDC design concept, the fuzzy controller is required to share the same number of rules and premise membership functions as those of the T-S fuzzy model, otherwise, it is referred to as non-PDC design concept in this paper. Stability analysis results under the non-PDC descign concept can be found in [63–65, 108–114].

The second type is of piecewise/switched Lyapunov function candidate [57, 115–121], which consists of some local Lyapunov function candidates. The piecewise/switched Lyapunov function candidate considers the operating domain as a union of its operating sub-domains. Corresponding to each operating sub-domain, an individual local Lyapunov function candidate is proposed for stability analysis. Comparing

with the quadratic Lyapunov function candidate, the piecewise/switched Lyapunov function candidate is able to produce less conservative stability analysis results. However, it will generally complicate the stability analysis as it requires to develop a condition to guarantee a smooth and continuous transition between the local Lyapunov function candidates for all connected operating sub-domains. A particular structure of the Lyapunov function matrices has been proposed to make sure that the piecewise/switched Lyapunov function candidate is valid for stability analysis and invertible for control synthesis [115, 119].

The third type is of fuzzy Lyapunov function candidate [122, 123] where the first and the second types are the subset of this one. The fuzzy Lyapunov function candidate consists of some local Lyapunov function candidates where the contribution of each is governed by the membership functions. Similar to the switched Lyapunov function candidate, as different local Lyapunov function candidates are considered in different operating sub-domains, less conservative stability results can be achieved compared with the first type. The membership functions ensure a smooth and continuous transition between the local Lyapunov function candidates of all connected operating sub-domains. Consequently, unlike the switched Lyapunov function candidate, in general, there is no particular structure of Lyapunov function matrices is required, the stability analysis is made easier. However, the derivative of membership functions will appear in the stability analysis, which makes the stability analysis complicated. Various enhancement techniques were proposed in [60, 61, 77, 124–138] for further relaxation of stability conditions and/or alleviation of difficulty in stability analysis resulting from the derivative terms of membership functions.

The one adopted in this thesis is the polynomial Lyapunov function candidate, in which the Lyapunov function is of polynomial form of the states [36]. When the order of the polynomial terms in the candidate reduces to zero, the polynomial Lyapunov function candidate turns out to the common quadratic Lyapunov function candidate. Therefore, the polynomial Lyapunov function candidate is a more general representation than the common quadratic Lyapunov function candidate. In [36], the authors compared quadratic Lyapunov function, piecewise Lyapunov function, and polynomial Lyapunov functions in the simulation example. The best performance was obtained by the polynomial Lyapunov function with proper order. It is also worth mentioning that in the works in [139], the two-step stability analysis of the PFMB control system was proposed. More general form of the polynomial Lyapunov function can be obtained by solving the convex problem in the two-step approach.

2.4 Improving the H_∞ Tracking Control Performance

The performance of FMB/PFMB control systems is another important issue to be consider during the controller design, and it can be the speed of response, constrains on input, output, control and so on [10] as mentioned before. Also there is a guaranteed cost approach introduced by Chang and Peng [140], which is able to provide an upper bound on a given performance index and the performance of the system is guaranteed to be less than the boundary. Guan and Chen applied this approach on T-S fuzzy systems with time delays [22] and Tanaka, etc. adopted this method in the stability analysis of polynomial fuzzy systems [38].

One of the most frequently used control performance index is based on the H_∞ norm. Form the definition of the H_∞ norm for the system transfer function, it shows largest possible gain from the input. The space-space solution to the H_∞ is reported in the famous DGKF paper [141], in this study, the H_∞ solution is related the solution of two algebraic Riccati equations to guarantee that the spectral radius is less than γ^2. After that, the LMI based approach for H_∞ control is reported in [142]. Afterwards, lots of the control research based on H_∞ are reported with success, for example, the works in [15–18] applied the H_∞ techniques into the fuzzy control systems.

In addition, the tracking performance can be judged and improved in terms of the H_∞ performance [76, 78, 80, 143, 144]. By using H_∞ performance index based approach [66, 80], the tracking error between the fuzzy model and the reference model can be attenuated, then the tracking performance can be further improved by compressing the H_∞ norm.

2.5 Useful Lemmas

In this thesis, the following lemmas are introduced, which play vital role in the analysis.

Lemma 1 (Schur complement)**.** *With matrices* $\mathbf{A}$*,* $\mathbf{B}$ *and* $\mathbf{C}$ *of appropriate dimensions and* $\mathbf{A} = \mathbf{A}^T, \mathbf{C} = \mathbf{C}^T$*, the following relation holds [104]:*

$$\begin{bmatrix} \mathbf{A} & \mathbf{B} \\ \mathbf{B}^T & \mathbf{C} \end{bmatrix} > 0 \Longleftrightarrow \mathbf{C} > 0, \mathbf{A} - \mathbf{B}\mathbf{C}^{-1}\mathbf{B}^T > 0$$

Lemma 2. *For any invertible polynomial matrix* $\mathbf{X}(\tilde{\mathbf{x}})$*, the following lemma holds:*

$$\frac{\partial \mathbf{X}(\tilde{\mathbf{x}})^{-1}}{\partial x_k} = -\mathbf{X}(\tilde{\mathbf{x}})^{-1}\frac{\partial \mathbf{X}(\tilde{\mathbf{x}})}{\partial x_k}\mathbf{X}(\tilde{\mathbf{x}})^{-1}. \tag{2.30}$$

Proof. Given that

$$\frac{\partial \mathbf{I}}{dx_k} = 0, \tag{2.31}$$

replacing $\mathbf{I}$ by $\mathbf{X}(\tilde{\mathbf{x}})^{-1}\mathbf{X}(\tilde{\mathbf{x}})$, (2.31) can be rewritten as

$$\frac{\partial \mathbf{X}(\tilde{\mathbf{x}})^{-1}\mathbf{X}(\tilde{\mathbf{x}})}{\partial x_k} = 0. \tag{2.32}$$

It follows that

$$\mathbf{X}(\tilde{\mathbf{x}})^{-1}\frac{\partial \mathbf{X}(\tilde{\mathbf{x}})}{\partial x_k} + \frac{\partial \mathbf{X}(\tilde{\mathbf{x}})^{-1}}{\partial x_k}\mathbf{X}(\tilde{\mathbf{x}}) = 0. \tag{2.33}$$

□

Lemma 3 (Jensen's Inequality)**.** *with* $\mathbf{b}(\varphi)$*,* $\mathbf{R} > 0$ *and* $t_\gamma > 0$*, the following equations alway holds [145]:*

$$-\int_{t-t_\gamma}^{t} \mathbf{b}(\varphi)^T\mathbf{R}\mathbf{b}(\varphi)d\varphi \leq -\frac{1}{t_\gamma}(\hat{\mathbf{v}}(t) - \hat{\mathbf{v}}(t-t_\gamma))^T\mathbf{R}(\hat{\mathbf{v}}(t) - \hat{\mathbf{v}}(t-t_\gamma)), \tag{2.34}$$

Proof. From Schur complement, it can be found that:

$$\begin{bmatrix} \mathbf{b}(\varphi)^T\mathbf{R}\mathbf{b}(\varphi) & \mathbf{b}(\varphi)^T \\ \mathbf{b}(\varphi) & \mathbf{R}^{-1} \end{bmatrix} \geq \mathbf{0}, \tag{2.35}$$

for any $t - t_\gamma \leq \varphi \leq t$, integrate the above equation from $t - h_s$ to t, we have:

$$\begin{bmatrix} \int_{t-t_\gamma}^{t} \mathbf{b}(\varphi)^T\mathbf{R}\mathbf{b}(\varphi)d\varphi & \int_{t-t_\gamma}^{t} \mathbf{b}(\varphi)^T d\varphi \\ \int_{t-t_\gamma}^{t} \mathbf{b}(\varphi)d\varphi & t_\gamma\mathbf{R}^{-1} \end{bmatrix} \geq \mathbf{0}, \tag{2.36}$$

By using Schur complement lemma again, (2.34) can be achieved. □

Chapter 3

Relaxation of the Stability Conditions of IT2 PFMB Control Systems

In this chapter, the stability analysis of IT2 PFMB control system will be conducted. The control objective in this chapter is to design proper polynomial feedback gains, which drive the value of state $\mathbf{x}(t)$ in of the nonlinear plant represented by an IT2 polynomial fuzzy model to $\mathbf{0}$. The block digram of the IT PFMB control system in this chapter is shown in Fig. 3.1. In this figure, it demonstrates that the states of the IT2 polynomial fuzzy model will be feedbacked to the IT2 polynomial fuzzy controller. The IT2 polynomial fuzzy controller generates control input $\mathbf{u}(t)$ to stabilize the nonlinear plant. To conduct the stability analysis by both MFI and MFD approaches, at first, the MFI stability conditions will be developed without considering the information of the IT2 membership functions. Then, considering the sub-domains of the membership functions, the polynomial approximation of the membership functions and the polynomial approximation in sub-domains of the membership functions, three approaches are presented to further relax the stability conditions. Both theoretical analysis and simulation results suggest the feasibility of the proposed approaches.

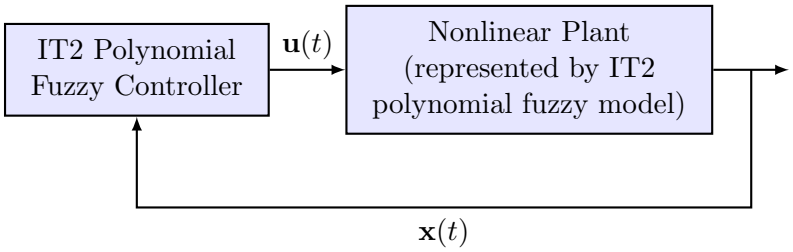

Figure 3.1: A block diagram of IT2 PFMB control systems.

3.1 Stability Analysis of IT2 PFMB Systems

The stability analysis of the IT2 PFMB systems is investigated in this section. In the following analysis in this chapter, for brevity, the time t associated with the variables is dropped for the situation without ambiguity. e.g., $\mathbf{x}(t)$ and $\hat{\mathbf{x}}(\mathbf{x}(t))$ are denoted as $\mathbf{x}$ and $\hat{\mathbf{x}}$, respectively. Also $\tilde{w}_i(\mathbf{x}(t))$ and $\tilde{m}_j(\mathbf{x}(t))$ are denoted as $\tilde{w}_i$ and $\tilde{m}_j$, respectively. From (2.2) and (2.14), we obtain the IT2 PFMB control system as follows:

$$\dot{\mathbf{x}} = \sum_{i=1}^{p}\sum_{j=1}^{c} \tilde{w}_i\tilde{m}_j(\mathbf{A}_i(\mathbf{x}) + \mathbf{B}_i(\mathbf{x})\mathbf{G}_j(\mathbf{x}))\hat{\mathbf{x}}. \tag{3.1}$$

From (3.1), denoting $\mathbf{x} = [x_1, x_2, \ldots, x_n]^T$ and $\hat{\mathbf{x}} = [\hat{x}_1, \hat{x}_2, \ldots, \hat{x}_N]^T$, we have:

$$\begin{aligned}\dot{\hat{\mathbf{x}}} &= \frac{\partial\hat{\mathbf{x}}}{\partial\mathbf{x}}\frac{d\mathbf{x}}{dt} = \mathbf{T}(\mathbf{x})\dot{\mathbf{x}} \\ &= \sum_{i=1}^{p}\sum_{j=1}^{c} \tilde{w}_i\tilde{m}_j(\tilde{\mathbf{A}}_i(\mathbf{x}) + \tilde{\mathbf{B}}_i(\mathbf{x})\mathbf{G}_j(\mathbf{x}))\hat{\mathbf{x}},\end{aligned} \tag{3.2}$$

where $\tilde{\mathbf{A}}_i(\mathbf{x}) = \mathbf{T}(\mathbf{x})\mathbf{A}_i(\mathbf{x})$, $\tilde{\mathbf{B}}_i(\mathbf{x}) = \mathbf{T}(\mathbf{x})\mathbf{B}_i(\mathbf{x})$, and $\mathbf{T}(\mathbf{x}) \in \Re^{N\times N}$ is a polynomial matrix with (i,j)th element is defined as $T_{i,j} = \partial\hat{x}_i(\mathbf{x})/\partial x_j$. Since $\hat{\mathbf{x}}$ is a vector of monomials of $\mathbf{x}$, $\hat{\mathbf{x}} = \mathbf{0}$ implies $\mathbf{x} = \mathbf{0}$, therefore, the stability of the augmented IT2 PFMB control system (3.2) implies that of the IT2 PFMB control system (3.1).

3.1.1 Sum-of-Squares-Based Stability Analysis

The following polynomial Lyapunov function candidate is employed to investigate the stability of the augmented IT2 PFMB control system (3.2).

$$V(t) = \hat{\mathbf{x}}^T\mathbf{X}(\tilde{\mathbf{x}})^{-1}\hat{\mathbf{x}}, \tag{3.3}$$

where $0 < \mathbf{X}(\tilde{\mathbf{x}}) = \mathbf{X}(\tilde{\mathbf{x}})^T \in \Re^{N\times N}$.

Remark 3.1. *To facilitate the stability analysis, it is defined that* $\mathbf{K} = \{k_1, k_2, \ldots, k_q\}$ *is the set of row numbers that the entire row of* $\mathbf{B}_i(\mathbf{x})$ *are all zeros for all* i. *Defining* $\tilde{\mathbf{x}} = (x_{k_1}, x_{k_2}, \ldots, x_{k_q})$, *it obtains* $\frac{\partial\mathbf{X}(\tilde{\mathbf{x}})^{-1}}{\partial x_j} = -\mathbf{X}(\tilde{\mathbf{x}})^{-1}\frac{\partial\mathbf{X}(\tilde{\mathbf{x}})}{\partial x_j}\mathbf{X}(\tilde{\mathbf{x}})^{-1}$ *and* $\dot{\mathbf{X}}(\tilde{\mathbf{x}})^{-1} = \sum_{k\in\mathbf{K}}\frac{\partial\mathbf{X}(\tilde{\mathbf{x}})^{-1}}{\partial x_k}\sum_{i=1}^{p}\tilde{w}_i\mathbf{A}_i^k(\mathbf{x})\hat{\mathbf{x}}$ *[36], where* $\mathbf{A}_i^k(\mathbf{x}) \in \Re^N$ *and* $\mathbf{B}_i^k(\mathbf{x}) \in \Re^m$, $i = 1, 2, \ldots, p$, $k = 1, 2, \ldots, n$ *denote the* k*-th row of* $\mathbf{A}_i(\mathbf{x})$ *and* $\mathbf{B}_i(\mathbf{x})$, *respectively.*

From (3.2) and (3.3), we have

$$\begin{aligned}\dot{V}(t) &= \dot{\hat{\mathbf{x}}}^T\mathbf{X}(\tilde{\mathbf{x}})^{-1}\hat{\mathbf{x}} + \hat{\mathbf{x}}^T\mathbf{X}(\tilde{\mathbf{x}})^{-1}\dot{\hat{\mathbf{x}}} + \hat{\mathbf{x}}^T\frac{d\mathbf{X}(\tilde{\mathbf{x}})^{-1}}{dt}\hat{\mathbf{x}} \\ &= \sum_{i=1}^{p}\sum_{j=1}^{c}\tilde{w}_i\tilde{m}_j\hat{\mathbf{x}}^T\Big(\big(\tilde{\mathbf{A}}_i(\mathbf{x}) + \tilde{\mathbf{B}}_i(\mathbf{x})\mathbf{G}_j(\mathbf{x})\big)^T\mathbf{X}(\tilde{\mathbf{x}})^{-1} \\ &\quad + \mathbf{X}(\tilde{\mathbf{x}})^{-1}\big(\tilde{\mathbf{A}}_i(\mathbf{x}) + \tilde{\mathbf{B}}_i(\mathbf{x})\mathbf{G}_j(\mathbf{x})\big)\Big)\hat{\mathbf{x}} \quad + \hat{\mathbf{x}}^T\frac{d\mathbf{X}(\tilde{\mathbf{x}})^{-1}}{dt}\hat{\mathbf{x}}.\end{aligned} \tag{3.4}$$

Let us denote $\tilde{w}_i\tilde{m}_j$ as $\tilde{h}_{ij}(\mathbf{x})$ and define $\mathbf{z} = \mathbf{X}(\tilde{\mathbf{x}})^{-1}\hat{\mathbf{x}}$ and $\mathbf{G}_j(\mathbf{x}) = \mathbf{N}_j(\mathbf{x})\mathbf{X}(\tilde{\mathbf{x}})^{-1}$, where $\mathbf{N}_j(\mathbf{x}) \in \Re^{m\times N}$, $j = 1, 2, \ldots, c$, is an arbitrary polynomial matrix to be determined. From Remark 3.1, (3.2), (3.3) and (3.4), we have:

$$\dot{V}(t) = \sum_{i=1}^{p}\sum_{j=1}^{c} \tilde{h}_{ij}(\mathbf{x})\mathbf{z}^T\mathbf{Q}_{ij}(\mathbf{x})\mathbf{z}, \tag{3.5}$$

where $\mathbf{Q}_{ij}(\mathbf{x}) = \tilde{\mathbf{A}}_i\mathbf{X}(\tilde{\mathbf{x}}) + \mathbf{X}(\tilde{\mathbf{x}})\tilde{\mathbf{A}}_i(\mathbf{x})^T + \tilde{\mathbf{B}}_i(\mathbf{x})\mathbf{N}_j(\mathbf{x}) + \mathbf{N}_j(\mathbf{x})^T\tilde{\mathbf{B}}_i(\mathbf{x})^T$
$- \sum_{k\in\mathbf{K}} \frac{\partial\mathbf{X}(\tilde{\mathbf{x}})}{\partial x_k}\mathbf{A}_i^k(\mathbf{x})\hat{\mathbf{x}}$, $i = 1, 2, \ldots, p$; $j= 1, 2, \ldots, c$.

Remark 3.2. *For IT2 PFMB control systems, the membership grades $\tilde{w}_i$ for all i are uncertain, which hinder the stability analysis using the techniques requiring the membership functions to be known, e.g., the PDC design. The most straightforward approach to guarantee the stability of the control systems is to require $\mathbf{X}(\tilde{\mathbf{x}}) > 0$ and $\mathbf{Q}_{ij}(\mathbf{x}) < 0$ for all i and j. According to Lyapunov stability theory, by satisfying these conditions $V(t) > 0$ and $\dot{V}(t) < 0$ (excluding $\mathbf{x} = \mathbf{0}$) can be achieved, which implies the asymptotic stability of* (3.1)*. However, the stability conditions will be very conservative as the membership functions $\tilde{h}_{ij}(\mathbf{x})$ are not considered in the stability analysis, which means that the stability conditions are unnecessarily valid for arbitrary membership functions. In order to include the specific membership functions into the analysis, some basic techniques were proposed in [45, 55] to utilize limited information of membership functions.*

3.1.2 Using Sub-domains to Include the Information of Membership Functions

To bring the information of the membership functions into the stability analysis, in this section, sub-domains based approach will be introduced to relax the basic stability conditions. It is worth noting that $\tilde{h}_{ij}(\mathbf{x})$ is a function of $\mathbf{x}$, which has infinite number of membership grades due to the continuous variable $\mathbf{x}$. Consequently, by incorporating the membership functions into the stability conditions, it is not practical to find a feasible solution to the stability conditions of infinite number. In this section, various techniques are proposed to bring the information of membership functions into the stability analysis, which avoids turning the number of stability conditions into infinite but still can achieve more relaxed stability conditions.

To facilitate the stability analysis, we first divide the whole operating domain Φ into L connected sub-domains, Φ_l, $l = 1, 2, \ldots, L$ such that $\Phi = \bigcup_{l=1}^{L}\Phi_l$. In each sub-domain, we denote the portion of $\tilde{h}_{ij}(\mathbf{x})$ where $\mathbf{x} \in \Phi_l$ (the portion of $\tilde{h}_{ij}(\mathbf{x})$ in the l-th sub-domain) as $\tilde{h}_{ijl}(\mathbf{x})$ such that $\tilde{h}_{ij}(\mathbf{x}) = \bigcup_{l=1}^{L}\tilde{h}_{ijl}(\mathbf{x})$.

To proceed further, we define constant scalars $\underline{h}_{ijl} \geq 0$ and $\overline{h}_{ijl} \geq 0$ as the lower and upper bound of the IT2 membership function $\tilde{h}_{ijl}(\mathbf{x})$ in the l-th sub-domains, respectively, satisfying $0 \leq \underline{h}_{ijl} \leq \tilde{h}_{ijl}(\mathbf{x}) \leq \overline{h}_{ijl} \leq 1$ for $\mathbf{x} \in \Phi_l$.We obtain

$\overline{h}_{ijl} - \underline{h}_{ijl} \geq \tilde{h}_{ijl}(\mathbf{x}) - \underline{h}_{ijl} \geq 0$. Therefore, through adopting $\underline{h}_{ijl}$ and $\overline{h}_{ijl}$ in the stability analysis, it is able to get rid of $\tilde{h}_{ijl}(\mathbf{x})$ to allow the stability conditions to be handled by convex programming techniques.

In the following, we conduct the stability analysis sub-domain by sub-domain by utilizing the information of $\tilde{h}_{ijl}(\mathbf{x})$ for $\mathbf{x} \in \Phi_l$. (3.5) is rewritten in the l-th sub-domain as follows:

$$\begin{aligned}\dot{V}(t) &= \sum_{i=1}^{p}\sum_{j=1}^{c} \tilde{h}_{ijl}(\mathbf{x})\mathbf{z}^T\mathbf{Q}_{ij}(\mathbf{x})\mathbf{z} \\ &= \sum_{i=1}^{p}\sum_{j=1}^{c} (\underline{h}_{ijl} + \tilde{h}_{ijl}(\mathbf{x}) - \underline{h}_{ijl})\mathbf{z}^T\mathbf{Q}_{ij}(\mathbf{x})\mathbf{z}, \mathbf{x} \in \Phi_l, \\ & \quad l = 1, 2, \ldots, L. \end{aligned} \tag{3.6}$$

Meanwhile, we define some non-negative matrices $\mathbf{Y}_{ijl}(\mathbf{x}) = \mathbf{Y}_{ijl}(\mathbf{x})^T \geq 0$, which are required to satisfy $\mathbf{Y}_{ijl}(\mathbf{x}) \geq \mathbf{Q}_{ij}(\mathbf{x})$. From (3.6), we have

$$\begin{aligned}\dot{V}(t) &= \sum_{i=1}^{p}\sum_{j=1}^{c} \underline{h}_{ijl}\mathbf{z}^T\mathbf{Q}_{ij}(\mathbf{x})\mathbf{z} + \sum_{i=1}^{p}\sum_{j=1}^{c} (\tilde{h}_{ijl} - \underline{h}_{ijl})\mathbf{z}^T\mathbf{Q}_{ij}(\mathbf{x})\mathbf{z} \\ &\leq \sum_{i=1}^{p}\sum_{j=1}^{c} \underline{h}_{ijl}\mathbf{z}^T\mathbf{Q}_{ij}(\mathbf{x})\mathbf{z} \\ &\quad + \sum_{i=1}^{p}\sum_{j=1}^{c} (\tilde{h}_{ijl}(\mathbf{x}) - \underline{h}_{ijl})\mathbf{z}^T\mathbf{Y}_{ijl}(\mathbf{x})\mathbf{z} \\ &= \sum_{i=1}^{p}\sum_{j=1}^{c} \mathbf{z}^T(\underline{h}_{ijl}\mathbf{Q}_{ij}(\mathbf{x}) + (\tilde{h}_{ijl}(\mathbf{x}) - \underline{h}_{ijl})\mathbf{Y}_{ijl}(\mathbf{x}))\mathbf{z}, \\ & \quad \mathbf{x} \in \Phi_l, l = 1, 2, \ldots, L. \end{aligned} \tag{3.7}$$

Then, (3.7) can be rewritten as follows:

$$V(t) \leq \sum_{i=1}^{p}\sum_{j=1}^{c} \mathbf{z}^T(\underline{h}_{ijl}\mathbf{Q}_{ij}(\mathbf{x}) + \delta_{ijl}\mathbf{Y}_{ijl}(\mathbf{x}))\mathbf{z}, \tag{3.8}$$

where $\delta_{ijl} = \overline{h}_{ijl} - \underline{h}_{ijl}$.

To further relax the stability analysis results, we bring the state information from each sub-domain into the stability analysis. Defining the slack matrices $\mathbf{M}_l(\mathbf{x}) = \mathbf{M}_l^T(\mathbf{x}) \in \Re^{N\times N} \geq 0$, $l = 1, 2, \ldots, L$, it follows from (3.8) that

$$\begin{aligned}\dot{V}(t) \leq \sum_{i=1}^{p}\sum_{j=1}^{c} \mathbf{z}^T \big(&\underline{h}_{ijl}\mathbf{Q}_{ij}(\mathbf{x}) + \delta_{ijl}\mathbf{Y}_{ijl}(\mathbf{x}) \\ &+ (\mathbf{x} - \underline{\mathbf{x}}_l)^T\mathbf{D}(\overline{\mathbf{x}}_l - \mathbf{x})\mathbf{M}_l(\mathbf{x})\big)\mathbf{z}, \end{aligned} \tag{3.9}$$

where $\underline{\mathbf{x}}_l \in \Re^N$ and $\overline{\mathbf{x}}_l \in \Re^N$ are the lower and upper bound of $\mathbf{x}$ in the l-th sub-domain, $l = 1, 2, \ldots, L$, $\mathbf{D} = \text{diag}\{d_1, d_2, \ldots, d_N\} \in \Re^{N\times N}$ is a diagonal matrix whose element is either 0 or 1. When $d_r = 0$, $r = 1, 2, \ldots, N$, the state information of x_r is not contained. Through the analysis, the results can be summarized as in the following theorem:

Theorem 3.1. *The IT2 PFMB system* (3.1)*, which is formed by a nonlinear plant represented by the IT2 polynomial fuzzy model* (2.12) *and the IT2 polynomial fuzzy controller* (2.28) *connected in a closed loop is guaranteed to be asymptotically stable if there exist polynomial matrices* $\mathbf{M}_l(\mathbf{x}) = \mathbf{M}_l(\mathbf{x})^T \in \Re^{N\times N}$, $\mathbf{N}_j(\mathbf{x}) \in \Re^{m\times N}$, $\mathbf{X}(\tilde{\mathbf{x}}) = \mathbf{X}(\tilde{\mathbf{x}})^T \in \Re^{N\times N}$, $\mathbf{Y}_{ijl}(\mathbf{x}) = \mathbf{Y}_{ijl}(\mathbf{x})^T \in \Re^{N\times N}$, $i = 1, 2, \ldots, p$, $j = 1, 2, \ldots, c$, $l = 1, 2, \ldots, L$, *such that the following SOS-based conditions are satisfied:*

$$
\begin{aligned}
&\nu^T(\mathbf{M}_l(\mathbf{x}) - \varepsilon_1(\mathbf{x})\mathbf{I})\nu \text{ is SOS}, \ \forall l;\\
&\nu^T(\mathbf{X}(\tilde{\mathbf{x}}) - \varepsilon_2(\tilde{\mathbf{x}})\mathbf{I})\nu \text{ is SOS};\\
&\nu^T(\mathbf{Y}_{ijl}(\mathbf{x}) - \varepsilon_3(\mathbf{x})\mathbf{I})\nu \text{ is SOS}, \ \forall i, j, l;\\
&\nu^T(\mathbf{Y}_{ijl}(\mathbf{x}) - \mathbf{Q}_{ij}(\mathbf{x}) - \varepsilon_4(\mathbf{x})\mathbf{I})\nu \text{ is SOS}, \forall i, j, l;\\
-&\nu^T \sum_{i=1}^{p}\sum_{j=1}^{c} \big(\underline{h}_{ijl}\mathbf{Q}_{ij}(\mathbf{x}) + \delta_{ijl}\mathbf{Y}_{ijl}(\mathbf{x})\\
&+ (\mathbf{x} - \underline{\mathbf{x}}_l)^T\mathbf{D}(\overline{\mathbf{x}}_l - \mathbf{x})\mathbf{M}_l(\mathbf{x}) + \varepsilon_5(\mathbf{x})\mathbf{I}\big)\nu \text{ is SOS}, \ \forall l,
\end{aligned}
$$

where $\nu \in \Re^N$ *is an arbitrary vector independent of* $\mathbf{x}$, $\hat{h}_{ijl}$ *and* δ_{ijl} *are predefined constants;* $\mathbf{D} = diag\{d_1, d_2, \ldots, d_N\} \in \Re^{N\times N}$ *is a predefined diagonal matrix;* $\varepsilon_1(\mathbf{x}) > 0$, $\varepsilon_2(\tilde{\mathbf{x}}) > 0$, $\varepsilon_3(\mathbf{x}) > 0$, $\varepsilon_4(\mathbf{x}) > 0$, $\varepsilon_5(\mathbf{x}) > 0$ *are predefined scalar polynomials;* $\underline{\mathbf{x}}_l$ *and* $\overline{\mathbf{x}}_l$ *are the predefined lower and upper bounds of system state* $\mathbf{x}$ *in the* l*-th sub-domain;* $\mathbf{Q}_{ij}(\mathbf{x}) = \tilde{\mathbf{A}}_i\mathbf{X}(\tilde{\mathbf{x}}) + \mathbf{X}(\tilde{\mathbf{x}})\tilde{\mathbf{A}}_i(\mathbf{x})^T + \tilde{\mathbf{B}}_i(\mathbf{x})\mathbf{N}_j(\mathbf{x}) + \mathbf{N}_j(\mathbf{x})^T\tilde{\mathbf{B}}_i(\mathbf{x})^T - \sum_{k\in\mathbf{K}} \frac{\partial \mathbf{X}(\tilde{\mathbf{x}})}{\partial x_k}\mathbf{A}_i^k(\mathbf{x})\hat{\mathbf{x}}$, *and the feedback gains are defined as* $\mathbf{G}_j(\mathbf{x}) = \mathbf{N}_j(\mathbf{x})\mathbf{X}(\tilde{\mathbf{x}})^{-1}$, $j = 1, 2, \ldots, c$.

Remark 3.3. *Referring to Theorem 3.1, the number of SOS variables is* $pcL + L + c + 1$ *and the number of SOS based stability conditions is* $2pcL + 2L + 1$*. The more sub-domains are divided, the richer information can be contained in the stability analysis and then the more relaxed stability analysis results can be achieved. However, when the number of sub-domains increases, the number of stability conditions will also increase, therefore, the computational burden on solving the stability conditions will increase as well.*

3.1.3 Using Polynomial Functions to Approximate the Membership Functions

The FOU contains a lot of information of IT2 membership functions carried by an infinite number of embedded type-1 membership functions. In order to take the information of FOU into the stability analysis, in the second method, we first construct

a set of embedded type-1 membership functions in polynomial form. Then, the stability analysis is developed based on the embedded type-1 polynomial membership functions which can be effectively dealt within the SOS-based stability analysis and the stability conditions can be solved numerically using SOSTOOLS [37]. From (3.6), getting rid of the index l (as no sub-domain is required), we have

$$\begin{aligned}\dot{V}(t) &= \sum_{i=1}^{p}\sum_{j=1}^{c} \tilde{h}_{ij}(\mathbf{x})\mathbf{z}^T\mathbf{Q}_{ij}(\mathbf{x})\mathbf{z} \\ &= \sum_{i=1}^{p}\sum_{j=1}^{c} (\hat{h}_{ij}(\mathbf{x}) + \tilde{h}_{ij}(\mathbf{x}) - \hat{h}_{ij}(\mathbf{x}))\mathbf{z}^T\mathbf{Q}_{ij}(\mathbf{x})\mathbf{z}. \end{aligned} \tag{3.10}$$

Considering that $\underline{\delta}_{ij}(\mathbf{x}) \leq \tilde{h}_{ij}(\mathbf{x}) - \hat{h}_{ij}(\mathbf{x}) \leq \overline{\delta}_{ij}(\mathbf{x})$, (3.10) can be rewritten as following:

$$\begin{aligned}\dot{V}(t) &= \sum_{i=1}^{p}\sum_{j=1}^{c} \tilde{h}_{ij}(\mathbf{x})\mathbf{z}^T\mathbf{Q}_{ij}(\mathbf{x})\mathbf{z} \\ &= \sum_{i=1}^{p}\sum_{j=1}^{c} (\hat{h}_{ij}(\mathbf{x}) + \tilde{h}_{ij}(\mathbf{x}) - \hat{h}_{ij}(\mathbf{x}) - \underline{\delta}_{ij}(\mathbf{x}) + \underline{\delta}_{ij}(\mathbf{x}))\mathbf{z}^T\mathbf{Q}_{ij}(\mathbf{x})\mathbf{z} \\ &= \sum_{i=1}^{p}\sum_{j=1}^{c} \big((\hat{h}_{ij}(\mathbf{x}) + \underline{\delta}_{ij}(\mathbf{x})) + (\tilde{h}_{ij}(\mathbf{x}) - \hat{h}_{ij}(\mathbf{x}) - \underline{\delta}_{ij}(\mathbf{x}))\big)\mathbf{z}^T\mathbf{Q}_{ij}(\mathbf{x})\mathbf{z}. \end{aligned} \tag{3.11}$$

In the following analysis, $\hat{h}_{ij}(\mathbf{x}) + \underline{\delta}_{ij}(\mathbf{x})$ will be denoted as $\underline{h}_{ij}(\mathbf{x})$ to lighten the burden of symbols. Since $\underline{\delta}_{ij}(\mathbf{x})$ and $\overline{\delta}_{ij}(\mathbf{x})$ are both bounded, there must exist constant scalars $\underline{\delta}_{ij}$ and $\overline{\delta}_{ij}$ satisfying $\underline{\delta}_{ij} \leq \underline{\delta}_{ij}(\mathbf{x})$ and $\overline{\delta}_{ij} \geq \overline{\delta}_{ij}(\mathbf{x})$ for all $\mathbf{x}$ (or in a domain of interest).

Similar to the stability analysis in the first method, we introduce a polynomial matrix $\mathbf{Y}_{ij}(\mathbf{x}) = \mathbf{Y}_{ij}^T(\mathbf{x}) \geq 0$ requiring $\mathbf{Y}_{ij}(\mathbf{x}) \geq \mathbf{Q}_{ij}(\mathbf{x})$ for all i and j. Denoting $\overline{\delta}_{ij} - \underline{\delta}_{ij}$ as δ_{ij}. It follows from (3.11) that

$$\begin{aligned}\dot{V}(t) &\leq \sum_{i=1}^{p}\sum_{j=1}^{c} (\hat{h}_{ij}(\mathbf{x}) + \underline{\delta}_{ij}(\mathbf{x}))\mathbf{z}^T\mathbf{Q}_{ij}(\mathbf{x})\mathbf{z} + \sum_{i=1}^{p}\sum_{j=1}^{c} \delta_{ij}\mathbf{z}^T\mathbf{Y}_{ij}(\mathbf{x})\mathbf{z} \\ &= \sum_{i=1}^{p}\sum_{j=1}^{c} \mathbf{z}^T(\underline{h}_{ij}(\mathbf{x})\mathbf{Q}_{ij}(\mathbf{x}) + \delta_{ij}\mathbf{Y}_{ij}(\mathbf{x}))\mathbf{z}. \end{aligned} \tag{3.12}$$

Along the same line of derivation, the stability analysis results can be summarized in the following theorem.

Theorem 3.2. *The IT2 PFMB system* (3.1)*, which is formed by a nonlinear plant represented by the IT2 polynomial fuzzy model* (2.12) *and the IT2 polynomial fuzzy controller* (2.28) *connected in a closed loop is guaranteed to be asymptotically stable if there exist polynomial matrices* $\mathbf{N}_j(\mathbf{x}) \in \Re^{m\times N}$, $\mathbf{X}(\tilde{\mathbf{x}}) = \mathbf{X}(\tilde{\mathbf{x}})^T \in \Re^{N\times N}$, $\mathbf{Y}_{ij}(\mathbf{x}) =$

$\mathbf{Y}_{ij}(\mathbf{x})^T \in \Re^{N\times N}$, *i = 1, 2, ..., p, j = 1, 2, ..., c, such that the following SOS-based conditions are satisfied:*

$$\begin{aligned}
&\nu^T(\mathbf{X}(\tilde{\mathbf{x}}) - \varepsilon_1(\tilde{\mathbf{x}})\mathbf{I})\nu \text{ is SOS};\\
&\nu^T(\mathbf{Y}_{ij}(\mathbf{x}) - \varepsilon_2(\mathbf{x})\mathbf{I})\nu \text{ is SOS}, \quad \forall i,j;\\
&\nu^T(\mathbf{Y}_{ij}(\mathbf{x}) - \mathbf{Q}_{ij}(\mathbf{x}) - \varepsilon_3(\mathbf{x})\mathbf{I})\nu \text{ is SOS}, \ \forall i,j;\\
-&\nu^T \sum_{i=1}^{p}\sum_{j=1}^{c} \left(\underline{h}_{ij}(\mathbf{x})\mathbf{Q}_{ij}(\mathbf{x}) + \delta_{ij}\mathbf{Y}_{ij}(\mathbf{x}) + \varepsilon_4(\mathbf{x})\mathbf{I}\right)\nu \text{ is SOS},
\end{aligned}$$

where $\nu \in \Re^N$ *is an arbitrary vector independent of* $\mathbf{x}$*;* $\underline{h}_{ij}(\mathbf{x})$ *is a chosen embedded type-1 membership functions in polynomial form;* δ_{ij} *is a pre-defined constant scalar satisfying* $\overline{\delta}_{ij} \geq |\hat{\delta}_{ij}(\mathbf{x})|$ *for all* $\mathbf{x}$ *(or in a domain of interest);* $\varepsilon_1(\tilde{\mathbf{x}}) > 0$*,* $\varepsilon_2(\mathbf{x}) > 0$*,* $\varepsilon_3(\mathbf{x}) > 0$*,* $\varepsilon_4(\mathbf{x}) > 0$ *are predefined polynomials,* $\mathbf{Q}_{ij}(\mathbf{x}) = \tilde{\mathbf{A}}_i\mathbf{X}(\tilde{\mathbf{x}}) + \mathbf{X}(\tilde{\mathbf{x}})\tilde{\mathbf{A}}_i(\mathbf{x})^T + \tilde{\mathbf{B}}_i(\mathbf{x})\mathbf{N}_j(\mathbf{x}) + \mathbf{N}_j(\mathbf{x})^T\tilde{\mathbf{B}}_i(\mathbf{x})^T - \sum_{k\in\mathbf{K}} \frac{\partial \mathbf{X}(\tilde{\mathbf{x}})}{\partial x_k}\mathbf{A}_i^k(\mathbf{x})\hat{\mathbf{x}}$*, and the feedback gains are defined as* $\mathbf{G}_j(\mathbf{x}) = \mathbf{N}_j(\mathbf{x})\mathbf{X}(\tilde{\mathbf{x}})^{-1}$*, j = 1, 2, ..., c.*

Remark 3.4. *Referring to Theorem 3.2, the number of SOS variables is* $(p+1)c+1$ *and the number of SOS based stability conditions is* $pc + 2$*. It can be seen that the number of variables and stability conditions are smaller than those in Theorem 3.1, Therefore, the computational burden on solving a feasible solution is reduced. However, when the embedded type-1 membership functions* $\underline{h}_{ij}(\mathbf{x})$ *is in a higher-order polynomial form, the requirement on the numerical accuracy will increase and sometimes makes the computation runs into numerical problems, which hinders the solving of stability conditions.*

3.1.4 Using Polynomial Functions in Sub-domains to Approximate the Membership Functions

As discussed above, the advantage of using sub-domains of membership functions in the first method is that more information of membership functions can be utilized for the relaxation of stability conditions as the number of sub-domains increases, but the drawback is the increase of computational burden. In the second method, embedded type-1 membership functions in polynomial form are utilized which are in favor of the SOS-based stability analysis and the polynomial functions contain information of the FOU and IT2 membership functions. However, when only a single embedded type-1 membership function is used for the approximation in the whole operating domain, the order of polynomial functions is in general required to be high resulting in difficulties when using numerical method to obtain a feasible solution to the stability conditions. In order to address these drawbacks, we combine the advantages of both the first and the second methods to come up with the third method in this section.

In the third method, we first divide the whole operating domain into some sub-domains as in the first method. Corresponding to each sub-domain, embedded type-1 membership functions in polynomial form are employed to extract the information of FOU and IT2 membership functions as in the second method. Instead of using the embedded type-1 membership functions through the whole domain, the embedded type-1 membership functions are the local ones which can be different from those in other sub-domains. Consequently, the local embedded type-1 membership functions will be less complicated compared with the ones in the second method. It follows from (3.6) that

$$\begin{aligned}\dot{V}(t) &= \sum_{i=1}^{p}\sum_{j=1}^{c} \mathbf{z}^T \tilde{h}_{ijl}(\mathbf{x})\mathbf{Q}_{ij}(\mathbf{x})\mathbf{z} \\ &= \sum_{i=1}^{p}\sum_{j=1}^{c} \mathbf{z}^T (\hat{h}_{ijl}(\mathbf{x}) + \tilde{h}_{ijl}(\mathbf{x}) - \hat{h}_{ijl}(\mathbf{x}))\mathbf{Q}_{ij}(\mathbf{x})\mathbf{z}, \end{aligned} \tag{3.13}$$

where $\underline{\delta}_{ijl}(\mathbf{x}) \leq \tilde{h}_{ijl}(\mathbf{x}) - \hat{h}_{ijl}(\mathbf{x}) \leq \overline{\delta}_{ijl}(\mathbf{x})$; $\hat{h}_{ijl}(\mathbf{x})$ is the local embedded type-1 membership function in polynomial form in the l-th sub-domain. As $\underline{\delta}_{ijl}(\mathbf{x})$ and $\overline{\delta}_{ijl}(\mathbf{x})$ are bounded, there exists constant scalars $\underline{\delta}_{ijl}$ satisfying $\underline{\delta}_{ijl} \leq \underline{\delta}_{ijl}(\mathbf{x})$ and $\overline{\delta}_{ijl}$ satisfying $\overline{\delta}_{ijl} \geq \overline{\delta}_{ijl}(\mathbf{x})$ for $\mathbf{x} \in \Phi_l$. Furthermore, with the consideration of the state information in each sub-domain, we have

$$\begin{aligned}\dot{V}(t) \leq & \sum_{i=1}^{p}\sum_{j=1}^{c} \mathbf{z}^T \big((\hat{h}_{ijl}(\mathbf{x}) + \underline{\delta}_{ijl})\mathbf{Q}_{ij}(\mathbf{x}) + (\overline{\delta}_{ijl} - \underline{\delta}_{ijl})\mathbf{Y}_{ijl}(\mathbf{x}) \\ & + (\mathbf{x} - \underline{\mathbf{x}}_l)^T \mathbf{D}(\overline{\mathbf{x}}_l - \mathbf{x})\mathbf{M}_l(\mathbf{x}) \big)\mathbf{z}, \\ = & \sum_{i=1}^{p}\sum_{j=1}^{c} \mathbf{z}^T \big(\underline{h}_{ijl}(\mathbf{x})\mathbf{Q}_{ij}(\mathbf{x}) + \delta_{ijl}\mathbf{Y}_{ijl}(\mathbf{x}) \\ & + (\mathbf{x} - \underline{\mathbf{x}}_l)^T \mathbf{D}(\overline{\mathbf{x}}_l - \mathbf{x})\mathbf{M}_l(\mathbf{x}) \big)\mathbf{z}, \\ & \mathbf{x} \in \Phi_l, l = 1, 2, \ldots, L, \end{aligned} \tag{3.14}$$

where $\underline{h}_{ijl}(\mathbf{x}) = \hat{h}_{ijl}(\mathbf{x}) + \underline{\delta}_{ijl}$ and $\delta_{ijl} = \overline{\delta}_{ijl} - \underline{\delta}_{ijl}$.

Along the same line of derivation, the stability analysis results can be summarized in the following theorem.

Theorem 3.3. *The IT2 PFMB system* (3.1)*, which is formed by a nonlinear plant represented by the IT2 polynomial fuzzy model* (2.12) *and the IT2 polynomial fuzzy controller* (2.28) *connected in a closed loop is guaranteed to be asymptotically stable if there exist polynomial matrices* $\mathbf{M}_l(\mathbf{x}) = \mathbf{M}_l(\mathbf{x})^T \in \Re^{N\times N}$, $\mathbf{N}_j(\mathbf{x}) \in \Re^{m\times N}$, $\mathbf{X}(\tilde{\mathbf{x}}) = \mathbf{X}(\tilde{\mathbf{x}})^T \in \Re^{N\times N}$, $\mathbf{Y}_{ijl}(\mathbf{x}) = \mathbf{Y}_{ijl}(\mathbf{x})^T \in \Re^{N\times N}$, $i = 1, 2, \ldots, p$, $j = 1, 2, \ldots, c$, $l = 1, 2, \ldots, L$, *such that the following SOS-based conditions are satisfied:*

$$\nu^T(\mathbf{M}_l(\mathbf{x}) - \varepsilon_1(\mathbf{x})\mathbf{I})\nu \text{ is SOS}, \forall l;$$

$$
\begin{aligned}
&\nu^T(\mathbf{X}(\tilde{\mathbf{x}}) - \varepsilon_2(\tilde{\mathbf{x}})\mathbf{I})\nu \text{ is SOS};\\
&\nu^T(\mathbf{Y}_{ijl}(\mathbf{x}) - \varepsilon_3(\mathbf{x})\mathbf{I})\nu \text{ is SOS}, \ \forall i,j,l;\\
&\nu^T(\mathbf{Y}_{ijl}(\mathbf{x}) - \mathbf{Q}_{ij}(\mathbf{x}) - \varepsilon_4(\mathbf{x})\mathbf{I})\nu \text{ is SOS}, \forall i,j,l;\\
-\nu^T &\sum_{i=1}^{p}\sum_{j=1}^{c}\big(\underline{h}_{ijl}(\mathbf{x})\mathbf{Q}_{ij}(\mathbf{x}) + \delta_{ijl}\mathbf{Y}_{ijl}(\mathbf{x})\\
&+ (\mathbf{x} - \underline{\mathbf{x}}_l)^T\mathbf{D}(\overline{\mathbf{x}}_l - \mathbf{x})\mathbf{M}_l(\mathbf{x}) + \varepsilon_5(\mathbf{x})\mathbf{I}\big)\nu \text{ is SOS}, \ \forall l,
\end{aligned}
$$

where $\nu \in \Re^N$ *is an arbitrary vector independent of* $\mathbf{x}$*;* $\underline{h}_{ijl}(\mathbf{x})$ *is a chosen embedded type-1 membership functions in polynomial form in the* l*-th sub-domain;* δ_{ijl} *is a pre-defined constant scalar;* $\varepsilon_1(\mathbf{x}) > 0$*,* $\varepsilon_2(\tilde{\mathbf{x}}) > 0$*,* $\varepsilon_3(\mathbf{x}) > 0$*,* $\varepsilon_4(\mathbf{x}) > 0$*,* $\varepsilon_5(\mathbf{x}) > 0$ *are predefined scalar polynomials;* $\underline{\mathbf{x}}_l$ *and* $\overline{\mathbf{x}}_l$ *are the predefined lower and upper bounds of system state* $\mathbf{x}$ *in the* l*-th sub-domain;* $\mathbf{Q}_{ij}(\mathbf{x}) = \tilde{\mathbf{A}}_i\mathbf{X}(\tilde{\mathbf{x}}) + \mathbf{X}(\tilde{\mathbf{x}})\tilde{\mathbf{A}}_i(\mathbf{x})^T + \tilde{\mathbf{B}}_i(\mathbf{x})\mathbf{N}_j(\mathbf{x}) + \mathbf{N}_j(\mathbf{x})^T\tilde{\mathbf{B}}_i(\mathbf{x})^T - \sum_{k\in\mathbf{K}}\frac{\partial\mathbf{X}(\tilde{\mathbf{x}})}{\partial x_k}\mathbf{A}_i^k(\mathbf{x})\hat{\mathbf{x}}$*, and the feedback gains are defined as* $\mathbf{G}_j(\mathbf{x}) = \mathbf{N}_j(\mathbf{x})\mathbf{X}(\tilde{\mathbf{x}})^{-1}$*,* $j = 1, 2, \ldots, c$*.*

Remark 3.5. *Referring to Theorem 3.3, the number of SOS variables is* $pcL + L + c + 1$ *and the number of SOS based stability conditions is* $2pcL + 2L + 1$*. It can be seen that the number of variables and stability conditions is the same as that in Theorem 3.1. However, thanks to the introduction of polynomial functions in every sub-domain, richer information of membership functions can be included in every sub-domain, thus the number of intervals can be reduced, which means better performance can be achieved with a smaller value of* L*. Therefore, the computational burden in Theorem 3.3 is less than its counterpart in Theorem 3.1. Also, the membership functions in sub-domains are less complicated than being considered as a whole, it is possible to use low-order polynomial functions to fulfill the approximation task, which avoids the numerical problems could occur in Theorem 3.2 when high-order polynomial functions are adopted.*

3.2 Simulation Examples

Example 1: Let us consider a three-rule polynomial fuzzy model in the form of (3.1) with $\hat{\mathbf{x}}(\mathbf{x}) = \mathbf{x} = [x_1 \quad x_2]^T$,

$$
\mathbf{A}_1(x_1) = \begin{bmatrix} 1.59 + 2.45x_1 & -7.29 - 0.89x_1 \\ 0.01 & -0.1 - 0.27x_1^2 \end{bmatrix},
$$

$$
\mathbf{A}_2(x_1) = \begin{bmatrix} 0.02 - 7.26x_1 - 0.05x_1^2 & -4.64x_1 \\ 0.35 - 0.28x_1 & -0.21 - 1.65x_1^2 \end{bmatrix},
$$

$$
\mathbf{A}_3(x_1) = \begin{bmatrix} -a + 0.37x_1 - 2.7x_1^2 & -4.33 - 2.73x_1^2 \\ 1.77x_1 & 0.05 - x_1^2 \end{bmatrix},
$$

$$\mathbf{B}_1(x_1) = \begin{bmatrix} 1 + 0.37x_1 + 1.28x_1^2 \\ 0 \end{bmatrix},$$

$$\mathbf{B}_2(x_1) = \begin{bmatrix} 8 + 0.23x_1^2 \\ 0 \end{bmatrix},$$

$$\mathbf{B}_3(x_1) = \begin{bmatrix} -b + 6 + 0.72x_1 + 1.55x_1^2 \\ -1 \end{bmatrix},$$

where a and b are constant system parameters. The membership functions are chosen as $\underline{w}_1(x_1) = 1 - 1/(1 + e^{(-x_1+3.5)})$, $\underline{w}_3(x_1) = 1 - 1/(1 + e^{(-x_1-3.5)})$, $\overline{w}_2(x_1) = 1 - \underline{w}_1(x_1) - \underline{w}_3(x_1)$, $\overline{w}_1(x_1) = 1 - 1/(1 + e^{(-x_1+2.5)})$, $\overline{w}_3(x_1) = 1 - 1/(1 + e^{(-x_1-2.5)})$, $\underline{w}_2(x_1) = 1 - \overline{w}_1(x_1) - \overline{w}_3(x_1)$, $\underline{m}_1(x_1) = \max(\min(1, (4.8 - x_1)/10), 0)$, $\overline{m}_1(x_1) = \max(\min(1, (5.2 - x_1)/10), 0)$, $\underline{m}_2(x_1) = 1 - \overline{m}_1(x_1)$ and $\overline{m}_2(x_1) = 1 - \underline{m}_1(x_1)$. The operation max means to pick the largest element and min means to pick the smallest element. The IT2 membership functions for the fuzzy model and fuzzy controller can be viewed in Fig. 3.2. Different style and color curves are plotted in the figure: the bold and normal black curves are for $\overline{w}_1(x_1)$ and $\underline{w}_1(x_1)$; the bold and normal green curves are for $\overline{w}_2(x_1)$ and $\underline{w}_2(x_1)$; the bold and normal red curves are for $\overline{w}_3(x_1)$ and $\underline{w}_3(x_1)$; the bold and normal cyan curves are for $\overline{m}_1(x_1)$ and $\underline{m}_1(x_1)$; the bold and normal magenta curves are for $\overline{m}_2(x_1)$ and $\underline{m}_2(x_1)$.

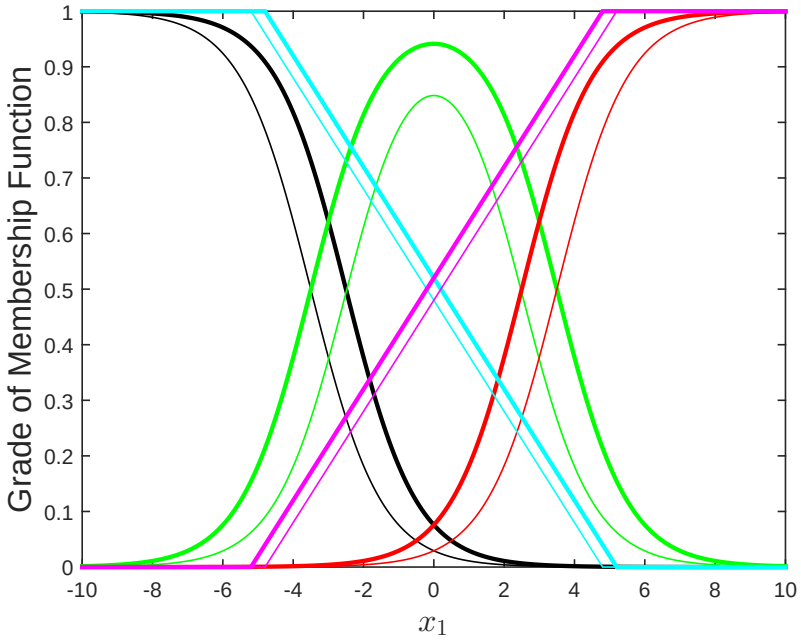

Figure 3.2: IT2 membership functions of the fuzzy model and fuzzy controller used in the simulation.

It should be noted that, in this example, the number of fuzzy rules and the membership functions employed for the polynomial fuzzy models and the polynomial fuzzy controllers are different, which can reduce the controller implementation cost when less number of membership functions is employed in the controller.

3.2.1 Simulations on Theorem 3.1

The stability conditions in Theorem 3.1 are employed to determine the stabilization region of the PFMB control system mentioned above with $60 \leq a \leq 100$ at the interval of 5 and $20 \leq b \leq 148$ at the interval of 4.

Referring to Theorem 3.1, we choose $\varepsilon_1(\mathbf{x}) = \varepsilon_2(\tilde{\mathbf{x}}) = \varepsilon_3(\mathbf{x}) = \varepsilon_4(\mathbf{x}) = \varepsilon_5(\mathbf{x}) = 0.001$; $\mathbf{X}(\tilde{\mathbf{x}})$ as a polynomial of degree 0; $\mathbf{N}_j(x_1)$, $j = 1, 2, \ldots, c$ as a polynomial with monomials in x_1 of degree 0 (for case 1) and degree 2 (for case 2); $\underline{\mathbf{x}}_l$ and $\overline{\mathbf{x}}_l$ are the boundaries of l-th sub-domain.

The stabilization regions are determined under 6, 8, 10 sub-domains for both cases of polynomial degrees for $\mathbf{N}_j(x_1)$ which are plotted in Figs. 3.3 to 3.5. It is observed that a larger stabilization region can be obtained by higher order polynomial matrices $\mathbf{N}_j(x_1)$ under the same number of sub-domains. When more sub-domains are employed, larger stabilization regions can be obtained. To verify the results, the phase plots of certain points in the stability regions are shown in Fig. 3.6. To obtain the phase plots, throughout this example, the membership functions $\tilde{w}_i(x_1)$ and $\tilde{m}_j(x_1)$ used in the simulations are gained from type reduction where $\underline{\lambda}_1(x_1) = (\sin(5x_1)+1)/2, \overline{\lambda}_1(x_1) = 1-\underline{\lambda}_1(x_1)$, $\underline{\lambda}_3(x_1) = (\cos(5x_1)+1)/2, \overline{\lambda}_3(x_1) = 1-\underline{\lambda}_3(x_1)$, $\underline{\kappa}_j(x_1) = \overline{\kappa}_j(x_1) = 0.5$, $j = 1, 2$. From the property of membership functions in (2.13) and (2.29), we have $\tilde{w}_2(x_1) = 1-\tilde{w}_1(x_1)-\tilde{w}_3(x_1)$. $\underline{h}_{ijl}$ and δ_{ijl} are defined by the membership functions and the number of sub-domains, and they are calculated sub-domain by sub-domain in the way explained in deduction of Theorem 3.1, their values can be viewed in Table 3.1 to 3.6. It can be found that all states started from different initial conditions approach $\mathbf{x} = \mathbf{0}$, which means the system is asymptotically stable. The solutions of the stability conditions in Theorem 3.1 are found numerically with SOSTOOLS.

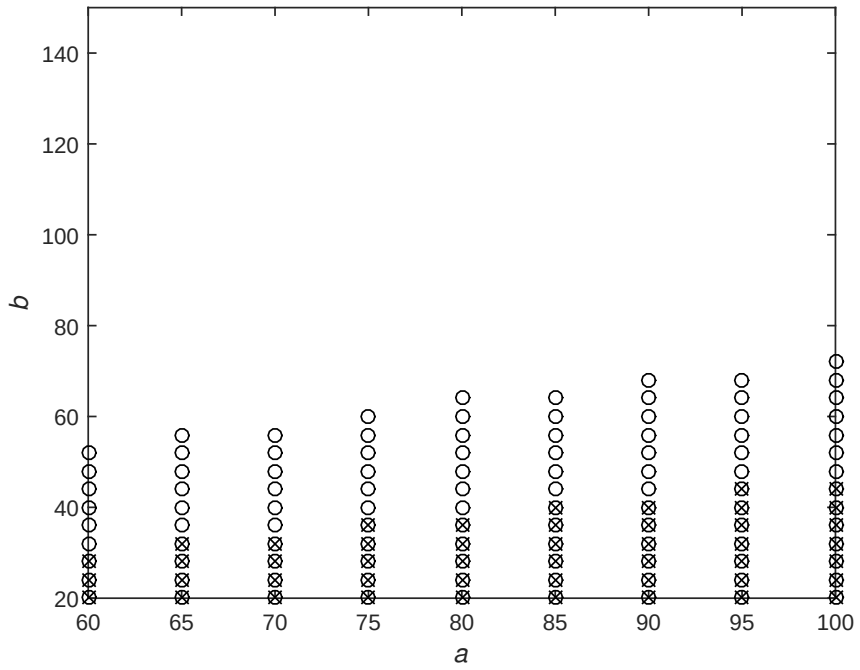

Figure 3.3: Stabilization regions given by Theorem 3.1 with $\mathbf{N}_j(\mathbf{x})$ of degree 0 and degree 2 indicated by "×" and "○", respectively. The number of sub-domains is 6.

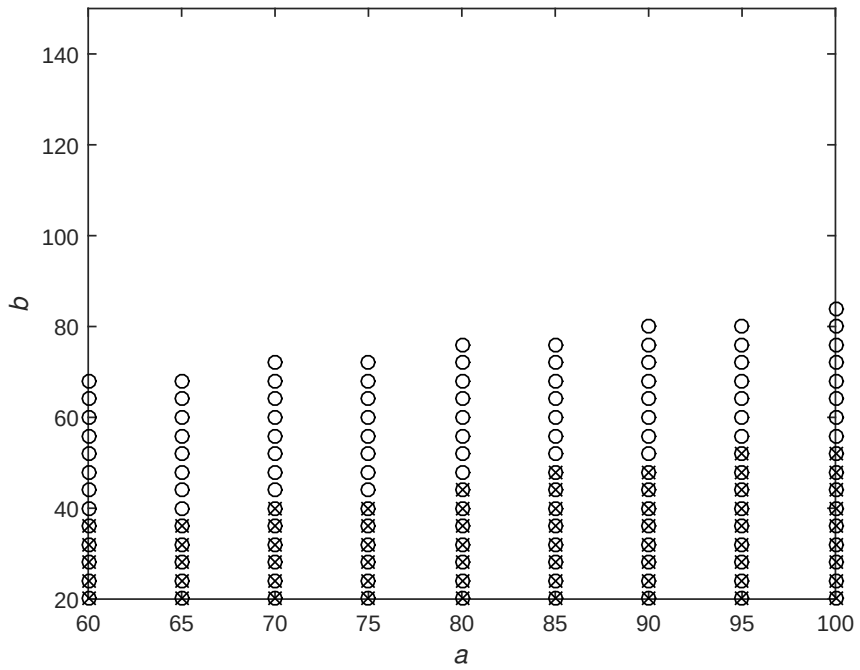

Figure 3.4: Stabilization regions given by Theorem 3.1 with $\mathbf{N}_j(\mathbf{x})$ of degree 0 and degree 2 indicated by "×" and "○", respectively. The number of sub-domains is 8.

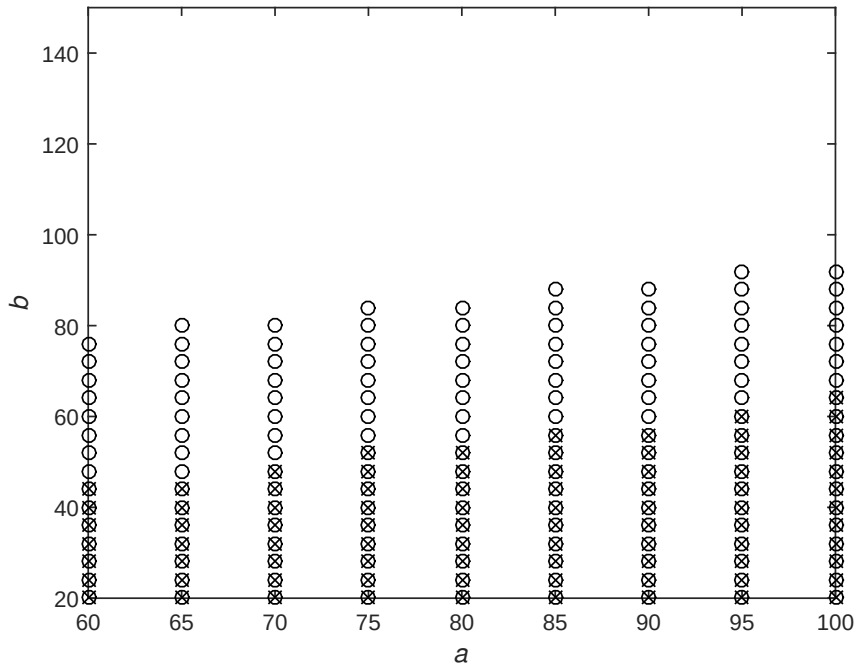

Figure 3.5: Stabilization regions given by Theorem 3.1 with $\mathbf{N}_j(\mathbf{x})$ of degree 0 and degree 2 indicated by "$\times$" and "$\circ$", respectively. The number of sub-domains is 10.

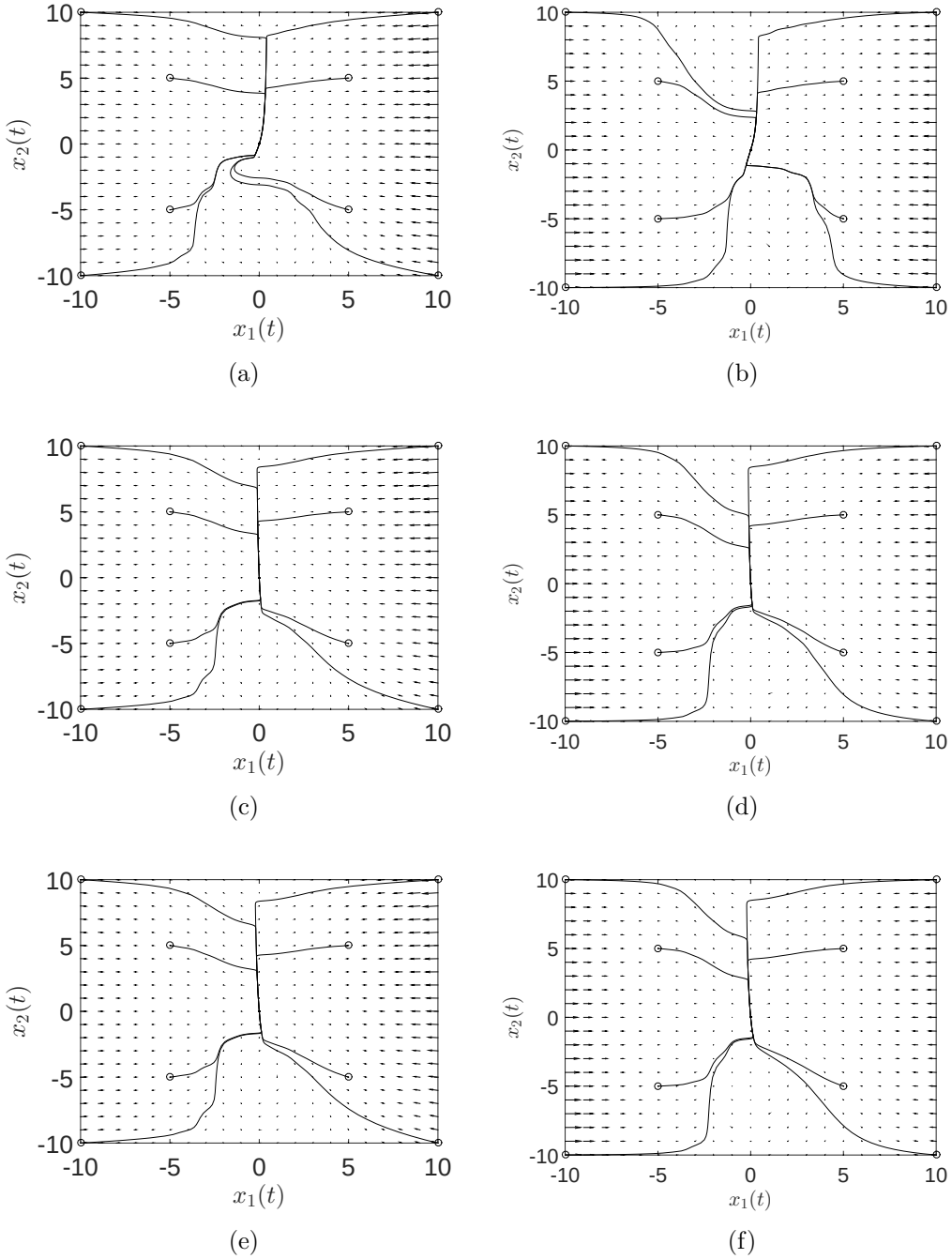

Figure 3.6: (a) and (b) are the phase plots of $x_1(t)$ and $x_2(t)$ for $a = 80$ and $b = 36$, $a = 80$ and $b = 44$ for Theorem 3.1 with $\mathbf{N}_j(\mathbf{x})$ of degree 0 and 2, respectively, and the number of sub-domains is 6; (c) and (d) are the phase plots of $x_1(t)$ and $x_2(t)$ for $a = 90$ and $b = 40$, $a = 90$ and $b = 60$ for Theorem 3.1 with $\mathbf{N}_j(\mathbf{x})$ of degree 0 and 2, respectively and the number of sub-domains is 8; (e) and (f) are the phase plots of $x_1(t)$ and $x_2(t)$ for $a = 80$ and $b = 40$, $a = 80$ and $b = 60$ for Theorem 3.1 with $\mathbf{N}_j(\mathbf{x})$ of degree 0 and 2, respectively and the number of sub-domains is 10. "$\circ$" indicates the initial condition of $\mathbf{x}$.

Table 3.1: The values of the approximation of the membership functions in 6 operating sub-domains.

$\underline{h}_{ijl}$	$l=1$	$l=2$	$l=3$
$\underline{h}_{1,1,l}$	9.5957×10^{-1}	1.3135×10^{-1}	1.4656×10^{-3}
$\underline{h}_{1,2,l}$	0	0	0
$\underline{h}_{2,1,l}$	2.8644×10^{-4}	4.1077×10^{-3}	1.1717×10^{-1}
$\underline{h}_{2,2,l}$	0	0	0
$\underline{h}_{3,1,l}$	7.1523×10^{-7}	1.0411×10^{-5}	3.0848×10^{-4}
$\underline{h}_{3,2,l}$	0	0	0
$\underline{h}_{ijl}$	$l=4$	$l=5$	$l=6$
$\underline{h}_{1,1,l}$	0	0	0
$\underline{h}_{1,2,l}$	3.0848×10^{-4}	1.0411×10^{-5}	7.1523×10^{-7}
$\underline{h}_{2,1,l}$	0	0	0
$\underline{h}_{2,2,l}$	1.1717×10^{-1}	4.1077×10^{-3}	2.8644×10^{-4}
$\underline{h}_{3,1,l}$	0	0	0
$\underline{h}_{3,2,l}$	1.4656×10^{-3}	1.3135×10^{-1}	9.5957×10^{-1}

Table 3.2: The values of $\delta_{i,j,l}$ in 6 operating sub-domains.

δ_{ijl}	$l=1$	$l=2$	$l=3$
$\delta_{1,1,l}$	4.0142×10^{-2}	8.6451×10^{-1}	8.8493×10^{-1}
$\delta_{1,2,l}$	1.3221×10^{-23}	1.4654×10^{-1}	1.4654×10^{-1}
$\delta_{2,1,l}$	4.0106×10^{-2}	5.5950×10^{-1}	4.5160×10^{-1}
$\delta_{2,2,l}$	1.3221×10^{-23}	9.0114×10^{-2}	5.6877×10^{-1}
$\delta_{3,1,l}$	1.0371×10^{-4}	2.4234×10^{-3}	6.7352×10^{-2}
$\delta_{3,2,l}$	1.3221×10^{-23}	4.8688×10^{-4}	3.7929×10^{-2}
δ_{ijl}	$l=4$	$l=5$	$l=6$
$\delta_{1,1,l}$	3.7929×10^{-2}	4.8688×10^{-4}	1.3221×10^{-23}
$\delta_{1,2,l}$	6.7352×10^{-2}	2.4234×10^{-3}	1.0371×10^{-4}
$\delta_{2,1,l}$	5.6877×10^{-1}	9.0114×10^{-2}	1.3221×10^{-23}
$\delta_{2,2,l}$	4.5160×10^{-1}	5.5950×10^{-1}	4.0106×10^{-2}
$\delta_{3,1,l}$	1.4654×10^{-1}	1.4654×10^{-1}	1.3221×10^{-23}
$\delta_{3,2,l}$	8.8493×10^{-1}	8.6451×10^{-1}	4.0142×10^{-2}

Table 3.3: The values of the approximation of the membership functions in 8 operating sub-domains.

$\underline{h}_{ijl}$	$l=1$	$l=2$	$l=3$	$l=4$
$\underline{h}_{1,1,l}$	9.8201×10^{-1}	8.0940×10^{-1}	9.4511×10^{-2}	5.0402×10^{-3}
$\underline{h}_{1,2,l}$	0	0	0	8.9780×10^{-3}
$\underline{h}_{2,1,l}$	3.1270×10^{-4}	3.1147×10^{-3}	3.8894×10^{-2}	3.4608×10^{-1}
$\underline{h}_{2,2,l}$	0	0	0	1.2333×10^{-2}
$\underline{h}_{3,1,l}$	7.8081×10^{-7}	7.8256×10^{-6}	9.4364×10^{-5}	1.0562×10^{-3}
$\underline{h}_{3,2,l}$	0	0	0	6.1816×10^{-5}
$\underline{h}_{ijl}$	$l=5$	$l=6$	$l=7$	$l=8$
$\underline{h}_{1,1,l}$	6.1816×10^{-5}	0	0	0
$\underline{h}_{1,2,l}$	1.0562×10^{-3}	9.4364×10^{-5}	7.8256×10^{-6}	7.8081×10^{-7}
$\underline{h}_{2,1,l}$	1.2333×10^{-2}	0	0	0
$\underline{h}_{2,2,l}$	3.4608×10^{-1}	3.8894×10^{-2}	3.1147×10^{-3}	3.1270×10^{-4}
$\underline{h}_{3,1,l}$	8.9780×10^{-3}	0	0	0
$\underline{h}_{3,2,l}$	5.0402×10^{-3}	9.4511×10^{-2}	8.0940×10^{-1}	9.8201×10^{-1}

Table 3.4: The values of $\delta_{i,j,l}$ in 8 operating sub-domains.

δ_{ijl}	$l=1$	$l=2$	$l=3$	$l=4$
$\delta_{1,1,l}$	1.7536×10^{-2}	1.8747×10^{-1}	8.6561×10^{-1}	3.9142×10^{-1}
$\delta_{1,2,l}$	1.3221×10^{-23}	4.3261×10^{-2}	1.5504×10^{-1}	1.4607×10^{-1}
$\delta_{2,1,l}$	1.7657×10^{-2}	1.7729×10^{-1}	5.5717×10^{-1}	2.4999×10^{-1}
$\delta_{2,2,l}$	1.3221×10^{-23}	1.8222×10^{-3}	1.8215×10^{-1}	5.1627×10^{-1}
$\delta_{3,1,l}$	4.4617×10^{-5}	5.3943×10^{-4}	4.9253×10^{-3}	3.6873×10^{-2}
$\delta_{3,2,l}$	1.3221×10^{-23}	5.5278×10^{-6}	1.6732×10^{-3}	3.7867×10^{-2}
δ_{ijl}	$l=5$	$l=6$	$l=7$	$l=8$
$\delta_{1,1,l}$	3.7867×10^{-2}	1.6732×10^{-3}	5.5278×10^{-6}	1.3221×10^{-23}
$\delta_{1,2,l}$	3.6873×10^{-2}	4.9253×10^{-3}	5.3943×10^{-4}	4.4617×10^{-5}
$\delta_{2,1,l}$	5.1627×10^{-1}	1.8215×10^{-1}	1.8222×10^{-3}	1.3221×10^{-23}
$\delta_{2,2,l}$	2.4999×10^{-1}	5.5717×10^{-1}	1.7729×10^{-1}	1.7657×10^{-2}
$\delta_{3,1,l}$	1.4607×10^{-1}	1.5504×10^{-1}	4.3261×10^{-2}	1.3221×10^{-23}
$\delta_{3,2,l}$	3.9142×10^{-1}	8.6561×10^{-1}	1.8747×10^{-1}	1.7536×10^{-2}

Table 3.5: The values of the approximation of the membership functions in 10 operating sub-domains.

$\underline{h}_{ijl}$	$l=1$	$l=2$	$l=3$	$l=4$
$\underline{h}_{1,1,l}$	9.8901×10^{-1}	9.2414×10^{-1}	5.2402×10^{-1}	7.8225×10^{-2}
$\underline{h}_{1,2,l}$	0	0	0	0
$\underline{h}_{2,1,l}$	3.5761×10^{-4}	2.4764×10^{-3}	1.7831×10^{-2}	1.2931×10^{-1}
$\underline{h}_{2,2,l}$	0	0	0	0
$\underline{h}_{3,1,l}$	8.9293×10^{-7}	6.2054×10^{-6}	4.5849×10^{-5}	3.4138×10^{-4}
$\underline{h}_{3,2,l}$	0	0	0	0
$\underline{h}_{ijl}$	$l=5$	$l=6$	$l=7$	$l=8$
$\underline{h}_{1,1,l}$	7.6461×10^{-3}	5.0003×10^{-4}	0	0
$\underline{h}_{1,2,l}$	1.0931×10^{-2}	1.9550×10^{-3}	3.4138×10^{-4}	4.5849×10^{-5}
$\underline{h}_{2,1,l}$	4.2414×10^{-1}	1.4567×10^{-1}	0	0
$\underline{h}_{2,2,l}$	1.4567×10^{-1}	4.2414×10^{-1}	1.2931×10^{-1}	1.7831×10^{-2}
$\underline{h}_{3,1,l}$	1.9550×10^{-3}	1.0931×10^{-2}	0	0
$\underline{h}_{3,2,l}$	5.0003×10^{-4}	7.6461×10^{-3}	7.8225×10^{-2}	5.2402×10^{-1}
$\underline{h}_{ijl}$	$l=9$	$l=10$		
$\underline{h}_{1,1,l}$	0	0		
$\underline{h}_{1,2,l}$	6.2054×10^{-6}	8.9293×10^{-7}		
$\underline{h}_{2,1,l}$	0	0		
$\underline{h}_{2,2,l}$	2.4764×10^{-3}	3.5761×10^{-4}		
$\underline{h}_{3,1,l}$	0	0		
$\underline{h}_{3,2,l}$	9.2414×10^{-1}	9.8901×10^{-1}		

Table 3.6: The values of $\delta_{i,j,l}$ in 10 operating sub-domains.

δ_{ijl}	$l=1$	$l=2$	$l=3$	$l=4$
$\delta_{1,1,l}$	1.0627×10^{-2}	7.3365×10^{-2}	4.5803×10^{-1}	7.9799×10^{-1}
$\delta_{1,2,l}$	1.3221×10^{-23}	1.3221×10^{-23}	1.1013×10^{-1}	1.4067×10^{-1}
$\delta_{2,1,l}$	1.0619×10^{-2}	7.3307×10^{-2}	3.7416×10^{-1}	4.7449×10^{-1}
$\delta_{2,2,l}$	1.3221×10^{-23}	1.3221×10^{-23}	3.7699×10^{-2}	2.4409×10^{-1}
$\delta_{3,1,l}$	2.6643×10^{-5}	1.9722×10^{-4}	1.3052×10^{-3}	7.3495×10^{-3}
$\delta_{3,2,l}$	1.3221×10^{-23}	1.3221×10^{-23}	1.5012×10^{-4}	3.2961×10^{-3}
δ_{ijl}	$l=5$	$l=6$	$l=7$	$l=8$
$\delta_{1,1,l}$	2.5663×10^{-1}	3.7429×10^{-2}	3.2961×10^{-3}	1.5012×10^{-4}
$\delta_{1,2,l}$	1.2973×10^{-1}	3.5974×10^{-2}	7.3495×10^{-3}	1.3052×10^{-3}
$\delta_{2,1,l}$	1.7965×10^{-1}	3.4319×10^{-1}	2.4409×10^{-1}	3.7699×10^{-2}
$\delta_{2,2,l}$	3.4319×10^{-1}	1.7965×10^{-1}	4.7449×10^{-1}	3.7416×10^{-1}
$\delta_{3,1,l}$	3.5974×10^{-2}	1.2973×10^{-1}	1.4067×10^{-1}	1.1013×10^{-1}
$\delta_{3,2,l}$	3.7429×10^{-2}	2.5663×10^{-1}	7.9799×10^{-1}	4.5803×10^{-1}
δ_{ijl}	$l=9$	$l=10$		
$\delta_{1,1,l}$	1.3221×10^{-23}	1.3221×10^{-23}		
$\delta_{1,2,l}$	1.9722×10^{-4}	2.6643×10^{-5}		
$\delta_{2,1,l}$	1.3221×10^{-23}	1.3221×10^{-23}		
$\delta_{2,2,l}$	7.3307×10^{-2}	1.0619×10^{-2}		
$\delta_{3,1,l}$	1.3221×10^{-23}	1.3221×10^{-23}		
$\delta_{3,2,l}$	7.3365×10^{-2}	1.0627×10^{-2}		

3.2.2 Simulations on Theorem 3.2

Along the same way in the above simulations, the stability conditions in Theorem 3.2 are employed to determine the stabilization region of the same PFMB control system. The simulations have been conducted under both 6th and 8th order polynomial approximation functions while other settings remain the same.

Referring to Theorem 3.2, we choose $\varepsilon_1(\tilde{\mathbf{x}}) = \varepsilon_2(\mathbf{x}) = \varepsilon_3(\mathbf{x}) = \varepsilon_4(\mathbf{x}) = 0.001$; $\mathbf{X}(\tilde{\mathbf{x}})$ as a polynomial of degree 0; $\mathbf{N}_j(x_1)$, $j = 1, 2, \ldots, c$ as a polynomial with monomials in x_1 of degree 0 (for case 1) and degree 2 (for case 2); $\underline{h}_{ij}(\mathbf{x})$ and δ_{ij} are defined by the membership functions and the order of the chosen polynomial functions, and they are calculated in the way explained in the deduction of Theorem 3.2. The values of the coefficients of the 6th and 8th order polynomial functions can be viewed in Table 3.7 and 3.8; the values $\delta_{11} = 0.1991$, $\delta_{12} = 0.0592$, $\delta_{21} = 0.2008$, $\delta_{22} = 0.2008$, $\delta_{31} = 0.0592$, $\delta_{32} = 0.1991$ for 6th order polynomial function; the values $\delta_{11} = 0.1991$, $\delta_{12} = 0.0592$, $\delta_{21} = 0.2008$, $\delta_{22} = 0.2008$, $\delta_{31} = 0.0592$, $\delta_{32} = 0.1991$ for 8th order polynomial function.

The stabilization region are shown in Figs. 3.7 and 3.8 for both cases of poly-

nomial degrees for $\mathbf{N}_j(x_1)$. It can be seen that a larger stabilization region can be obtained using higher order polynomial matrices $\mathbf{N}_j(x_1)$. Furthermore, using higher order polynomial functions in the approximation is able to obtain a larger stabilization region. The phase plots under initial conditions are shown in Fig. 3.9. It can be seen that all state started with different initial positions approach $\mathbf{x} = \mathbf{0}$, which shows the asymptotic stability of the system.

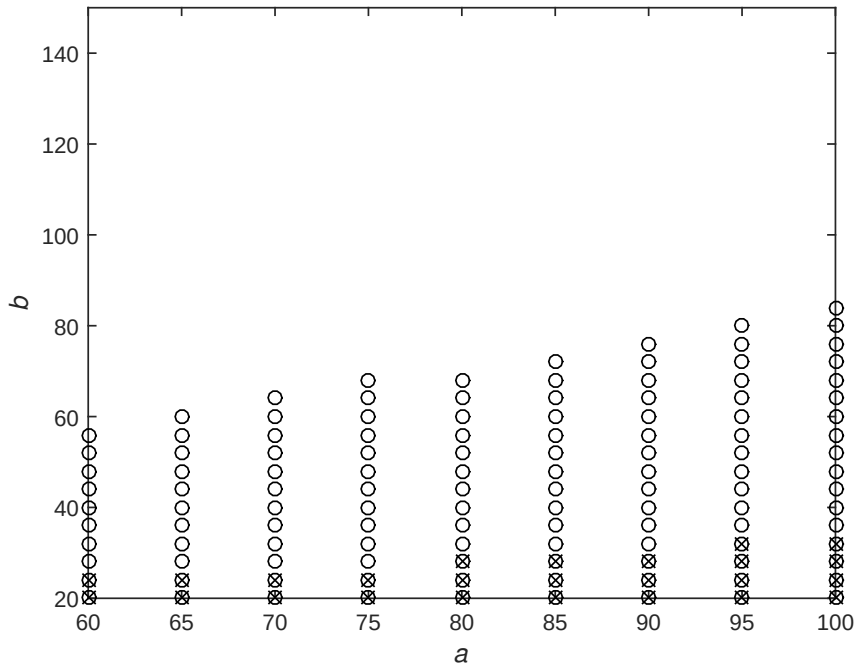

Figure 3.7: Stabilization regions given by Theorem 3.2 with $\mathbf{N}_j(\mathbf{x})$ of degree 0 and degree 2 indicated by "×" and "○", respectively. The order of polynomial functions is 6.

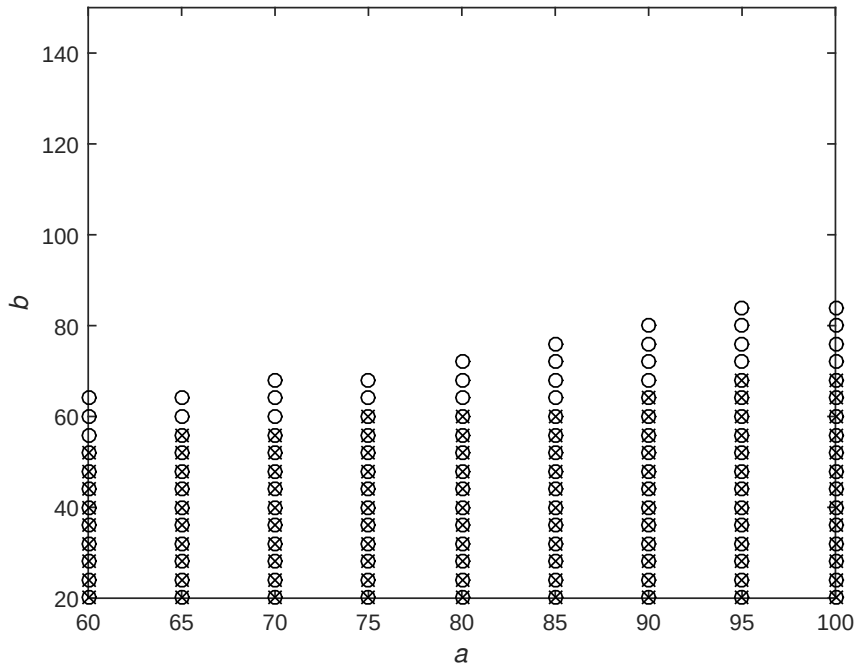

Figure 3.8: Stabilization regions given by Theorem 3.2 with $\mathbf{N}_j(\mathbf{x})$ of degree 0 and degree 2 indicated by "$\times$" and "$\circ$", respectively. The order of polynomial functions is 8.

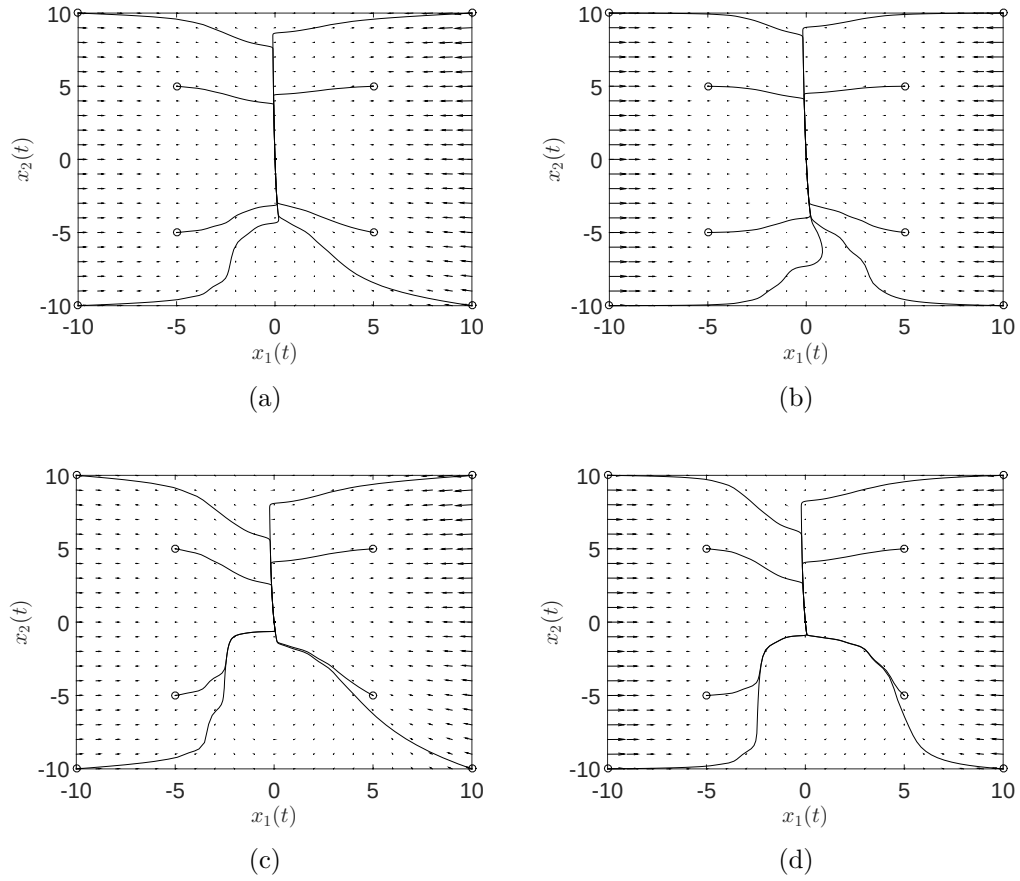

Figure 3.9: (a) and (b) are the phase plots of $x_1(t)$ and $x_2(t)$ for $a = 100$ and $b = 32$ for Theorem 3.2 with $\mathbf{N}_j(\mathbf{x})$ of degree 0 and 2, respectively, and the order of the polynomial functions is 6. (c) and (d) are the phase plots of $x_1(t)$ and $x_2(t)$ for $a = 80$ and $b = 60$ for Theorem 3.2 with $\mathbf{N}_j(\mathbf{x})$ of degree 0 and 2, respectively, and the order of the polynomial functions is 8. "$\circ$" indicates the initial condition of $\mathbf{x}$.

Table 3.7: The coefficients for the 6th order polynomial function.

$\underline{h}_{ij}(x_1)$	x_1^6	x_1^5	x_1^4	x_1^3
$\underline{h}_{1,1}$	2.0754×10^{-6}	4.4880×10^{-6}	-4.0477×10^{-4}	-1.3396×10^{-4}
$\underline{h}_{1,2}$	8.5422×10^{-8}	-3.6486×10^{-6}	-2.8445×10^{-6}	4.9279×10^{-4}
$\underline{h}_{2,1}$	-2.1608×10^{-6}	-1.1928×10^{-5}	4.0762×10^{-4}	1.6617×10^{-3}
$\underline{h}_{2,2}$	-2.1608×10^{-6}	1.1928×10^{-5}	4.0762×10^{-4}	-1.6617×10^{-3}
$\underline{h}_{3,1}$	8.5422×10^{-8}	3.6486×10^{-6}	-2.8445×10^{-6}	-4.9279×10^{-4}
$\underline{h}_{3,2}$	2.0754×10^{-6}	-4.4880×10^{-6}	-4.0477×10^{-4}	1.3396×10^{-4}
$\underline{h}_{ij}(x_1)$	x_1^2	x_1^1	x_1^0	
$\underline{h}_{1,1}$	2.4946×10^{-2}	-7.5773×10^{-2}	1.3908×10^{-2}	
$\underline{h}_{1,2}$	-8.7412×10^{-4}	-1.5152×10^{-2}	4.0279×10^{-2}	
$\underline{h}_{2,1}$	-2.4072×10^{-2}	-5.3949×10^{-2}	4.4581×10^{-1}	
$\underline{h}_{2,2}$	-2.4072×10^{-2}	5.3949×10^{-2}	4.4581×10^{-1}	
$\underline{h}_{3,1}$	-8.7412×10^{-4}	1.5152×10^{-2}	4.0279×10^{-2}	
$\underline{h}_{3,2}$	2.4946×10^{-2}	7.5773×10^{-2}	1.3908×10^{-2}	

Table 3.8: The coefficients for the 8th order polynomial function.

$\underline{h}_{ij}(x_1)$	x_1^8	x_1^7	x_1^6	x_1^5
$\underline{h}_{1,1}$	-1.4915×10^{-8}	-2.9821×10^{-7}	4.8598×10^{-6}	5.2665×10^{-5}
$\underline{h}_{1,2}$	-1.3323×10^{-8}	1.0198×10^{-7}	2.5727×10^{-6}	-2.0124×10^{-5}
$\underline{h}_{2,1}$	2.8238×10^{-8}	2.9710×10^{-7}	-7.4324×10^{-6}	-5.9925×10^{-5}
$\underline{h}_{2,2}$	2.8238×10^{-8}	-2.9710×10^{-7}	-7.4324×10^{-6}	5.9925×10^{-5}
$\underline{h}_{3,1}$	-1.3323×10^{-8}	-1.0198×10^{-7}	2.5727×10^{-6}	2.0124×10^{-5}
$\underline{h}_{3,2}$	-1.4915×10^{-8}	2.9821×10^{-7}	4.8598×10^{-6}	-5.2665×10^{-5}
$\underline{h}_{ij}(x_1)$	x_1^4	x_1^3	x_1^2	x_1^1
$\underline{h}_{1,1}$	-5.6543×10^{-4}	-2.3240×10^{-3}	2.7867×10^{-2}	-5.1436×10^{-2}
$\underline{h}_{1,2}$	-1.4635×10^{-4}	1.2417×10^{-3}	1.7354×10^{-3}	-2.3475×10^{-2}
$\underline{h}_{2,1}$	7.1178×10^{-4}	3.8437×10^{-3}	-2.9603×10^{-2}	-7.8195×10^{-2}
$\underline{h}_{2,2}$	7.1178×10^{-4}	-3.8437×10^{-3}	-2.9603×10^{-2}	7.8195×10^{-2}
$\underline{h}_{3,1}$	-1.4635×10^{-4}	-1.2417×10^{-3}	1.7354×10^{-3}	2.3475×10^{-2}
$\underline{h}_{3,2}$	-5.6543×10^{-4}	2.3240×10^{-3}	2.7867×10^{-2}	5.1436×10^{-2}
$\underline{h}_{ij}(x_1)$	x_1^0			
$\underline{h}_{1,1}$	5.7923×10^{-3}			
$\underline{h}_{1,2}$	3.3029×10^{-2}			
$\underline{h}_{2,1}$	4.6118×10^{-1}			
$\underline{h}_{2,2}$	4.6118×10^{-1}			
$\underline{h}_{3,1}$	3.3029×10^{-2}			
$\underline{h}_{3,2}$	5.7923×10^{-3}			

3.2.3 Simulations on Theorem 3.3

The stability conditions in Theorem 3.3 are employed to determine the stabilization region of the same PFMB control system. Referring to Theorem 3.3, we choose $\varepsilon_1(\mathbf{x}) = \varepsilon_2(\tilde{\mathbf{x}}) = \varepsilon_3(\mathbf{x}) = \varepsilon_4(\mathbf{x}) = \varepsilon_5(\mathbf{x}) = 0.001$; $\mathbf{X}(\tilde{\mathbf{x}})$ as a polynomial of degree 0; $\mathbf{N}_j(x_1)$, $j = 1, 2, \ldots, c$ as a polynomial with monomials in x_1 of degree 0 (for case 1) and degree 2 (for case 2); $\underline{h}_{ijl}(\mathbf{x})$ and δ_{ijl} are defined by the membership functions and the order of the chosen polynomial functions as well as the number of sub-domains and they are calculated in the way explained in the deduction of Theorem 3.3; $\underline{\mathbf{x}}_l$ and $\overline{\mathbf{x}}_l$ are the boundaries of l-th sub-domain.

With the same settings as above, the simulations have been done under 4, 8, 12 sub-domains using 2-nd or 4-th order polynomial approximation functions for both cases of polynomial degrees for $\mathbf{N}_j(x_1)$. The stabilization regions are shown in Figs. 3.10 to 3.12. It can be seen that a larger stabilization region can be produced with higher order polynomial matrices $\mathbf{N}_j(x_1)$. The phase plots of system states with different initial conditions are shown in Fig. 3.13. It can be seen that all states start from different initial conditions approach $\mathbf{x} = \mathbf{0}$. Comparing with Theorems

3.1 and 3.2, the stability conditions in Theorem 3.3 are the most relaxed one which is evident by the largest stability region offered.

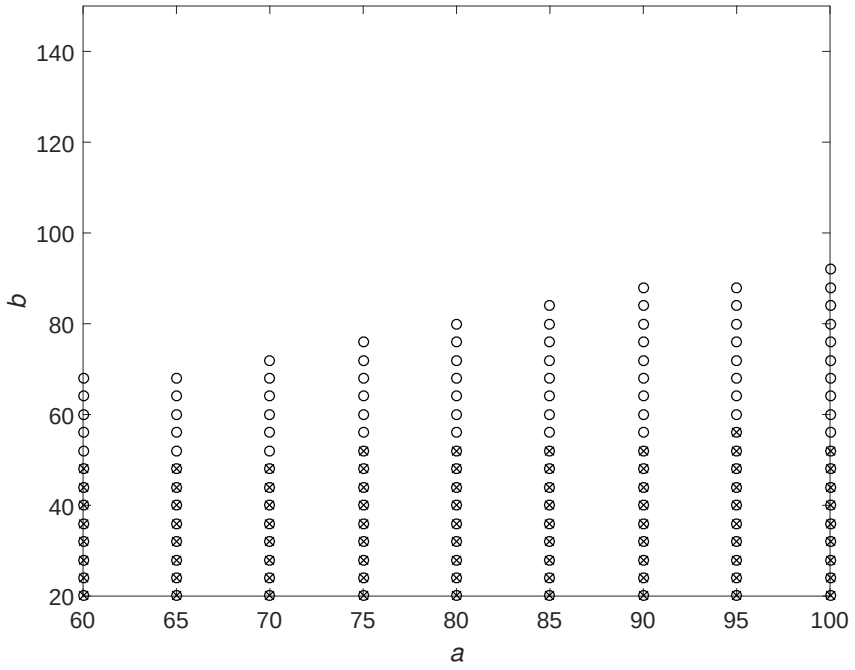

Figure 3.10: Stabilization regions given by Theorem 3.3 with $\mathbf{N}_j(\mathbf{x})$ of degree 0 and degree 2 indicated by "×" and "○", respectively. The number of sub-domains and order of polynomial functions are 4 and 4, respectively.

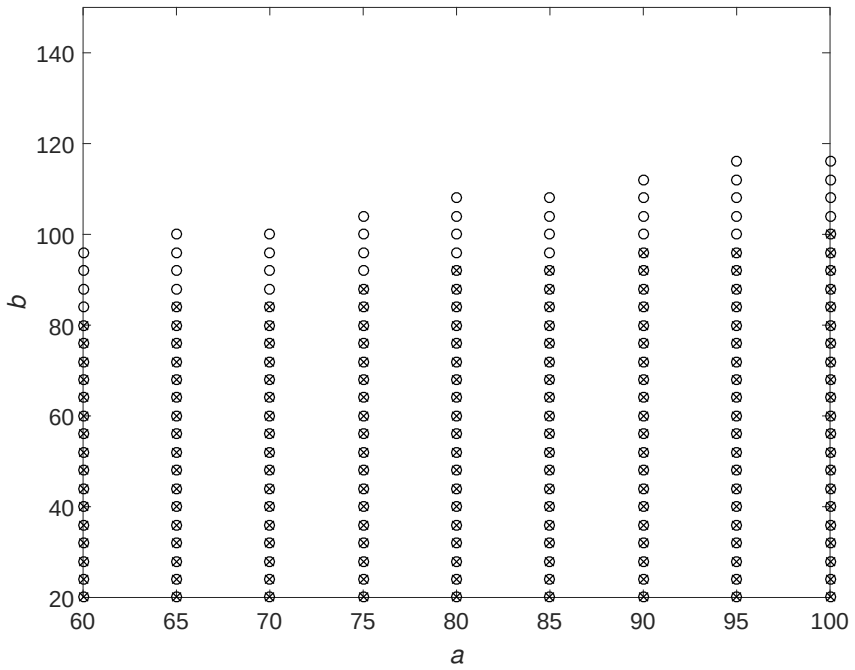

Figure 3.11: Stabilization regions given by Theorem 3.3 with $\mathbf{N}_j(\mathbf{x})$ of degree 0 and degree 2 indicated by "×" and "○", respectively. The number of sub-domains and order of polynomial functions are 8 and 2, respectively.

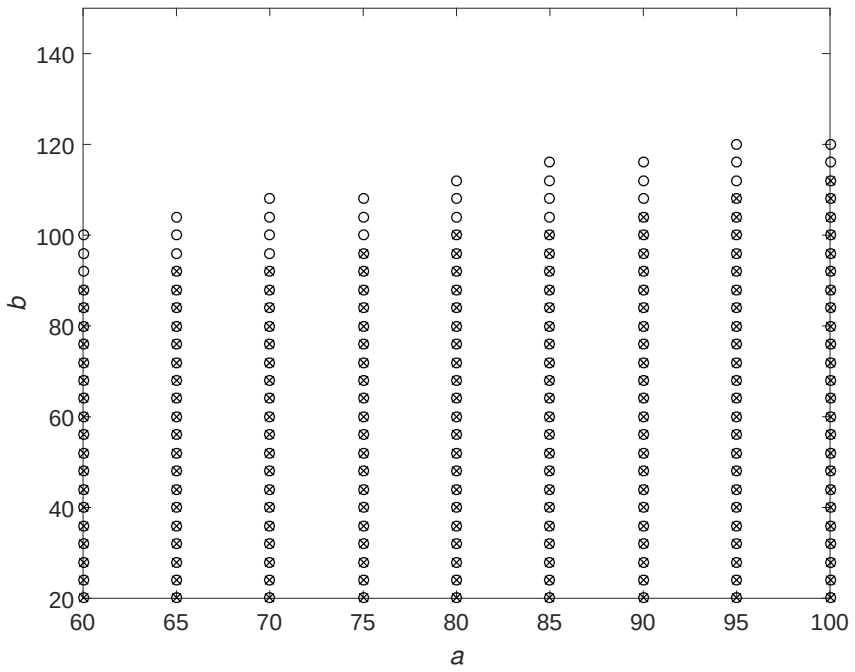

Figure 3.12: Stabilization regions given by Theorem 3.3 with $\mathbf{N}_j(\mathbf{x})$ of degree 0 and degree 2 indicated by "$\times$" and "$\circ$", respectively. The number of sub-domains and order of polynomial functions are 12 and 2, respectively.

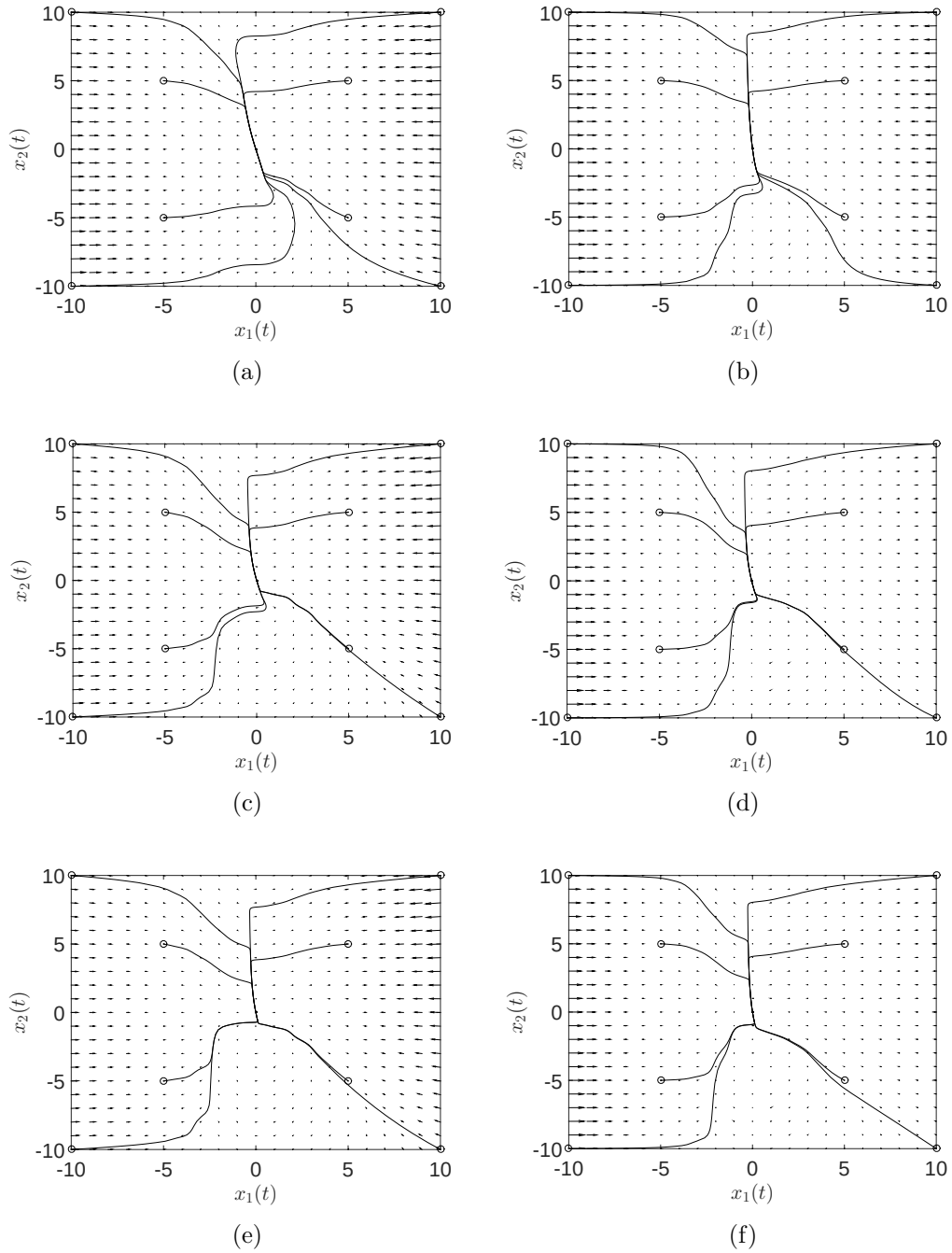

Figure 3.13: (a) and (b) are the phase plots of $x_1(t)$ and $x_2(t)$ for $a = 80$ and $b = 48$ for Theorem 3.3 with $\mathbf{N}_j(\mathbf{x})$ of degree 0 and 2, respectively and the number of sub-domains is 4 and the order of polynomial functions is 4; (c) and (d) are the phase plots of $x_1(t)$ and $x_2(t)$ for $a = 70$ and $b = 80$ for Theorem 3.3 with $\mathbf{N}_j(\mathbf{x})$ of degree 0 and 2 receptively and the number of sub-domains is 8 and the order of polynomial functions is 2; (e) and (f) are the phase plots of $x_1(t)$ and $x_2(t)$ for $a = 100$ and $b = 100$ for Theorem 3.3 with $\mathbf{N}_j(\mathbf{x})$ of degree 0 and 2, respectively and the number of sub-domains is 12 and the order of polynomial functions is 2. "$\circ$" indicates the initial condition of $\mathbf{x}$.

Table 3.9: The approximation of the membership functions for the 4 sub-domains and 4th order polynomial approximation function.

$\underline{h}_{1,1,l}$	$l=1$	$l=2$	$l=3$	$l=4$
x_1^4	-5.5157×10^{-4}	-2.4135×10^{-3}	1.4216×10^{-4}	5.0151×10^{-8}
x_1^3	-1.8813×10^{-2}	-1.7446×10^{-2}	-1.9714×10^{-3}	-1.5670×10^{-6}
x_1^2	-2.4186×10^{-1}	8.4027×10^{-4}	1.0286×10^{-2}	1.8135×10^{-5}
x_1^1	-1.3939	-3.0593×10^{-2}	-2.4512×10^{-2}	-9.2061×10^{-5}
x_1^0	-2.1206	-7.8198×10^{-2}	1.4656×10^{-2}	1.7202×10^{-4}

Table 3.10: The approximation of the membership functions for the 4 sub-domains and 4th order polynomial approximation function.

$\underline{h}_{1,2,l}$	$l=1$	$l=2$	$l=3$	$l=4$
x_1^4	1.3956×10^{-4}	6.1315×10^{-4}	5.2929×10^{-5}	1.4654×10^{-6}
x_1^3	4.3615×10^{-3}	9.7257×10^{-3}	-8.6045×10^{-4}	-5.0332×10^{-5}
x_1^2	5.0487×10^{-2}	3.3282×10^{-2}	5.5743×10^{-3}	6.5106×10^{-4}
x_1^1	2.5636×10^{-1}	5.3428×10^{-3}	-1.7632×10^{-2}	-3.7704×10^{-3}
x_1^0	4.7913×10^{-1}	-1.6988×10^{-4}	1.4656×10^{-2}	8.1524×10^{-3}

Table 3.11: The approximation of the membership functions for the 4 sub-domains and 4th order polynomial approximation function.

$\underline{h}_{2,1,l}$	$l=1$	$l=2$	$l=3$	$l=4$
x_1^4	3.9261×10^{-4}	2.2031×10^{-3}	-5.9782×10^{-4}	1.7881×10^{-5}
x_1^3	1.3841×10^{-2}	1.5208×10^{-2}	1.0319×10^{-2}	-5.5870×10^{-4}
x_1^2	1.8424×10^{-1}	-1.0226×10^{-2}	-3.9756×10^{-2}	6.4659×10^{-3}
x_1^1	1.1009	-9.0602×10^{-2}	-7.3708×10^{-2}	-3.2825×10^{-2}
x_1^0	2.4577	3.5101×10^{-1}	4.1689×10^{-1}	6.1335×10^{-2}

Table 3.12: The approximation of the membership functions for the 4 sub-domains and 4th order polynomial approximation function.

$\underline{h}_{2,2,l}$	$l=1$	$l=2$	$l=3$	$l=4$
x_1^4	1.7881×10^{-5}	-5.9782×10^{-4}	2.2031×10^{-3}	3.9261×10^{-4}
x_1^3	5.5870×10^{-4}	-1.0319×10^{-2}	-1.5208×10^{-2}	-1.3841×10^{-2}
x_1^2	6.4659×10^{-3}	-3.9756×10^{-2}	-1.0226×10^{-2}	1.8424×10^{-1}
x_1^1	3.2825×10^{-2}	7.3708×10^{-2}	9.0602×10^{-2}	-1.1009
x_1^0	6.1335×10^{-2}	4.1689×10^{-1}	3.5101×10^{-1}	2.4577

Table 3.13: The approximation of the membership functions for the 4 sub-domains and 4th order polynomial approximation function.

$\underline{h}_{3,1,l}$	$l=1$	$l=2$	$l=3$	$l=4$
x_1^4	1.4654×10^{-6}	5.2929×10^{-5}	6.1315×10^{-4}	1.3956×10^{-4}
x_1^3	5.0332×10^{-5}	8.6045×10^{-4}	-9.7257×10^{-3}	-4.3615×10^{-3}
x_1^2	6.5106×10^{-4}	5.5743×10^{-3}	3.3282×10^{-2}	5.0487×10^{-2}
x_1^1	3.7704×10^{-3}	1.7632×10^{-2}	-5.3428×10^{-3}	-2.5636×10^{-1}
x_1^0	8.1524×10^{-3}	1.4656×10^{-2}	-1.6988×10^{-4}	4.7913×10^{-1}

Table 3.14: The approximation of the membership functions for the 4 sub-domains and 4th order polynomial approximation function.

$\underline{h}_{3,2,l}$	$l=1$	$l=2$	$l=3$	$l=4$
x_1^4	5.0151×10^{-8}	1.4216×10^{-4}	-2.4135×10^{-3}	-5.5157×10^{-4}
x_1^3	1.5670×10^{-6}	1.9714×10^{-3}	1.7446×10^{-2}	1.8813×10^{-2}
x_1^2	1.8135×10^{-5}	1.0286×10^{-2}	8.4027×10^{-4}	-2.4186×10^{-1}
x_1^1	9.2061×10^{-5}	2.4512×10^{-2}	3.0593×10^{-2}	1.3939
x_1^0	1.7202×10^{-4}	1.4656×10^{-2}	-7.8198×10^{-2}	-2.1206

Table 3.15: The δ_{ijl} for the 4 sub-domains and 4th order polynomial approximation function.

δ_{ijl}	$l=1$	$l=2$	$l=3$	$l=4$
$\delta_{1,1,l}$	1.0550×10^{-1}	1.9912×10^{-1}	2.3273×10^{-2}	3.4935×10^{-6}
$\delta_{1,2,l}$	1.0657×10^{-3}	5.9190×10^{-2}	2.3273×10^{-2}	3.4586×10^{-4}
$\delta_{2,1,l}$	1.0585×10^{-1}	2.0077×10^{-1}	6.0846×10^{-2}	1.0692×10^{-3}
$\delta_{2,2,l}$	1.0692×10^{-3}	6.0846×10^{-2}	2.0077×10^{-1}	1.0585×10^{-1}
$\delta_{3,1,l}$	3.4586×10^{-4}	2.3273×10^{-2}	5.9190×10^{-2}	1.0657×10^{-3}
$\delta_{3,2,l}$	3.4935×10^{-6}	2.3273×10^{-2}	1.9912×10^{-1}	1.0550×10^{-1}

Table 3.16: The approximation of the membership functions for the 8 sub-domains and second order polynomial approximation function.

$\underline{h}_{1,1,l}$	$l=1$	$l=2$	$l=3$	$l=4$
x_1^2	-1.7477×10^{-3}	-1.9118×10^{-2}	-9.8406×10^{-3}	3.9205×10^{-2}
x_1^1	-3.4261×10^{-2}	-2.8019×10^{-1}	-3.1944×10^{-1}	-2.0508×10^{-3}
x_1^0	8.2336×10^{-1}	-1.1362×10^{-1}	-5.7345×10^{-1}	-4.8453×10^{-2}
$\underline{h}_{1,1,l}$	$l=5$	$l=6$	$l=7$	$l=8$
x_1^2	4.4508×10^{-3}	2.2648×10^{-4}	5.3265×10^{-7}	0
x_1^1	-1.9198×10^{-2}	-2.0457×10^{-3}	-6.9567×10^{-6}	0
x_1^0	1.4656×10^{-2}	4.3169×10^{-3}	2.1772×10^{-5}	0

Table 3.17: Theapproximation of the membership functions for the 8 sub-domains and second order polynomial approximation function.

$\underline{h}_{1,2,l}$	$l=1$	$l=2$	$l=3$	$l=4$
x_1^2	0	1.4895×10^{-3}	-2.2976×10^{-2}	2.4816×10^{-3}
x_1^1	0	1.9457×10^{-2}	-1.3439×10^{-1}	-2.3774×10^{-2}
x_1^0	0	6.0902×10^{-2}	-1.2513×10^{-1}	-7.7108×10^{-3}
$\underline{h}_{1,2,l}$	$l=5$	$l=6$	$l=7$	$l=8$
x_1^2	2.9255×10^{-3}	4.2358×10^{-4}	5.3143×10^{-5}	4.4081×10^{-6}
x_1^1	-1.5183×10^{-2}	-4.1908×10^{-3}	-7.7608×10^{-4}	-8.6345×10^{-5}
x_1^0	1.4656×10^{-2}	9.6841×10^{-3}	2.7532×10^{-3}	4.1634×10^{-4}

Table 3.18: The approximation of the membership functions for the 8 sub-domains and second order polynomial approximation function.

$\underline{h}_{2,1,l}$	$l=1$	$l=2$	$l=3$	$l=4$
x_1^2	1.7433×10^{-3}	1.7384×10^{-2}	7.7370×10^{-3}	-4.2131×10^{-2}
x_1^1	3.4175×10^{-2}	2.5747×10^{-1}	2.0360×10^{-1}	-1.1313×10^{-1}
x_1^0	1.6490×10^{-1}	9.2729×10^{-1}	8.3062×10^{-1}	3.5046×10^{-1}
$\underline{h}_{2,1,l}$	$l=5$	$l=6$	$l=7$	$l=8$
x_1^2	-6.9324×10^{-3}	2.4429×10^{-2}	1.9000×10^{-4}	0
x_1^1	-1.0458×10^{-1}	-2.4400×10^{-1}	-2.4816×10^{-3}	0
x_1^0	4.2011×10^{-1}	5.8063×10^{-1}	7.7665×10^{-3}	0

Table 3.19: The approximation of the membership functions for the 8 sub-domains and second order polynomial approximation function.

$\underline{h}_{2,2,l}$	$l=1$	$l=2$	$l=3$	$l=4$
x_1^2	0	1.9000×10^{-4}	2.4429×10^{-2}	-6.9324×10^{-3}
x_1^1	0	2.4816×10^{-3}	2.4400×10^{-1}	1.0458×10^{-1}
x_1^0	0	7.7665×10^{-3}	5.8063×10^{-1}	4.2011×10^{-1}
$\underline{h}_{2,2,l}$	$l=5$	$l=6$	$l=7$	$l=8$
x_1^2	-4.2131×10^{-2}	7.7370×10^{-3}	1.7384×10^{-2}	1.7433×10^{-3}
x_1^1	1.1313×10^{-1}	-2.0360×10^{-1}	-2.5747×10^{-1}	-3.4175×10^{-2}
x_1^0	3.5046×10^{-1}	8.3062×10^{-1}	9.2729×10^{-1}	1.6490×10^{-1}

Table 3.20: The approximation of the membership functions for the 8 sub-domains and second order polynomial approximation function.

$\underline{h}_{3,1,l}$	$l=1$	$l=2$	$l=3$	$l=4$
x_1^2	4.4081×10^{-6}	5.3143×10^{-5}	4.2358×10^{-4}	2.9255×10^{-3}
x_1^1	8.6345×10^{-5}	7.7608×10^{-4}	4.1908×10^{-3}	1.5183×10^{-2}
x_1^0	4.1634×10^{-4}	2.7532×10^{-3}	9.6841×10^{-3}	1.4656×10^{-2}
$\underline{h}_{3,1,l}$	$l=5$	$l=6$	$l=7$	$l=8$
x_1^2	2.4816×10^{-3}	-2.2976×10^{-2}	1.4895×10^{-3}	0
x_1^1	2.3774×10^{-2}	1.3439×10^{-1}	-1.9457×10^{-2}	0
x_1^0	-7.7108×10^{-3}	-1.2513×10^{-1}	6.0902×10^{-2}	0

Table 3.21: The approximation of the membership functions for the 8 sub-domains and second order polynomial approximation function.

$\underline{h}_{3,2,l}$	$l=1$	$l=2$	$l=3$	$l=4$
x_1^2	0	5.3265×10^{-7}	2.2648×10^{-4}	4.4508×10^{-3}
x_1^1	0	6.9567×10^{-6}	2.0457×10^{-3}	1.9198×10^{-2}
x_1^0	0	2.1772×10^{-5}	4.3169×10^{-3}	1.4656×10^{-2}
$\underline{h}_{3,2,l}$	$l=5$	$l=6$	$l=7$	$l=8$
x_1^2	3.9205×10^{-2}	-9.8406×10^{-3}	-1.9118×10^{-2}	-1.7477×10^{-3}
x_1^1	2.0508×10^{-3}	3.1944×10^{-1}	2.8019×10^{-1}	3.4261×10^{-2}
x_1^0	-4.8453×10^{-2}	-5.7345×10^{-1}	-1.1362×10^{-1}	8.2336×10^{-1}

Table 3.22: The δ_{ijl} for the 8 sub-domains and second order polynomial approximation function.

δ_{ijl}	$l=1$	$l=2$	$l=3$	$l=4$
$\delta_{1,1,l}$	1.1293×10^{-2}	1.0550×10^{-1}	1.9912×10^{-1}	1.7329×10^{-1}
$\delta_{1,2,l}$	0	1.0657×10^{-3}	5.7765×10^{-2}	5.9190×10^{-2}
$\delta_{2,1,l}$	1.1322×10^{-2}	1.0585×10^{-1}	2.0077×10^{-1}	1.7646×10^{-1}
$\delta_{2,2,l}$	0	1.0692×10^{-3}	5.8820×10^{-2}	6.0846×10^{-2}
$\delta_{3,1,l}$	2.8696×10^{-5}	3.4586×10^{-4}	3.1652×10^{-3}	2.3273×10^{-2}
$\delta_{3,2,l}$	0	3.4935×10^{-6}	1.0551×10^{-3}	2.3273×10^{-2}
δ_{ijl}	$l=5$	$l=6$	$l=7$	$l=8$
$\delta_{1,1,l}$	2.3273×10^{-2}	1.0551×10^{-3}	3.4935×10^{-6}	0
$\delta_{1,2,l}$	2.3273×10^{-2}	3.1652×10^{-3}	3.4586×10^{-4}	2.8696×10^{-5}
$\delta_{2,1,l}$	6.0846×10^{-2}	5.8820×10^{-2}	1.0692×10^{-3}	00
$\delta_{2,2,l}$	1.7646×10^{-1}	2.0077×10^{-1}	1.0585×10^{-1}	1.1322×10^{-2}
$\delta_{3,1,l}$	5.9190×10^{-2}	5.7765×10^{-2}	1.0657×10^{-3}	0
$\delta_{3,2,l}$	1.7329×10^{-1}	1.9912×10^{-1}	1.0550×10^{-1}	1.1293×10^{-2}

Table 3.23: The approximation of the membership functions for the 12 sub-domains and second order polynomial approximation function.

$\underline{h}_{1,1,l}$	$l=1$	$l=2$	$l=3$	$l=4$
x_1^2	-1.0942×10^{-3}	-5.5458×10^{-3}	-2.8236×10^{-2}	-2.7605×10^{-2}
x_1^1	-2.2298×10^{-2}	-9.4774×10^{-2}	-3.8622×10^{-1}	-4.6740×10^{-1}
x_1^0	8.8225×10^{-1}	5.7427×10^{-1}	-4.1583×10^{-1}	-8.7343×10^{-1}
$\underline{h}_{1,1,l}$	$l=5$	$l=6$	$l=7$	$l=8$
x_1^2	4.2339×10^{-2}	3.0876×10^{-2}	6.5389×10^{-3}	9.7253×10^{-4}
x_1^1	1.4363×10^{-3}	-1.5778×10^{-2}	-2.2627×10^{-2}	-6.4410×10^{-3}
x_1^0	-8.3528×10^{-2}	-2.0256×10^{-2}	1.4656×10^{-2}	9.9265×10^{-3}
$\underline{h}_{1,1,l}$	$l=9$	$l=10$	$l=11$	$l=12$
x_1^2	1.2080×10^{-4}	1.6295×10^{-6}	0	0
x_1^1	-1.1689×10^{-3}	-1.9665×10^{-5}	0	0
x_1^0	2.7332×10^{-3}	5.8194×10^{-5}	0	0

Table 3.24: The approximation of the membership functions for the 12 sub-domains and second order polynomial approximation function.

$\underline{h}_{1,2,l}$	$l=1$	$l=2$	$l=3$	$l=4$
x_1^2	0	0	4.5391×10^{-3}	-1.7199×10^{-2}
x_1^1	0	0	5.4790×10^{-2}	-8.5779×10^{-2}
x_1^0	0	0	1.6217×10^{-1}	-1.8507×10^{-2}
$\underline{h}_{1,2,l}$	$l=5$	$l=6$	$l=7$	$l=8$
x_1^2	-1.5992×10^{-2}	5.5379×10^{-3}	3.7465×10^{-3}	1.1345×10^{-3}
x_1^1	-9.8216×10^{-2}	-1.8534×10^{-2}	-1.6542×10^{-2}	-8.4295×10^{-3}
x_1^0	-7.8803×10^{-2}	-3.6254×10^{-4}	1.4656×10^{-2}	1.4684×10^{-2}
$\underline{h}_{1,2,l}$	$l=9$	$l=10$	$l=11$	$l=12$
x_1^2	2.8420×10^{-4}	7.4833×10^{-5}	1.4465×10^{-5}	2.7386×10^{-6}
x_1^1	-3.0323×10^{-3}	-1.0287×10^{-3}	-2.4648×10^{-4}	-5.5785×10^{-5}
x_1^0	7.8455×10^{-3}	3.4740×10^{-3}	1.0388×10^{-3}	2.8195×10^{-4}

Table 3.25: The approximation of the membership functions for the 12 sub-domains and second order polynomial approximation function.

$\underline{h}_{2,1,l}$	$l=1$	$l=2$	$l=3$	$l=4$
x_1^2	1.0914×10^{-3}	5.5313×10^{-3}	2.3039×10^{-2}	2.2199×10^{-2}
x_1^1	2.2243×10^{-2}	9.4527×10^{-2}	3.2337×10^{-1}	3.2376×10^{-1}
x_1^0	1.1246×10^{-1}	3.9953×10^{-1}	1.1154	1.0825
$\underline{h}_{2,1,l}$	$l=5$	$l=6$	$l=7$	$l=8$
x_1^2	-4.3474×10^{-2}	-3.4623×10^{-2}	-1.2077×10^{-2}	1.5020×10^{-2}
x_1^1	-1.0987×10^{-1}	-1.0076×10^{-1}	-9.5907×10^{-2}	-1.9178×10^{-1}
x_1^0	3.6036×10^{-1}	3.8260×10^{-1}	4.2054×10^{-1}	5.0520×10^{-1}
$\underline{h}_{2,1,l}$	$l=9$	$l=10$	$l=11$	$l=12$
x_1^2	2.2200×10^{-2}	5.8104×10^{-4}	0	0
x_1^1	-2.2522×10^{-1}	-7.0120×10^{-3}	0	0
x_1^0	5.5404×10^{-1}	2.0751×10^{-2}	0	0

Table 3.26: The approximation of the membership functions for the 12 sub-domains and second order polynomial approximation function.

$\underline{h}_{2,2,l}$	$l=1$	$l=2$	$l=3$	$l=4$
x_1^2	0	0	5.8104×10^{-4}	2.2200×10^{-2}
x_1^1	0	0	7.0120×10^{-3}	2.2522×10^{-1}
x_1^0	0	0	2.0751×10^{-2}	5.5404×10^{-1}
$\underline{h}_{2,2,l}$	$l=5$	$l=6$	$l=7$	$l=8$
x_1^2	1.5020×10^{-2}	-1.2077×10^{-2}	-3.4623×10^{-2}	-4.3474×10^{-2}
x_1^1	1.9178×10^{-1}	9.5907×10^{-2}	1.0076×10^{-1}	1.0987×10^{-1}
x_1^0	5.0520×10^{-1}	4.2054×10^{-1}	3.8260×10^{-1}	3.6036×10^{-1}
$\underline{h}_{2,2,l}$	$l=9$	$l=10$	$l=11$	$l=12$
x_1^2	2.2199×10^{-2}	2.3039×10^{-2}	5.5313×10^{-3}	1.0914×10^{-3}
x_1^1	-3.2376×10^{-1}	-3.2337×10^{-1}	-9.4527×10^{-2}	-2.2243×10^{-2}
x_1^0	1.0825	1.1154	3.9953×10^{-1}	1.1246×10^{-1}

Table 3.27: The approximation of the membership functions for the 12 sub-domains and second order polynomial approximation function.

$\underline{h}_{3,1,l}$	$l=1$	$l=2$	$l=3$	$l=4$
x_1^2	2.7386×10^{-6}	1.4465×10^{-5}	7.4833×10^{-5}	2.8420×10^{-4}
x_1^1	5.5785×10^{-5}	2.4648×10^{-4}	1.0287×10^{-3}	3.0323×10^{-3}
x_1^0	2.8195×10^{-4}	1.0388×10^{-3}	3.4740×10^{-3}	7.8455×10^{-3}
$\underline{h}_{3,1,l}$	$l=5$	$l=6$	$l=7$	$l=8$
x_1^2	1.1345×10^{-3}	3.7465×10^{-3}	5.5379×10^{-3}	-1.5992×10^{-2}
x_1^1	8.4295×10^{-3}	1.6542×10^{-2}	1.8534×10^{-2}	9.8216×10^{-2}
x_1^0	1.4684×10^{-2}	1.4656×10^{-2}	-3.6254×10^{-4}	-7.8803×10^{-2}
$\underline{h}_{3,1,l}$	$l=9$	$l=10$	$l=11$	$l=12$
x_1^2	-1.7199×10^{-2}	4.5391×10^{-3}	0	0
x_1^1	8.5779×10^{-2}	-5.4790×10^{-2}	0	0
x_1^0	-1.8507×10^{-2}	1.6217×10^{-1}	0	0

Table 3.28: The approximation of the membership functions for the 12 sub-domains and second order polynomial approximation function.

$\underline{h}_{3,2,l}$	$l=1$	$l=2$	$l=3$	$l=4$
x_1^2	0	0	1.6295×10^{-6}	1.2080×10^{-4}
x_1^1	0	0	1.9665×10^{-5}	1.1689×10^{-3}
x_1^0	0	0	5.8194×10^{-5}	2.7332×10^{-3}
$\underline{h}_{3,2,l}$	$l=5$	$l=6$	$l=7$	$l=8$
x_1^2	9.7253×10^{-4}	6.5389×10^{-3}	3.0876×10^{-2}	4.2339×10^{-2}
x_1^1	6.4410×10^{-3}	2.2627×10^{-2}	1.5778×10^{-2}	-1.4363×10^{-3}
x_1^0	9.9265×10^{-3}	1.4656×10^{-2}	-2.0256×10^{-2}	-8.3528×10^{-2}
$\underline{h}_{3,2,l}$	$l=9$	$l=10$	$l=11$	$l=12$
x_1^2	-2.7605×10^{-2}	-2.8236×10^{-2}	-5.5458×10^{-3}	-1.0942×10^{-3}
x_1^1	4.6740×10^{-1}	3.8622×10^{-1}	9.4774×10^{-2}	2.2298×10^{-2}
x_1^0	-8.7343×10^{-1}	-4.1583×10^{-1}	5.7427×10^{-1}	8.8225×10^{-1}

Table 3.29: The δ_{ijl} for the 12 sub-domains and second order polynomial approximation function.

δ_{ijl}	$l=1$	$l=2$	$l=3$	$l=4$
$\delta_{1,1,l}$	4.9938×10^{-3}	2.5093×10^{-2}	1.0550×10^{-1}	1.9888×10^{-1}
$\delta_{1,2,l}$	0	0	1.0657×10^{-3}	3.9872×10^{-2}
$\delta_{2,1,l}$	5.0063×10^{-3}	2.5159×10^{-2}	1.0585×10^{-1}	2.0042×10^{-1}
$\delta_{2,2,l}$	0	0	1.0692×10^{-3}	4.0181×10^{-2}
$\delta_{3,1,l}$	1.2514×10^{-5}	6.5805×10^{-5}	3.4586×10^{-4}	1.5409×10^{-3}
$\delta_{3,2,l}$	0	0	3.4935×10^{-6}	3.0891×10^{-4}
δ_{ijl}	$l=5$	$l=6$	$l=7$	$l=8$
$\delta_{1,1,l}$	1.9912×10^{-1}	1.1033×10^{-1}	2.3273×10^{-2}	3.1850×10^{-3}
$\delta_{1,2,l}$	5.9190×10^{-2}	5.5080×10^{-2}	2.3273×10^{-2}	6.3796×10^{-3}
$\delta_{2,1,l}$	2.0077×10^{-1}	1.1671×10^{-1}	5.8266×10^{-2}	6.0846×10^{-2}
$\delta_{2,2,l}$	6.0846×10^{-2}	5.8266×10^{-2}	1.1671×10^{-1}	2.0077×10^{-1}
$\delta_{3,1,l}$	6.3796×10^{-3}	2.3273×10^{-2}	5.5080×10^{-2}	5.9190×10^{-2}
$\delta_{3,2,l}$	3.1850×10^{-3}	2.3273×10^{-2}	1.1033×10^{-1}	1.9912×10^{-1}
δ_{ijl}	$l=9$	$l=10$	$l=11$	$l=12$
$\delta_{1,1,l}$	3.0891×10^{-4}	3.4935×10^{-6}	0	0
$\delta_{1,2,l}$	1.5409×10^{-3}	3.4586×10^{-4}	6.5805×10^{-5}	1.2514×10^{-5}
$\delta_{2,1,l}$	4.0181×10^{-2}	1.0692×10^{-3}	0	0
$\delta_{2,2,l}$	2.0042×10^{-1}	1.0585×10^{-1}	2.5159×10^{-2}	5.0063×10^{-3}
$\delta_{3,1,l}$	3.9872×10^{-2}	1.0657×10^{-3}	0	0
$\delta_{3,2,l}$	1.9888×10^{-1}	1.0550×10^{-1}	2.5093×10^{-2}	4.9938×10^{-3}

The stability analysis of IT2 PFMB control system is limitedly investigated in the literature. For comparison purposes, we compare the results using the basic stability conditions in Remark 3.2 that there is no stability region can be found, which shows the effectiveness of the proposed stability conditions. To probe further, we employ the stability conditions for type-1 PFMB control system in [1], which offers less conservative stability conditions among some recently published results. The embedded type-1 membership functions taking the average of the lower and upper membership functions are used for the stability conditions in [1]. The stability regions given by the stability conditions in [1] are shown in Fig. 3.14. It can be seen that the stability regions given by Theorems 3.1 to 3.3 are larger in size, which demonstrates the superiority of the proposed stability analysis results.

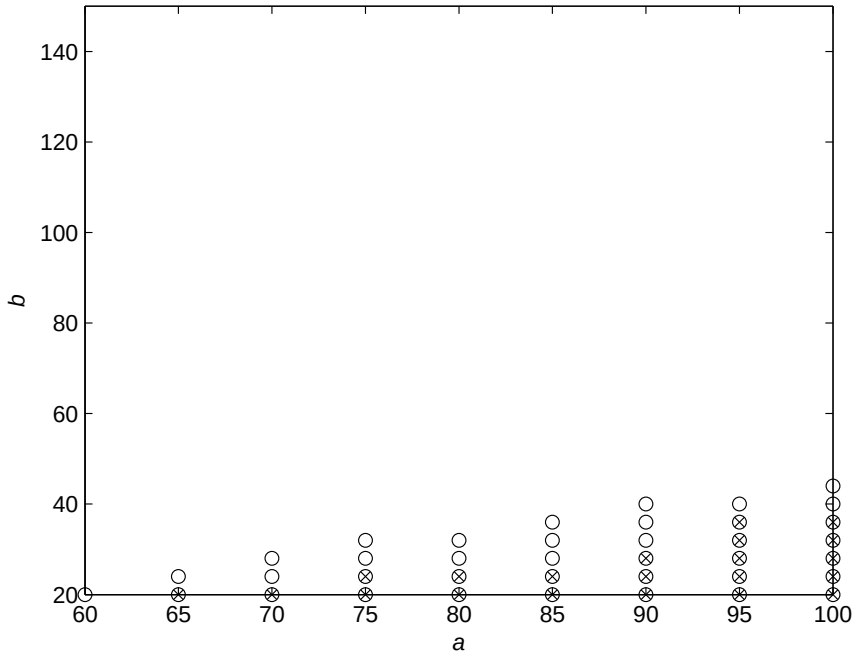

Figure 3.14: Stabilization regions given by the method used in [1] with $\mathbf{N}_j(\mathbf{x})$ of degree 0 and degree 2 indicated by "$\times$" and "$\circ$", respectively.

3.2.4 Inverted Pendulum

Example 2: In this example, the stability of an inverted pendulum is investigated to verify the applicability of the proposed approaches. The inverted pendulum is an open-loop unstable nonlinear system so the control task is to apply the developed stability conditions to find the proper feedback gains which can stabilize the inverted pendulum system. The dynamic equation for the inverted pendulum [45] is given by

$$\ddot{\theta} = \frac{g\sin(\theta(t)) - am_pS\dot{\theta}(t)^2\sin(2\theta(t))/2 - a\cos(\theta(t))u(t)}{4S/3 - am_pS\cos^2(\theta(t))}, \tag{3.15}$$

where $\theta(t)$ is the angular displacement of the inverted pendulum, $g = 9.8\ \mathrm{m/s^2}$, $m_p \in [m_{p_{\min}} \quad m_{p_{\max}}] = [0.5 \quad 1]$ kg is the mass of the pendulum, $M_c \in [M_{c_{\min}} \quad M_{c_{\max}}] = [18 \quad 20]$ kg is the mass of the cart, $a = \frac{1}{m_p + M_c}$, $2S = 1\mathrm{m}$ is the length of the pendulum, and $u(t)$ is the force applied on the cart. m_p and M_c are treated as the parameter uncertainties.

The following 4-rule polynomial fuzzy model is adopted to describe the inverted pendulum:

$$\begin{aligned}
&\text{Rule } i : \text{IF } f_1(\mathbf{x}(t)) \text{ is } \tilde{M}_1^i \text{ AND } f_2(\mathbf{x}(t)) \text{ is } \tilde{M}_2^i \\
&\text{THEN } \dot{\mathbf{x}}(t) = \mathbf{A}_i(\mathbf{x}(t))\hat{\mathbf{x}}(\mathbf{x}(t)) + \mathbf{B}_i(\mathbf{x}(t))\mathbf{u}(t), \\
&\qquad i = 1, 2, 3, 4.
\end{aligned} \tag{3.16}$$

After combining all the fuzzy rules, we have:

$$\dot{\mathbf{x}}(t) = \sum_{i=1}^{4} \tilde{w}_i \big(\mathbf{A}_i(\mathbf{x}(t))\hat{\mathbf{x}}(\mathbf{x}(t)) + \mathbf{B}_i(\mathbf{x}(t))\mathbf{u}(t) \big), \tag{3.17}$$

where

$$\hat{\mathbf{x}}(t) = \mathbf{x}(t) = [x_1(t) \quad x_2(t)]^T = [\theta(t) \quad \dot{\theta}(t)]^T,$$
$$x_1(t) \in [\frac{-5\pi}{12} \quad \frac{5\pi}{12}], \quad x_2(t) \in [-4 \quad 4],$$

$$\mathbf{A}_1 = \mathbf{A}_2 = \begin{bmatrix} 0 & 1 \\ f_{1_{\min}} & 0 \end{bmatrix}, \quad \mathbf{A}_3 = \mathbf{A}_4 = \begin{bmatrix} 0 & 1 \\ f_{1_{\max}} & 0 \end{bmatrix},$$
$$\mathbf{B}_1 = \mathbf{B}_3 = \begin{bmatrix} 0 \\ f_{2_{\min}} \end{bmatrix}, \quad \mathbf{B}_2 = \mathbf{B}_4 = \begin{bmatrix} 0 \\ f_{2_{\max}} \end{bmatrix},$$

$$f_1(\mathbf{x}(t)) = \frac{g - am_pSx_2(t)^2\cos(x_1(t))}{4S/3 - am_pS\cos^2(x_1(t))}\left(\frac{\sin(x_1(t))}{x_1(t)}\right),$$
$$f_2(\mathbf{x}(t)) = \frac{-a\cos(x_1(t))}{4S/3 - am_pS\cos^2(x_1(t))}.$$

In the polynomial fuzzy modeling process, the Taylor series is firstly used to approximate the lower and upper bounds of original nonlinear terms $f_1(\mathbf{x}(t))$ and $f_2(\mathbf{x}(t))$ in $\mathbf{A}_i$ and $\mathbf{B}_i$ are obtained as follows:

$$\underline{f}_1(x_1(t)) = -2.7142x_1(t)^2 + 14.6466,$$
$$\overline{f}_1(x_1(t)) = -2.5842x_1(t)^2 + 15.3041,$$
$$\underline{f}_2(x_1(t)) = 0.0360x_1(t)^2 - 0.0828,$$
$$\overline{f}_2(x_1(t)) = 0.0398x_1(t)^2 - 0.0741.$$

The approximations for $f_1(x_1(t))$ and $f_2(x_1(t))$ can be viewed in Fig. 3.15 and 3.16. In Fig. 3.15 and 3.16, the black curves are the Taylor series used as the upper and lower boundaries while the green curves are the possible values $f_1(x_1(t))$ or $f_2(x_1(t))$ with uncertainty.

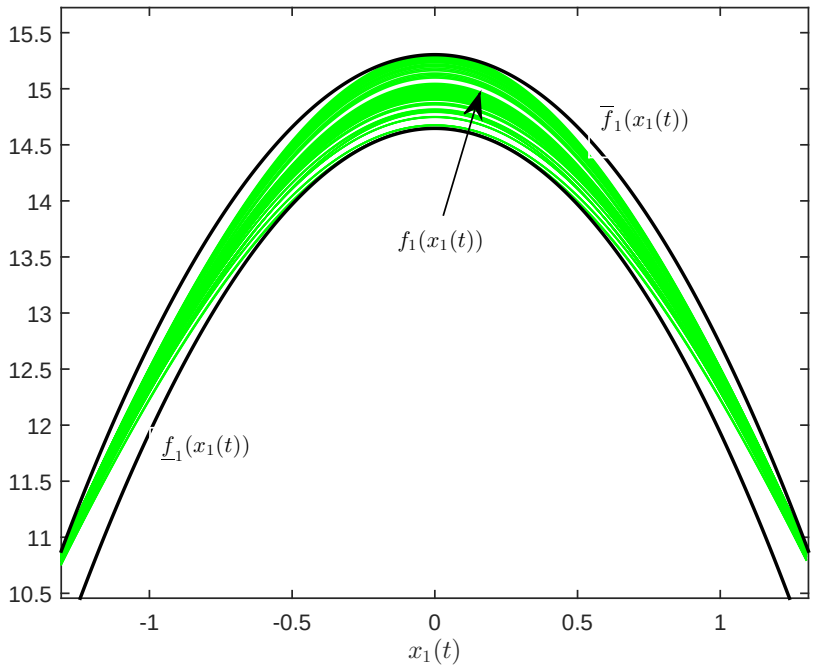

Figure 3.15: The approximation of the nonlinear term $f_1(x_1(t))$ by Taylor series.

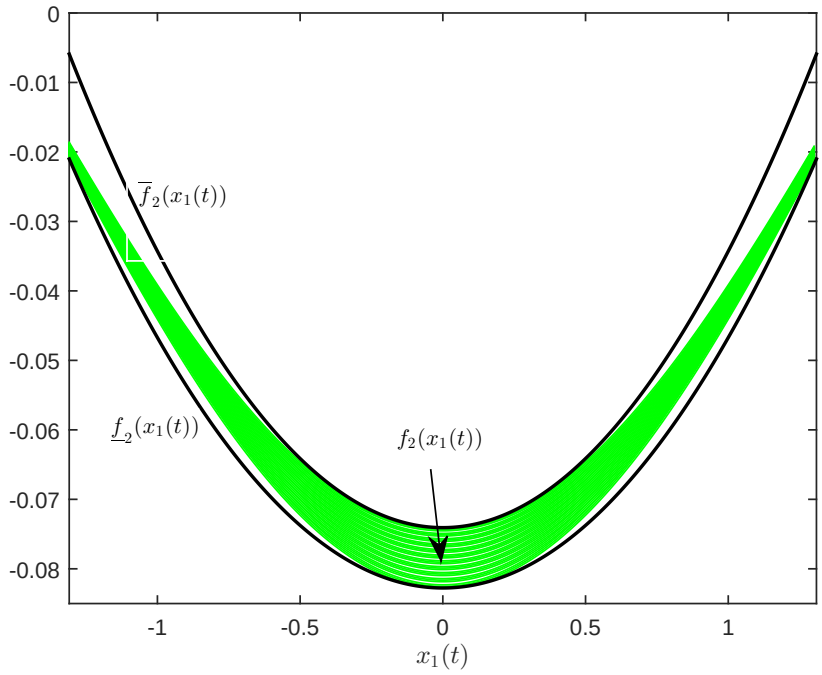

Figure 3.16: The approximation of the nonlinear term $f_2(x_1(t))$ by Taylor series.

To extract more information from the FOU of the IT2 membership functions, we define $f_{1nom}(x_1(t)) = \overline{f}_1(x_1(t)) - \underline{f}_1(x_1(t))$ and $f_{2nom}(x_1(t)) = \overline{f}_2(x_1(t)) - \underline{f}_2(x_1(t))$, by the definition, we can calculate the values of $f_{1nom}(x_1(t))$ and $f_{2nom}(x_1(t))$ as

$$f_{1nom}(x_1(t)) = 0.1299x_1(t)^2 + 0.6575,$$

$$f_{2nom}(x_1(t)) = 0.0037x_1(t)^2 + 0.0087.$$

Then, the constant lower and upper bounds $\underline{f}_{1c}$ and $\overline{f}_{1c}$ for $f_1(x_1(t)) - f_{1nom}(x_1(t))$, respectively; $\underline{f}_{2c}$ and $\overline{f}_{2c}$ for $f_2(x_1(t)) - f_{2nom}(x_1(t))$, respectively, are shown in Fig. 3.17 and 3.18

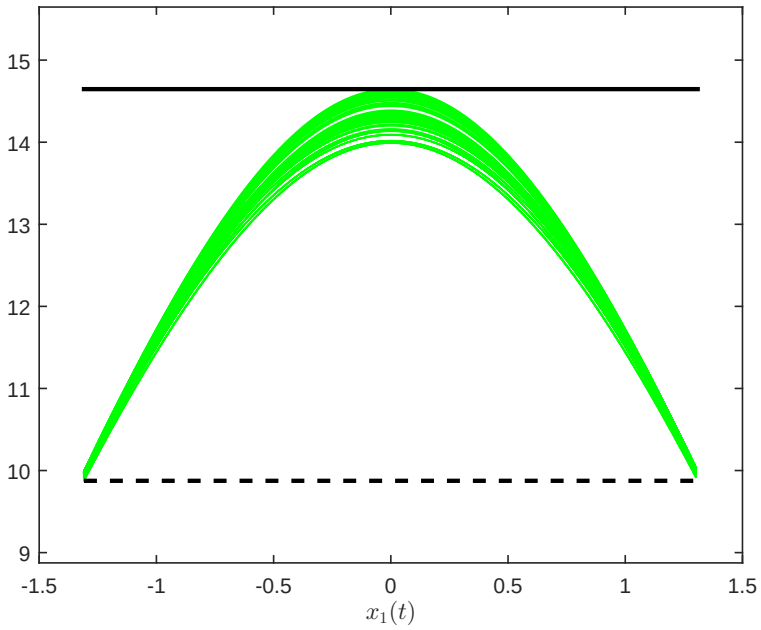

Figure 3.17: The lower and upper bounds for the nonlinear term $f_1(x_1(t)) - f_{1nom}(x_1(t))$.

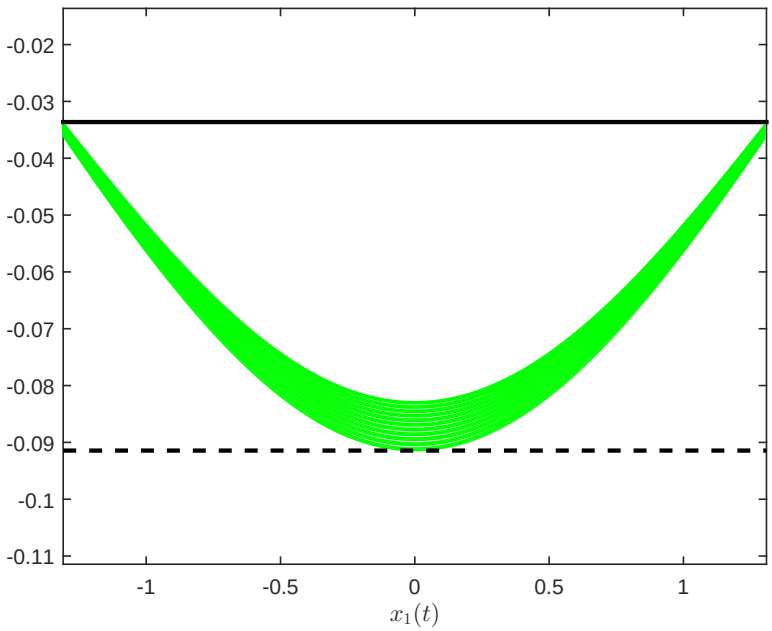

Figure 3.18: The lower and upper bounds for the nonlinear term $f_2(x_1(t)) - f_{2nom}(x_1(t))$.

After that, the polynomial forms of $f_{1min}(x_1(t))$, $f_{1max}(x_1(t))$, $f_{2min}(x_1(t))$ and $f_{2max}(x_1(t))$ can be calculated as follows:

$$
\begin{aligned}
f_{1min}(x_1(t)) &= f_{1nom}(x_1(t)) + \underline{f}_{1c} = 0.12996x_1(t)^2 + 10.5323 \\
f_{1max}(x_1(t)) &= f_{1nom}(x_1(t)) + \overline{f}_{1c} = 0.1299x_1(t)^2 + 15.3041 \\
f_{2min}(x_1(t)) &= f_{2nom}(x_1(t)) + \underline{f}_{2c} = 0.0037x_1(t)^2 - 0.0828 \\
f_{2max}(x_1(t)) &= f_{2nom}(x_1(t)) + \overline{f}_{2c} = 0.0037x_1(t)^2 - 0.0249
\end{aligned}
$$

The IT2 membership functions are defined as shown in Table 3.30 and the lower and upper grades of membership are respectively defined as:

$$
\begin{aligned}
w_i^L(\mathbf{x}(t)) &= \underline{\mu}_{\tilde{M}_1^i}(\mathbf{x}(t)) \times \underline{\mu}_{\tilde{M}_2^i}(\mathbf{x}(t)), \\
w_i^U(\mathbf{x}(t)) &= \overline{\mu}_{\tilde{M}_1^i}(\mathbf{x}(t)) \times \overline{\mu}_{\tilde{M}_2^i}(\mathbf{x}(t))
\end{aligned}
$$

The shape of the IT2 membership functions can be viewed in Fig. 3.19. In the figures, the black curves represent the upper membership functions $w_i^U(\mathbf{x}(t))$ while the blue curves represent the lower membership functions $w_i^L(\mathbf{x}(t))$.

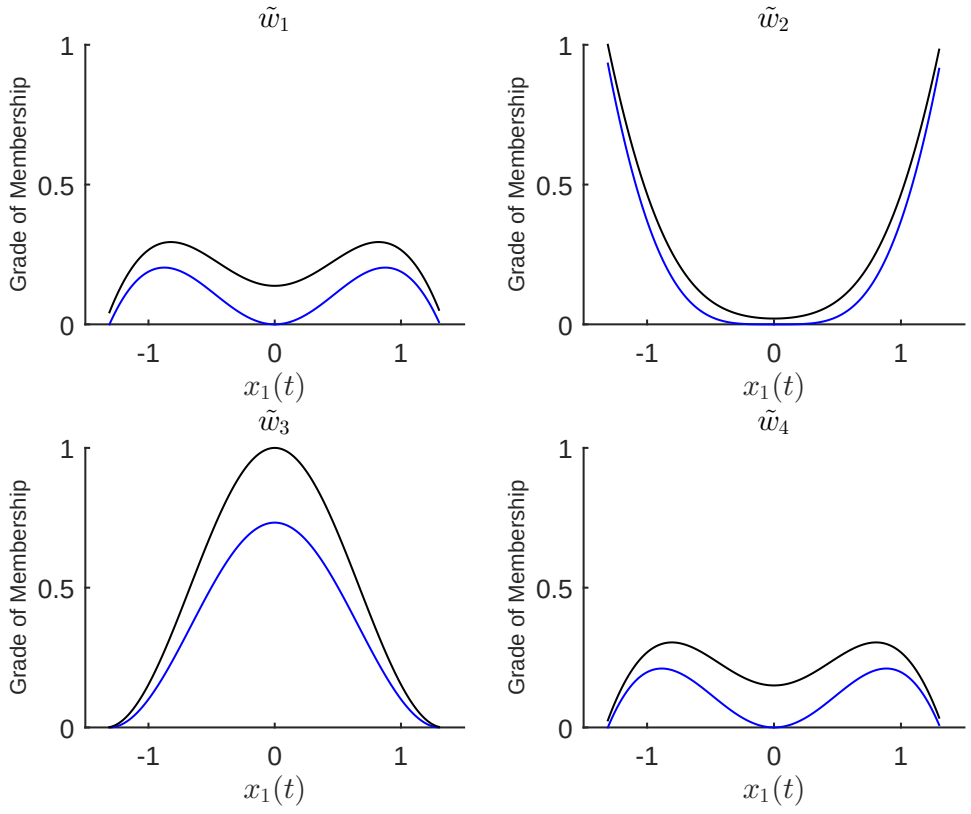

Figure 3.19: The shape of the IT2 membership functions for the inverted pendulum.

Based the IT2 PFMB fuzzy model, a two-rule IT2 polynomial fuzzy controller is adopted to stabilize the inverted pendulum for each control approach we propose

in the chapter. The following 2-rule IT2 polynomial fuzzy controller is adopted to describe the inverted pendulum:

$$\begin{aligned} &\text{Rule } j: \text{IF } x_1(t) \text{ is } \tilde{N}^j \\ &\qquad \text{THEN } u(t) = \mathbf{G}_j \mathbf{x}(t), \quad j = 1, 2. \end{aligned} \tag{3.18}$$

After combining of all the fuzzy rules, we have

$$u(t) = m_1 \mathbf{G}_1 \mathbf{x}(t) + m_2 \mathbf{G}_2 \mathbf{x}(t). \tag{3.19}$$

The membership functions are defined:

$$\overline{m}_1(\mathbf{x}(t)) = \begin{cases} 0 & \text{for } \mathbf{x}(t) < -\frac{5\pi}{12} \\ \frac{\mathbf{x}(t)+5\pi/12}{5\pi/12} & \text{for } -\frac{5\pi}{12} \leq \mathbf{x}(t) \leq 0 \\ \frac{5\pi/12-\mathbf{x}(t)}{5\pi/12} & \text{for } 0 \leq \mathbf{x}(t) \leq \frac{5\pi}{12} \\ 0 & \text{for } \mathbf{x}(t) > \frac{5\pi}{12} \end{cases} \tag{3.20}$$

$$\underline{m}_1(\mathbf{x}(t)) = \begin{cases} 0 & \text{for } \mathbf{x}(t) < -\frac{5\pi}{12} \\ \frac{0.9(\mathbf{x}(t)+5\pi/12)}{5\pi/12} & \text{for } -\frac{5\pi}{12} \leq \mathbf{x}(t) \leq 0 \\ \frac{0.9(5\pi/12-\mathbf{x}(t))}{5\pi/12} & \text{for } 0 \leq \mathbf{x}(t) \leq \frac{5\pi}{12} \\ 0 & \text{for } \mathbf{x}(t) > \frac{5\pi}{12} \end{cases} \tag{3.21}$$

$\overline{m}_2(x_1(t)) = \overline{\mu}_{\tilde{N}^2}(x_1(t)) = 1 - \underline{m}_1(x_1(t))$, $\underline{m}_2(x_1(t)) = \underline{\mu}_{\tilde{N}^2}(x_1(t)) = 1 - \overline{m}_1(x_1(t))$, $m_1(x_1(t)) = \mu_{\tilde{N}^1}(x_1(t))$, $m_2(x_1(t)) = \mu_{\tilde{N}^2}(x_1(t))) = 1 - m_1(x_1(t))$. The type reductions for the controller $\underline{\kappa}_j(x_1(t)) = \overline{\kappa}_j(x_1(t)) = 0.5$, $j = 1, 2$.

Table 3.30: Lower and Upper Membership Functions for the Interval Type-2 Fuzzy Model of the Inverted Pendulum.

Lower and upper membership functions	
$\underline{\mu}_{\tilde{M}_1^1}(f_1(\mathbf{x}(t))) = \underline{\mu}_{\tilde{M}_1^2}(f_1(\mathbf{x}(t)))$ $= \frac{f_{1\max} - f_1(\mathbf{x}(t))}{f_{1\max} - f_{1\min}}$;	$\underline{\mu}_{\tilde{M}_2^1}(f_2(\mathbf{x}(t))) = \underline{\mu}_{\tilde{M}_2^3}(f_2(\mathbf{x}(t)))$ $= \frac{f_{2\max} - f_2(\mathbf{x}(t))}{f_{2\max} - f_{2\min}}$;
$\overline{\mu}_{\tilde{M}_1^3}(f_1(\mathbf{x}(t))) = \overline{\mu}_{\tilde{M}_1^4}(f_1(\mathbf{x}(t)))$ $= \frac{f_1(\mathbf{x}(t)) - f_{1\min}}{f_{1\max} - f_{1\min}}$;	$\overline{\mu}_{\tilde{M}_2^2}(f_2(\mathbf{x}(t))) = \overline{\mu}_{\tilde{M}_2^4}(f_2(\mathbf{x}(t)))$ $= \frac{f_2(\mathbf{x}(t)) - f_{2\min}}{f_{2\max} - f_{2\min}}$
with $x_2(t) = 0, m_p = m_{p\max}$ $= 1$kg and $M_c = M_{c\min} = 18$kg	with $m_p = m_{p\max}$ $= 1$kg and $M_c = M_{c\max} = 20$kg
$\overline{\mu}_{\tilde{M}_1^1}(f_1(\mathbf{x}(t))) = \overline{\mu}_{\tilde{M}_1^2}(f_1(\mathbf{x}(t)))$ $= \frac{f_{1\max} - f_1(\mathbf{x}(t))}{f_{1\max} - f_{1\min}}$;	$\overline{\mu}_{\tilde{M}_2^1}(f_2(\mathbf{x}(t))) = \overline{\mu}_{\tilde{M}_2^3}(f_2(\mathbf{x}(t)))$ $= \frac{f_{2\max} - f_2(\mathbf{x}(t))}{f_{2\max} - f_{2\min}}$
$\underline{\mu}_{\tilde{M}_1^3}(f_1(\mathbf{x}(t))) = \underline{\mu}_{\tilde{M}_1^4}(f_1(\mathbf{x}(t)))$ $= \frac{f_1(\mathbf{x}(t)) - f_{1\min}}{f_{1\max} - f_{1\min}}$;	$\underline{\mu}_{\tilde{M}_2^2}(f_2(\mathbf{x}(t))) = \underline{\mu}_{\tilde{M}_2^4}(f_2(\mathbf{x}(t)))$ $= \frac{f_2(\mathbf{x}(t)) - f_{2\min}}{f_{2\max} - f_{2\min}}$;
with $x_2(t) = x_{2\max}, m_p = m_{p\max}$ $= 1$kg and $M_c = M_{c\min} = 18$kg	with $m_p = m_{p\min} = 0.5$kg and $M_c = M_{c\min} = 18$kg

During the simulations, we set $m_p = 0.75$kg and $M_c = 19$kg. Based on Theorem 3.1, the number of sub-domains is 15 and the feedback gains have been achieved as $\mathbf{G}_1 = [3058.7702 \quad 903.6783]$, $\mathbf{G}_2 = [8307.3853 \quad 2486.3838]$, and $\mathbf{X} = [0.2146 \quad -0.6796; -0.6796 \quad 2.2660]$, the values of $\underline{h}_{ijl}$ and δ_{ijl} can be found in Tables 3.31 and 3.32. Based on Theorem 3.2, the order of the polynomial functions is 8 and the feedback gains have been achieved as $\mathbf{G}_1 = [2330.4394 \quad 712.2114]$, $\mathbf{G}_2 = [57737.7092 \quad 18208.0045]$ and $\mathbf{X} = [0.5926 \quad -1.867; -1.867 \quad 5.925]$, the values of $\underline{h}_{ij}(\mathbf{x})$ can be found in Tables 3.33 and δ_{ij} are 0.1377, 0.0418, 0.3403, 0.1501, 0.0698, 0.0874, 0.1229, 0.0738, respectively. Based on Theorem 3.3, the number of sub-domains is 10 and the order of the polynomial functions is 2. The feedback gains have been achieved as $\mathbf{G}_1 = [2605.0379 \quad 777.2866]$, $\mathbf{G}_2 = [6387.7014 \quad 1971.6072]$ and $\mathbf{X} = [0.1024 \quad -0.3104; -0.3104 \quad 0.9994]$, the coefficients of $\underline{h}_{ijl}(\mathbf{x})$ and δ_{ijl} can be found in Tables 3.34 to 3.42. The state response for all the three methods are shown in Figs. 3.20 to 3.22. In those figures, the bold solid curves are under the initial condition $\mathbf{x}(0) = [\frac{5\pi}{12}, 0]$, the regular solid curves are under the condition $\mathbf{x}(0) = [\frac{\pi}{6}, 0]$, the bold dash curves are under the initial condition $\mathbf{x}(0) = [-\frac{5\pi}{12}, 0]$ and the regular dash curves are under the initial condition $\mathbf{x}(0) = [-\frac{\pi}{6}, 0]$. It can be found that all the methods can obtain the proper feedback gains, which can stabilize the inverted pendulum system.

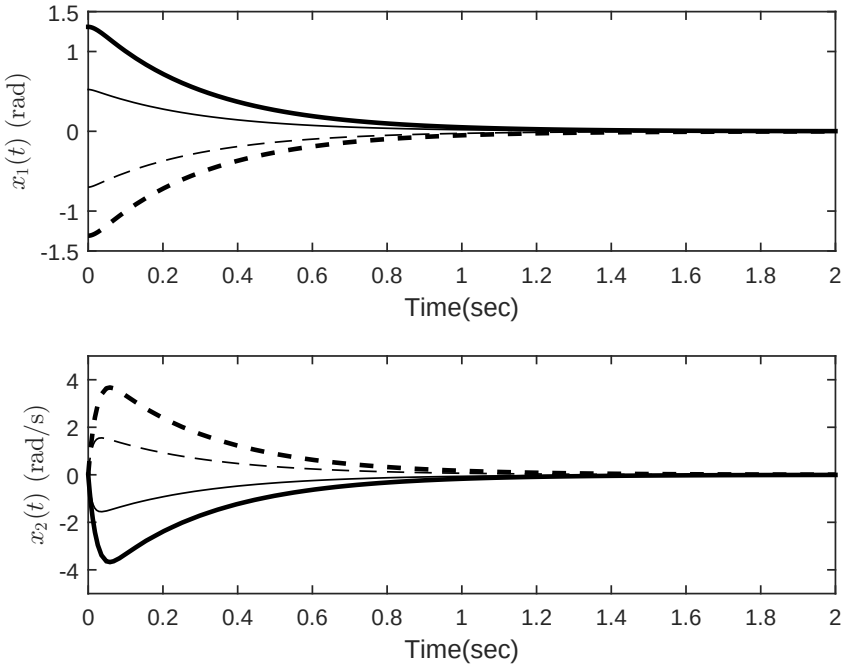

Figure 3.20: The top figure is the responses of $x_1(t)$; The figure below is the responses of $x_2(t)$. The number of sub-domains is 15.

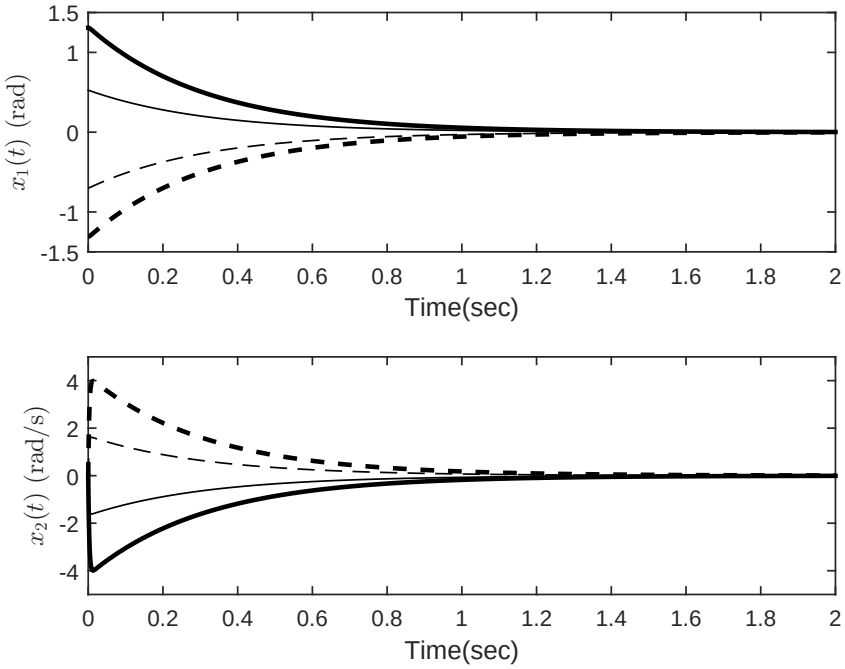

Figure 3.21: The top figure is the responses of $x_1(t)$; The figure below is the responses of $x_2(t)$. The order of polynomial functions is 4.

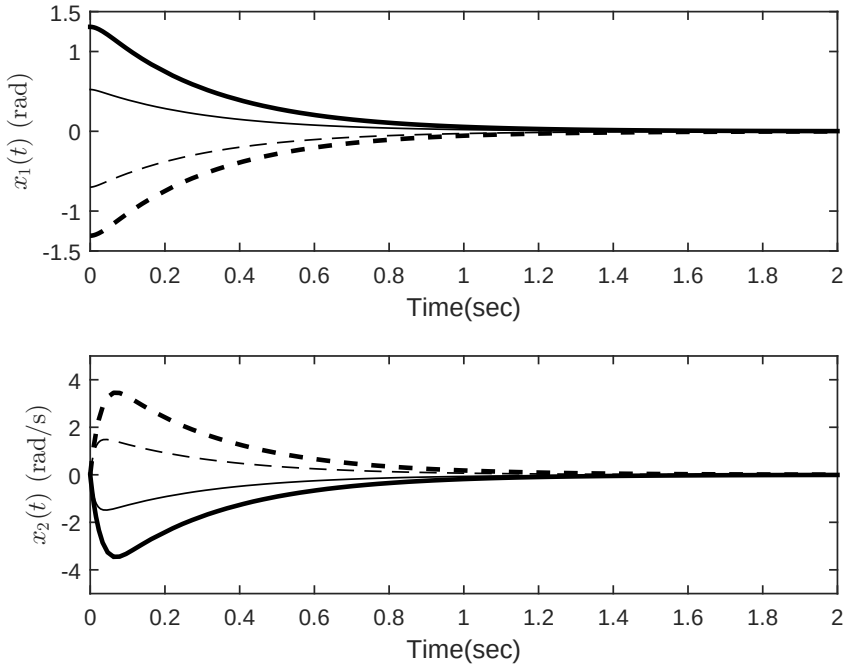

Figure 3.22: The top figure is the responses of $x_1(t)$; The figure below is the responses of $x_2(t)$. The number of sub-domains is 10 and the order of polynomial functions is 2.

Table 3.31: The values of the approximation of the membership functions in 15 operating sub-domains.

$\underline{h}_{ijl}$	$l=1$	$l=2$	$l=3$	$l=4$
$\underline{h}_{1,1,l}$	0	0	4.7031×10^{-2}	7.0439×10^{-2}
$\underline{h}_{1,2,l}$	0	6.8176×10^{-2}	5.5666×10^{-2}	2.7433×10^{-2}
$\underline{h}_{2,1,l}$	0	0	2.5932×10^{-2}	8.6085×10^{-2}
$\underline{h}_{2,2,l}$	0	0	4.9174×10^{-2}	7.2567×10^{-2}
$\underline{h}_{3,1,l}$	0	1.1565×10^{-1}	1.1846×10^{-1}	7.1041×10^{-2}
$\underline{h}_{3,2,l}$	4.7802×10^{-1}	2.1985×10^{-1}	8.2821×10^{-2}	2.3339×10^{-2}
$\underline{h}_{4,1,l}$	0	0	9.2163×10^{-2}	1.5409×10^{-1}
$\underline{h}_{4,2,l}$	3.5628×10^{-16}	1.2307×10^{-1}	1.2201×10^{-1}	7.1933×10^{-2}
$\underline{h}_{ijl}$	$l=5$	$l=6$	$l=7$	$l=8$
$\underline{h}_{1,1,l}$	5.7074×10^{-2}	2.7512×10^{-2}	0	0
$\underline{h}_{1,2,l}$	8.7599×10^{-3}	4.6988×10^{-4}	0	0
$\underline{h}_{2,1,l}$	1.9074×10^{-1}	3.2676×10^{-1}	4.7178×10^{-1}	6.0729×10^{-1}
$\underline{h}_{2,2,l}$	5.7459×10^{-2}	2.7508×10^{-2}	0	0
$\underline{h}_{3,1,l}$	3.0492×10^{-2}	4.2885×10^{-3}	0	0
$\underline{h}_{3,2,l}$	3.4250×10^{-3}	4.9829×10^{-5}	0	0
$\underline{h}_{4,1,l}$	1.8437×10^{-1}	1.3440×10^{-1}	0	0
$\underline{h}_{4,2,l}$	3.0697×10^{-2}	4.2879×10^{-3}	0	0
$\underline{h}_{ijl}$	$l=9$	$l=10$	$l=11$	$l=12$
$\underline{h}_{1,1,l}$	0	2.5654×10^{-2}	5.5882×10^{-2}	7.1115×10^{-2}
$\underline{h}_{1,2,l}$	0	2.9456×10^{-4}	8.1020×10^{-3}	2.6277×10^{-2}
$\underline{h}_{2,1,l}$	4.7828×10^{-1}	3.3256×10^{-1}	1.9748×10^{-1}	8.9069×10^{-2}
$\underline{h}_{2,2,l}$	0	2.5644×10^{-2}	5.6237×10^{-2}	7.3217×10^{-2}
$\underline{h}_{3,1,l}$	0	3.5317×10^{-3}	2.9045×10^{-2}	6.8673×10^{-2}
$\underline{h}_{3,2,l}$	0	0	3.1299×10^{-3}	2.1470×10^{-2}
$\underline{h}_{4,1,l}$	0	1.3122×10^{-1}	1.8139×10^{-1}	1.5650×10^{-1}
$\underline{h}_{4,2,l}$	0	3.5304×10^{-3}	2.9229×10^{-2}	6.9536×10^{-2}
$\underline{h}_{ijl}$	$l=13$	$l=14$	$l=15$	
$\underline{h}_{1,1,l}$	4.8397×10^{-2}	3.1935×10^{-3}	3.7174×10^{-5}	
$\underline{h}_{1,2,l}$	5.4400×10^{-2}	6.9670×10^{-2}	5.0240×10^{-3}	
$\underline{h}_{2,1,l}$	2.8573×10^{-2}	0	0	
$\underline{h}_{2,2,l}$	5.0594×10^{-2}	3.3955×10^{-3}	4.3574×10^{-5}	
$\underline{h}_{3,1,l}$	1.1656×10^{-1}	1.1867×10^{-1}	7.9094×10^{-3}	
$\underline{h}_{3,2,l}$	7.8945×10^{-2}	2.1157×10^{-1}	4.6328×10^{-1}	
$\underline{h}_{4,1,l}$	9.5255×10^{-2}	5.7835×10^{-3}	4.2456×10^{-5}	
$\underline{h}_{4,2,l}$	1.1997×10^{-1}	1.2617×10^{-1}	8.5626×10^{-3}	

Table 3.32: The values of $\delta_{i,j,l}$ in 15 operating sub-domains.

δ_{ijl}	$l=1$	$l=2$	$l=3$	$l=4$
$\delta_{1,1,l}$	2.6274×10^{-2}	7.4757×10^{-2}	7.2553×10^{-2}	7.4253×10^{-2}
$\delta_{1,2,l}$	9.8318×10^{-2}	4.6323×10^{-2}	5.8834×10^{-2}	7.1576×10^{-2}
$\delta_{2,1,l}$	7.4208×10^{-3}	5.0715×10^{-2}	1.2034×10^{-1}	2.2039×10^{-1}
$\delta_{2,2,l}$	2.5565×10^{-2}	7.5792×10^{-2}	7.4564×10^{-2}	7.9411×10^{-2}
$\delta_{3,1,l}$	1.8862×10^{-1}	1.0246×10^{-1}	9.9653×10^{-2}	1.2092×10^{-1}
$\delta_{3,2,l}$	5.2198×10^{-1}	3.7442×10^{-1}	2.3369×10^{-1}	1.3355×10^{-1}
$\delta_{4,1,l}$	5.0512×10^{-2}	1.4504×10^{-1}	1.4747×10^{-1}	1.5001×10^{-1}
$\delta_{4,2,l}$	1.8388×10^{-1}	9.9090×10^{-2}	1.0015×10^{-1}	1.2674×10^{-1}
δ_{ijl}	$l=5$	$l=6$	$l=7$	$l=8$
$\delta_{1,1,l}$	8.9359×10^{-2}	1.1892×10^{-1}	1.3763×10^{-1}	1.3786×10^{-1}
$\delta_{1,2,l}$	6.0869×10^{-2}	4.3892×10^{-2}	2.7949×10^{-2}	2.0723×10^{-2}
$\delta_{2,1,l}$	3.1484×10^{-1}	3.9656×10^{-1}	5.2822×10^{-1}	3.9271×10^{-1}
$\delta_{2,2,l}$	9.8747×10^{-2}	1.2870×10^{-1}	1.4987×10^{-1}	1.5083×10^{-1}
$\delta_{3,1,l}$	1.0830×10^{-1}	8.3315×10^{-2}	4.8936×10^{-2}	2.2859×10^{-2}
$\delta_{3,2,l}$	6.4476×10^{-2}	2.6771×10^{-2}	1.0024×10^{-2}	3.5662×10^{-3}
$\delta_{4,1,l}$	1.2788×10^{-1}	1.7785×10^{-1}	2.6230×10^{-1}	1.6377×10^{-1}
$\delta_{4,2,l}$	1.1564×10^{-1}	8.9019×10^{-2}	5.2762×10^{-2}	2.4884×10^{-2}
δ_{ijl}	$l=9$	$l=10$	$l=11$	$l=12$
$\delta_{1,1,l}$	1.3786×10^{-1}	1.2054×10^{-1}	9.0311×10^{-2}	7.4140×10^{-2}
$\delta_{1,2,l}$	2.7408×10^{-2}	4.3089×10^{-2}	6.0250×10^{-2}	7.0945×10^{-2}
$\delta_{2,1,l}$	5.2172×10^{-1}	4.0046×10^{-1}	3.2037×10^{-1}	2.2588×10^{-1}
$\delta_{2,2,l}$	1.5083×10^{-1}	1.3021×10^{-1}	9.9616×10^{-2}	7.9446×10^{-2}
$\delta_{3,1,l}$	4.7473×10^{-2}	8.1945×10^{-2}	1.0759×10^{-1}	1.2023×10^{-1}
$\delta_{3,2,l}$	9.5668×10^{-3}	2.6314×10^{-2}	6.2006×10^{-2}	1.2998×10^{-1}
$\delta_{4,1,l}$	2.5940×10^{-1}	1.7927×10^{-1}	1.2910×10^{-1}	1.4991×10^{-1}
$\delta_{4,2,l}$	5.1212×10^{-2}	8.7565×10^{-2}	1.1444×10^{-1}	1.2698×10^{-1}
δ_{ijl}	$l=13$	$l=14$	$l=15$	
$\delta_{1,1,l}$	7.2792×10^{-2}	7.3930×10^{-2}	2.8239×10^{-2}	
$\delta_{1,2,l}$	6.0437×10^{-2}	4.5166×10^{-2}	9.4472×10^{-2}	
$\delta_{2,1,l}$	1.2368×10^{-1}	5.3896×10^{-2}	8.3844×10^{-3}	
$\delta_{2,2,l}$	7.4897×10^{-2}	7.5141×10^{-2}	2.7476×10^{-2}	
$\delta_{3,1,l}$	1.0224×10^{-1}	1.0014×10^{-1}	1.8271×10^{-1}	
$\delta_{3,2,l}$	2.2813×10^{-1}	3.6728×10^{-1}	5.1405×10^{-1}	
$\delta_{4,1,l}$	1.4807×10^{-1}	1.4278×10^{-1}	5.4192×10^{-2}	
$\delta_{4,2,l}$	1.0236×10^{-1}	9.6156×10^{-2}	1.7929×10^{-1}	

Table 3.33: The coefficients for the 6th order polynomial function.

$\underline{h}_{ij}(x_1)$	x_1^6	x_1^5	x_1^4	x_1^3
$\underline{h}_{1,1}$	1.0145×10^{-1}	3.1014×10^{-4}	-2.8436×10^{-1}	-4.8375×10^{-4}
$\underline{h}_{1,2}$	-5.3016×10^{-2}	-2.6151×10^{-4}	-2.2206×10^{-3}	4.0788×10^{-4}
$\underline{h}_{2,1}$	-5.5728×10^{-1}	-3.9947×10^{-3}	1.9424	6.2306×10^{-3}
$\underline{h}_{2,2}$	1.0461×10^{-1}	3.2663×10^{-4}	-2.8677×10^{-1}	-5.0947×10^{-4}
$\underline{h}_{3,1}$	-2.9856×10^{-2}	-1.5559×10^{-4}	-1.6686×10^{-1}	2.4269×10^{-4}
$\underline{h}_{3,2}$	-2.3363×10^{-4}	1.2647×10^{-4}	3.0810×10^{-1}	-1.9726×10^{-4}
$\underline{h}_{4,1}$	4.1803×10^{-1}	3.4263×10^{-3}	-1.1541	-5.3441×10^{-3}
$\underline{h}_{4,2}$	-2.5098×10^{-2}	-1.3680×10^{-4}	-1.9543×10^{-1}	2.1339×10^{-4}
$\underline{h}_{ij}(x_1)$	x_1^2	x_1^1	x_1^0	
$\underline{h}_{1,1}$	1.1524×10^{-1}	1.3834×10^{-4}	1.3144×10^{-1}	
$\underline{h}_{1,2}$	1.4673×10^{-1}	-1.1663×10^{-4}	1.8073×10^{-2}	
$\underline{h}_{2,1}$	-2.2525	-1.7816×10^{-3}	9.0301×10^{-1}	
$\underline{h}_{2,2}$	1.0339×10^{-1}	1.4570×10^{-4}	1.4319×10^{-1}	
$\underline{h}_{3,1}$	3.8561×10^{-1}	-6.9408×10^{-5}	2.0092×10^{-2}	
$\underline{h}_{3,2}$	5.5146×10^{-2}	5.6405×10^{-5}	3.9041×10^{-3}	
$\underline{h}_{4,1}$	6.7062×10^{-1}	1.5281×10^{-3}	1.8649×10^{-1}	
$\underline{h}_{4,2}$	4.0930×10^{-1}	-6.1030×10^{-5}	2.2118×10^{-2}	

Table 3.34: The approximation of the membership functions for the 10 sub-domains and second order polynomial approximation function.

$\underline{h}_{1,1,l}$	$l=1$	$l=2$	$l=3$	$l=4$
x_1^2	4.6620×10^{-1}	-1.5161×10^{-1}	-3.6559×10^{-1}	-1.4877×10^{-1}
x_1^1	1.2938	-1.5449×10^{-2}	-3.7100×10^{-1}	-1.5630×10^{-1}
x_1^0	8.9399×10^{-1}	1.9920×10^{-1}	5.1453×10^{-2}	1.0476×10^{-1}
$\underline{h}_{1,1,l}$	$l=5$	$l=6$	$l=7$	$l=8$
x_1^2	3.0068×10^{-1}	3.0850×10^{-1}	-1.3684×10^{-1}	-3.6492×10^{-1}
x_1^1	8.2222×10^{-2}	-8.3993×10^{-2}	1.4685×10^{-1}	3.7007×10^{-1}
x_1^0	1.3729×10^{-1}	1.3736×10^{-1}	1.0659×10^{-1}	5.1774×10^{-2}
$\underline{h}_{1,1,l}$	$l=9$	$l=10$		
x_1^2	-1.6484×10^{-1}	4.4270×10^{-1}		
x_1^1	3.9599×10^{-2}	-1.2386		
x_1^0	1.8822×10^{-1}	8.6166×10^{-1}		

Table 3.35: The approximation of the membership functions for the 10 sub-domains and second order polynomial approximation function.

$\underline{h}_{1,2,l}$	$l=1$	$l=2$	$l=3$	$l=4$
x_1^2	-1.2312	-4.9023×10^{-1}	-1.4781×10^{-2}	1.5498×10^{-1}
x_1^1	-2.5025	-9.3982×10^{-1}	-1.7729×10^{-1}	1.3093×10^{-2}
x_1^0	-1.1653	-3.3994×10^{-1}	-3.3337×10^{-2}	2.0223×10^{-2}
$\underline{h}_{1,2,l}$	$l=5$	$l=6$	$l=7$	$l=8$
x_1^2	1.5431×10^{-1}	1.5460×10^{-1}	1.5630×10^{-1}	-5.2047×10^{-3}
x_1^1	1.4497×10^{-2}	-1.4597×10^{-2}	-1.4119×10^{-2}	1.6478×10^{-1}
x_1^0	2.0678×10^{-2}	2.0685×10^{-2}	2.0417×10^{-2}	-2.9289×10^{-2}
$\underline{h}_{1,2,l}$	$l=9$	$l=10$		
x_1^2	-4.7111×10^{-1}	-1.2057		
x_1^1	9.0486×10^{-1}	2.4425		
x_1^0	-3.2403×10^{-1}	-1.1302		

Table 3.36: The approximation of the membership functions for the 10 sub-domains and second order polynomial approximation function.

$\underline{h}_{2,1,l}$	$l=1$	$l=2$	$l=3$	$l=4$
x_1^2	4.6112×10^{-1}	9.5347×10^{-1}	8.5752×10^{-1}	1.5201×10^{-1}
x_1^1	1.1691	2.2217	2.0959	1.3701
x_1^0	7.4097×10^{-1}	1.3043	1.2646	1.0767
$\underline{h}_{2,1,l}$	$l=5$	$l=6$	$l=7$	$l=8$
x_1^2	-9.0836×10^{-1}	-9.0140×10^{-1}	1.2296×10^{-1}	8.4426×10^{-1}
x_1^1	8.1044×10^{-1}	-8.1455×10^{-1}	-1.3471	-2.0784
x_1^0	1.0006	1.0010	1.0722	1.2589
$\underline{h}_{2,1,l}$	$l=9$	$l=10$		
x_1^2	9.6006×10^{-1}	4.8314×10^{-1}		
x_1^1	-2.2337	-1.2208		
x_1^0	1.3098	7.7124×10^{-1}		

Table 3.37: The approximation of the membership functions for the 10 sub-domains and second order polynomial approximation function.

$\underline{h}_{2,2,l}$	$l=1$	$l=2$	$l=3$	$l=4$
x_1^2	5.1289×10^{-1}	-1.3647×10^{-1}	-3.7773×10^{-1}	-1.6290×10^{-1}
x_1^1	1.4040	2.8767×10^{-2}	-3.7045×10^{-1}	-1.5910×10^{-1}
x_1^0	9.5822×10^{-1}	2.2886×10^{-1}	6.3592×10^{-2}	1.1569×10^{-1}
$\underline{h}_{2,2,l}$	$l=5$	$l=6$	$l=7$	$l=8$
x_1^2	3.0798×10^{-1}	3.1630×10^{-1}	-1.5055×10^{-1}	-3.7758×10^{-1}
x_1^1	9.0541×10^{-2}	-9.2437×10^{-2}	1.4931×10^{-1}	3.7020×10^{-1}
x_1^0	1.4969×10^{-1}	1.4976×10^{-1}	1.1758×10^{-1}	6.3693×10^{-2}
$\underline{h}_{2,2,l}$	$l=9$	$l=10$		
x_1^2	-1.5071×10^{-1}	4.8851×10^{-1}		
x_1^1	-2.7661×10^{-3}	-1.3467		
x_1^0	2.1704×10^{-1}	9.2468×10^{-1}		

Table 3.38: The approximation of the membership functions for the 10 sub-domains and second order polynomial approximation function.

$\underline{h}_{3,1,l}$	$l=1$	$l=2$	$l=3$	$l=4$
x_1^2	-1.7554	-8.3022×10^{-1}	-1.1326×10^{-1}	2.2662×10^{-1}
x_1^1	-3.5318	-1.5870	-4.4344×10^{-1}	-6.7275×10^{-2}
x_1^0	-1.5715	-5.4761×10^{-1}	-9.0216×10^{-2}	1.4338×10^{-2}
$\underline{h}_{3,1,l}$	$l=5$	$l=6$	$l=7$	$l=8$
x_1^2	1.7454×10^{-1}	1.7018×10^{-1}	2.3041×10^{-1}	-9.6629×10^{-2}
x_1^1	-8.1975×10^{-2}	8.3076×10^{-2}	6.4334×10^{-2}	4.2169×10^{-1}
x_1^0	1.4060×10^{-2}	1.4007×10^{-2}	1.4895×10^{-2}	-8.3172×10^{-2}
$\underline{h}_{3,1,l}$	$l=9$	$l=10$		
x_1^2	-8.0397×10^{-1}	-1.7260		
x_1^1	1.5390	3.4628		
x_1^0	-5.2576×10^{-1}	-1.5311		

Table 3.39: The approximation of the membership functions for the 10 sub-domains and second order polynomial approximation function.

$\underline{h}_{3,2,l}$	$l=1$	$l=2$	$l=3$	$l=4$
x_1^2	2.5301	1.6412	8.6529×10^{-1}	3.3563×10^{-1}
x_1^1	3.8098	1.9434	7.1162×10^{-1}	1.3990×10^{-1}
x_1^0	1.6508	6.6944×10^{-1}	1.7901×10^{-1}	2.3737×10^{-2}
$\underline{h}_{3,2,l}$	$l=5$	$l=6$	$l=7$	$l=8$
x_1^2	7.8867×10^{-2}	7.6635×10^{-2}	3.2396×10^{-1}	8.4483×10^{-1}
x_1^1	-7.1441×10^{-3}	7.5977×10^{-3}	-1.3072×10^{-1}	-6.8485×10^{-1}
x_1^0	2.2232×10^{-3}	2.2106×10^{-3}	2.1973×10^{-2}	1.7033×10^{-1}
$\underline{h}_{3,2,l}$	$l=9$	$l=10$		
x_1^2	1.6148	2.5027		
x_1^1	-1.8952	-3.7452		
x_1^0	6.4749×10^{-1}	1.6130		

Table 3.40: The approximation of the membership functions for the 10 sub-domains and second order polynomial approximation function.

$\underline{h}_{4,1,l}$	$l=1$	$l=2$	$l=3$	$l=4$
x_1^2	8.7218×10^{-1}	-1.3713×10^{-1}	-8.1111×10^{-1}	-9.3551×10^{-1}
x_1^1	2.4218	2.9662×10^{-1}	-7.8530×10^{-1}	-9.4063×10^{-1}
x_1^0	1.6757	5.5502×10^{-1}	1.1963×10^{-1}	7.2030×10^{-2}
$\underline{h}_{4,1,l}$	$l=5$	$l=6$	$l=7$	$l=8$
x_1^2	-4.7664×10^{-1}	-4.8665×10^{-1}	-9.2984×10^{-1}	-8.2383×10^{-1}
x_1^1	-7.1822×10^{-1}	7.2261×10^{-1}	9.3607×10^{-1}	8.0189×10^{-1}
x_1^0	9.9676×10^{-2}	9.9304×10^{-2}	7.2923×10^{-2}	1.1427×10^{-1}
$\underline{h}_{4,1,l}$	$l=9$	$l=10$		
x_1^2	-1.6425×10^{-1}	8.3891×10^{-1}		
x_1^1	-2.4703×10^{-1}	-2.3437		
x_1^0	5.3245×10^{-1}	1.6299		

Table 3.41: The approximation of the membership functions for the 10 sub-domains and second order polynomial approximation function.

$\underline{h}_{4,2,l}$	$l=1$	$l=2$	$l=3$	$l=4$
x_1^2	-1.8439	-8.9784×10^{-1}	-1.4843×10^{-1}	2.2216×10^{-1}
x_1^1	-3.6736	-1.6852	-4.9073×10^{-1}	-8.1536×10^{-2}
x_1^0	-1.6229	-5.7624×10^{-1}	-9.8865×10^{-2}	1.4630×10^{-2}
$\underline{h}_{4,2,l}$	$l=5$	$l=6$	$l=7$	$l=8$
x_1^2	1.7953×10^{-1}	1.7495×10^{-1}	2.2661×10^{-1}	-1.3070×10^{-1}
x_1^1	-9.0200×10^{-2}	9.1369×10^{-2}	7.8075×10^{-2}	4.6756×10^{-1}
x_1^0	1.5312×10^{-2}	1.5254×10^{-2}	1.5287×10^{-2}	-9.1356×10^{-2}
$\underline{h}_{4,2,l}$	$l=9$	$l=10$		
x_1^2	-8.7077×10^{-1}	-1.8140		
x_1^1	1.6357	3.6032		
x_1^0	-5.5370×10^{-1}	-1.5816		

Table 3.42: The values of $\delta_{i,j,l}$ in 10 sub-domains and second order polynomial approximation function.

δ_{ijl}	$l=1$	$l=2$	$l=3$	$l=4$
$\delta_{1,1,l}$	1.9484×10^{-2}	4.7033×10^{-2}	7.7075×10^{-2}	1.0784×10^{-1}
$\delta_{1,2,l}$	2.7531×10^{-2}	4.1153×10^{-2}	4.1923×10^{-2}	3.8262×10^{-2}
$\delta_{2,1,l}$	9.6909×10^{-3}	5.3756×10^{-2}	1.3973×10^{-1}	2.4828×10^{-1}
$\delta_{2,2,l}$	1.7818×10^{-2}	4.9137×10^{-2}	8.4720×10^{-2}	1.1851×10^{-1}
$\delta_{3,1,l}$	6.3379×10^{-2}	7.0933×10^{-2}	7.0916×10^{-2}	6.1923×10^{-2}
$\delta_{3,2,l}$	8.8342×10^{-2}	8.6590×10^{-2}	6.2603×10^{-2}	3.0159×10^{-2}
$\delta_{4,1,l}$	3.7702×10^{-2}	8.2447×10^{-2}	1.1525×10^{-1}	1.2322×10^{-1}
$\delta_{4,2,l}$	5.5663×10^{-2}	7.3143×10^{-2}	7.4138×10^{-2}	6.7932×10^{-2}
δ_{ijl}	$l=5$	$l=6$	$l=7$	$l=8$
$\delta_{1,1,l}$	1.3769×10^{-1}	1.3769×10^{-1}	1.0877×10^{-1}	7.8031×10^{-2}
$\delta_{1,2,l}$	2.6223×10^{-2}	2.5871×10^{-2}	3.7954×10^{-2}	4.1906×10^{-2}
$\delta_{2,1,l}$	3.4382×10^{-1}	3.4234×10^{-1}	2.5158×10^{-1}	1.4290×10^{-1}
$\delta_{2,2,l}$	1.5012×10^{-1}	1.5011×10^{-1}	1.1949×10^{-1}	8.5813×10^{-2}
$\delta_{3,1,l}$	4.0716×10^{-2}	3.9936×10^{-2}	6.1422×10^{-2}	7.0861×10^{-2}
$\delta_{3,2,l}$	9.5257×10^{-3}	9.1378×10^{-3}	2.9295×10^{-2}	6.1582×10^{-2}
$\delta_{4,1,l}$	1.2453×10^{-1}	1.2304×10^{-1}	1.2325×10^{-1}	1.1588×10^{-1}
$\delta_{4,2,l}$	4.4543×10^{-2}	4.3678×10^{-2}	6.7407×10^{-2}	7.4294×10^{-2}
δ_{ijl}	$l=9$	$l=10$		
$\delta_{1,1,l}$	4.7940×10^{-2}	2.0240×10^{-2}		
$\delta_{1,2,l}$	4.1324×10^{-2}	2.8190×10^{-2}		
$\delta_{2,1,l}$	5.5793×10^{-2}	1.0439×10^{-2}		
$\delta_{2,2,l}$	5.0220×10^{-2}	1.8609×10^{-2}		
$\delta_{3,1,l}$	7.0978×10^{-2}	6.3788×10^{-2}		
$\delta_{3,2,l}$	8.6268×10^{-2}	8.8056×10^{-2}		
$\delta_{4,1,l}$	8.3734×10^{-2}	3.9046×10^{-2}		
$\delta_{4,2,l}$	7.3373×10^{-2}	5.6481×10^{-2}		

3.3 Conclusion

In this chapter, the stability analysis of PFMB control system equipped with IT2 membership functions has been conducted. The imperfectly matched membership functions have been considered and the information of IT2 membership functions has been contained in the analysis, which contributes to further relaxation of the stability conditions. Three approaches for developing the stability conditions of the IT2 PFMB control systems have been proposed. The first approach is able to achieve more relaxed stability conditions through utilizing the information of membership functions in sub-domains. The second approach can relax the sta-

bility conditions by introducing polynomial-approximation-functions instead. The third approach can obtain relaxed stability conditions by employing polynomial-approximation-functions to approximate the original IT2 membership functions in sub-domains. Simulation examples have been presented to show the effectiveness of the proposed approaches.

Chapter 4

Output-Feedback Tracking Control Design of IT2 PFMB Control System

In this chapter, the output tracking control issues of polynomial-fuzzy-model-based (PFMB) systems equipped with mismatched interval type-2 (IT2) membership functions are investigated. The output-feedback tracking control system is shown in Fig. 4.1 and the control objective is to attenuate the difference between the output of the nonlinear plant represented by an IT2 polynomial fuzzy model ($\mathbf{y}(t)$) and the reference model ($\mathbf{y_r}(t)$) as much as possible by proper control input $\mathbf{u}(t)$. The output-feedback IT2 polynomial fuzzy controller connected with the nonlinear plant in a closed loop drives the system states of the nonlinear plant to track those of a stable reference model. The system stability is investigated based on the Lyapunov stability theory under the sum-of-squares (SOS)-based analysis approach and the SOS-based stability conditions are derived subjecting to an H_∞ performance. In addition, the IT2 polynomial fuzzy controller does not need to share the same membership functions with the plant. Moreover, the information of membership functions is included in the analysis to facilitate the analysis and relax the stability conditions. Numerical and experimental examples are presented to verify the effectiveness of the proposed tracking control approach.

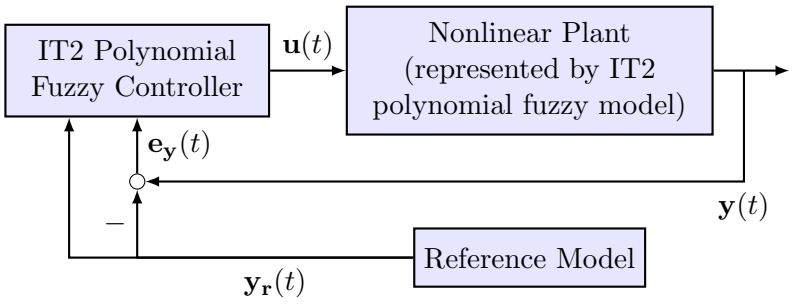

Figure 4.1: A block diagram of IT2 PFMB output feedback tracking control systems.

4.1 Reference Model and IT2 Polynomial Fuzzy Controller

The IT2 fuzzy model used in the tracking control system is defined in the same way in Chapter 2, which can be found in section 2.2.1. Here we need only define the reference model used to be tracked and the IT2 fuzzy controller for tracking design.

4.1.1 Reference Model

A stable reference model is defined as follows:

$$\begin{aligned}\dot{\mathbf{x}}_{\mathbf{r}}(t) &= \mathbf{A}_{\mathbf{r}}\hat{\mathbf{x}}_{\mathbf{r}}(\mathbf{x}_{\mathbf{r}}(t)) + \mathbf{B}_{\mathbf{r}}\mathbf{r}(t),\\ \mathbf{y}_{\mathbf{r}}(t) &= \mathbf{C}\hat{\mathbf{x}}_{\mathbf{r}}(\mathbf{x}_{\mathbf{r}}(t)),\end{aligned} \tag{4.1}$$

where $\mathbf{x}_{\mathbf{r}}(t) \in \Re^n$ is the state vector of the reference model, which needs to be followed by the fuzzy model, $\hat{\mathbf{x}}_{\mathbf{r}}(\mathbf{x}_{\mathbf{r}}(t)) \in \Re^N$ is a vector of monomials in $\mathbf{x}_{\mathbf{r}}(t)$ as the entries, $\mathbf{A}_{\mathbf{r}} \in \Re^{n\times N}$ and $\mathbf{B}_{\mathbf{r}} \in \Re^{n\times m}$ are the constant system and input matrices, respectively, $\mathbf{r}(t) \in \Re^m$ is the reference input vector, $\mathbf{y}_{\mathbf{r}}(t) \in \Re^q$ is the output vector of the reference model.

4.1.2 IT2 Output-Feedback Polynomial Fuzzy Controller

An output-feedback polynomial fuzzy controller is proposed to drive the system states of the nonlinear plant in the form of (2.12) to follow those of the stable reference model (4.1).

Define the state error in polynomial form as

$$\hat{\mathbf{e}}(t) = \hat{\mathbf{x}}(\mathbf{x}(t)) - \hat{\mathbf{x}}_{\mathbf{r}}(\mathbf{x}_{\mathbf{r}}(t)). \tag{4.2}$$

From (2.12), (4.1) and (4.2), the output error is defined as follows:

$$\mathbf{e}_{\mathbf{y}}(t) = \mathbf{y}(t) - \mathbf{y}_{\mathbf{r}}(t) = \mathbf{C}\hat{\mathbf{e}}(t). \tag{4.3}$$

An output-feedback IT2 polynomial fuzzy controller with c rules is employed to stabilise the plant represented by the IT2 polynomial fuzzy model (2.12). The format of the IT2 polynomial fuzzy controller is as follows:

$$\begin{aligned}\text{Rule } j : \text{IF } g_1(\mathbf{y}(t)) \text{ is } \tilde{N}_1^j \text{ AND } \cdots \text{ AND } g_\Omega(\mathbf{y}(t)) \text{ is } \tilde{N}_\Omega^j\\ \text{THEN } \mathbf{u}(t) = \mathbf{F}_j(\mathbf{h}(t))\mathbf{e}_{\mathbf{y}}(t) + \mathbf{G}_j(\mathbf{h}(t))\mathbf{y}_{\mathbf{r}}(t),\end{aligned} \tag{4.4}$$

where $\tilde{N}_\beta^j$ is an IT2 fuzzy term of rule j corresponding to function $g_\beta(\mathbf{y}(t))$, where $\beta = 1, 2, \ldots, \Omega$ and $j = 1, 2, \ldots, c$; Ω is a positive integer. Define $\mathbf{h}(t) =$

$[\mathbf{y}(t) \quad \mathbf{y_r}(t)]$. $\mathbf{F}_j(\mathbf{h}(t)) \in \Re^{m\times q}$ and $\mathbf{G}_j(\mathbf{h}(t)) \in \Re^{m\times q}$, $j = 1, 2,\ldots, c$, are the polynomial gains to be determined. Along the same way in fuzzy model, the membership grade function of the j-th rule is within the following interval sets:

$$\tilde{m}_j(\mathbf{y}(t)) \in [\prod_{\beta=1}^{\Omega} \underline{\mu}_{\tilde{N}_\beta^j}(g_\beta(\mathbf{y}(t))), \prod_{\beta=1}^{\Omega} \overline{\mu}_{\tilde{N}_\beta^j}(g_\beta(\mathbf{y}(t)))], \quad j = 1, 2, \ldots, c \tag{4.5}$$

and we define

$$m_j^L(\mathbf{y}(t)) = \prod_{r=1}^{\Omega} \underline{\mu}_{\tilde{N}_\beta^j}(g_\beta(\mathbf{y}(t))), \tag{4.6}$$

$$m_j^U(\mathbf{y}(t)) = \prod_{r=1}^{\Omega} \overline{\mu}_{\tilde{N}_\beta^j}(g_\beta(\mathbf{y}(t))), \tag{4.7}$$

in which $0 \leq \overline{\mu}_{\tilde{N}_\beta^j}(g_\beta(\mathbf{y}(t))) \leq 1$ and $0 \leq \underline{\mu}_{\tilde{N}_\beta^i}(g_\beta(\mathbf{y}(t))) \leq 1$ denote the upper and lower grades of membership governed by the upper and lower membership functions, respectively. By the definition of IT2 membership functions, the property $0 \leq \underline{\mu}_{\tilde{N}_\beta^j}(g_\beta(\mathbf{y}(t))) \leq \overline{\mu}_{\tilde{N}_\beta^j}(g_\beta(\mathbf{y}(t))) \leq 1$ holds and further leads to the $0 \leq m_j^L(\mathbf{y}(t)) \leq m_j^U(\mathbf{y}(t)) \leq 1$ valid for all j.

Also we define $\tilde{m}_j(\mathbf{y}(t))$ as follows:

$$\tilde{m}_j(\mathbf{y}(t)) = \underline{\kappa}_j(\mathbf{y}(t))m_j^L(\mathbf{y}(t)) + \overline{\kappa}_j(\mathbf{y}(t))m_j^U(\mathbf{y}(t)), \tag{4.8}$$

$$0 \leq \underline{\kappa}_j(\mathbf{y}(t)) \leq 1, \tag{4.9}$$

$$0 \leq \overline{\kappa}_j(\mathbf{y}(t)) \leq 1, \tag{4.10}$$

$$\underline{\kappa}_j(\mathbf{y}(t)) + \overline{\kappa}_j(\mathbf{y}(t)) = 1 \; \forall \; j, \tag{4.11}$$

where $\underline{\kappa}_j(\mathbf{y}(t))$ and $\overline{\kappa}_j(\mathbf{y}(t))$ are nonlinear functions to be determined.

The IT2 polynomial fuzzy controller is described by

$$\mathbf{u}(t) = \sum_{j=1}^{c} \tilde{m}_j(\mathbf{y}(t))(\mathbf{F}_j(\mathbf{h}(t))\mathbf{C}\hat{\mathbf{e}}(t) + \mathbf{G}_j(\mathbf{h}(t))\mathbf{y_r}(t)), \tag{4.12}$$

where

$$\sum_{i=1}^{c} \tilde{m}_j(\mathbf{y}(t)) = 1, \quad \tilde{m}_j(\mathbf{y}(t)) \geq 0 \; \forall \; j. \tag{4.13}$$

4.2 Stability Analysis

For brevity, in the following analysis in this chapter, $\tilde{w}_i(\mathbf{y}(t))$ is denoted as $\tilde{w}_i$ and $\tilde{m}_j(\mathbf{y}(t))$ is denoted as $\tilde{m}_j$, also the time t associated with the variables is dropped for the situation without ambiguity, e.g., $\mathbf{h}(t)$, $\mathbf{x}(t)$, $\hat{\mathbf{x}}_\mathbf{r}(\mathbf{x}_\mathbf{r}(t))$ and $\hat{\mathbf{x}}(\mathbf{x}(t))$ are denoted as $\mathbf{h}$, $\mathbf{x}$, $\hat{\mathbf{x}}_\mathbf{r}(\mathbf{x}_\mathbf{r})$ and $\hat{\mathbf{x}}(\mathbf{x})$, respectively.

Considering the polynomial fuzzy model (2.12) and the output-feedback polynomial fuzzy controller (4.4), we have the following close-loop dynamic equation:

$$\dot{\mathbf{x}} = \sum_{i=1}^{p}\sum_{j=1}^{c} \tilde{w}_i\tilde{m}_j(\mathbf{A}_i(\mathbf{x})+\mathbf{B}_i(\mathbf{x})\mathbf{F}_j(\mathbf{h})\mathbf{C})\hat{\mathbf{e}}+\sum_{i=1}^{p}\sum_{j=1}^{c} \tilde{w}_i\tilde{m}_j(\mathbf{A}_i(\mathbf{x})+\mathbf{B}_i(\mathbf{x})\mathbf{G}_j(\mathbf{h})\mathbf{C})\hat{\mathbf{x}}_\mathbf{r}(\mathbf{x}_\mathbf{r}), \tag{4.14}$$

in which $\mathbf{x} = [x_1, x_2, \ldots, x_n]^T$ and $\hat{\mathbf{x}}(\mathbf{x}) = [\hat{x}_1(\mathbf{x}), \hat{x}_2(\mathbf{x}), \ldots, \hat{x}_N(\mathbf{x})]$.

The relationship between $\dot{\hat{\mathbf{x}}}$ and $\dot{\mathbf{x}}$ is as follows:

$$\dot{\hat{\mathbf{x}}} = \frac{\partial\hat{\mathbf{x}}}{\partial\mathbf{x}}\frac{d\mathbf{x}}{dt} = \mathbf{T}(\mathbf{x})\dot{\mathbf{x}}, \tag{4.15}$$

in which $\mathbf{T}(\mathbf{x}) \in \Re^{N\times n}$ with its $\alpha\beta$-th element $T_{\alpha\beta}(\mathbf{x})$ defined as

$$T_{\alpha\beta}(\mathbf{x}) = \frac{\partial\hat{x}_\alpha(\mathbf{x})}{\partial x_\beta}, \alpha = 1, 2, \ldots, N; \beta = 1, 2, \ldots, n. \tag{4.16}$$

Through combining (4.14) with (4.15), the polynomial dynamic model can be obtained as follows:

$$\dot{\hat{\mathbf{x}}} = \sum_{i=1}^{p}\sum_{j=1}^{c} \tilde{w}_i\tilde{m}_j(\tilde{\mathbf{A}}_i(\mathbf{x})+\tilde{\mathbf{B}}_i(\mathbf{x})\mathbf{F}_j(\mathbf{h})\mathbf{C})\hat{\mathbf{e}}+\sum_{i=1}^{p}\sum_{j=1}^{c} \tilde{w}_i\tilde{m}_j(\tilde{\mathbf{A}}_i(\mathbf{x})+\tilde{\mathbf{B}}_i(\mathbf{x})\mathbf{G}_j(\mathbf{h})\mathbf{C})\hat{\mathbf{x}}_\mathbf{r}(\mathbf{x}_\mathbf{r}), \tag{4.17}$$

where $\tilde{\mathbf{A}}_i(\mathbf{x}) = \mathbf{T}(\mathbf{x})\mathbf{A}_i(\mathbf{x})$, $\tilde{\mathbf{B}}_i(\mathbf{x}) = \mathbf{T}(\mathbf{x})\mathbf{B}_i(\mathbf{x})$. Similarly, denote $\mathbf{x}_\mathbf{r} = [x_{r_1}, x_{r_2}, \ldots, x_{r_n}]^T$ and $\hat{\mathbf{x}}(\mathbf{x}_\mathbf{r}) = [\hat{x}_{r_1}(\mathbf{x}_\mathbf{r}), \hat{x}_{r_2}(\mathbf{x}_\mathbf{r}), \ldots, \hat{x}_{r_N}(\mathbf{x}_\mathbf{r})]^T$. From (4.1), we have the polynomial dynamic model for the reference model:

$$\dot{\hat{\mathbf{x}}}(\mathbf{x}_\mathbf{r}) = \frac{\partial\hat{\mathbf{x}}_\mathbf{r}(\mathbf{x}_\mathbf{r})}{\partial\mathbf{x}_\mathbf{r}}\frac{d\mathbf{x}_\mathbf{r}}{dt} = \mathbf{H}(\mathbf{x}_\mathbf{r})\dot{\mathbf{x}}_\mathbf{r} = \tilde{\mathbf{A}}_\mathbf{r}\hat{\mathbf{x}}(\mathbf{x}_\mathbf{r}) + \tilde{\mathbf{B}}_\mathbf{r}\mathbf{r}, \tag{4.18}$$

where $\tilde{\mathbf{A}}_\mathbf{r} = \mathbf{H}(\mathbf{x}_\mathbf{r})\mathbf{A}_\mathbf{r}$, $\tilde{\mathbf{B}}_\mathbf{r} = \mathbf{H}(\mathbf{x}_\mathbf{r})\mathbf{B}_\mathbf{r}$ and $\mathbf{H}(\mathbf{x}_\mathbf{r}) \in \Re^{N\times n}$ with its $\alpha\beta$-th element is defined as

$$H_{\alpha\beta}(\mathbf{x}_\mathbf{r}) = \frac{\partial\hat{x}_{r_\alpha}(\mathbf{x})}{\partial x_{r_\beta}}, \alpha = 1, 2, \ldots, N; \beta = 1, 2, \ldots, n. \tag{4.19}$$

From the polynomial dynamic models for the plant and reference, the state error can be achieved as

$$\begin{aligned}
\dot{\hat{\mathbf{e}}} &= \dot{\hat{\mathbf{x}}}(\mathbf{x}) - \dot{\hat{\mathbf{x}}}(\mathbf{x}_\mathbf{r}) \\
&= \sum_{i=1}^{p}\sum_{j=1}^{c} \tilde{w}_i\tilde{m}_j(\tilde{\mathbf{A}}_i(\mathbf{x}) + \tilde{\mathbf{B}}_i(\mathbf{x})\mathbf{F}_j(\mathbf{h})\mathbf{C})\hat{\mathbf{e}} \\
&+ \sum_{i=1}^{p}\sum_{j=1}^{c} \tilde{w}_i\tilde{m}_j(\tilde{\mathbf{A}}_i(\mathbf{x}) - \tilde{\mathbf{A}}_\mathbf{r} + \tilde{\mathbf{B}}_i(\mathbf{x})\mathbf{G}_j(\mathbf{h})\mathbf{C})\hat{\mathbf{x}}_\mathbf{r}(\mathbf{x}_\mathbf{r}) - \tilde{\mathbf{B}}_\mathbf{r}\mathbf{r}.
\end{aligned} \tag{4.20}$$

4.2.1 Basic Stability Analysis

To facilitate the stability analysis of error system (4.20), we define an augmented vector $\hat{\mathbf{v}} = \mathbf{\Gamma}^{-1}\hat{\mathbf{e}}$, where $\mathbf{\Gamma} = [\mathbf{C}^T(\mathbf{C}\mathbf{C}^T)^{-1} \quad ortc(\mathbf{C}^T)] \in \Re^{N\times N}$ and ortc$(\mathbf{C}^T)$ denotes the orthogonal complement of $\mathbf{C}^T$ [71, 80]. Consequently, we have $\mathbf{C}\mathbf{\Gamma} = [\mathbf{I}_l \quad \mathbf{0}]$, where $\mathbf{I}_q \in \Re^{q\times q}$ is the identity matrix.

Furthermore, we define $0 < \mathbf{X}(\tilde{\mathbf{x}}) = \mathbf{X}(\tilde{\mathbf{x}})^T = \begin{bmatrix} \mathbf{X}_{11} & 0 \\ 0 & \mathbf{X}_{22}(\tilde{\mathbf{x}}) \end{bmatrix} \in \Re^{N\times N}$ [71, 80], $\mathbf{X}_{11} \in \Re^{q\times q}$ and $\mathbf{X}_{22}(\tilde{\mathbf{x}}) \in \Re^{(N-q)\times(N-q)}$; $\tilde{\mathbf{x}} = (x_{j_1}, x_{j_2}, \ldots, x_{j_q}, x_{r_{k_1}}, x_{r_{k_2}}, \ldots, x_{r_{k_s}})$; the row indices $\mathbf{J} = \{j_1, j_2, \ldots, j_q\}$ and $\mathbf{K} = \{k_1, k_2, \ldots, k_s\}$ are the rows indicating that the entire row of $\mathbf{B}_i(\mathbf{x_r})$ and $\mathbf{B_r}(\mathbf{x})$ are all zeros, respectively [36]. As $\mathbf{X}(\tilde{\mathbf{x}})$ is required to be positive definite, it implies that the inverse of $\mathbf{X}_{11}$ and $\mathbf{X}_{22}(\tilde{\mathbf{x}})$ exist.

Using the fact that $\mathbf{F}_j(\mathbf{h})\mathbf{C}\mathbf{\Gamma}\mathbf{X}(\tilde{\mathbf{x}}) = [\mathbf{M}_j(\mathbf{h}) \quad \mathbf{0}]$ and $\mathbf{G}_j(\mathbf{h})\mathbf{C}\mathbf{\Gamma}\mathbf{X}(\tilde{\mathbf{x}}) = [\mathbf{N}_j(\mathbf{h}) \quad \mathbf{0}]$, where $\mathbf{M}_j(\mathbf{h}) = \mathbf{F}_j(\mathbf{h})\mathbf{X}_{11} \in \Re^{m\times q}$ and $\mathbf{N}_j(\mathbf{h}) = \mathbf{G}_j(\mathbf{h})\mathbf{X}_{11} \in \Re^{m\times q}$, it follows from (4.20) and the augmented vector $\hat{\mathbf{v}}$ that we obtain the augmented system dynamics $\dot{\hat{\mathbf{v}}}$ as follows:

$$
\begin{aligned}
\dot{\hat{\mathbf{v}}} &= \mathbf{\Gamma}^{-1}\dot{\hat{\mathbf{e}}} \\
&= \sum_{i=1}^{p}\sum_{j=1}^{c} \tilde{w}_i\tilde{m}_j(\mathbf{\Gamma}^{-1}\tilde{\mathbf{A}}_i(\mathbf{x}) + \mathbf{\Gamma}^{-1}\tilde{\mathbf{B}}_i(\mathbf{x})\mathbf{F}_j(\mathbf{h})\mathbf{C})\hat{\mathbf{e}} \\
&+ \sum_{i=1}^{p}\sum_{j=1}^{c} \tilde{w}_i\tilde{m}_j(\mathbf{\Gamma}^{-1}(\tilde{\mathbf{A}}_i(\mathbf{x}) - \tilde{\mathbf{A}}_{\mathbf{r}}) + \mathbf{\Gamma}^{-1}\tilde{\mathbf{B}}_i(\mathbf{x})\mathbf{G}_j(\mathbf{h})\mathbf{C})\hat{\mathbf{x}}_{\mathbf{r}}(\mathbf{x_r}) - \mathbf{\Gamma}^{-1}\tilde{\mathbf{B}}_{\mathbf{r}}\mathbf{r} \\
&= \sum_{i=1}^{p}\sum_{j=1}^{c} \tilde{w}_i\tilde{m}_j(\mathbf{\Gamma}^{-1}\tilde{\mathbf{A}}_i(\mathbf{x})\mathbf{\Gamma}\mathbf{X}(\tilde{\mathbf{x}}) + \mathbf{\Gamma}^{-1}\tilde{\mathbf{B}}_i(\mathbf{x})\mathbf{F}_j(\mathbf{h})\mathbf{C}\mathbf{\Gamma}\mathbf{X}(\tilde{\mathbf{x}}))\mathbf{X}(\tilde{\mathbf{x}})^{-1}\mathbf{\Gamma}^{-1}\hat{\mathbf{e}} \\
&+ \sum_{i=1}^{p}\sum_{j=1}^{c} \tilde{w}_i\tilde{m}_j(\mathbf{\Gamma}^{-1}(\tilde{\mathbf{A}}_i(\mathbf{x}) - \tilde{\mathbf{A}}_{\mathbf{r}})\mathbf{\Gamma}\mathbf{X}(\tilde{\mathbf{x}}) + \mathbf{\Gamma}^{-1}\tilde{\mathbf{B}}_i(\mathbf{x})\mathbf{G}_j(\mathbf{h})\mathbf{C}\mathbf{\Gamma}\mathbf{X}(\tilde{\mathbf{x}}))\mathbf{X}(\tilde{\mathbf{x}})^{-1}\mathbf{\Gamma}^{-1}\hat{\mathbf{x}}_{\mathbf{r}}(\mathbf{x_r}) \\
&- \mathbf{\Gamma}^{-1}\tilde{\mathbf{B}}_{\mathbf{r}}\mathbf{r} \\
&= \sum_{i=1}^{p}\sum_{j=1}^{c} \tilde{w}_i\tilde{m}_j(\mathbf{\Gamma}^{-1}\tilde{\mathbf{A}}_i(\mathbf{x})\mathbf{\Gamma}\mathbf{X}(\tilde{\mathbf{x}}) + \mathbf{\Gamma}^{-1}\tilde{\mathbf{B}}_i(\mathbf{x}) \times [\mathbf{M}_j(\mathbf{h}) \quad \mathbf{0}])\mathbf{X}(\tilde{\mathbf{x}})^{-1}\hat{\mathbf{v}} \\
&+ \sum_{i=1}^{p}\sum_{j=1}^{c} \tilde{w}_i\tilde{m}_j(\mathbf{\Gamma}^{-1}(\tilde{\mathbf{A}}_i(\mathbf{x}) - \tilde{\mathbf{A}}_{\mathbf{r}})\mathbf{\Gamma}\mathbf{X}(\tilde{\mathbf{x}}) + \mathbf{\Gamma}^{-1}\tilde{\mathbf{B}}_i(\mathbf{x}) \\
&\times [\mathbf{N}_j(\mathbf{h}) \quad \mathbf{0}])\mathbf{X}(\tilde{\mathbf{x}})^{-1}\mathbf{\Gamma}^{-1}\hat{\mathbf{x}}_{\mathbf{r}}(\mathbf{x_r}) - \mathbf{\Gamma}^{-1}\tilde{\mathbf{B}}_{\mathbf{r}}\mathbf{r} \\
&= \sum_{i=1}^{p}\sum_{j=1}^{c} \tilde{w}_i\tilde{m}_j\mathbf{\Phi}_{ij}(\mathbf{x}, \mathbf{x_r})\mathbf{z}, \qquad (4.21)
\end{aligned}
$$

where $\mathbf{\Phi}_{ij}(\mathbf{x}, \mathbf{x_r}) = [\mathbf{\Phi}_{ij}^{(1)}(\mathbf{x}, \mathbf{x_r}) \quad \mathbf{\Phi}_{ij}^{(2)}(\mathbf{x}, \mathbf{x_r}) \quad \mathbf{\Phi}_{ij}^{(3)}(\mathbf{x}, \mathbf{x_r})]$, $\mathbf{\Phi}_{ij}^{(1)}(\mathbf{x}, \mathbf{x_r}) = \mathbf{\Gamma}^{-1}\tilde{\mathbf{A}}_i(\mathbf{x})\mathbf{\Gamma}\mathbf{X}(\tilde{\mathbf{x}}) + \mathbf{\Gamma}^{-1}\tilde{\mathbf{B}}_i(\mathbf{x}) \times [\mathbf{M}_j(\mathbf{h}) \quad \mathbf{0}]$, $\mathbf{\Phi}_{ij}^{(2)}(\mathbf{x}, \mathbf{x_r}) = \mathbf{\Gamma}^{-1}(\tilde{\mathbf{A}}_i(\mathbf{x}) - \tilde{\mathbf{A}}_{\mathbf{r}})\mathbf{\Gamma} + \mathbf{\Gamma}^{-1}\tilde{\mathbf{B}}_i(\mathbf{x}) \times [\mathbf{N}_j(\mathbf{h}) \quad \mathbf{0}]$,

$\mathbf{\Phi}_{ij}^{(3)}(\mathbf{x},\mathbf{x_r}) = -\mathbf{\Gamma}^{-1}\tilde{\mathbf{B}}_\mathbf{r}$, $\mathbf{z} = \begin{bmatrix}\mathbf{z}_1\\ \mathbf{z}_2\\ \mathbf{z}_3\end{bmatrix} = \begin{bmatrix}\mathbf{X}(\tilde{\mathbf{x}})^{-1}\hat{\mathbf{v}}\\ \mathbf{X}(\tilde{\mathbf{x}})^{-1}\mathbf{\Gamma}^{-1}\mathbf{x_r}\\ \mathbf{r}\end{bmatrix} = \begin{bmatrix}\mathbf{X}(\tilde{\mathbf{x}})^{-1}\mathbf{\Gamma}^{-1}\hat{\mathbf{e}}\\ \mathbf{X}(\tilde{\mathbf{x}})^{-1}\mathbf{\Gamma}^{-1}\mathbf{x_r}\\ \mathbf{r}\end{bmatrix}$. Before proceeding further, the lemma 2 is introduced to support the stability analysis.

With Lemma 2, the term $\frac{d\mathbf{X}(\tilde{\mathbf{x}})^{-1}}{dt}$ appearing in the following analysis can be written as follows.

$$\begin{aligned}\frac{d\mathbf{X}(\tilde{\mathbf{x}})^{-1}}{dt} &= \sum_{k=1}^{n}\Big(\frac{\partial\mathbf{X}(\tilde{\mathbf{x}})^{-1}}{\partial x_k}\dot{x}_k + \frac{\partial\mathbf{X}(\tilde{\mathbf{x}})^{-1}}{\partial x_{rk}}\dot{x}_{rk}\Big)\\ &= -\sum_{k\in\mathbf{J}}\mathbf{X}(\tilde{\mathbf{x}})^{-1}\Big(\frac{\partial\mathbf{X}(\tilde{\mathbf{x}})}{\partial x_k}\sum_{i=1}^{p}w_i\mathbf{A}_i^{(k)}(\mathbf{x})\hat{\mathbf{x}}(\mathbf{x})\Big)\mathbf{X}(\tilde{\mathbf{x}})^{-1}\\ &\quad -\sum_{k\in\mathbf{K}}\mathbf{X}(\tilde{\mathbf{x}})^{-1}\Big(\frac{\partial\mathbf{X}(\tilde{\mathbf{x}})}{\partial x_{rk}}\mathbf{A}_r^{(k)}(\mathbf{x})\hat{\mathbf{x}}_\mathbf{r}(\mathbf{x_r})\Big)\mathbf{X}(\tilde{\mathbf{x}})^{-1}. \qquad (4.22)\end{aligned}$$

Consider the following polynomial Lyapunov function candidate to investigate the stability of the augmented system (4.21):

$$V(t) = \hat{\mathbf{v}}^T\mathbf{X}(\tilde{\mathbf{x}})^{-1}\hat{\mathbf{v}}. \qquad (4.23)$$

It follows from (4.21) and (4.23) that we have

$$\begin{aligned}\dot{V}(t) &= \dot{\hat{\mathbf{v}}}^T\mathbf{X}(\tilde{\mathbf{x}})^{-1}\hat{\mathbf{v}} + \hat{\mathbf{v}}^T\mathbf{X}(\tilde{\mathbf{x}})^{-1}\dot{\hat{\mathbf{v}}} + \hat{\mathbf{v}}^T\frac{d\mathbf{X}(\tilde{\mathbf{x}})^{-1}}{dt}\hat{\mathbf{v}}\\ &= \sum_{i=1}^{p}\sum_{j=1}^{c}\tilde{w}_i\tilde{m}_j\mathbf{z}^T\mathbf{\Phi}_{ij}(\mathbf{x},\mathbf{x_r})\mathbf{z}_1 + \mathbf{z}_1^T\sum_{i=1}^{p}\sum_{j=1}^{c}\tilde{w}_i\tilde{m}_j\mathbf{\Phi}_{ij}\mathbf{z} \qquad (4.24)\\ &\quad + \mathbf{z}_1^T\Big(\sum_{k\in\mathbf{J}}\frac{\partial\mathbf{X}(\tilde{\mathbf{x}})}{\partial x_k}\mathbf{A}_i^{(k)}(\mathbf{x})\hat{\mathbf{x}}(\mathbf{x}) - \sum_{k\in\mathbf{K}}\frac{\partial\mathbf{X}(\tilde{\mathbf{x}})}{\partial x_{rk}}\mathbf{A}_r^{(k)}(\mathbf{x})\hat{\mathbf{x}}_\mathbf{r}(\mathbf{x_r})\Big)\mathbf{z}_1\\ &= \sum_{i=1}^{p}\sum_{j=1}^{c}\tilde{w}_i\tilde{m}_j\mathbf{z}^T\mathbf{\Xi}_{ij}(\mathbf{x},\mathbf{x_r})\mathbf{z} - \mathbf{z}_1^T\mathbf{z}_1 + \sigma_1^2\mathbf{z}_2^T\mathbf{z}_2 + \sigma_2^2\mathbf{z}_3^T\mathbf{z}_3, \qquad (4.25)\end{aligned}$$

where $\mathbf{\Xi}_{ij}(\mathbf{x},\mathbf{x_r}) = \begin{bmatrix}\mathbf{\Xi}_{ij}^{(11)}(\mathbf{x},\mathbf{x_r}) & * & *\\ \mathbf{\Phi}_{ij}^{(2)}(\mathbf{x},\mathbf{x_r})^T & -\sigma_1^2\mathbf{I} & *\\ \mathbf{\Phi}_{ij}^{(3)}(\mathbf{x},\mathbf{x_r})^T & \mathbf{0} & -\sigma_2^2\mathbf{I}\end{bmatrix}$, $\mathbf{\Xi}_{ij}^{11}(\mathbf{x},\mathbf{x_r}) = \mathbf{\Phi}_{ij}^{(1)}(\mathbf{x},\mathbf{x_r}) + \mathbf{\Phi}_{ij}^{(1)}(\mathbf{x},\mathbf{x_r})^T + \mathbf{I} - \sum_{k\in\mathbf{J}}\frac{\partial\mathbf{X}(\tilde{\mathbf{x}})}{\partial x_k}\mathbf{A}_i^{(k)}(\mathbf{x})\hat{\mathbf{x}}(\mathbf{x}) - \sum_{k\in\mathbf{K}}\frac{\partial\mathbf{X}(\tilde{\mathbf{x}})}{\partial x_{rk}}\mathbf{A}_r^{(k)}(\mathbf{x})\hat{\mathbf{x}}_\mathbf{r}(\mathbf{x_r})$.

When

$$\sum_{i=1}^{p}\sum_{j=1}^{c}\tilde{w}_i\tilde{m}_j\mathbf{\Xi}_{ij}(\mathbf{x},\mathbf{x_r}) < 0, \qquad (4.26)$$

we have

$$\dot{V}(t) \le -\mathbf{z}_1^T\mathbf{z}_1 + \sigma_1^2\mathbf{z}_2^T\mathbf{z}_2 + \sigma_2^2\mathbf{z}_3^T\mathbf{z}_3. \qquad (4.27)$$

Considering the termination time of control t_f and taking integration on both

sides of (4.27) with respect to time t, we obtain the following H_∞ performance:

$$\frac{\int_0^{t_f} \mathbf{z}_1^T \mathbf{z}_1 - V(0)}{\int_0^{t_f} (\sigma_1^2 \mathbf{z}_2^T \mathbf{z}_2 + \sigma_2^2 \mathbf{z}_3^T \mathbf{z}_3) dt} \leq 1, \tag{4.28}$$

where the tracking performance can be improved with smaller values of $\sigma_1 > 0$ and $\sigma_2 > 0$.

In order to ensure (4.26) to be valid, the basic stability condition can be derived by requiring $\mathbf{\Xi}_{ij}(\mathbf{x}, \mathbf{x_r}) < 0$ for all i and j. The basic results can be summarized as the following theorem [80]:

Theorem 4.1. *The IT2 PFMB system (4.14), which is formed by a nonlinear plant represented by the IT2 polynomial fuzzy model and the IT2 polynomial fuzzy controller connected in a closed loop, in which the states are driven to follow those of the stable reference model (4.1) subject to H_∞ performance (4.28) if there exist polynomial matrices $\mathbf{M}_j(\mathbf{h}) \in \Re^{m \times q}$, $\mathbf{N}_j(\mathbf{h}) \in \Re^{m \times q}$, $\mathbf{X}(\tilde{\mathbf{x}}) = \mathbf{X}(\tilde{\mathbf{x}})^T \in \Re^{N \times N}$ such that the following SOS-based conditions are satisfied:*

$$\begin{aligned} &\nu^T(\mathbf{X}(\tilde{\mathbf{x}}) - \varepsilon_1(\tilde{\mathbf{x}})\mathbf{I})\nu \text{ is SOS}; \\ &-\rho^T(\mathbf{\Xi}_{ij}(\mathbf{x}, \mathbf{x_r}) + \varepsilon_2(\mathbf{x}, \mathbf{x_r})\mathbf{I})\rho \text{ is SOS} \quad \forall i, j, \end{aligned} \tag{4.29}$$

where $\nu \in \Re^N$ is an arbitrary vector independent of $\mathbf{x}$ and $\mathbf{x_r}$, $\rho \in \Re^{2N+m}$ is an arbitrary vector independent of $\mathbf{x}$ and $\mathbf{x_r}$, $\varepsilon_1(\tilde{\mathbf{x}}) > 0$, $\varepsilon_2(\mathbf{x}, \mathbf{x_r}) > 0$ are predefined scalar polynomials.

Remark 4.1. *From Theorem 4.1, it can be found that the stability conditions are clear and straightforward. However, the information of the membership functions has not been included in the conditions, which means the stability conditions in Theorem 4.1 are unnecessarily valid for all kinds of membership functions. In the real application, only the specific membership functions adopted in the plants and controllers need to be considered. Therefore, there is conservativeness lying in the basic stability conditions. In order to reduce the conservativeness and further relax the stability conditions, the membership-function-dependent analysis will be introduced in the following section.*

4.2.2 Membership-Function-Dependent Stability Analysis

In order to guarantee the stability of the system, the stability condition (4.26) has to be satisfied. However, as $\tilde{w}_i \tilde{m}_j \equiv \tilde{h}_{ij}(\mathbf{y})$ is a function of $\mathbf{y}$, the stability condition (4.26) has to be satisfied for all values of membership grades implying an infinite number of stability conditions. Consequently, when the membership functions $\tilde{h}_{ij}(\mathbf{y})$ are incorporated into the stability conditions, it is not practical to find a feasible solution to the stability conditions of infinite number. In this section, we propose

a technique to bring the information of membership functions into the stability analysis, which avoids turning the number of stability conditions into infinity but still can achieve more relaxed stability conditions.

To facilitate the stability analysis and bring the information of membership functions into the analysis, a discretization process is applied to the membership functions. The whole operating domain Φ is divided into L connected sub-domains, Φ_l, $l = 1, 2, \ldots, L$ such that $\Phi = \bigcup_{l=1}^{L} \Phi_l$. We denote the portion of $\tilde{h}_{ij}(\mathbf{y})$ where $\mathbf{y} \in \Phi_l$ (the portion of $\tilde{h}_{ij}(\mathbf{y})$ in the l-th sub-domain) as $\tilde{h}_{ijl}$ such that $\tilde{h}_{ij}(\mathbf{y}) = \bigcup_{l=1}^{L} \tilde{h}_{ijl}(\mathbf{y})$. Then we can construct the linear and upper linear function in very sub-domain, which guarantee that the FOU in sub-domains is between the upper and lower linear functions.

In the following, we conduct the stability analysis sub-domain by sub-domain by utilizing the information of $\tilde{h}_{ijl}(\mathbf{y})$ for $\mathbf{y} \in \Phi_l$. Once the control system operated in every sub-domain is guaranteed to be stable, the whole control system is guaranteed to be a stable one. We can then rewrite the basic stability condition in the l-th sub-domain as follows:

$$\begin{aligned}
&\sum_{i=1}^{p}\sum_{j=1}^{c} \tilde{h}_{ijl}(\mathbf{y})\mathbf{z}^T\boldsymbol{\Xi}_{ij}(\mathbf{x},\mathbf{x_r})\mathbf{z} \\
&= \sum_{i=1}^{p}\sum_{j=1}^{c} (\underline{h}_{ijl}(\mathbf{y}) + \tilde{h}_{ijl}(\mathbf{y}) - \underline{h}_{ijl}(\mathbf{y}))\mathbf{z}^T\boldsymbol{\Xi}_{ij}(\mathbf{x},\mathbf{x_r})\mathbf{z} < 0, \mathbf{x} \in \Phi_l, l = 1, 2, \ldots, L,
\end{aligned} \tag{4.30}$$

where $\underline{h}_{ijl}(\mathbf{y}) \geq 0$ is a function, which is an estimate of $h_{ijl}(\mathbf{y})$ to be determined and it is always hold that $\underline{h}_{ijl}(\mathbf{y}) \leq h_{ijl}(\mathbf{y})$. Meanwhile, we define some non-negative matrices $\mathbf{Y}_{ijl}(\mathbf{x},\mathbf{x_r}) = \mathbf{Y}_{ijl}(\mathbf{x},\mathbf{x_r})^T \in \Re^{(2N+m)\times(2N+m)} \geq 0$, which is required to satisfy the condition that $\mathbf{Y}_{ijl}(\mathbf{x},\mathbf{x_r}) \geq \boldsymbol{\Xi}_{ij}(\mathbf{x},\mathbf{x_r})$. From (4.30), we have

$$\begin{aligned}
&\sum_{i=1}^{p}\sum_{j=1}^{c} \tilde{h}_{ijl}(\mathbf{y})\mathbf{z}^T\boldsymbol{\Xi}_{ij}(\mathbf{x},\mathbf{x_r})\mathbf{z} \\
&\leq \sum_{i=1}^{p}\sum_{j=1}^{c} \hat{h}_{ijl}(\mathbf{y})\mathbf{z}^T\boldsymbol{\Xi}_{ij}(\mathbf{x},\mathbf{x_r})\mathbf{z} + \sum_{i=1}^{p}\sum_{j=1}^{c} (\tilde{h}_{ijl}(\mathbf{y}) - \underline{h}_{ijl}(\mathbf{y}))\mathbf{z}^T\mathbf{Y}_{ijl}(\mathbf{x},\mathbf{x_r})\mathbf{z} \\
&= \sum_{i=1}^{p}\sum_{j=1}^{c} \mathbf{z}^T\big(\underline{h}_{ijl}(\mathbf{y})\boldsymbol{\Xi}_{ij}(\mathbf{x},\mathbf{x_r}) + (\tilde{h}_{ijl}(\mathbf{y}) - \underline{h}_{ijl}(\mathbf{y}))\mathbf{Y}_{ijl}(\mathbf{x},\mathbf{x_r})\big)\mathbf{z}, \mathbf{x} \in \Phi_l, \\
&l = 1, 2, \ldots, L.
\end{aligned} \tag{4.31}$$

In every sub-domain, we define the functions $\overline{h}_{ijl}(\mathbf{y}) \geq \tilde{h}_{ijl}(\mathbf{y})$. Then the stability condition can be bounded as follows:

$$\sum_{i=1}^{p}\sum_{j=1}^{c} \tilde{h}_{ijl}(\mathbf{y})\mathbf{z}^T\boldsymbol{\Xi}_{ij}(\mathbf{x},\mathbf{x_r})\mathbf{z}$$

$$\leq \sum_{i=1}^{p}\sum_{j=1}^{c} \mathbf{z}^T(\underline{h}_{ijl}(\mathbf{y})\mathbf{\Xi}_{ij}(\mathbf{x},\mathbf{x_r}) + (\overline{h}_{ijl}(\mathbf{y}) - \underline{h}_{ijl}(\mathbf{y}))\mathbf{Y}_{ijl}(\mathbf{x},\mathbf{x_r}))\mathbf{z}$$
$$= \sum_{i=1}^{p}\sum_{j=1}^{c} \mathbf{z}^T(\hat{h}_{ijl}(\mathbf{y})\mathbf{\Xi}_{ij}(\mathbf{x},\mathbf{x_r}) + \delta_{ijl}(\mathbf{y})\mathbf{Y}_{ijl}(\mathbf{x},\mathbf{x_r}))\mathbf{z} < 0, \tag{4.32}$$

where $\delta_{ijl}(\mathbf{y}) = \overline{h}_{ijl}(\mathbf{y}) - \underline{h}_{ijl}(\mathbf{y})$.

In order to further relax the stability analysis results, we bring the state information from each sub-domain into the stability analysis. Defining the slack matrices $\mathbf{S}_l(\mathbf{y}) = \mathbf{S}_l^T(\mathbf{y}) \in \Re^{N\times N} \geq 0$, $l = 1, 2,\ldots, L$, it follows from (4.32) that

$$\dot{V}(t) \leq \sum_{i=1}^{p}\sum_{j=1}^{c} \mathbf{z}^T(\hat{h}_{ijl}(\mathbf{y})\mathbf{\Xi}_{ij}(\mathbf{x},\mathbf{x_r}) + \delta_{ijl}(\mathbf{y})\mathbf{Y}_{ijl}(\mathbf{x},\mathbf{x_r}))\mathbf{z}$$
$$\leq \sum_{i=1}^{p}\sum_{j=1}^{c} \mathbf{z}^T\big(\underline{h}_{ijl}(\mathbf{y})\mathbf{\Xi}_{ij}(\mathbf{x},\mathbf{x_r}) + \delta_{ijl}(\mathbf{y})\mathbf{Y}_{ijl}(\mathbf{x},\mathbf{x_r}) + (\mathbf{y} - \underline{\mathbf{y}}_l)^T\mathbf{D}(\overline{\mathbf{y}}_l - \mathbf{y})\mathbf{S}_l(\mathbf{y})\big)\mathbf{z}, \tag{4.33}$$

where $\underline{\mathbf{y}}_l \in \Re^q$ and $\overline{\mathbf{y}}_l \in \Re^q$ are the lower and upper bound of $\mathbf{y}$ in the l-th sub-domain, $l = 1, 2, \ldots, L$; $\mathbf{D} = \text{diag}\{d_1, d_2, \ldots, d_q\} \in \Re^{q\times q}$ is a diagonal matrix whose element is either 0 or 1. When $d_r = 0$, $r = 1, 2,\ldots, m$, the state information of y_r is not included. Combining the stability condition in (4.26) with the information of membership functions, the results can be summarized as in the following theorem.

Theorem 4.2. *The IT2 PFMB system (4.14), which is formed by a nonlinear plant represented by the IT2 polynomial fuzzy model and the IT2 polynomial fuzzy controller connected in a closed loop, in which the states are driven to follow those of the stable reference model (4.1) subject to H_∞ performance (4.28) if there exist polynomial matrices $\mathbf{S}_l(\mathbf{y}) = \mathbf{S}_l(\mathbf{y})^T \in \Re^{N\times N} \geq 0$, $\mathbf{F}_j(\mathbf{h}) \in \Re^{m\times q}$, $\mathbf{G}_j(\mathbf{h}) \in \Re^{m\times q}$, $\mathbf{X}(\tilde{\mathbf{x}}) = \mathbf{X}(\tilde{\mathbf{x}})^T \in \Re^{N\times N}$, $\mathbf{Y}_{ijl}(\mathbf{x},\mathbf{x_r}) = \mathbf{Y}_{ijl}(\mathbf{x},\mathbf{x_r})^T \in \Re^{N\times N}$, $i = 1, 2, \ldots, p$, $j = 1, 2, \ldots, c$, $l = 1, 2, \ldots, L$, such that the following SOS-based conditions are satisfied:*

$$\begin{aligned}
&\nu^T(\mathbf{S}_l(\mathbf{y}) - \varepsilon_1(\mathbf{y})\mathbf{I})\nu \text{ is SOS} \quad \forall l;\\
&\nu^T(\mathbf{X}(\tilde{\mathbf{x}}) - \varepsilon_2(\tilde{\mathbf{x}})\mathbf{I})\nu \text{ is SOS};\\
&\rho^T(\mathbf{Y}_{ijl}(\mathbf{x},\mathbf{x_r}) - \varepsilon_3(\mathbf{x},\mathbf{x_r})\mathbf{I})\rho \text{ is SOS} \quad \forall i,j,l;\\
&\rho^T(\mathbf{Y}_{ijl}(\mathbf{x},\mathbf{x_r}) - \mathbf{\Xi}_{ij}(\mathbf{x},\mathbf{x_r}) - \varepsilon_4(\mathbf{x},\mathbf{x_r})\mathbf{I})\rho \text{ is SOS} \quad \forall i,j,l;\\
&-\rho^T\big(\sum_{i=1}^{p}\sum_{j=1}^{c}(\underline{h}_{ijl}(\mathbf{y})\mathbf{\Xi}_{ij}(\mathbf{x},\mathbf{x_r}) + \delta_{ijl}(\mathbf{y})\mathbf{Y}_{ijl}(\mathbf{x},\mathbf{x_r})) +\\
&(\mathbf{y} - \underline{\mathbf{y}}_l)^T\mathbf{D}(\overline{\mathbf{y}}_l - \mathbf{y})\mathbf{S}_l(\mathbf{y}) + \varepsilon_5(\mathbf{x},\mathbf{x_r},\mathbf{y})\mathbf{I}\big)\rho \text{ is SOS} \quad \forall l,
\end{aligned} \tag{4.34}$$

where $\nu \in \Re^N$ is an arbitrary vector independent of $\mathbf{x}$, $\mathbf{x_y}$ and $\mathbf{y}$, $\rho \in \Re^{2N+m}$ is an arbitrary vector independent of $\mathbf{x}$, $\mathbf{x_r}$ and $\mathbf{y}$, $\hat{h}_{ijl}(\mathbf{y})$ and $\delta_{ijl}(\mathbf{y})$ are linear functions defined by $\overline{h}_{ijl}(\mathbf{y})$ and $\underline{h}_{ijl}(\mathbf{y})$; $\mathbf{D} = diag\{d_1, d_2, \ldots, d_q\} \in \Re^{q\times q}$ is a predefined di-

agonal matrix; $\varepsilon_1(\mathbf{y}) > 0$, $\varepsilon_2(\tilde{\mathbf{x}}) > 0$, $\varepsilon_3(\mathbf{x}, \mathbf{x_r}) > 0$, $\varepsilon_4(\mathbf{x}, \mathbf{x_r}) > 0$, $\varepsilon_5(\mathbf{x}, \mathbf{x_r}, \mathbf{y}) > 0$ *are predefined scalar polynomials for numerical reason;* $\underline{\mathbf{y}}_l$ *and* $\overline{\mathbf{y}}_l$ *are the predefined lower and upper bounds of* $\mathbf{y}$ *in the l-th sub-domain.*

4.3 Simulation Examples

4.3.1 Numerical Example

Example 1: To demonstrate the effectiveness of the proposed approach, we design a polynomial fuzzy control system equipped with different model and control fuzzy rules to track the states of the reference using only the system output.

Let us consider a three-rule polynomial fuzzy model with $\hat{\mathbf{x}}(\mathbf{x}) = \mathbf{x} = [x_1 \quad x_2]^T$,

$$\mathbf{A}_1(x_1) = \begin{bmatrix} 0.59 - 0.12x_1 & -7.29 - 1.82x_1 \\ 0.01 & -2.85 \end{bmatrix},$$

$$\mathbf{A}_2(x_1) = \begin{bmatrix} 0.02 + 2.25x_1 & -4.64 + 0.72x_1 \\ 0.35 & -8.56 \end{bmatrix},$$

$$\mathbf{A}_3(x_1) = \begin{bmatrix} 0.73 + 0.45x_1 & 8.45 + 2.13x_1 \\ 0.26 & -15.43 \end{bmatrix},$$

$$\mathbf{B}_1(x_1) = \begin{bmatrix} 1 + 1.35x_1 + 2.33x_1^2 \\ 0 \end{bmatrix},$$

$$\mathbf{B}_2(x_1) = \begin{bmatrix} 8 - 0.62x_1 \\ 0 \end{bmatrix},$$

$$\mathbf{B}_3(x_1) = \begin{bmatrix} 4 - 0.73x_1 + 3.35x_1^2 \\ 0.8 \end{bmatrix},$$

$$\mathbf{C} = [1 \quad 0].$$

Give that $\mathbf{C} = [1 \quad 0]$, we have the output $\mathbf{y} = \mathbf{C}\hat{\mathbf{x}}(\mathbf{x}) = x_1$ in this simulation. The membership functions are chosen as $\underline{w}_1(x_1) = 1 - 1/(1 + e^{(-x_1+3.5)})$, $\underline{w}_3(x_1) = 1 - 1/(1 + e^{(-x_1-3.5)})$, $\overline{w}_2(x_1) = 1 - \underline{w}_1(x_1) - \underline{w}_3(x_1)$; $\overline{w}_1(x_1) = 1 - 1/(1 + e^{(-x_1+2.5)})$, $\overline{w}_3(x_1) = 1 - 1/(1 + e^{(-x_1-2.5)})$, $\underline{w}_2(x_1) = 1 - \overline{w}_1(x_1) - \overline{w}_3(x_1)$;

$$\underline{m}_1(x_1) = \begin{cases} 1 & \text{for } x_1 < -5.2 \\ \frac{-x_1+4.8}{10} & \text{for } -5.2 \leq x_1 \leq 4.8 \\ 0 & \text{for } x_1 > 4.8 \end{cases}, \tag{4.35}$$

$$\overline{m}_1(x_1) = \begin{cases} 1 & \text{for } x_1 < -4.8 \\ \frac{-x_1+5.2}{10} & \text{for } -4.8 \leq x_1 \leq 5.2 \\ 0 & \text{for } x_1 > 5.2 \end{cases}, \tag{4.36}$$

$\underline{m}_2(x_1) = 1 - \overline{m}_1(x_1)$ and $\overline{m}_2(x_1) = 1 - \underline{m}_1(x_1)$.

For the reference model, the system and input matrices are

$$\mathbf{A}_r = \begin{bmatrix} -1.5 & -1 \\ -0.3 & -8.5 \end{bmatrix},$$

$$\mathbf{B}_r = \begin{bmatrix} 1 \\ 0 \end{bmatrix},$$

and the output matrix is $\mathbf{C} = [1 \quad 0]$.

It should be noted in this example that the number of fuzzy rules and the membership functions employed for the polynomial model and the polynomial fuzzy controller are different, which can reduce the controller implementation cost when a less number of membership functions is employed in the controller.

Referring to Theorem 4.2, we choose $\varepsilon_1(\mathbf{y}) = \varepsilon_2(\tilde{\mathbf{x}}) = \varepsilon_3(\mathbf{x}, \mathbf{x_r}) = \varepsilon_4(\mathbf{x}, \mathbf{x_r}) = \varepsilon_5(\mathbf{x}, \mathbf{x_y}, \mathbf{y}) = 0.001$; $\mathbf{X}(\tilde{\mathbf{x}})$ as a polynomial of degree 0; $\mathbf{M}_j(x_1)$ and $\mathbf{N}_j(x_1)$, $j = 1, 2, \ldots, c$ are polynomials with monomials in x_1 of degree 0, $\mathbf{S}_l(x_1)$ is of degree 0. Throughout this example, the membership functions $\tilde{w}_i(x_1)$ and $\tilde{m}_j(x_1)$ used in the simulations are gained from type reduction in (2.8) and (4.8) where $\underline{\lambda}_1(x_1) = (\sin(5x_1)+1)/2, \overline{\lambda}_1(x_1) = 1-\underline{\lambda}_1(x_1)$, $\underline{\lambda}_3(x_1) = (\cos(5x_1)+1)/2, \overline{\lambda}_3(x_1) = 1-\underline{\lambda}_3(x_1)$, $\tilde{w}_2(x_1) = 1 - \tilde{w}_1(x_1) - \tilde{w}_3(x_1)$, $\underline{\kappa}_j(x_1) = \overline{\kappa}_j(x_1) = 0.5$, $j = 1, 2$. The number of sub-domains used in the simulation is 20, i.e., $L = 20$. The values of the coefficients of $\underline{h}_{ijl}(\mathbf{y})$ and $\delta_{ijl}(\mathbf{y})$ can be viewed in Table 4.1 to 4.12.

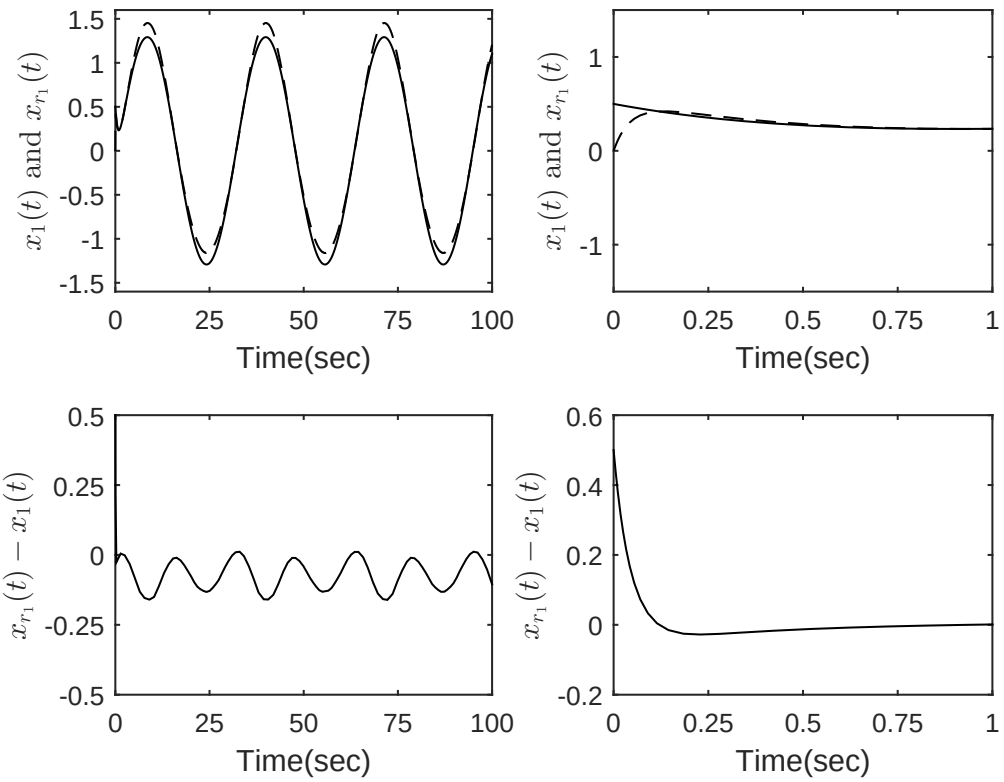

Figure 4.2: Tracking control performance for $x_1(t)$ with $\sigma_1 = 2.4212$ and $\sigma_2 = 0.1507$. On the top left hand side, the sub-figure shows the simulation time from 0 to 100 seconds, on the top right hand side, the simulation time is from 0 to 1 second. The dashed curves are for the controlled trajectory of the response in the fuzzy system $(x_1(t))$, and the solid curves are the trajectory of response in the reference model $(x_{r_1}(t))$. The low two sub-figures show the difference between $x_1(t)$ and $x_{r_1}(t)$.

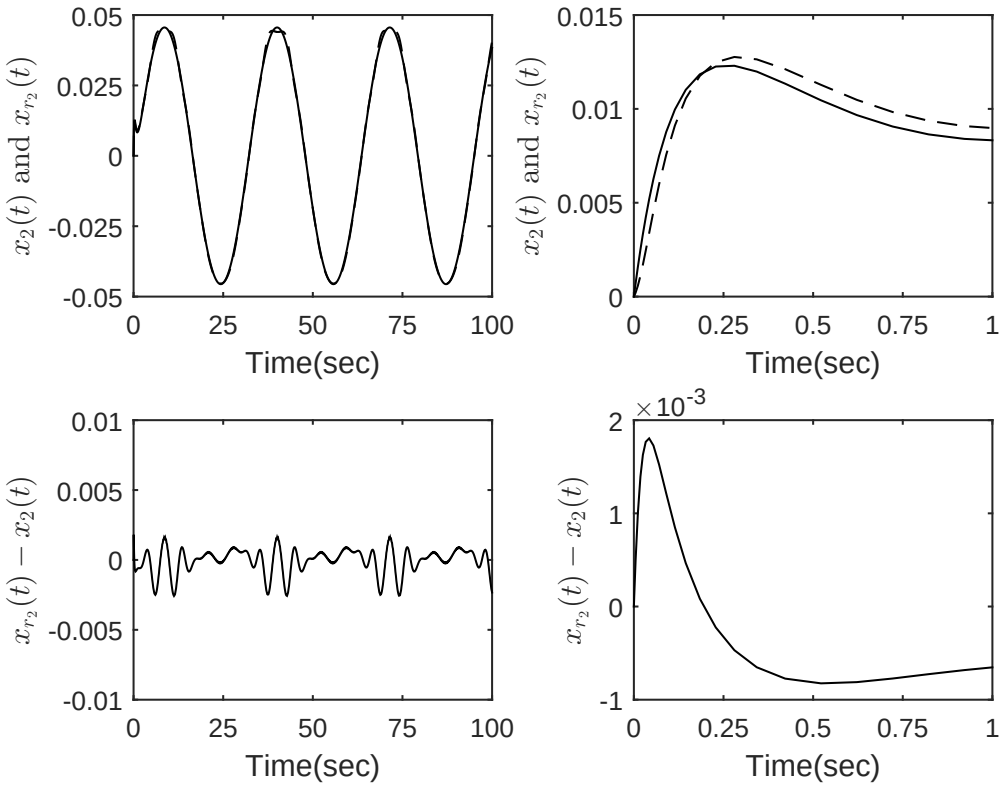

Figure 4.3: Tracking control performance for $x_2(t)$ with $\sigma_1 = 2.4212$ and $\sigma_2 = 0.1507$. On the top left hand side, the sub-figure shows the simulation time from 0 to 100 seconds, on the top right hand side, the simulation time is from 0 to 1 second. The dashed curves are for the controlled trajectory of the response in the fuzzy system $(x_2(t))$, and the solid curves are the trajectory of response in the reference model $(x_{r_2}(t))$. The below two sub-figures show the difference between $x_2(t)$ and $x_{r_2}(t)$.

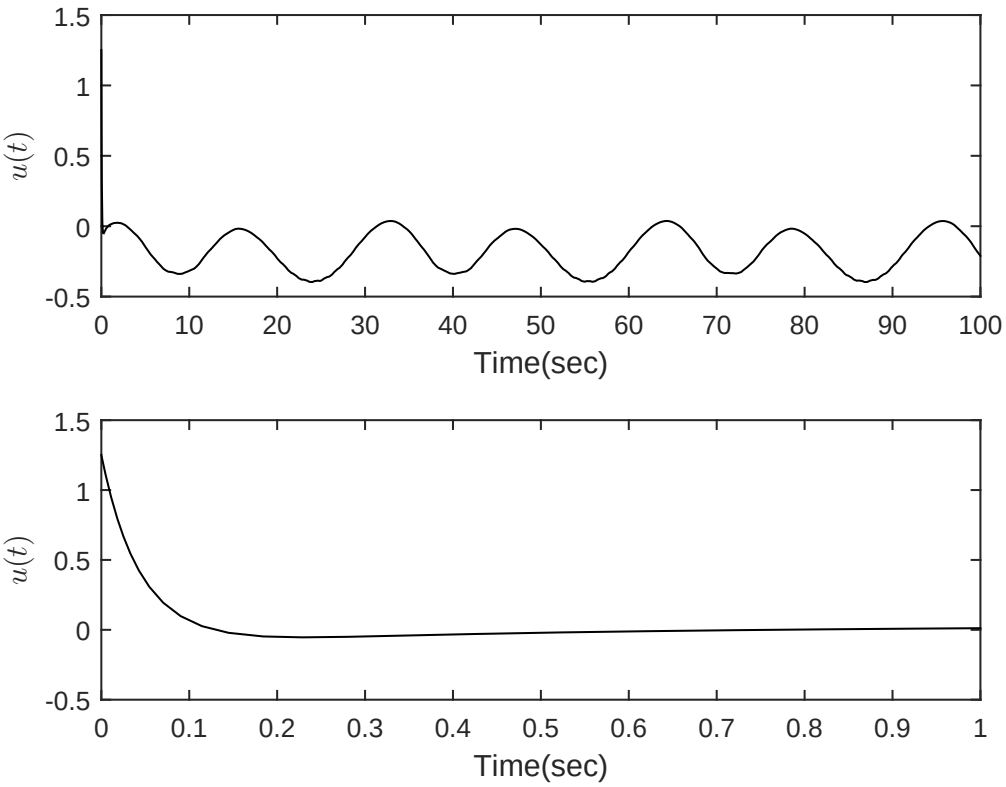

Figure 4.4: The control input with $\sigma_1 = 2.4212$ and $\sigma_2 = 0.1507$. On the top side, the sub-figure shows the simulation time from 0 to 100 seconds, on the down side, the simulation time is from 0 to 1 second.

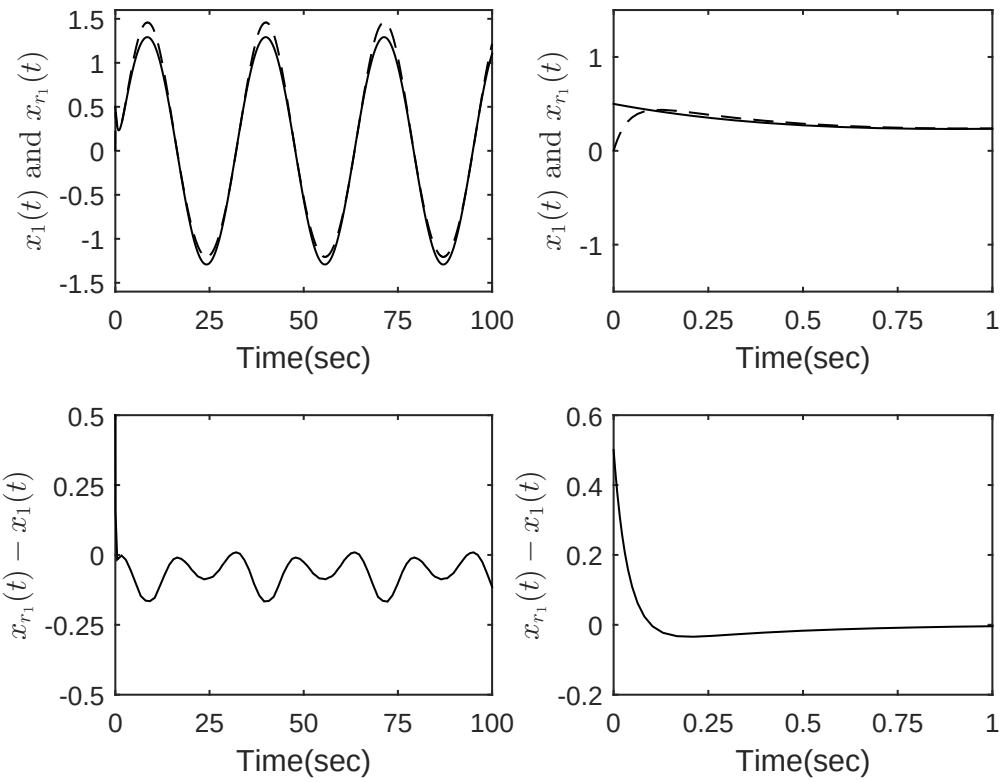

Figure 4.5: Tracking control performance for $x_1(t)$ with $\sigma_1 = 10$ and $\sigma_2 = 10$. On the top left hand side, the sub-figure shows the simulation time from 0 to 100 seconds, on the top right hand side, the simulation time is from 0 to 1 second. The dashed curves are for the controlled trajectory of the response in the fuzzy system ($x_1(t)$), and the solid curves are the trajectory of response in the reference model ($x_{r_1}(t)$). The below two sub-figures show the difference between $x_1(t)$ and $x_{r_1}(t)$.

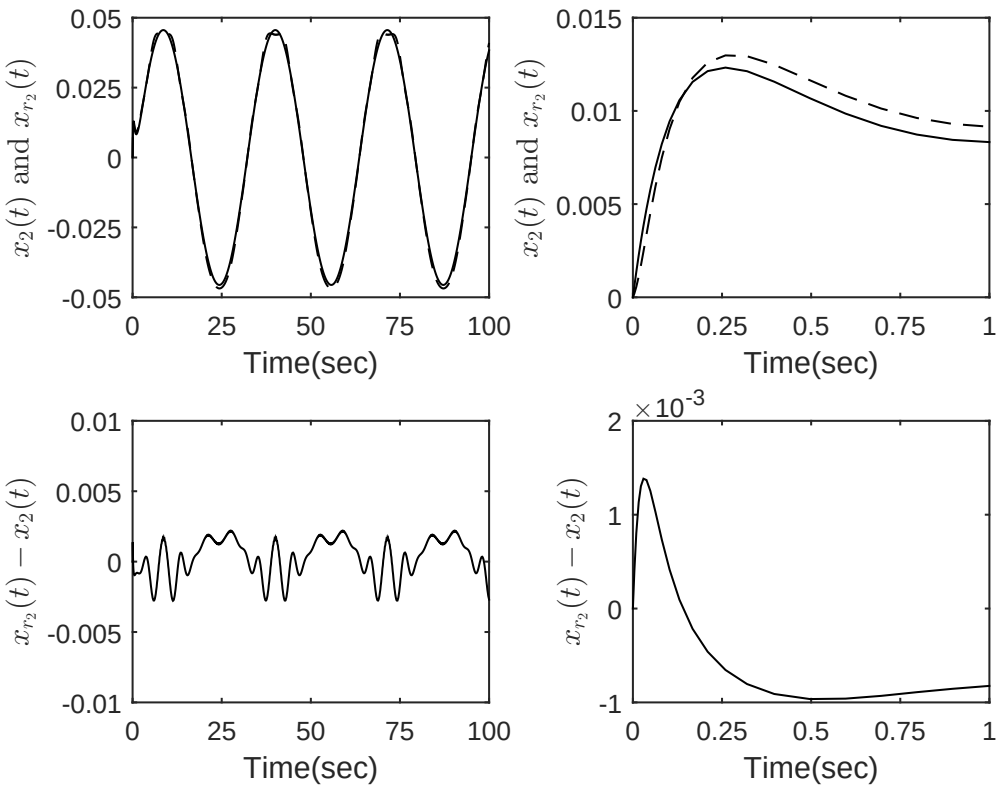

Figure 4.6: Tracking control performance for $x_2(t)$ with $\sigma_1 = 10$ and $\sigma_2 = 10$. On the top left hand side, the sub-figure shows the simulation time from 0 to 100 seconds, on the top right hand side, the simulation time is from 0 to 1 second. The dashed curves are for the controlled trajectory of the response in the fuzzy system ($x_2(t)$), and the solid curves are the trajectory of response in the reference model ($x_{r_2}(t)$). The below two sub-figures show the difference between $x_2(t)$ and $x_{r_2}(t)$.

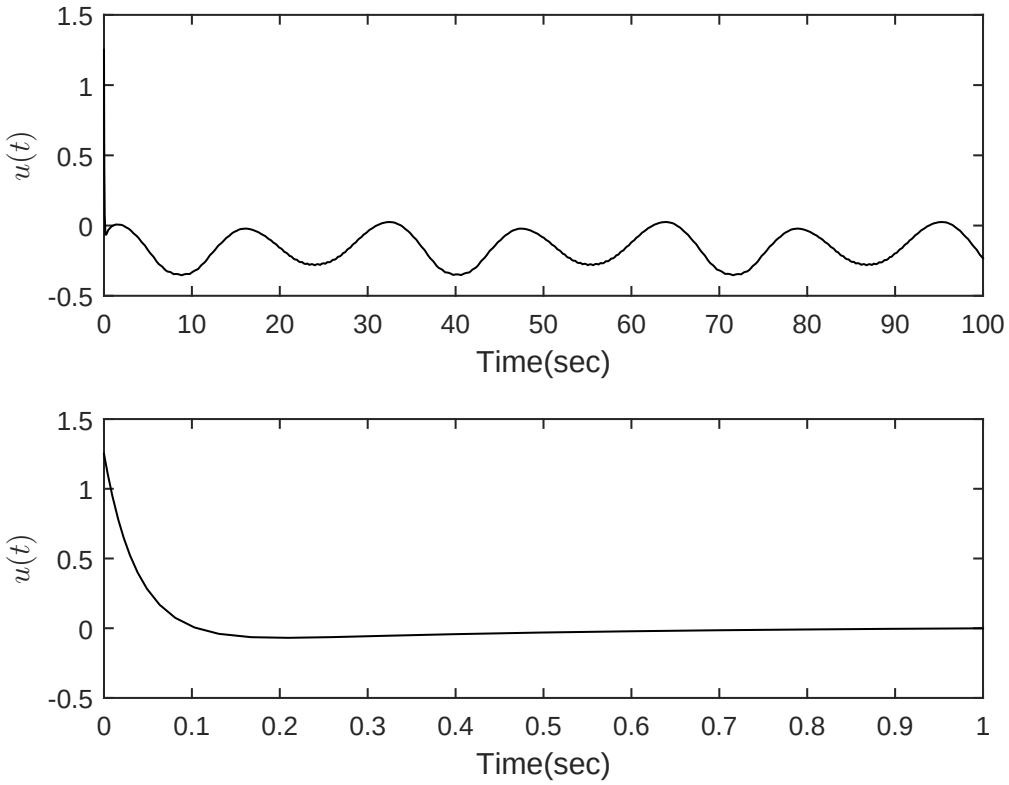

Figure 4.7: The control input with $\sigma_1 = 2.4212$ and $\sigma_2 = 0.1507$. On the top side, the sub-figure shows the simulation time from 0 to 100 seconds, on the down side, the simulation time is from 0 to 1 second.

The simulations have been done under two cases according to different sets of H_∞ performance parameters of σ_1 and σ_2. The proposed fuzzy controller is employed to control the nonlinear plant subject to the initial conditions $\mathbf{x}(0) = [0 \quad 0]^T$ and $\mathbf{x_r}(0) = [0.5 \quad 0]^T$.

In the first case, we investigate the tracking performance with the smallest values of σ_1 and σ_2. To obtain the smallest values of σ_1 and σ_2, the summation of σ_1 and σ_2 can be set as the objective function in SOSTOOLS and further be minimized to achieve better performance. In the second case, we consider $\sigma_1 = \sigma_2 = 10$ as sufficiently large set of values to investigate the tracking performance for comparison purposes.

Through the two cases, the influence of H_∞ performance parameters σ_1 and σ_2 can be demonstrated through performing time response simulation. For the first case, by solving the solution to Theorem 4.2, we obtained $\mathbf{X} = \begin{bmatrix} 3.3796 & 0.1823 \\ 0.1823 & 0.2735 \end{bmatrix}$ and the feedback gains as $\mathbf{F}_1 = -3.3649$, $\mathbf{F}_2 = -2.9116$, $\mathbf{G}_1 = -0.0569$, $\mathbf{G}_2 = -0.0570$. The time response simulations are shown in Figs. 4.2 to 4.4 under $\sigma_1 = 2.4212$ and $\sigma_2 = 0.1507$.

For the second case, by solving the solution to Theorem 4.2, we obtained $\mathbf{X} =$

$\begin{bmatrix} 0.2225 & -0.0452 \\ -0.0452 & 0.4919 \end{bmatrix}$ and the feedback gains as $\mathbf{F}_1 = -4.2141$, $\mathbf{F}_2 = -3.0289$, $\mathbf{G}_1 = -0.0700$ and $\mathbf{G}_2 = -0.0318$. The time response simulations are shown in Fig. 4.5 and 4.6 under $\sigma_1 = 10$ and $\sigma_2 = 10$.

It can be seen from Figs. 4.2 to 4.6 that when σ_1 and σ_2 are small, the performance of the tracking control is decent that the states of fuzzy model can track closely the those of the reference model. But when the value of σ_1 and σ_2 are increased to 10 in the second case, the tracking error becomes obvious, especially for $x_1(t)$ in Fig. 4.5 that the tracking error of $x_1(t)$ is larger than its counterparts in the first cases. In Fig. 4.6, there are also some higher spikes in the error of $x_2(t)$, which are larger than their counterparts in the first case. From the simulation results, it reveals that good tracking performance can be achieved by using smaller values of σ_1 and σ_2, which verify the analysis result.

Remark 4.2. *When Theorem 4.1 in [80] is applied to facilitate the stability analysis, there is no feasible solution can be found. It can be seen that through incorporating the information of membership functions into the stability analysis, the analysis results can be further relaxed by adopting Theorem 4.2.*

Table 4.1: The coefficients of the approximation of the membership functions in 20 operating sub-domains.

$\underline{h}_{1,1,l}$	$l=1$	$l=2$	$l=3$	$l=4$
x_1^1	-2.5690×10^{-3}	-6.9168×10^{-3}	-1.8325×10^{-2}	-4.6546×10^{-2}
x_1^0	9.7281×10^{-1}	9.3368×10^{-1}	8.4241×10^{-1}	6.4487×10^{-1}
$\underline{h}_{1,1,l}$	$l=5$	$l=6$	$l=7$	$l=8$
x_1^1	-1.2292×10^{-1}	-2.5388×10^{-1}	-2.6673×10^{-1}	-1.6878×10^{-1}
x_1^0	1.8663×10^{-1}	-4.6819×10^{-1}	-5.1958×10^{-1}	-2.2572×10^{-1}
$\underline{h}_{1,1,l}$	$l=9$	$l=10$	$l=11$	$l=12$
x_1^1	-7.3779×10^{-2}	-2.6331×10^{-2}	-8.2447×10^{-3}	-2.5738×10^{-3}
x_1^0	-3.5725×10^{-2}	1.1723×10^{-2}	1.1723×10^{-2}	6.0525×10^{-3}
$\underline{h}_{1,1,l}$	$l=13$	$l=14$	$l=15$	$l=16$
x_1^1	-6.9042×10^{-4}	-2.1458×10^{-4}	0	0
x_1^0	2.2858×10^{-3}	8.5831×10^{-4}	0	0
$\underline{h}_{1,1,l}$	$l=17$	$l=18$	$l=19$	$l=20$
x_1^1	0	0	0	0
x_1^0	0	0	0	0

Table 4.2: The coefficients of the approximation of the membership functions in 20 operating sub-domains.

$\underline{h}_{1,2,l}$	$l=1$	$l=2$	$l=3$	$l=4$
x_1^1	0	0	0	0
x_1^0	0	0	0	0
$\underline{h}_{1,2,l}$	$l=5$	$l=6$	$l=7$	$l=8$
x_1^1	0	0	6.7957×10^{-2}	-1.6980×10^{-2}
x_1^0	0	0	2.7183×10^{-1}	1.7017×10^{-2}
$\underline{h}_{1,2,l}$	$l=9$	$l=10$	$l=11$	$l=12$
x_1^1	-2.3373×10^{-2}	-1.4443×10^{-2}	-7.2967×10^{-3}	-3.3417×10^{-3}
x_1^0	4.2311×10^{-3}	1.3161×10^{-2}	1.3161×10^{-2}	9.2058×10^{-3}
$\underline{h}_{1,2,l}$	$l=13$	$l=14$	$l=15$	$l=16$
x_1^1	-1.4553×10^{-3}	-6.2860×10^{-4}	-2.5882×10^{-4}	-1.1398×10^{-4}
x_1^0	5.4329×10^{-3}	2.9530×10^{-3}	1.4738×10^{-3}	7.4962×10^{-4}
$\underline{h}_{1,2,l}$	$l=17$	$l=18$	$l=19$	$l=20$
x_1^1	-4.1559×10^{-5}	-1.5290×10^{-5}	-5.6249×10^{-6}	-2.0526×10^{-6}
x_1^0	3.1510×10^{-4}	1.3122×10^{-4}	5.3897×10^{-5}	2.1747×10^{-5}

Table 4.3: The coefficients of the approximation of the membership functions in 20 operating sub-domains.

$\underline{h}_{2,1,l}$	$l=1$	$l=2$	$l=3$	$l=4$
x_1^1	8.2080×10^{-4}	2.2413×10^{-3}	6.0343×10^{-3}	1.6338×10^{-2}
x_1^0	8.6970×10^{-3}	2.1482×10^{-2}	5.1826×10^{-2}	1.2395×10^{-1}
$\underline{h}_{2,1,l}$	$l=5$	$l=6$	$l=7$	$l=8$
x_1^1	4.1989×10^{-2}	8.3802×10^{-2}	1.3838×10^{-1}	1.2571×10^{-1}
x_1^0	2.7786×10^{-1}	4.8692×10^{-1}	7.0522×10^{-1}	6.6722×10^{-1}
$\underline{h}_{2,1,l}$	$l=9$	$l=10$	$l=11$	$l=12$
x_1^1	4.1391×10^{-2}	-5.0016×10^{-2}	-1.0764×10^{-1}	-1.3729×10^{-1}
x_1^0	4.9858×10^{-1}	4.0718×10^{-1}	4.0718×10^{-1}	4.3683×10^{-1}
$\underline{h}_{2,1,l}$	$l=13$	$l=14$	$l=15$	$l=16$
x_1^1	-9.8545×10^{-2}	-6.3707×10^{-2}	0	0
x_1^0	3.5934×10^{-1}	2.5483×10^{-1}	0	0
$\underline{h}_{2,1,l}$	$l=17$	$l=18$	$l=19$	$l=20$
x_1^1	0	0	0	0
x_1^0	0	0	0	0

Table 4.4: The coefficients of the approximation of the membership functions in 20 operating sub-domains.

$\underline{h}_{2,2,l}$	$l=1$	$l=2$	$l=3$	$l=4$
x_1^1	0	0	0	0
x_1^0	0	0	0	0
$\underline{h}_{2,2,l}$	$l=5$	$l=6$	$l=7$	$l=8$
x_1^1	0	0	6.3707×10^{-2}	9.8545×10^{-2}
x_1^0	0	0	2.5483×10^{-1}	3.5934×10^{-1}
$\underline{h}_{2,2,l}$	$l=9$	$l=10$	$l=11$	$l=12$
x_1^1	1.3729×10^{-1}	1.0764×10^{-1}	5.0016×10^{-2}	-4.1391×10^{-2}
x_1^0	4.3683×10^{-1}	4.0718×10^{-1}	4.0718×10^{-1}	4.9858×10^{-1}
$\underline{h}_{2,2,l}$	$l=13$	$l=14$	$l=15$	$l=16$
x_1^1	-1.2571×10^{-1}	-1.3838×10^{-1}	-8.3802×10^{-2}	-4.1989×10^{-2}
x_1^0	6.6722×10^{-1}	7.0522×10^{-1}	4.8692×10^{-1}	2.7786×10^{-1}
$\underline{h}_{2,2,l}$	$l=17$	$l=18$	$l=19$	$l=20$
x_1^1	-1.6338×10^{-2}	-6.0343×10^{-3}	-2.2413×10^{-3}	-8.2080×10^{-4}
x_1^0	1.2395×10^{-1}	5.1826×10^{-2}	2.1482×10^{-2}	8.6970×10^{-3}

Table 4.5: The coefficients of the approximation of the membership functions in 20 operating sub-domains.

$\underline{h}_{3,1,l}$	$l=1$	$l=2$	$l=3$	$l=4$
x_1^1	2.0526×10^{-6}	5.6249×10^{-6}	1.5290×10^{-5}	4.1559×10^{-5}
x_1^0	2.1747×10^{-5}	5.3897×10^{-5}	1.3122×10^{-4}	3.1510×10^{-4}
$\underline{h}_{3,1,l}$	$l=5$	$l=6$	$l=7$	$l=8$
x_1^1	1.1398×10^{-4}	2.5882×10^{-4}	6.2860×10^{-4}	1.4553×10^{-3}
x_1^0	7.4962×10^{-4}	1.4738×10^{-3}	2.9530×10^{-3}	5.4329×10^{-3}
$\underline{h}_{3,1,l}$	$l=9$	$l=10$	$l=11$	$l=12$
x_1^1	3.3417×10^{-3}	7.2967×10^{-3}	1.4443×10^{-2}	2.3373×10^{-2}
x_1^0	9.2058×10^{-3}	1.3161×10^{-2}	1.3161×10^{-2}	4.2311×10^{-3}
$\underline{h}_{3,1,l}$	$l=13$	$l=14$	$l=15$	$l=16$
x_1^1	1.6980×10^{-2}	-6.7957×10^{-2}	0	0
x_1^0	1.7017×10^{-2}	2.7183×10^{-1}	0	0
$\underline{h}_{3,1,l}$	$l=17$	$l=18$	$l=19$	$l=20$
x_1^1	0	0	0	0
x_1^0	0	0	0	0

Table 4.6: The coefficients of the approximation of the membership functions in 20 operating sub-domains.

$\underline{h}_{3,2,l}$	$l=1$	$l=2$	$l=3$	$l=4$
x_1^1	0	0	0	0
x_1^0	0	0	0	0
$\underline{h}_{3,2,l}$	$l=5$	$l=6$	$l=7$	$l=8$
x_1^1	0	0	2.1458×10^{-4}	6.9042×10^{-4}
x_1^0	0	0	8.5831×10^{-4}	2.2858×10^{-3}
$\underline{h}_{3,2,l}$	$l=9$	$l=10$	$l=11$	$l=12$
x_1^1	2.5738×10^{-3}	8.2447×10^{-3}	2.6331×10^{-2}	7.3779×10^{-2}
x_1^0	6.0525×10^{-3}	1.1723×10^{-2}	1.1723×10^{-2}	-3.5725×10^{-2}
$\underline{h}_{3,2,l}$	$l=13$	$l=14$	$l=15$	$l=16$
x_1^1	1.6878×10^{-1}	2.6673×10^{-1}	2.5388×10^{-1}	1.2292×10^{-1}
x_1^0	-2.2572×10^{-1}	-5.1958×10^{-1}	-4.6819×10^{-1}	1.8663×10^{-1}
$\underline{h}_{3,2,l}$	$l=17$	$l=18$	$l=19$	$l=20$
x_1^1	4.6546×10^{-2}	1.8325×10^{-2}	6.9168×10^{-3}	2.5690×10^{-3}
x_1^0	6.4487×10^{-1}	8.4241×10^{-1}	9.3368×10^{-1}	9.7281×10^{-1}

Table 4.7: The coefficients of $\delta_{1,1,l}$ in 20 operating sub-domains.

$\delta_{1,1,l}$	$l=1$	$l=2$	$l=3$	$l=4$
x_1^1	1.7426×10^{-3}	4.6602×10^{-3}	1.2249×10^{-2}	3.0092×10^{-2}
x_1^0	1.8435×10^{-2}	4.4693×10^{-2}	1.0541×10^{-1}	2.3031×10^{-1}
$\delta_{1,1,l}$	$l=5$	$l=6$	$l=7$	$l=8$
x_1^1	8.5817×10^{-2}	1.1059×10^{-1}	-1.6354×10^{-2}	-6.9809×10^{-2}
x_1^0	5.6465×10^{-1}	6.8852×10^{-1}	1.8074×10^{-1}	2.0377×10^{-2}
$\delta_{1,1,l}$	$l=9$	$l=10$	$l=11$	$l=12$
x_1^1	-8.4946×10^{-2}	-4.7327×10^{-2}	-1.8890×10^{-2}	-6.2216×10^{-3}
x_1^0	-9.8969×10^{-3}	2.7723×10^{-2}	2.7723×10^{-2}	1.5054×10^{-2}
$\delta_{1,1,l}$	$l=13$	$l=14$	$l=15$	$l=16$
x_1^1	-1.9300×10^{-3}	-5.0071×10^{-4}	-1.6909×10^{-4}	-1.1056×10^{-5}
x_1^0	6.4708×10^{-3}	2.1830×10^{-3}	8.5649×10^{-4}	6.6333×10^{-5}
$\delta_{1,1,l}$	$l=17$	$l=18$	$l=19$	$l=20$
x_1^1	-4.9740×10^{-41}	2.9464×10^{-40}	4.7682×10^{-40}	-3.9398×10^{-40}
x_1^0	1.3221×10^{-23}	1.3221×10^{-23}	1.3221×10^{-23}	1.3221×10^{-23}

Table 4.8: The coefficients of $\delta_{1,2,l}$ in 20 operating sub-domains.

$\delta_{1,2,l}$	$l=1$	$l=2$	$l=3$	$l=4$
x_1^1	-2.2299×10^{-40}	3.8012×10^{-39}	-5.7050×10^{-40}	-1.9361×10^{-39}
x_1^0	1.3221×10^{-23}	1.3221×10^{-23}	1.3221×10^{-23}	1.3221×10^{-23}
$\delta_{1,2,l}$	$l=5$	$l=6$	$l=7$	$l=8$
x_1^1	1.9242×10^{-2}	8.5951×10^{-2}	-2.9430×10^{-2}	-3.3336×10^{-4}
x_1^0	1.1545×10^{-1}	4.4900×10^{-1}	-1.2528×10^{-2}	7.4763×10^{-2}
$\delta_{1,2,l}$	$l=9$	$l=10$	$l=11$	$l=12$
x_1^1	-2.6415×10^{-2}	-2.2729×10^{-2}	-1.3976×10^{-2}	-6.9213×10^{-3}
x_1^0	2.2599×10^{-2}	2.6285×10^{-2}	2.6285×10^{-2}	1.9231×10^{-2}
$\delta_{1,2,l}$	$l=13$	$l=14$	$l=15$	$l=16$
x_1^1	-3.1178×10^{-3}	-1.3278×10^{-3}	-5.6949×10^{-4}	-2.3537×10^{-4}
x_1^0	1.1624×10^{-2}	6.2538×10^{-3}	3.2205×10^{-3}	1.5499×10^{-3}
$\delta_{1,2,l}$	$l=17$	$l=18$	$l=19$	$l=20$
x_1^1	-8.7022×10^{-5}	-3.2021×10^{-5}	-1.1781×10^{-5}	-4.3507×10^{-6}
x_1^0	6.5981×10^{-4}	2.7480×10^{-4}	1.1288×10^{-4}	4.6013×10^{-5}

Table 4.9: The coefficients of $\delta_{2,1,l}$ in 20 operating sub-domains.

$\delta_{2,1,l}$	$l=1$	$l=2$	$l=3$	$l=4$
x_1^1	1.7458×10^{-3}	4.6691×10^{-3}	1.2274×10^{-2}	3.0160×10^{-2}
x_1^0	1.8469×10^{-2}	4.4778×10^{-2}	1.0561×10^{-1}	2.3082×10^{-1}
$\delta_{2,1,l}$	$l=5$	$l=6$	$l=7$	$l=8$
x_1^1	6.4450×10^{-2}	8.0899×10^{-2}	3.9054×10^{-2}	-5.1538×10^{-2}
x_1^0	4.3656×10^{-1}	5.1880×10^{-1}	3.5143×10^{-1}	7.9648×10^{-2}
$\delta_{2,1,l}$	$l=9$	$l=10$	$l=11$	$l=12$
x_1^1	-6.6635×10^{-2}	-3.0827×10^{-2}	1.2965×10^{-3}	1.2146×10^{-2}
x_1^0	4.9454×10^{-2}	8.5262×10^{-2}	8.5262×10^{-2}	7.4413×10^{-2}
$\delta_{2,1,l}$	$l=13$	$l=14$	$l=15$	$l=16$
x_1^1	-2.5801×10^{-2}	-2.7666×10^{-2}	-4.1594×10^{-2}	-3.6444×10^{-3}
x_1^0	1.5031×10^{-1}	1.5590×10^{-1}	2.1161×10^{-1}	2.1867×10^{-2}
$\delta_{2,1,l}$	$l=17$	$l=18$	$l=19$	$l=20$
x_1^1	-4.9740×10^{-41}	2.9464×10^{-40}	4.7682×10^{-40}	-3.9398×10^{-40}
x_1^0	1.3221×10^{-23}	1.3221×10^{-23}	1.3221×10^{-23}	1.3221×10^{-23}

Table 4.10: The coefficients of $\delta_{2,2,l}$ in 20 operating sub-domains.

$\delta_{2,2,l}$	$l=1$	$l=2$	$l=3$	$l=4$
x_1^1	-2.2299×10^{-40}	3.8012×10^{-39}	-5.7050×10^{-40}	-1.9361×10^{-39}
x_1^0	1.3221×10^{-23}	1.3221×10^{-23}	1.3221×10^{-23}	1.3221×10^{-23}
$\delta_{2,2,l}$	$l=5$	$l=6$	$l=7$	$l=8$
x_1^1	3.6444×10^{-3}	4.1594×10^{-2}	2.7666×10^{-2}	2.5801×10^{-2}
x_1^0	2.1867×10^{-2}	2.1161×10^{-1}	1.5590×10^{-1}	1.5031×10^{-1}
$\delta_{2,2,l}$	$l=9$	$l=10$	$l=11$	$l=12$
x_1^1	-1.2146×10^{-2}	-1.2965×10^{-3}	3.0827×10^{-2}	6.6635×10^{-2}
x_1^0	7.4413×10^{-2}	8.5262×10^{-2}	8.5262×10^{-2}	4.9454×10^{-2}
$\delta_{2,2,l}$	$l=13$	$l=14$	$l=15$	$l=16$
x_1^1	5.1538×10^{-2}	-3.9054×10^{-2}	-8.0899×10^{-2}	-6.4450×10^{-2}
x_1^0	7.9648×10^{-2}	3.5143×10^{-1}	5.1880×10^{-1}	4.3656×10^{-1}
$\delta_{2,2,l}$	$l=17$	$l=18$	$l=19$	$l=20$
x_1^1	-3.0160×10^{-2}	-1.2274×10^{-2}	-4.6691×10^{-3}	-1.7458×10^{-3}
x_1^0	2.3082×10^{-1}	1.0561×10^{-1}	4.4778×10^{-2}	1.8469×10^{-2}

Table 4.11: The coefficients of $\delta_{3,1,l}$ in 20 operating sub-domains.

$\delta_{3,1,l}$	$l=1$	$l=2$	$l=3$	$l=4$
x_1^1	4.3507×10^{-6}	1.1781×10^{-5}	3.2021×10^{-5}	8.7022×10^{-5}
x_1^0	4.6013×10^{-5}	1.1288×10^{-4}	2.7480×10^{-4}	6.5981×10^{-4}
$\delta_{3,1,l}$	$l=5$	$l=6$	$l=7$	$l=8$
x_1^1	2.3537×10^{-4}	5.6949×10^{-4}	1.3278×10^{-3}	3.1178×10^{-3}
x_1^0	1.5499×10^{-3}	3.2205×10^{-3}	6.2538×10^{-3}	1.1624×10^{-2}
$\delta_{3,1,l}$	$l=9$	$l=10$	$l=11$	$l=12$
x_1^1	6.9213×10^{-3}	1.3976×10^{-2}	2.2729×10^{-2}	2.6415×10^{-2}
x_1^0	1.9231×10^{-2}	2.6285×10^{-2}	2.6285×10^{-2}	2.2599×10^{-2}
$\delta_{3,1,l}$	$l=13$	$l=14$	$l=15$	$l=16$
x_1^1	3.3336×10^{-4}	2.9430×10^{-2}	-8.5951×10^{-2}	-1.9242×10^{-2}
x_1^0	7.4763×10^{-2}	-1.2528×10^{-2}	4.4900×10^{-1}	1.1545×10^{-1}
$\delta_{3,1,l}$	$l=17$	$l=18$	$l=19$	$l=20$
x_1^1	-4.9740×10^{-41}	2.9464×10^{-40}	4.7682×10^{-40}	-3.9398×10^{-40}
x_1^0	1.3221×10^{-23}	1.3221×10^{-23}	1.3221×10^{-23}	1.3221×10^{-23}

Table 4.12: The coefficients of $\delta_{3,2,l}$ in 20 operating sub-domains.

$\delta_{3,2,l}$	$l=1$	$l=2$	$l=3$	$l=4$
x_1^1	-2.2299×10^{-40}	3.8012×10^{-39}	-5.7050×10^{-40}	-1.9361×10^{-39}
x_1^0	1.3221×10^{-23}	1.3221×10^{-23}	1.3221×10^{-23}	1.3221×10^{-23}
$\delta_{3,2,l}$	$l=5$	$l=6$	$l=7$	$l=8$
x_1^1	1.1056×10^{-5}	1.6909×10^{-4}	5.0071×10^{-4}	1.9300×10^{-3}
x_1^0	6.6333×10^{-5}	8.5649×10^{-4}	2.1830×10^{-3}	6.4708×10^{-3}
$\delta_{3,2,l}$	$l=9$	$l=10$	$l=11$	$l=12$
x_1^1	6.2216×10^{-3}	1.8890×10^{-2}	4.7327×10^{-2}	8.4946×10^{-2}
x_1^0	1.5054×10^{-2}	2.7723×10^{-2}	2.7723×10^{-2}	-9.8969×10^{-3}
$\delta_{3,2,l}$	$l=13$	$l=14$	$l=15$	$l=16$
x_1^1	6.9809×10^{-2}	1.6354×10^{-2}	-1.1059×10^{-1}	-8.5817×10^{-2}
x_1^0	2.0377×10^{-2}	1.8074×10^{-1}	6.8852×10^{-1}	5.6465×10^{-1}
$\delta_{3,2,l}$	$l=17$	$l=18$	$l=19$	$l=20$
x_1^1	-3.0092×10^{-2}	-1.2249×10^{-2}	-4.6602×10^{-3}	-1.7426×10^{-3}
x_1^0	2.3031×10^{-1}	1.0541×10^{-1}	4.4693×10^{-2}	1.8435×10^{-2}

4.3.2 Inverted Pendulum

Example 2: In this example, the tracking control design of an inverted pendulum will be investigated to verify the effectiveness of the proposed approach. The inverted pendulum is an open-loop unstable nonlinear system, which requires a well-designed controller to stabilize the system and further drive the states of the fuzzy model to track those of the reference model. The dynamic equation of the inverted pendulum [45] is given by

$$\ddot{\theta}(t)=\frac{g\sin(\theta(t))-am_pS\dot{\theta}(t)^2\sin(2\theta(t))/2-a\cos(\theta(t))u(t)}{4S/3-am_pS\cos^2(\theta(t))}, \tag{4.37}$$

where $\theta(t)$ is the angular displacement of the inverted pendulum, $g=9.8\ \mathrm{m/s^2}$, $m_p\in[m_{p_{\min}}\quad m_{p_{\max}}]=[0.5\quad 1]$ kg is the mass of the pendulum, $M_c\in[M_{c_{\min}}\quad M_{c_{\max}}]=[18\quad 20]$ kg is the mass of the cart, $a=\frac{1}{m_p+M_c}$, $2S=1\mathrm{m}$ is the length of the pendulum, and $u(t)$ is the force applied on the cart. In the investigation, m_p and M_c are treated as the parameter uncertainties. To transform the dynamic equation of the inverted pendulum into state variable models, $\theta(t)$ and $\dot{\theta}(t)$ are treated as the state variables. Also by considering the uncertainties in the plant, we can construct an IT2 PFMB fuzzy model.

The 4-rule polynomial fuzzy model can be adopted to describe the inverted pendulum as follows:

Rule i : IF $f_1(\mathbf{x}(t))$ is $\tilde{M}_1^i$ AND $f_2(\mathbf{x}(t))$ is $\tilde{M}_2^i$

$$\text{THEN } \dot{\mathbf{x}}(t) = \mathbf{A}_i(\mathbf{x}(t))\hat{\mathbf{x}}(\mathbf{x}(t)) + \mathbf{B}_i(\mathbf{x}(t))\mathbf{u}(t), \quad i = 1, 2, 3, 4. \tag{4.38}$$

Blending all the fuzzy rules together, we have:

$$\dot{\mathbf{x}}(t) = \sum_{i=1}^{4} \tilde{w}_i\big(\mathbf{A}_i(\mathbf{x}(t))\hat{\mathbf{x}}(\mathbf{x}(t)) + \mathbf{B}_i(\mathbf{x}(t))\mathbf{u}(t)\big), \tag{4.39}$$

where

$$\hat{\mathbf{x}}(t) = \mathbf{x}(t) = [x_1(t) \quad x_2(t)]^T = [\theta(t) \quad \dot{\theta}(t)]^T,$$
$$x_1(t) \in [\frac{-5\pi}{12} \quad \frac{5\pi}{12}], \quad x_2(t) \in [-5 \quad 5],$$

$$\mathbf{A}_1 = \mathbf{A}_2 = \begin{bmatrix} 0 & 1 \\ f_{1_{\min}} & 0 \end{bmatrix}, \quad \mathbf{A}_3 = \mathbf{A}_4 = \begin{bmatrix} 0 & 1 \\ f_{1_{\max}} & 0 \end{bmatrix},$$

$$\mathbf{B}_1 = \mathbf{B}_3 = \begin{bmatrix} 0 \\ f_{2_{\min}} \end{bmatrix}, \quad \mathbf{B}_2 = \mathbf{B}_4 = \begin{bmatrix} 0 \\ f_{2_{\max}} \end{bmatrix}, \quad \mathbf{C} = \begin{bmatrix} 1 & 0 \\ 0 & 1 \end{bmatrix}.$$

The IT2 membership functions for the fuzzy model are defined as shown in Table 4.13.

In Table 4.13, we have

$$f_1(\mathbf{x}(t)) = \frac{g - am_pSx_2(t)^2\cos(x_1(t))}{4S/3 - am_pS\cos^2(x_1(t))}\left(\frac{\sin(x_1(t))}{x_1(t)}\right),$$
$$f_2(\mathbf{x}(t)) = \frac{-a\cos(x_1(t))}{4S/3 - am_pS\cos^2(x_1(t))}.$$

Adopting the same techniques reported in Chapter 3, the minimum and maximum values of f_1 and f_2 can be obtained in polynomial functions as follows:

$$f_{1_{\min}}(\mathbf{x}(t)) = 0.12996x_1(t)^2 + 10.5323,$$

$$f_{1_{\max}}(\mathbf{x}(t)) = 0.1299x_1(t)^2 + 15.3041,$$

$$f_{2_{\min}}(\mathbf{x}(t)) = 0.0037x_1(t)^2 - 0.0828,$$

$$f_{2_{\max}}(\mathbf{x}(t)) = 0.0037x_1(t)^2 - 0.0249.$$

The lower and upper grades of membership are respectively defined as:

$$w_i^L(\mathbf{x}(t)) = \underline{\mu}_{\tilde{M}_1^i}(\mathbf{x}(t)) \times \underline{\mu}_{\tilde{M}_2^i}(\mathbf{x}(t)),$$
$$w_i^U(\mathbf{x}(t)) = \overline{\mu}_{\tilde{M}_1^i}(\mathbf{x}(t)) \times \overline{\mu}_{\tilde{M}_2^i}(\mathbf{x}(t))$$

for all i.

Table 4.13: Lower and Upper Membership Functions for the Interval Type-2 Fuzzy Model of the Inverted Pendulum.

Lower and upper membership functions	
$\underline{\mu}_{\tilde{M}_1^1}(f_1(\mathbf{x}(t))) = \underline{\mu}_{\tilde{M}_1^2}(f_1(\mathbf{x}(t)))$ $= \frac{f_{1\max} - f_1(\mathbf{x}(t))}{f_{1\max} - f_{1\min}}$;	$\underline{\mu}_{\tilde{M}_2^1}(f_2(\mathbf{x}(t))) = \underline{\mu}_{\tilde{M}_2^3}(f_2(\mathbf{x}(t)))$ $= \frac{f_{2\max} - f_2(\mathbf{x}(t))}{f_{2\max} - f_{2\min}}$;
$\overline{\mu}_{\tilde{M}_1^3}(f_1(\mathbf{x}(t))) = \overline{\mu}_{\tilde{M}_1^4}(f_1(\mathbf{x}(t)))$ $= \frac{f_1(\mathbf{x}(t)) - f_{1\min}}{f_{1\max} - f_{1\min}}$;	$\overline{\mu}_{\tilde{M}_2^2}(f_2(\mathbf{x}(t))) = \overline{\mu}_{\tilde{M}_2^4}(f_2(\mathbf{x}(t)))$ $= \frac{f_2(\mathbf{x}(t)) - f_{2\min}}{f_{2\max} - f_{2\min}}$
with $x_2(t) = 0, m_p = m_{p\max}$ $= 1$kg and $M_c = M_{c\min} = 18$kg	with $m_p = m_{p\max}$ $= 1$kg and $M_c = M_{c\max} = 20$kg
$\overline{\mu}_{\tilde{M}_1^1}(f_1(\mathbf{x}(t))) = \overline{\mu}_{\tilde{M}_1^2}(f_1(\mathbf{x}(t)))$ $= \frac{f_{1\max} - f_1(\mathbf{x}(t))}{f_{1\max} - f_{1\min}}$;	$\overline{\mu}_{\tilde{M}_2^1}(f_2(\mathbf{x}(t))) = \overline{\mu}_{\tilde{M}_2^3}(f_2(\mathbf{x}(t)))$ $= \frac{f_{2\max} - f_2(\mathbf{x}(t))}{f_{2\max} - f_{2\min}}$
$\underline{\mu}_{\tilde{M}_1^3}(f_1(\mathbf{x}(t))) = \underline{\mu}_{\tilde{M}_1^4}(f_1(\mathbf{x}(t)))$ $= \frac{f_1(\mathbf{x}(t)) - f_{1\min}}{f_{1\max} - f_{1\min}}$;	$\underline{\mu}_{\tilde{M}_2^2}(f_2(\mathbf{x}(t))) = \underline{\mu}_{\tilde{M}_2^4}(f_2(\mathbf{x}(t)))$ $= \frac{f_2(\mathbf{x}(t)) - f_{2\min}}{f_{2\max} - f_{2\min}}$;
with $x_2(t) = x_{2\max}, m_p = m_{p\max}$ $= 1$kg and $M_c = M_{c\min} = 18$kg	with $m_p = m_{p\min} = 0.5$kg and $M_c = M_{c\min} = 18$kg

Based the IT2 PFMB fuzzy model, a two-rule IT2 polynomial fuzzy controller is adopted to drive the states of the inverted pendulum to track those of the reference model.

The following two-rule IT2 polynomial fuzzy controller is adopted to describe the inverted pendulum:

$$\begin{aligned} &\text{Rule } j: \text{IF } x_1(t) \text{ is } \tilde{N}^j \\ &\qquad \text{THEN } \mathbf{u}(t) = \mathbf{F}_j \mathbf{e}_{\mathbf{y}(t)} + \mathbf{G}_j \mathbf{y}_\mathbf{r}(t), \quad j = 1, 2. \end{aligned} \tag{4.40}$$

After combining of all the fuzzy rules, we have

$$\mathbf{u}(t) = \tilde{m}_1(x_1(t))(\mathbf{F}_1 \mathbf{e}_{\mathbf{y}(t)} + \mathbf{G}_1 \mathbf{y}_\mathbf{r}(t)) + \tilde{m}_2(x_1(t))(\mathbf{F}_2 \mathbf{e}_{\mathbf{y}(t)} + \mathbf{G}_2 \mathbf{y}_\mathbf{r}(t)), \tag{4.41}$$

where $\tilde{m}_1(x_1(t))$ and $\tilde{m}_2(x_1(t))$ are the IT2 membership functions of the polynomial fuzzy controller.

The upper and lower bounds of the membership functions of the fuzzy controller are defined as follows:

$$\overline{m}_1(x_1(t)) = \begin{cases} 0 & \text{for } x_1(t) < -\frac{5\pi}{12} \\ \frac{x_1(t) + 5\pi/12}{5\pi/12} & \text{for } -\frac{5\pi}{12} \le x_1(t) \le 0 \\ \frac{5\pi/12 - x_1(t)}{5\pi/12} & \text{for } 0 \le x_1(t) \le \frac{5\pi}{12} \\ 0 & \text{for } x_1(t) > \frac{5\pi}{12} \end{cases} \tag{4.42}$$

$$\underline{m}_1(x_1(t)) = \begin{cases} 0 & \text{for } x_1(t) < -\frac{5\pi}{12} \\ \frac{0.9(x_1(t)+5\pi/12)}{5\pi/12} & \text{for } -\frac{5\pi}{12} \leq x_1(t) \leq 0 \\ \frac{0.9(5\pi/12-x_1(t))}{5\pi/12} & \text{for } 0 \leq x_1(t) \leq \frac{5\pi}{12} \\ 0 & \text{for } x_1(t) > \frac{5\pi}{12} \end{cases} \tag{4.43}$$

$\overline{m}_2(x_1(t)) = 1-\underline{m}_1(x_1(t))$, $\underline{m}_2(x_1(t)) = 1-\overline{m}_1(x_1(t))$, and $\tilde{m}_2(x_1(t)) = 1-\tilde{m}_1(x_1(t))$. The type reductions for the controller $\underline{\kappa}_j(x_1(t)) = \overline{\kappa}_j(x_1(t)) = 0.5$, $j = 1, 2$.

The reference model has been chosen as $\mathbf{A_r} = \begin{bmatrix} 0 & 1 \\ -4 & -4 \end{bmatrix}$, $\mathbf{B_r} = \begin{bmatrix} 0 \\ 1 \end{bmatrix}$ and $r(t) = 5\sin(0.3t)$.

During the simulation, the m_p is set as 1kg and M_c is set as 19kg. Based on Theorem 4.2, the number of sub-domains is 10 and other parameters are set as the same with those in example 1, $\varepsilon_1(\mathbf{y}) = \varepsilon_2(\tilde{\mathbf{x}}) = \varepsilon_3(\mathbf{x}, \mathbf{x_r}) = \varepsilon_4(\mathbf{x}, \mathbf{x_r}) = \varepsilon_5(\mathbf{x}, \mathbf{x_y}, \mathbf{y}) = 0.001$; $\mathbf{X}(\tilde{\mathbf{x}})$ as a polynomial of degree 0; $\mathbf{M}_j(x_1(t))$ and $\mathbf{N}_j(x_1(t))$, $j = 1, 2, \ldots, c$ are polynomials with monomials in x_1 of degree 0, $\mathbf{S}_l(x_1(t))$ is of degree 0. The values of $\underline{h}_{ijl}$ and δ_{ijl} can be viewed in Table 4.14 and 4.15. The fuzzy controller is employed to control the nonlinear plant subject to the initial condition $\mathbf{x}(0) = [5\pi/12 \quad 0]$ and $\mathbf{x_r}(0) = [-5\pi/12 \quad 0.05]$. The feedback gains have been obtained as $\mathbf{F}_1 = [44636.7534 \quad 18384.4640]$, $\mathbf{F}_2 = [25535.9221 \quad 10547.3473]$, $\mathbf{G}_1 = [514.6375 \quad 132.4442]$, $\mathbf{G}_2 = [229.2499 \quad 41.8540]$, and $\mathbf{X} = \begin{bmatrix} 0.7264 & -1.7412 \\ -1.7412 & 4.4447 \end{bmatrix}$. The minimum values of σ_1 and σ_2 have been achieved as 0.002976 and 0.004911, respectively. Also the tracking performance can be viewed in Fig. 4.8 and 4.9, it can bee seen that the fuzzy controller is able to drive the system states to follow the reference model closely.

For comparison purposes, the simulation with $\sigma_1 = \sigma_2 = 0.2$ has also been conducted under the same other conditions. The feedback gains in this case have been obtained as $\mathbf{F}_1 = [11521.0017 \quad 2902.4726]$, $\mathbf{F}_2 = [6049.1505 \quad 1519.1870]$, $\mathbf{G}_1 = [72.5468 \quad 18.8362]$, $\mathbf{G}_2 = [247.4591 \quad 48.3076]$, $\mathbf{X} = \begin{bmatrix} 0.1945 & -0.7295 \\ -0.7295 & 2.8924 \end{bmatrix}$. The simulation results can be viewed in Figs. 4.10 and 4.11. It can be seen that the system states can also follow those of the reference model. However, from Figs. 4.8 to 4.11, it is clear that the error of $x_1(t)$ and $x_2(t)$ in Figs. 4.10 and 4.11 is much larger than the error in Figs. 4.8 and 4.9. Therefore, it is verified again that smaller values of σ_1 and σ_2 are able to provide better tracking performance.

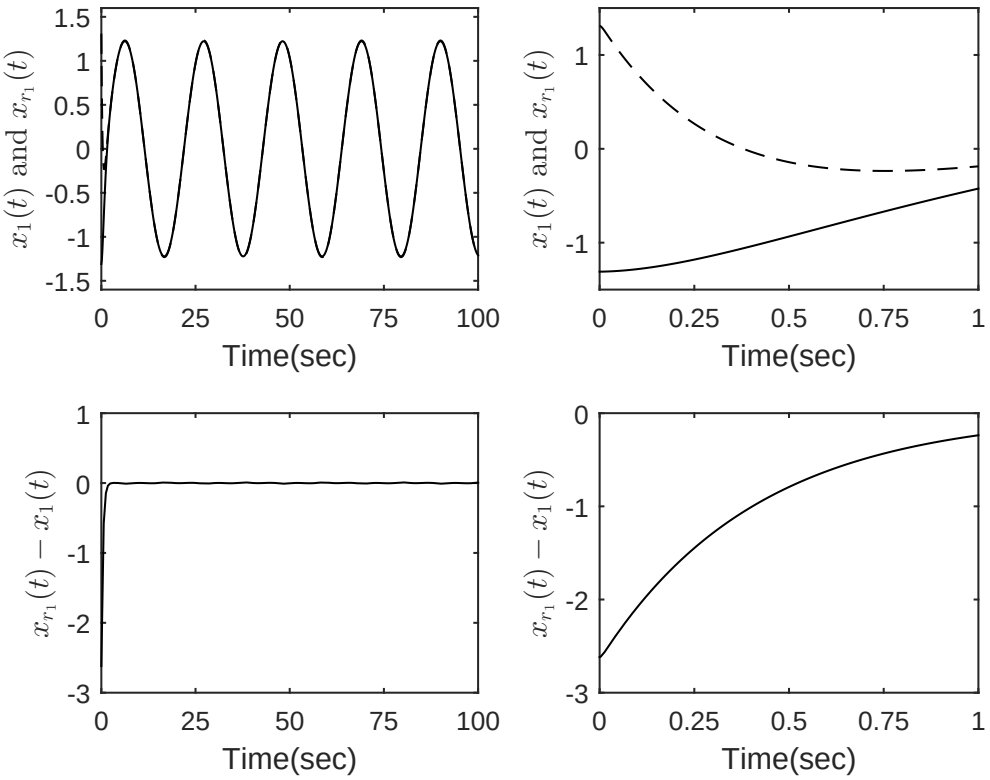

Figure 4.8: Tracking control performance for $x_1(t)$ with $\sigma_1 = 0.002976$ and $\sigma_2 = 0.004911$. On the top left hand side, the sub-figure shows the simulation time from 0 to 100 seconds, on the top right hand side, the simulation time is from 0 to 1 second. The dashed curves are for the controlled trajectory of the response in the fuzzy system ($x_1(t)$), and the solid curves are the trajectory of response in the reference model ($x_{r_1}(t)$). The below two sub-figures show the difference between $x_1(t)$ and $x_{r_1}(t)$.

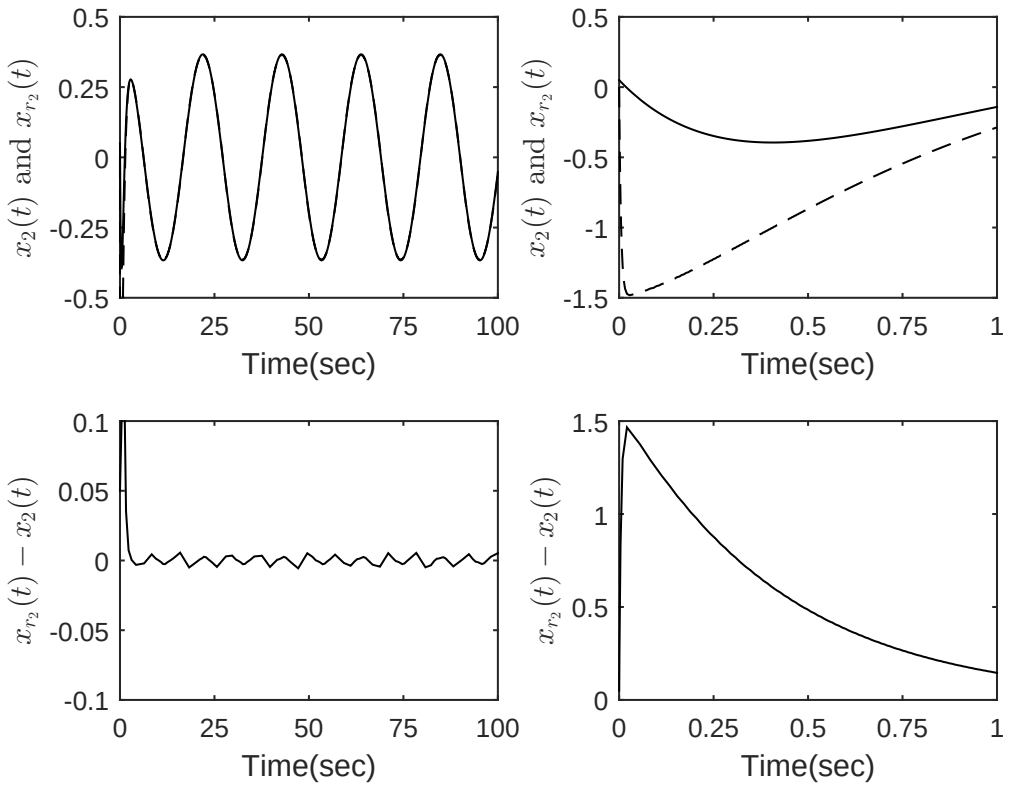

Figure 4.9: Tracking control performance for $x_1(t)$ with $\sigma_1 = 0.002976$ and $\sigma_2 = 0.004911$. On the top left hand side, the sub-figure shows the simulation time from 0 to 100 seconds, on the top right hand side, the simulation time is from 0 to 1 second. The dashed curves are for the controlled trajectory of the response in the fuzzy system ($x_2(t)$), and the solid curves are the trajectory of response in the reference model ($x_{r_2}(t)$). The below two sub-figures show the difference between $x_2(t)$ and $x_{r_2}(t)$.

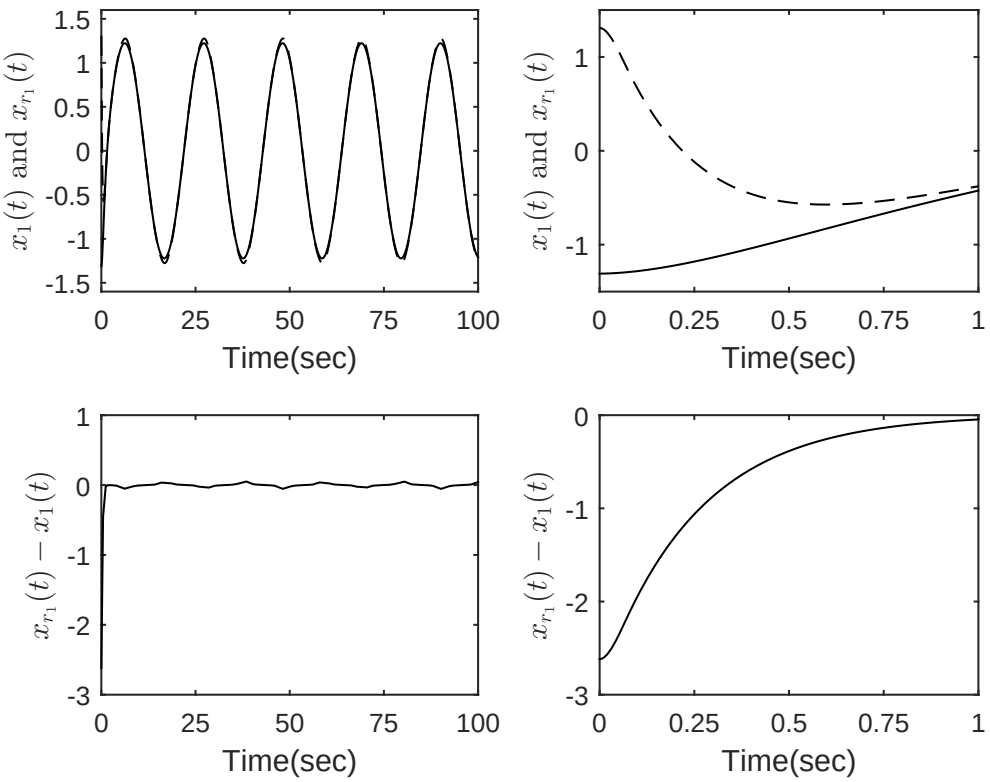

Figure 4.10: Tracking control performance for $x_1(t)$ with $\sigma_1 = 0.2$ and $\sigma_2 = 0.2$. On the top left hand side, the sub-figures show the simulation time from 0 to 100 seconds, on the top right hand side, the simulation time is from 0 to 1 second. The dashed curves are for the controlled trajectory of the response in the fuzzy system $(x_1(t))$, and the solid curves are the trajectory of response in the reference model $(x_{r_1}(t))$. The below two sub-figures show the difference between $x_1(t)$ and $x_{r_1}(t)$.

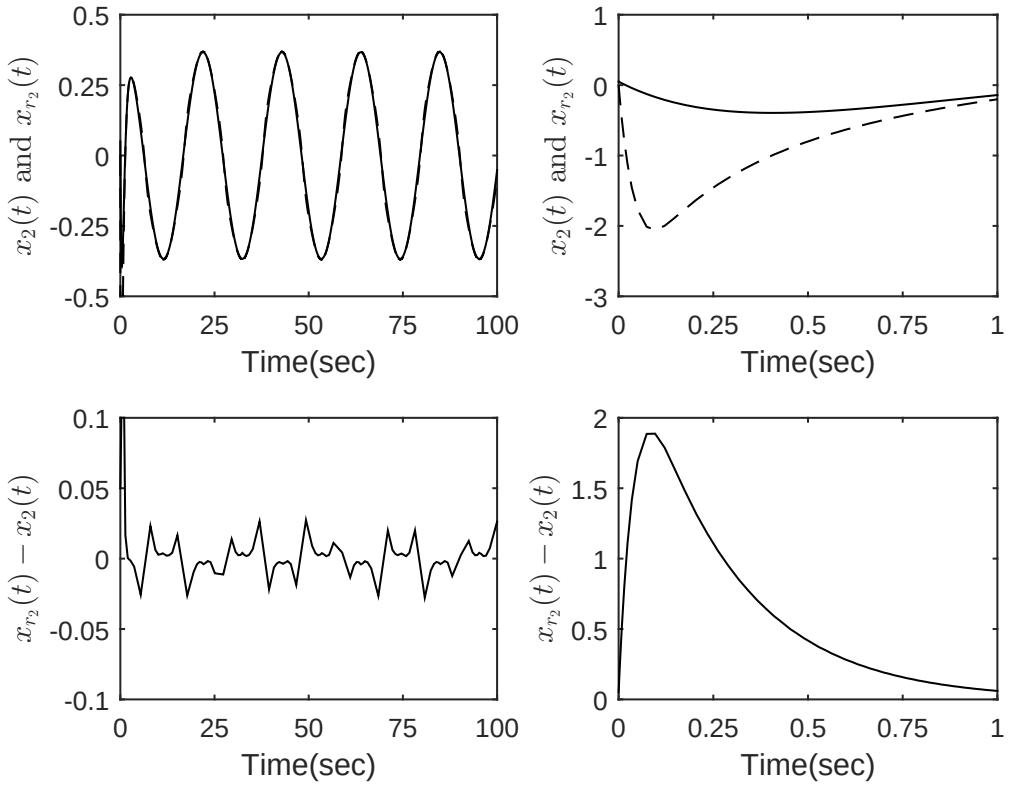

Figure 4.11: Tracking control performance for $x_2(t)$ with $\sigma_1 = 0.2$ and $\sigma_2 = 0.2$. On the top left hand side, the sub-figure shows the simulation time from 0 to 100 seconds, on the top right hand side, the simulation time is from 0 to 1 second. The dashed curves are for the controlled trajectory of the response in the fuzzy system $(x_2(t))$, and the solid curves are the trajectory of response in the reference model $(x_{r_2}(t))$. The below two sub-figures show the difference between $x_2(t)$ and $x_{r_2}(t)$.

Remark 4.3. *In this example, the PFMB control system equipped with the interval type-2 membership functions have been constructed from a real inverted pendulum case, also the mismatched fuzzy rule sets are adopted in the IT2 polynomial fuzzy model and IT polynomial fuzzy controller, which means the fuzzy model does not share the same fuzzy rules with the fuzzy controller. For the 4-rule IT2 polynomial fuzzy model, we managed to use a 2-rule IT2 polynomial fuzzy controller to drive the states of plant to follow those of the reference model. It can be seen that the tracking performance is good. Also, by using less number of rules, the implementation cost can be reduced and the design flexibility can be enhanced.*

Table 4.14: The coefficients of the approximation of the membership functions in 10 operating sub-domains.

$\underline{h}_{ijl}$	$l=1$	$l=2$	$l=3$	$l=4$
$\underline{h}_{1,1,l}$	0	0	6.8347×10^{-2}	0
$\underline{h}_{1,2,l}$	0	5.5666×10^{-2}	1.3230×10^{-2}	0
$\underline{h}_{2,1,l}$	0	0	8.3299×10^{-2}	2.4769×10^{-1}
$\underline{h}_{2,2,l}$	0	0	6.9125×10^{-2}	0
$\underline{h}_{3,1,l}$	-1.1699×10^{-16}	1.1856×10^{-1}	4.7824×10^{-2}	0
$\underline{h}_{3,2,l}$	3.0362×10^{-1}	7.2715×10^{-2}	4.7781×10^{-3}	0
$\underline{h}_{4,1,l}$	-4.4684×10^{-32}	0	1.5409×10^{-1}	1.3463×10^{-1}
$\underline{h}_{4,2,l}$	3.5628×10^{-16}	1.2210×10^{-1}	4.7964×10^{-2}	0
$\underline{h}_{ijl}$	$l=5$	$l=6$	$l=7$	$l=8$
$\underline{h}_{1,1,l}$	-2.8449×10^{-16}	-2.8449×10^{-16}	0	6.7507×10^{-2}
$\underline{h}_{1,2,l}$	0	0	0	1.2603×10^{-2}
$\underline{h}_{2,1,l}$	4.7178×10^{-1}	4.7838×10^{-1}	2.5368×10^{-1}	8.7626×10^{-2}
$\underline{h}_{2,2,l}$	0	0	0	6.8245×10^{-2}
$\underline{h}_{3,1,l}$	-2.4241×10^{-19}	-2.4241×10^{-19}	0	4.5226×10^{-2}
$\underline{h}_{3,2,l}$	0	0	0	4.4372×10^{-3}
$\underline{h}_{4,1,l}$	2.9290×10^{-4}	2.9290×10^{-4}	1.3238×10^{-2}	1.5650×10^{-1}
$\underline{h}_{4,2,l}$	0	0	0	4.5731×10^{-2}
$\underline{h}_{ijl}$	$l=9$	$l=10$		
$\underline{h}_{1,1,l}$	3.2547×10^{-3}	4.3739×10^{-5}		
$\underline{h}_{1,2,l}$	5.4368×10^{-2}	5.0240×10^{-3}		
$\underline{h}_{2,1,l}$	0	0		
$\underline{h}_{2,2,l}$	3.4296×10^{-3}	4.7351×10^{-5}		
$\underline{h}_{3,1,l}$	1.1667×10^{-1}	7.9094×10^{-3}		
$\underline{h}_{3,2,l}$	6.9312×10^{-2}	2.9330×10^{-1}		
$\underline{h}_{4,1,l}$	6.1316×10^{-3}	7.4545×10^{-5}		
$\underline{h}_{4,2,l}$	1.2004×10^{-1}	8.5626×10^{-3}		

Table 4.15: The coefficients of $\delta_{i,j,l}$ in 10 operating sub-domains.

δ_{ijl}	$l=1$	$l=2$	$l=3$	$l=4$
$\delta_{1,1,l}$	4.9353×10^{-2}	1.2284×10^{-1}	8.3813×10^{-2}	1.5216×10^{-1}
$\delta_{1,2,l}$	1.2598×10^{-1}	7.0315×10^{-2}	8.4341×10^{-2}	5.6608×10^{-2}
$\delta_{2,1,l}$	2.2799×10^{-2}	1.4616×10^{-1}	3.1520×10^{-1}	5.2271×10^{-1}
$\delta_{2,2,l}$	4.9217×10^{-2}	1.2767×10^{-1}	9.1405×10^{-2}	1.6053×10^{-1}
$\delta_{3,1,l}$	2.3012×10^{-1}	1.1156×10^{-1}	1.4451×10^{-1}	1.1319×10^{-1}
$\delta_{3,2,l}$	6.9638×10^{-1}	3.6488×10^{-1}	1.5211×10^{-1}	4.4052×10^{-2}
$\delta_{4,1,l}$	9.4257×10^{-2}	2.5028×10^{-1}	1.6764×10^{-1}	1.8710×10^{-1}
$\delta_{4,2,l}$	2.3305×10^{-1}	1.1096×10^{-1}	1.5108×10^{-1}	1.1975×10^{-1}
δ_{ijl}	$l=5$	$l=6$	$l=7$	$l=8$
$\delta_{1,1,l}$	1.3773×10^{-1}	1.3773×10^{-1}	1.5162×10^{-1}	8.4114×10^{-2}
$\delta_{1,2,l}$	2.7949×10^{-2}	2.7408×10^{-2}	5.5437×10^{-2}	8.3604×10^{-2}
$\delta_{2,1,l}$	5.2801×10^{-1}	5.2141×10^{-1}	7.1912×10^{-1}	3.2016×10^{-1}
$\delta_{2,2,l}$	1.5018×10^{-1}	1.5018×10^{-1}	1.6076×10^{-1}	9.2516×10^{-2}
$\delta_{3,1,l}$	4.8936×10^{-2}	4.7473×10^{-2}	1.1081×10^{-1}	1.4484×10^{-1}
$\delta_{3,2,l}$	1.0024×10^{-2}	9.5668×10^{-3}	4.2197×10^{-2}	1.4702×10^{-1}
$\delta_{4,1,l}$	2.7401×10^{-1}	2.6896×10^{-1}	3.1041×10^{-1}	1.6715×10^{-1}
$\delta_{4,2,l}$	5.2762×10^{-2}	5.1212×10^{-2}	1.1731×10^{-1}	1.5238×10^{-1}
δ_{ijl}	$l=9$	$l=10$		
$\delta_{1,1,l}$	1.2188×10^{-1}	5.1537×10^{-2}		
$\delta_{1,2,l}$	7.2516×10^{-2}	1.2186×10^{-1}		
$\delta_{2,1,l}$	1.5202×10^{-1}	2.4748×10^{-2}		
$\delta_{2,2,l}$	1.2599×10^{-1}	5.1534×10^{-2}		
$\delta_{3,1,l}$	1.1491×10^{-1}	2.2367×10^{-1}		
$\delta_{3,2,l}$	3.5607×10^{-1}	6.8403×10^{-1}		
$\delta_{4,1,l}$	2.4625×10^{-1}	9.8495×10^{-2}		
$\delta_{4,2,l}$	1.1178×10^{-1}	2.2326×10^{-1}		

4.4 Conclusion

In this chapter, the tracking control issues based on IT2 PFMB control systems have been investigated. In the analysis, the system output is used for the controller instead of full states. The mismatched premise membership functions approach has been adopted to render the control system more flexibly and the information of membership functions is included in the stability analysis to relax the stability conditions. The stability conditions subject to an H_∞ performance are obtained in the form of SOS, which can be solved efficiently through a third-party Matlab toolbox SOSTOOLS. Both numerical simulation example and experimental simulation have been presented to show the effectiveness of the proposed control approach.

Chapter 5

Output-Feedback Tracking Control Design of Sampled-data IT2 PFMB Control System

In this chapter, the stability and performance of the polynomial fuzzy-model-based (PFMB) tracking control systems based on sampled-data structure are investigated through an interval type-2 (IT2) approach. The diagram of the IT2 PFMB sampled-data output-feedback (SDOF) tracking control system can be viewed in Fig. 5.1. The control objective is to design proper feedback gains of the IT2 SDOF polynomial fuzzy controller which can drive the states of the polynomial model to follow those of the reference model. In Fig. 5.1, h_s is the sampling period, t_γ is the time at the γ-th sampling instant, sampled $\mathbf{y}(t_\gamma)$ is the sampled output of the IT2 polynomial fuzzy model, $\mathbf{y_r}(t_\gamma)$ is the sampled output of the reference model and $\mathbf{u}(t)$ is the control input. The stability conditions are developed using only the output of the system instead of the full states, which gives the control design more flexibility. The stability conditions are summarized in terms of sum-of-square (SOS) based on Lyapunov stability theory. In the analysis, both the membership-function-dependent and membership-function-independent cases are investigated and it can be seen that by utilizing the information of membership functions, the stability conditions can be further relaxed. Also, the stability conditions are derived according to an H_∞ performance. In addition, by considering the sample error as the uncertainties of membership functions, the characters of sampling process can be captured by the IT2 membership functions, which facilitates the analysis. Numerical and experimental examples are presented to verify the effectiveness of the proposed tracking control approach.

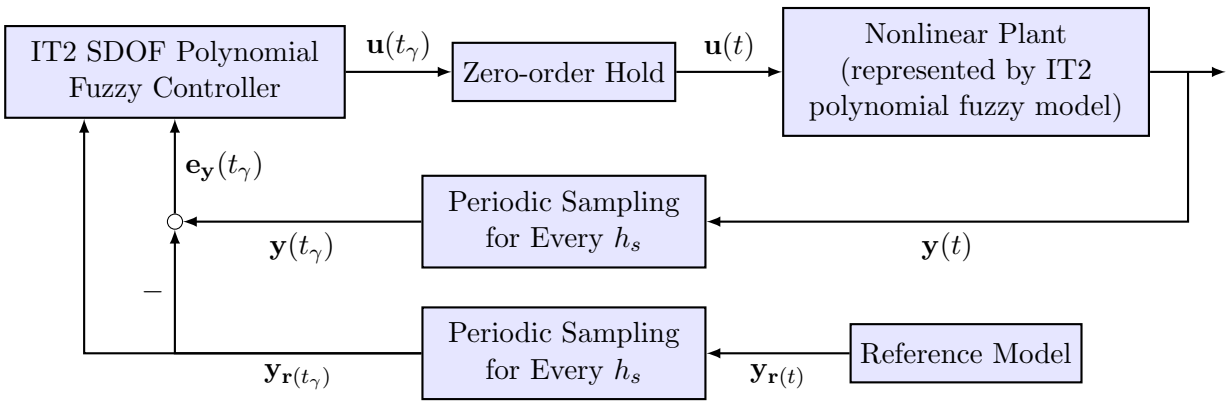

Figure 5.1: A block diagram of IT2 PFMB SDOF tracking control systems.

5.1 IT2 Sampled-Data Output-Feedback Polynomial Fuzzy Controller

The IT2 fuzzy model and the reference model used in the tracking control system is defined in the same way as in Chapters 2 and 4, which can be found in section 2.2.1 and 4.1.1. Here we need only define the IT2 sampled-data output-feedback polynomial fuzzy controller.

Define the state error (or tracking error of states) as follows:

$$\hat{\mathbf{e}}(t) = \hat{\mathbf{x}}(\mathbf{x}(t)) - \hat{\mathbf{x}}_{\mathbf{r}}(\mathbf{x}_{\mathbf{r}}(t)). \tag{5.1}$$

From (2.2.1), (4.1) and (5.1), the output error is defined as follows:

$$\mathbf{e_y}(t) = \mathbf{y}(t) - \mathbf{y_r}(t) = \mathbf{C}\hat{\mathbf{e}}(t). \tag{5.2}$$

An IT2 SDOF polynomial fuzzy controller with c rules is employed to drive the states of the nonlinear plant represented by the IT2 polynomial fuzzy model (2.2.1) to follow those of the reference model (4.1) where the tracking error $\hat{\mathbf{e}}(t)$ is characterized by H_∞ performance.

The format of the IT2 SDOF polynomial fuzzy controller is as follows:

$$\begin{aligned} \text{Rule } j : \text{IF } g_1(\mathbf{y}(t_\gamma)) \text{ is } \tilde{N}_1^j \text{ AND } \cdots \text{ AND } g_\Omega(\mathbf{y}(t_\gamma)) \text{ is } \tilde{N}_\Omega^j \\ \text{THEN } \mathbf{u}(t) = \mathbf{F}_j(\mathbf{h}(t_\gamma))\mathbf{e_y}(t_\gamma) + \mathbf{G}_j(\mathbf{h}(t_\gamma))\mathbf{y_r}(t_\gamma), \end{aligned} \tag{5.3}$$

where $\tilde{N}_\beta^j$ is an IT2 fuzzy term of rule j corresponding to function $g_\beta(\mathbf{y}(t))$, where $\beta = 1, 2, \ldots, \Omega$ and $j = 1, 2, \ldots, c$; Ω is a positive integer. $t_\gamma = t - \tau(t)$, for $t_\gamma < t \leq t_{\gamma+1}$, $0 \leq \tau(t) \leq h_s$, h_s is the sampling period and t_γ is the time at the γ-th sampling instant. Define $\mathbf{h}(t_\gamma) = [\mathbf{y}(t_\gamma) \quad \mathbf{y_r}(t_\gamma)]$, and $\mathbf{F}_j(\mathbf{h}(t_\gamma)) \in \Re^{m\times q}$ and $\mathbf{G}_j(\mathbf{h}(t_\gamma)) \in \Re^{m\times q}$, $j = 1, 2, \ldots, c$, as the polynomial feedback gains to be

determined. The firing strength of the j-th rule is within the following interval sets:

$$\tilde{m}_j(\mathbf{y}(t_\gamma)) \in [m_j^L(\mathbf{y}(t_\gamma)), m_j^U(\mathbf{y}(t_\gamma))], \quad j = 1, 2, \ldots, c, \tag{5.4}$$

where

$$m_j^L(\mathbf{y}(t_\gamma)) = \prod_{r=1}^{\Omega} \underline{\mu}_{\tilde{N}_\beta^j}(g_\beta(\mathbf{y}(t_\gamma))), \tag{5.5}$$

$$m_j^U(\mathbf{y}(t_\gamma)) = \prod_{r=1}^{\Omega} \overline{\mu}_{\tilde{N}_\beta^j}(g_\beta(\mathbf{y}(t_\gamma))), \tag{5.6}$$

in which $0 \leq \overline{\mu}_{\tilde{N}_\beta^j}(g_\beta(\mathbf{y}(t_\gamma))) \leq 1$ and $0 \leq \underline{\mu}_{\tilde{N}_\beta^i}(g_\beta(\mathbf{y}(t_\gamma))) \leq 1$ denote the upper and lower grades of membership governed by the upper and lower membership functions, respectively. By the definition of IT2 membership functions, the property $0 \leq \underline{\mu}_{\tilde{N}_\beta^j}(g_\beta(\mathbf{y}(t_\gamma))) \leq \overline{\mu}_{\tilde{N}_\beta^j}(g_\beta(\mathbf{y}(t_\gamma))) \leq 1$ holds and further leads to $0 \leq m_j^L(\mathbf{y}(t_\gamma)) \leq m_j^U(\mathbf{y}(t_\gamma)) \leq 1$, which is valid for all j.

Inspired by [55], $\tilde{m}_j(\mathbf{y}(t_\gamma))$ is defined as follows:

$$\begin{aligned}
\tilde{m}_j(\mathbf{y}(t_\gamma)) =& \frac{\underline{\kappa}_j(\mathbf{y}(t_\gamma))m_j^L(\mathbf{y}(t_\gamma)) + \overline{\kappa}_j(\mathbf{y}(t_\gamma))m_j^U(\mathbf{y}(t_\gamma))}{\sum_{k=1}^{c}\left(\underline{\kappa}_k(\mathbf{y}(t_\gamma))m_k^L(\mathbf{y}(t_\gamma)) + \overline{\kappa}_k(\mathbf{y}(t_\gamma))m_k^U(\mathbf{y}(t_\gamma))\right)} \\
& \geq 0, && (5.7)\\
& 0 \leq \underline{\kappa}_j(\mathbf{y}(t_\gamma)) \leq 1, && (5.8)\\
& 0 \leq \overline{\kappa}_j(\mathbf{y}(t_\gamma)) \leq 1, && (5.9)\\
& \underline{\kappa}_j(\mathbf{y}(t_\gamma)) + \overline{\kappa}_j(\mathbf{y}(t_\gamma)) = 1, \ \forall\ j, && (5.10)
\end{aligned}$$

where $\underline{\kappa}_j(\mathbf{y}(t_\gamma))$ and $\overline{\kappa}_j(\mathbf{y}(t_\gamma))$ are nonlinear functions to be determined.

The IT2 SDOF polynomial fuzzy controller is described by

$$\mathbf{u}(t) = \sum_{j=1}^{c} \tilde{m}_j(\mathbf{y}(t_\gamma))(\mathbf{F}_j(\mathbf{h}(t_\gamma))\mathbf{e}_\mathbf{y}(t_\gamma) + \mathbf{G}_j(\mathbf{h}(t_\gamma))\mathbf{y}_\mathbf{r}(t_\gamma)) \tag{5.11}$$

where

$$\sum_{i=1}^{c} \tilde{m}_j(\mathbf{y}(t_\gamma)) = 1, \quad \tilde{m}_j(\mathbf{y}(t_\gamma)) \geq 0 \ \forall\ j. \tag{5.12}$$

The IT2 SDOF polynomial fuzzy controller in (5.11) becomes a full-state feedback one when $\mathbf{C}$ is a full rank matrix, e.g., $\mathbf{C} = \mathbf{I}$, which means that the analysis in this chapter is also valid for the full-state feedback case.

5.2 Stability Analysis

The tracking control problem for the IT2 SDOF PFMB control system, formed by the IT2 polynomial fuzzy model (2.2.1), reference model (4.1) and the SDOF

polynomial fuzzy controller (5.1), is considered through stability analysis in this section. The tracking performance is characterized by an H_∞ performance index. Both sets of MFI and MFD stability conditions are obtained to determine the system stability and synthesize the feedback gains.

For brevity, in the following analysis in this chapter, the time t associated with the variables is dropped for the situation without ambiguity, e.g., $\hat{\mathbf{e}}(t)$, $\mathbf{e_y}(t)$, $\mathbf{x}(t)$, $\hat{\mathbf{x}}_\mathbf{r}(\mathbf{x_r}(t))$ and $\hat{\mathbf{x}}(\mathbf{x}(t))$ are denoted as $\hat{\mathbf{e}}$, $\mathbf{e_y}$, $\mathbf{x}$, $\hat{\mathbf{x}}_\mathbf{r}(\mathbf{x_r})$ and $\hat{\mathbf{x}}(\mathbf{x})$, respectively. In matrices, "*" denotes the transposed element at the corresponding position.

5.2.1 Basic MFI Stability Conditions with H_∞ Performance

Connecting the IT2 polynomial fuzzy model (2.2.1) and the IT2 SDOF polynomial fuzzy controller (5.1), we get the closed-loop dynamic equation as follows:

$$\begin{aligned}\dot{\mathbf{x}} &= \sum_{i=1}^{p}\sum_{j=1}^{c} \tilde{w}_i(\mathbf{x})\tilde{m}_j(\mathbf{y}(t_\gamma))(\mathbf{A}_i(\mathbf{x})\hat{\mathbf{x}} + \mathbf{B}_i(\mathbf{x})\mathbf{u}) \\ &= \sum_{i=1}^{p}\sum_{j=1}^{c} \tilde{w}_i(\mathbf{x})\tilde{m}_j(\mathbf{y}(t_\gamma))\big(\mathbf{A}_i(\mathbf{x})\hat{\mathbf{x}} \\ &\quad + \mathbf{B}_i(\mathbf{x})(\mathbf{F}_j(\mathbf{h}(t_\gamma))\mathbf{e_y}(t_\gamma) + \mathbf{G}_j(\mathbf{h}(t_\gamma))\mathbf{y_r}(t_\gamma))\big), \end{aligned} \tag{5.13}$$

in which $\mathbf{x} = [x_1, x_2, \ldots, x_n]^T$ and $\hat{\mathbf{x}}(\mathbf{x}) = [\hat{x}_1(\mathbf{x}), \hat{x}_2(\mathbf{x}), \ldots, \hat{x}_N(\mathbf{x})]$.

Let us consider the relationship between $\dot{\hat{\mathbf{x}}}$ and $\dot{\mathbf{x}}$, which can be linked together by $\mathbf{T}(\mathbf{x})$ as follows:

$$\dot{\hat{\mathbf{x}}} = \frac{\partial \hat{\mathbf{x}}}{\partial \mathbf{x}}\frac{d\mathbf{x}}{dt} = \mathbf{T}(\mathbf{x})\dot{\mathbf{x}}, \tag{5.14}$$

in which $\mathbf{T}(\mathbf{x}) \in \Re^{N\times n}$ with its $\alpha\beta$-th element $T_{\alpha\beta}(\mathbf{x})$ defined as

$$T_{\alpha\beta}(\mathbf{x}) = \frac{\partial \hat{x}_\alpha(\mathbf{x})}{\partial x_\beta}, \alpha = 1, 2, \ldots, N; \beta = 1, 2, \ldots, n. \tag{5.15}$$

From (5.13) and (5.14), we have

$$\begin{aligned}\dot{\hat{\mathbf{x}}} &= \sum_{i=1}^{p}\sum_{j=1}^{c} \tilde{w}_i(\mathbf{x})\tilde{m}_j(\mathbf{y}(t_\gamma))(\tilde{\mathbf{A}}_i(\mathbf{x})\hat{\mathbf{x}} + \tilde{\mathbf{B}}_i(\mathbf{x})\mathbf{u}) \\ &= \sum_{i=1}^{p}\sum_{j=1}^{c} \tilde{w}_i(\mathbf{x})\tilde{m}_j(\mathbf{y}(t_\gamma))\big(\tilde{\mathbf{A}}_i(\mathbf{x})\hat{\mathbf{x}} \\ &\quad + \tilde{\mathbf{B}}_i(\mathbf{x})(\mathbf{F}_j(\mathbf{h}(t_\gamma))\mathbf{e_y}(t_\gamma) + \mathbf{G}_j(\mathbf{h}(t_\gamma))\mathbf{y_r}(t_\gamma))\big), \end{aligned} \tag{5.16}$$

where $\tilde{\mathbf{A}}_i(\mathbf{x}) = \mathbf{T}(\mathbf{x})\mathbf{A}_i(\mathbf{x})$, $\tilde{\mathbf{B}}_i(\mathbf{x}) = \mathbf{T}(\mathbf{x})\mathbf{B}_i(\mathbf{x})$.

Denote $\mathbf{x_r} = [x_{r_1}, x_{r_2}, \ldots, x_{r_n}]^T$ and $\hat{\mathbf{x}}_\mathbf{r}(\mathbf{x_r}) = [\hat{x}_{r_1}(\mathbf{x_r}), \hat{x}_{r_2}(\mathbf{x_r}), \ldots, \hat{x}_{r_N}(\mathbf{x_r})]^T$.

From (4.1), we have the polynomial dynamic model for the reference model:

$$\dot{\hat{\mathbf{x}}}_{\mathbf{r}}(\mathbf{x}_{\mathbf{r}}) = \frac{\partial \hat{\mathbf{x}}_{\mathbf{r}}(\mathbf{x}_{\mathbf{r}})}{\partial \mathbf{x}_{\mathbf{r}}} \frac{d\mathbf{x}_{\mathbf{r}}}{dt} = \mathbf{H}(\mathbf{x}_{\mathbf{r}})\dot{\mathbf{x}}_{\mathbf{r}} = \tilde{\mathbf{A}}_{\mathbf{r}}(\mathbf{x}_{\mathbf{r}})\hat{\mathbf{x}}(\mathbf{x}_{\mathbf{r}}) + \tilde{\mathbf{B}}_{\mathbf{r}}(\mathbf{x}_{\mathbf{r}})\mathbf{r}, \tag{5.17}$$

where $\tilde{\mathbf{A}}_{\mathbf{r}}(\mathbf{x}_{\mathbf{r}}) = \mathbf{H}(\mathbf{x}_{\mathbf{r}})\mathbf{A}_{\mathbf{r}}$, $\tilde{\mathbf{B}}_{\mathbf{r}}(\mathbf{x}_{\mathbf{r}}) = \mathbf{H}(\mathbf{x}_{\mathbf{r}})\mathbf{B}_{\mathbf{r}}$ and $\mathbf{H}(\mathbf{x}_{\mathbf{r}}) \in \Re^{N\times n}$ with its $\alpha\beta$-th element is defined as

$$H_{\alpha\beta}(\mathbf{x}_{\mathbf{r}}) = \frac{\partial \hat{x}_{r_\alpha}(\mathbf{x})}{\partial x_{r_\beta}}, \alpha = 1, 2, \ldots, N; \beta = 1, 2, \ldots, n. \tag{5.18}$$

Also, from (5.1), combining the reference model (4.1) with (5.16), $\dot{\hat{\mathbf{e}}}$ can be expressed as follows:

$$\begin{aligned}
\dot{\hat{\mathbf{e}}} = & \sum_{i=1}^{p}\sum_{j=1}^{c} \tilde{w}_i(\mathbf{x})\tilde{m}_j(\mathbf{y}(t_\gamma))\big(\tilde{\mathbf{A}}_i(\mathbf{x})\hat{\mathbf{e}} \\
& + \tilde{\mathbf{B}}_i(\mathbf{x})\mathbf{F}_j(\mathbf{h}(t_\gamma))\mathbf{C}\hat{\mathbf{e}}(t_\gamma)\big) \\
& + \sum_{i=1}^{p}\sum_{j=1}^{c} \tilde{w}_i(\mathbf{x})\tilde{m}_j(\mathbf{y}(t_\gamma))\big((\tilde{\mathbf{A}}_i(\mathbf{x}) - \tilde{\mathbf{A}}_{\mathbf{r}}(\mathbf{x}_{\mathbf{r}}))\hat{\mathbf{x}}_{\mathbf{r}}(\mathbf{x}_{\mathbf{r}}) \\
& + \tilde{\mathbf{B}}_i(\mathbf{x})\mathbf{G}_j(\mathbf{h}(t_\gamma))\mathbf{C}\hat{\mathbf{x}}_{\mathbf{r}}(\mathbf{x}_{\mathbf{r}}(t_\gamma))\big) - \tilde{\mathbf{B}}_{\mathbf{r}}(\mathbf{x}_{\mathbf{r}})\mathbf{r}.
\end{aligned} \tag{5.19}$$

The control objective is to design the feedback gains $\mathbf{F}_j(\mathbf{h}(t_\gamma))$ and $\mathbf{G}_j(\mathbf{h}(t_\gamma))$, and the membership functions for the IT2 SDOF polynomial fuzzy controller for the realization of the tracking control such that the tracking error $\hat{\mathbf{e}}$ defined in (5.1) is characterized by H_∞ performance with the consideration of system stability.

In order to adopt the Lyapunov approach to develop the stability conditions, we define $0 < \mathbf{X}(\tilde{\mathbf{x}}) = \mathbf{X}(\tilde{\mathbf{x}})^T \in \Re^{N\times N}$, $\tilde{\mathbf{x}} = (x_{j_1}, x_{j_2}, \ldots, x_{j_o}, x_{r_{k_1}}, x_{r_{k_2}}, \ldots, x_{r_{k_s}})$. The row indices $\mathbf{J} = \{j_1, j_2, \ldots, j_o\}$ and $\mathbf{K} = \{k_1, k_2, \ldots, k_s\}$ are the rows indicating that the entire rows of $\mathbf{B}_i(\mathbf{x})$ and $\mathbf{B}_{\mathbf{r}}(\mathbf{x}_{\mathbf{r}})$ are all zeros, respectively, [36]. Inspired by the work in [71, 80], we choose

$$\mathbf{X}(\tilde{\mathbf{x}}) = \begin{bmatrix} \mathbf{X}_{11} & \mathbf{0} \\ \mathbf{0} & \mathbf{X}_{22}(\tilde{\mathbf{x}}) \end{bmatrix}, \tag{5.20}$$

where $\mathbf{X}_{11} \in \Re^{q\times q}$ and $\mathbf{X}_{22}(\tilde{\mathbf{x}}) \in \Re^{(N-q)\times(N-q)}$. As $\mathbf{X}(\tilde{\mathbf{x}})$ is required to be positive definite, it implies that the inverse of $\mathbf{X}_{11}$, $\mathbf{X}_{22}(\tilde{\mathbf{x}})$ and $\mathbf{X}(\tilde{\mathbf{x}})$ exist.

In addition, we define

$$\mathbf{\Gamma} = [\mathbf{C}^T(\mathbf{C}\mathbf{C}^T)^{-1} \quad \text{ortc}(\mathbf{C}^T)], \tag{5.21}$$

where $\mathbf{\Gamma} \in \Re^{N\times N}$ and $\text{ortc}(\mathbf{C}^T)$ denotes the orthogonal complement of $\mathbf{C}^T$ [71, 80].

From the definition of $\mathbf{\Gamma}$ we have

$$\mathbf{C\Gamma} = [\mathbf{I}_l \quad \mathbf{0}], \tag{5.22}$$

where $\mathbf{I}_l \in \Re^{l\times l}$ is the identity matrix.

To facilitate the stability analysis, we further define an augment vector as $\hat{\mathbf{v}}$ and

$$\hat{\mathbf{v}} = \mathbf{\Gamma}^{-1}\hat{\mathbf{e}}. \tag{5.23}$$

The augment vector can be regarded as the system states observation from the error signal $\hat{\mathbf{e}}$ which demonstrates a linear mapping relationship. In the following, it would be easier to investigate the dynamics of $\hat{\mathbf{e}}$ instead. From (5.23), we have the dynamics of $\hat{\mathbf{v}}$ as follows:

$$\begin{aligned}
\dot{\hat{\mathbf{v}}} &= \mathbf{\Gamma}^{-1}\dot{\hat{\mathbf{e}}} \\
&= \sum_{i=1}^{p}\sum_{j=1}^{c} \tilde{w}_i(\mathbf{x})\tilde{m}_j(\mathbf{y}(t_\gamma))\big(\mathbf{\Gamma}^{-1}\tilde{\mathbf{A}}_i(\mathbf{x})\mathbf{\Gamma}\mathbf{X}(\tilde{\mathbf{x}})\mathbf{X}^{-1}(\tilde{\mathbf{x}})\mathbf{\Gamma}^{-1}\hat{\mathbf{e}} \\
&+ \mathbf{\Gamma}^{-1}\tilde{\mathbf{B}}_i(\mathbf{x})\mathbf{F}_j(\mathbf{h}(t_\gamma))\mathbf{C\Gamma}\mathbf{X}(\tilde{\mathbf{x}})\mathbf{X}^{-1}(\tilde{\mathbf{x}})\mathbf{\Gamma}^{-1}\hat{\mathbf{e}}(t_\gamma)\big) \\
&+ \sum_{i=1}^{p}\sum_{j=1}^{c} \tilde{w}_i(\mathbf{x})\tilde{m}_j(\mathbf{y}(t_\gamma))\big(\mathbf{\Gamma}^{-1}((\tilde{\mathbf{A}}_i(\mathbf{x}) - \tilde{\mathbf{A}}_{\mathbf{r}}(\mathbf{x}_{\mathbf{r}})) \\
&\mathbf{\Gamma}\mathbf{X}(\tilde{\mathbf{x}})\mathbf{X}^{-1}(\tilde{\mathbf{x}})\mathbf{\Gamma}^{-1}\hat{\mathbf{x}}_{\mathbf{r}}(\mathbf{x}_{\mathbf{r}}) + \mathbf{\Gamma}^{-1}\tilde{\mathbf{B}}_i(\mathbf{x})\mathbf{G}_j(\mathbf{h}(t_\gamma)) \\
&\mathbf{C\Gamma}\mathbf{X}(\tilde{\mathbf{x}})\mathbf{X}^{-1}(\tilde{\mathbf{x}})\mathbf{\Gamma}^{-1}\hat{\mathbf{x}}_{\mathbf{r}}(\mathbf{x}_{\mathbf{r}}(t_\gamma))\big) - \mathbf{\Gamma}^{-1}\tilde{\mathbf{B}}_{\mathbf{r}}(\mathbf{x}_{\mathbf{r}})\mathbf{r}.
\end{aligned} \tag{5.24}$$

From the definition of $\mathbf{\Gamma}$ in (5.21), we can simplify $\mathbf{F}_j(\mathbf{h}(t_\gamma))\mathbf{C\Gamma}\mathbf{X}(\tilde{\mathbf{x}})$ and $\mathbf{G}_j(\mathbf{h}(t_\gamma))\mathbf{C\Gamma}\mathbf{X}(\tilde{\mathbf{x}})$ as

$$\mathbf{F}_j(\mathbf{h}(\mathbf{t}_\gamma))\mathbf{C\Gamma}\mathbf{X}(\tilde{\mathbf{x}}) = [\mathbf{M}_j(\mathbf{h}(t_\gamma)) \quad \mathbf{0}], \tag{5.25}$$

$$\mathbf{G}_j(\mathbf{h}(\mathbf{t}_\gamma))\mathbf{C\Gamma}\mathbf{X}(\tilde{\mathbf{x}}) = [\mathbf{N}_j(\mathbf{h}(t_\gamma)) \quad \mathbf{0}]. \tag{5.26}$$

It follows from (5.24) that

$$\begin{aligned}
\dot{\hat{\mathbf{v}}} &= \sum_{i=1}^{p}\sum_{j=1}^{c} \tilde{w}_i(\mathbf{x})\tilde{m}_j(\mathbf{y}(t_\gamma))\big(\mathbf{\Gamma}^{-1}\tilde{\mathbf{A}}_i(\mathbf{x})\mathbf{\Gamma}\mathbf{X}(\tilde{\mathbf{x}})\mathbf{X}^{-1}(\tilde{\mathbf{x}})\hat{\mathbf{v}} \\
&+ \mathbf{\Gamma}^{-1}\tilde{\mathbf{B}}_i(\mathbf{x}) \times [\mathbf{M}_j(\mathbf{h}(t_\gamma)) \quad \mathbf{0}]\mathbf{X}(\tilde{\mathbf{x}})^{-1}\hat{\mathbf{v}}(t_\gamma)\big) \\
&+ \sum_{i=1}^{p}\sum_{j=1}^{c} \tilde{w}_i(\mathbf{x})\tilde{m}_j(\mathbf{y}(t_\gamma))\big(\mathbf{\Gamma}^{-1}(\tilde{\mathbf{A}}_i(\mathbf{x}) - \tilde{\mathbf{A}}_{\mathbf{r}}(\mathbf{x}_{\mathbf{r}})) \\
&\mathbf{\Gamma}\mathbf{X}(\tilde{\mathbf{x}})\mathbf{X}^{-1}(\tilde{\mathbf{x}})\mathbf{\Gamma}^{-1}\hat{\mathbf{x}}_{\mathbf{r}}(\mathbf{x}_{\mathbf{r}}) + \mathbf{\Gamma}^{-1}\tilde{\mathbf{B}}_i(\mathbf{x})[\mathbf{N}_j(\mathbf{h}(t_\gamma)) \quad \mathbf{0}] \\
&\mathbf{X}^{-1}(\tilde{\mathbf{x}})\mathbf{\Gamma}^{-1}\hat{\mathbf{x}}_{\mathbf{r}}(\mathbf{x}_{\mathbf{r}}(t_\gamma))\big) - \mathbf{\Gamma}^{-1}\tilde{\mathbf{B}}_{\mathbf{r}}(\mathbf{x}_{\mathbf{r}})\mathbf{r} \\
&= \sum_{i=1}^{p}\sum_{j=1}^{c} \tilde{w}_i(\mathbf{x})\tilde{m}_j(\mathbf{y}(t_\gamma))\Phi_{ij}(\mathbf{x}, \mathbf{x}_{\mathbf{r}})\mathbf{z}
\end{aligned} \tag{5.27}$$

where $\Phi_{ij}(\mathbf{x},\mathbf{x_r}) = [\Phi_{ij}^{(1)}(\mathbf{x},\mathbf{x_r}) \quad \Phi_{ij}^{(2)}(\mathbf{x},\mathbf{x_r}) \quad \Phi_{ij}^{(3)}(\mathbf{x},\mathbf{x_r}) \quad \Phi_{ij}^{(4)}(\mathbf{x},\mathbf{x_r}) \quad \Phi_{ij}^{(5)}(\mathbf{x},\mathbf{x_r})]$, $\Phi_{ij}^{(1)}(\mathbf{x},\mathbf{x_r}) = \mathbf{\Gamma}^{-1}\tilde{\mathbf{A}}_i(\mathbf{x})\mathbf{\Gamma}\mathbf{X}(\tilde{\mathbf{x}})$, $\Phi_{ij}^{(2)}(\mathbf{x},\mathbf{x_r}) = \mathbf{\Gamma}^{-1}(\tilde{\mathbf{A}}_i(\mathbf{x}) - \tilde{\mathbf{A}}_{\mathbf{r}}(\mathbf{x_r}))\mathbf{\Gamma}\mathbf{X}(\tilde{\mathbf{x}})$, $\Phi_{ij}^{(3)}(\mathbf{x},\mathbf{x_r}) = \mathbf{\Gamma}^{-1}\tilde{\mathbf{B}}_i(\mathbf{x})[\mathbf{M}_j(\mathbf{h}(t_\gamma)) \quad \mathbf{0}]$, $\Phi_{ij}^{(4)}(\mathbf{x},\mathbf{x_r}) = \mathbf{\Gamma}^{-1}\tilde{\mathbf{B}}_i(\mathbf{x})[\mathbf{N}_j(\mathbf{h}(t_\gamma)) \quad \mathbf{0}]$, $\Phi_{ij}^{(5)}(\mathbf{x},\mathbf{x_r}) = -\mathbf{\Gamma}^{-1}\tilde{\mathbf{B}}_{\mathbf{r}}(\mathbf{x_r})$, $\mathbf{z} = \begin{bmatrix} \mathbf{z}_1 \\ \mathbf{z}_2 \\ \mathbf{z}_3 \\ \mathbf{z}_4 \\ \mathbf{z}_5 \end{bmatrix} = \begin{bmatrix} \mathbf{X}(\tilde{\mathbf{x}})^{-1}\hat{\mathbf{v}}(t) \\ \mathbf{X}(\tilde{\mathbf{x}})^{-1}\mathbf{\Gamma}^{-1}\hat{\mathbf{x}}_{\mathbf{r}} \\ \mathbf{X}(\tilde{\mathbf{x}})^{-1}\hat{\mathbf{v}}(t_\gamma) \\ \mathbf{X}(\tilde{\mathbf{x}})^{-1}\mathbf{\Gamma}^{-1}\hat{\mathbf{x}}_{\mathbf{r}}(\mathbf{x_r}(t_\gamma)) \\ \mathbf{r} \end{bmatrix}$.

To investigate the stability of the IT2 PFMB SDOF control system, the following Lyapunov-krasovskii functional is adopted:

$$V(t) = \hat{\mathbf{v}}^T\mathbf{X}(\tilde{\mathbf{x}})^{-1}\hat{\mathbf{v}} + \int_{h_s}^{0}\int_{t+\sigma}^{t} \dot{\hat{\mathbf{v}}}(\varphi)^T\mathbf{R}\dot{\hat{\mathbf{v}}}(\varphi)d\varphi d\sigma, \tag{5.28}$$

where $0 \leq \mathbf{R} = \mathbf{R}^T \in \Re^{N\times N}$.

By taking the derivative of $V(t)$, we have

$$\begin{aligned}\dot{V}(t) = {} & \dot{\hat{\mathbf{v}}}^T\mathbf{X}(\tilde{\mathbf{x}})^{-1}\hat{\mathbf{v}} + \hat{\mathbf{v}}^T\mathbf{X}(\tilde{\mathbf{x}})^{-1}\dot{\hat{\mathbf{v}}} + \hat{\mathbf{v}}^T\frac{d\mathbf{X}(\tilde{\mathbf{x}})^{-1}}{dt}\hat{\mathbf{v}}(t) \\ & + h_s\dot{\hat{\mathbf{v}}}^T\mathbf{R}\dot{\hat{\mathbf{v}}} - \int_{t-h_s}^{t}\dot{\hat{\mathbf{v}}}(\varphi)^T\mathbf{R}\dot{\hat{\mathbf{v}}}(\varphi)d\varphi.\end{aligned} \tag{5.29}$$

Remark 5.1. *To facilitate the stability analysis, it is defined that* $\mathbf{J} = \{j_1, j_2, \ldots, j_o\}$ *is the set of row numbers that the entire row of* $\mathbf{B}_i(\mathbf{x})$ *for all* i *and* $\mathbf{K} = \{k_1, k_2, \ldots, k_s\}$ *is the set of row numbers that the entire row of* $\mathbf{B}_{\mathbf{r}}(\mathbf{x_r})$ *are all zeros. Defining* $\tilde{\mathbf{x}} = (x_{j_1}, x_{j_2}, \ldots, x_{j_o}, x_{r_{k_1}}, x_{r_{k_2}}, \ldots, x_{r_{k_s}})$ *as before, it obtains that* $\frac{\partial\mathbf{X}(\tilde{\mathbf{x}})^{-1}}{\partial x_g} = -\mathbf{X}(\tilde{\mathbf{x}})^{-1}\frac{\partial\mathbf{X}(\tilde{\mathbf{x}})}{\partial x_g}\mathbf{X}(\tilde{\mathbf{x}})^{-1}$ *and* $\frac{d\mathbf{X}(\tilde{\mathbf{x}})^{-1}}{dt} = \sum_{k=1}^{n}(\frac{\partial\mathbf{X}(\tilde{\mathbf{x}})^{-1}}{\partial x_k}\frac{dx_k}{dt} + \frac{\partial\mathbf{X}(\tilde{\mathbf{x}})^{-1}}{\partial x_{r_k}}\frac{dx_{r_k}}{dt}) = -\sum_{g\in\mathbf{J}}\mathbf{X}(\tilde{\mathbf{x}})^{-1}\big(\frac{\partial\mathbf{X}(\tilde{\mathbf{x}})}{\partial x_g}\sum_{i=1}^{p}\tilde{w}_i\mathbf{A}_i^{(g)}(\mathbf{x})\hat{\mathbf{x}}(\mathbf{x})\big)\mathbf{X}(\tilde{\mathbf{x}})^{-1} - \sum_{g\in\mathbf{K}}\mathbf{X}(\tilde{\mathbf{x}})^{-1}\big(\frac{\partial\mathbf{X}(\tilde{\mathbf{x}})^{-1}}{\partial x_{r_g}}\mathbf{A}_r^{(g)}(\mathbf{x_r})\hat{\mathbf{x}}_{\mathbf{r}}(\mathbf{x_r})\big)\mathbf{X}(\tilde{\mathbf{x}})^{-1}$ *[36],* $\mathbf{A}_i^{(g)}(\mathbf{x})$ *and* $\mathbf{A}_r^{(g)}(\mathbf{x_r})$ *denote the* g*-th row of* $\mathbf{A}_i(\mathbf{x})$ *and* $\mathbf{A}_r(\mathbf{x_r})$*, respectively.*

From Lemma 3, when $\tau \leq h_s$, we have

$$\begin{aligned}& -\frac{1}{\tau}(\hat{\mathbf{v}}(t) - \hat{\mathbf{v}}(t-\tau))^T\mathbf{R}(\hat{\mathbf{v}}(t) - \hat{\mathbf{v}}(t-\tau)) \leq \\ & -\frac{1}{h_s}(\hat{\mathbf{v}}(t) - \hat{\mathbf{v}}(t-\tau))^T\mathbf{R}(\hat{\mathbf{v}}(t) - \hat{\mathbf{v}}(t-\tau)).\end{aligned} \tag{5.30}$$

Applying Lemma 3 to deal with the integral term in (5.29), combining with (5.30) and using the fact that $\mathbf{z}_1 = \mathbf{X}(\tilde{\mathbf{x}})^{-1}\hat{\mathbf{v}}$, we have

$$\begin{aligned}\dot{V}(t) \leq {} & \dot{\hat{\mathbf{v}}}^T\mathbf{X}(\tilde{\mathbf{x}})^{-1}\hat{\mathbf{v}} + \hat{\mathbf{v}}^T\mathbf{X}(\tilde{\mathbf{x}})^{-1}\dot{\hat{\mathbf{v}}} + \hat{\mathbf{v}}^T\frac{d\mathbf{X}(\tilde{\mathbf{x}})^{-1}}{dt}\hat{\mathbf{v}} + h_s\dot{\hat{\mathbf{v}}}^T\mathbf{R}\dot{\hat{\mathbf{v}}} \\ & - \frac{1}{h_s}(\hat{\mathbf{v}} - \hat{\mathbf{v}}(t-\tau))^T\mathbf{R}(\hat{\mathbf{v}} - \hat{\mathbf{v}}(t-\tau))\end{aligned}$$

$$
\begin{aligned}
&= \dot{\hat{\mathbf{v}}}^T \mathbf{z}_1 + \mathbf{z}_1^T \dot{\hat{\mathbf{v}}} + \hat{\mathbf{v}}^T \frac{d\mathbf{X}(\tilde{\mathbf{x}})^{-1}}{dt} \hat{\mathbf{v}} + h_s \dot{\hat{\mathbf{v}}}^T \mathbf{R} \dot{\hat{\mathbf{v}}} - \frac{1}{h_s} (\hat{\mathbf{v}} - \hat{\mathbf{v}}(t_\gamma)^T \mathbf{R} (\hat{\mathbf{v}} - \hat{\mathbf{v}}(t_\gamma)) \\
&= \mathbf{z}^T \sum_{i=1}^{p} \sum_{j=1}^{c} \tilde{w}_i(\mathbf{x}) \tilde{m}_j(\mathbf{y}(t_\gamma)) \Phi_{ij}^T(\mathbf{x}, \mathbf{x_r}) \mathbf{z}_1 \\
&+ \mathbf{z}_1^T \sum_{i=1}^{p} \sum_{j=1}^{c} \tilde{w}_i(\mathbf{x}) \tilde{m}_j(\mathbf{y}(t_\gamma)) \Phi_{i,j}(\mathbf{x}, \mathbf{x_r}) \mathbf{z} + \hat{\mathbf{v}}^T \frac{d\mathbf{X}(\tilde{\mathbf{x}})^{-1}}{dt} \hat{\mathbf{v}} \\
&+ h_s \mathbf{z}^T \big(\sum_{i=1}^{p} \sum_{j=1}^{c} \tilde{w}_i(\mathbf{x}) \tilde{m}_j(\mathbf{y}(t_\gamma)) \Phi_{ij}^T(\mathbf{x}, \mathbf{x_r}) \mathbf{R} \sum_{i=1}^{p} \sum_{j=1}^{c} \tilde{w}_i(\mathbf{x}) \tilde{m}_j(\mathbf{y}(t_\gamma)) \Phi_{i,j}(\mathbf{x}, \mathbf{x_r}) \big) \mathbf{z} \\
&- \frac{1}{h_s} (\hat{\mathbf{v}}(t) - \hat{\mathbf{v}}((t_\gamma))^T \mathbf{R} (\hat{\mathbf{v}}(t) - \hat{\mathbf{v}}(t_\gamma)). \qquad (5.31)
\end{aligned}
$$

To facilitate the stability analysis, the last term in the right hand side of (5.31) can be expressed as

$$
\sum_{i=1}^{p} \sum_{j=1}^{c} \tilde{w}_i(\mathbf{x}) \tilde{m}_j(\mathbf{y}(t_\gamma)) \mathbf{z}^T \mathbf{\Lambda} \mathbf{z} = -\frac{1}{h_s} (\hat{\mathbf{v}}(t) - \hat{\mathbf{v}}(t_\gamma)^T \mathbf{R} (\hat{\mathbf{v}}(t) - \hat{\mathbf{v}}(t_\gamma)), \qquad (5.32)
$$

where

$$
\mathbf{\Lambda} = \begin{bmatrix}
-\frac{1}{h_s}\mathbf{M} & \mathbf{0} & \frac{1}{h_s}\mathbf{M} & \mathbf{0} & \mathbf{0} \\
\mathbf{0} & \mathbf{0} & \mathbf{0} & \mathbf{0} & \mathbf{0} \\
\frac{1}{h_s}\mathbf{M} & \mathbf{0} & -\frac{1}{h_s}\mathbf{M} & \mathbf{0} & \mathbf{0} \\
\mathbf{0} & \mathbf{0} & \mathbf{0} & \mathbf{0} & \mathbf{0} \\
\mathbf{0} & \mathbf{0} & \mathbf{0} & \mathbf{0} & \mathbf{0}
\end{bmatrix}, \qquad (5.33)
$$

in which $\mathbf{\Lambda} \in \Re^{(4N+m)\times(4N+m)}$ and $\mathbf{M} = \mathbf{X}(\tilde{\mathbf{x}})\mathbf{R}\mathbf{X}(\tilde{\mathbf{x}}) \in \Re^{N\times N}$.

Considering the following 3 terms in the right hand side of (5.31)

$$
\begin{aligned}
&\mathbf{z}^T \sum_{i=1}^{p} \sum_{j=1}^{c} \tilde{w}_i(\mathbf{x}) \tilde{m}_j(\mathbf{y}(t_\gamma)) \Phi_{ij}^T(\mathbf{x}, \mathbf{x_r}) \mathbf{z}_1 \\
&+ \mathbf{z}_1 \sum_{i=1}^{p} \sum_{j=1}^{c} \tilde{w}_i(\mathbf{x}) \tilde{m}_j(\mathbf{y}(t_\gamma)) \Phi_{i,j}^T(\mathbf{x}, \mathbf{x_r}) \mathbf{z} + \hat{\mathbf{v}}^T \frac{d\mathbf{X}(\tilde{\mathbf{x}})^{-1}}{dt} \hat{\mathbf{v}} \qquad (5.34)
\end{aligned}
$$

which can be rewritten as

$$
\begin{aligned}
&\sum_{i=1}^{p} \sum_{j=1}^{c} w_i(\mathbf{x}) m_j(\mathbf{y}(t_\gamma)) \mathbf{z}^T \mathbf{\Delta}_{ij}(\mathbf{x}, \mathbf{x_r}) \mathbf{z} - \mathbf{z}_1^T \mathbf{z}_1 - \mathbf{z}_3^T \mathbf{z}_3 \\
&+ \sigma_1 \mathbf{z}_2^T \mathbf{z}_2 + \sigma_2 \mathbf{z}_4^T \mathbf{z}_4 + \sigma_3 \mathbf{z}_5^T \mathbf{z}_5, \qquad (5.35)
\end{aligned}
$$

where

$$\mathbf{\Delta}_{ij}(\mathbf{x},\mathbf{x_r}) = \begin{bmatrix} \mathbf{\Delta}_{ij}^{(11)}(\mathbf{x},\mathbf{x_r}) & * & * & * & * \\ \mathbf{\Phi}_{ij}^{(2)}(\mathbf{x},\mathbf{x_r})^T & -\sigma_1\mathbf{I} & \mathbf{0} & \mathbf{0} & \mathbf{0} \\ \mathbf{\Phi}_{ij}^{(3)}(\mathbf{x},\mathbf{x_r})^T & \mathbf{0} & \mathbf{I} & \mathbf{0} & \mathbf{0} \\ \mathbf{\Phi}_{ij}^{(4)}(\mathbf{x},\mathbf{x_r})^T & \mathbf{0} & \mathbf{0} & -\sigma_2\mathbf{I} & \mathbf{0} \\ \mathbf{\Phi}_{ij}^{(5)}(\mathbf{x},\mathbf{x_r})^T & \mathbf{0} & \mathbf{0} & \mathbf{0} & -\sigma_3\mathbf{I} \end{bmatrix} \tag{5.36}$$

where $\mathbf{\Delta}_{ij}^{(11)}(\mathbf{x},\mathbf{x_r}) = \mathbf{\Phi}_{ij}^{(1)}(\mathbf{x},\mathbf{x_r}) + \mathbf{\Phi}_{ij}^{(1)}(\mathbf{x},\mathbf{x_r})^T - \sum_{g\in\mathbf{J}} \frac{\partial \mathbf{X}(\tilde{\mathbf{x}})}{\partial x_g}\mathbf{A}_i^{(g)}(\mathbf{x})\hat{\mathbf{x}}(\mathbf{x})$
$- \sum_{g\in\mathbf{K}} \frac{\partial \mathbf{X}(\tilde{\mathbf{x}})}{\partial x_{g_k}}\mathbf{A}_r^{(g)}(\mathbf{x})\hat{\mathbf{x}}_\mathbf{r}(\mathbf{x_r}) + \mathbf{I}$; $\mathbf{I}$ is the identify matrix of compatible dimensions; $\sigma_1 > 0$, $\sigma_2 > 0$ and $\sigma_3 > 0$ are scalars to be determined which are related to the tracking performance characterized by an H_∞ performance index to be discussed in the following.

With (5.32) and (5.35), (5.31) can be written as follows:

$$\dot{V}(t) \leq \mathbf{z}^T\mathbf{\Theta}(\mathbf{x},\mathbf{x_r})\mathbf{z} - \mathbf{z}_1^T\mathbf{z}_1 - \mathbf{z}_3^T\mathbf{z}_3 + \sigma_1\mathbf{z}_2^T\mathbf{z}_2 + \sigma_2\mathbf{z}_4^T\mathbf{z}_4 + \sigma_3\mathbf{z}_5^T\mathbf{z}_5, \tag{5.37}$$

where

$$\begin{aligned}\mathbf{\Theta}(\mathbf{x},\mathbf{x_r}) = &\sum_{i=1}^{p}\sum_{j=1}^{c} \tilde{w}_i(\mathbf{x})\tilde{m}_j(\mathbf{y}(t_\gamma))(\mathbf{\Delta}_{ij}(\mathbf{x},\mathbf{x_r}) + \mathbf{\Lambda}) \\ &+ h_s\big(\sum_{i=1}^{p}\sum_{j=1}^{c} \tilde{w}_i(\mathbf{x})\tilde{m}_j(\mathbf{y}(t_\gamma))\Phi_{ij}^T(\mathbf{x},\mathbf{x_r})\mathbf{R}\sum_{i=k}^{p}\sum_{j=l}^{c} \tilde{w}_k(\mathbf{x})\tilde{m}_l(\mathbf{y}(t_\gamma))\Phi_{k,l}(\mathbf{x},\mathbf{x_r})\big).\end{aligned} \tag{5.38}$$

If $\mathbf{\Theta}(\mathbf{x},\mathbf{x_r}) < 0$ can be achieved, we obtain

$$\dot{V}(t) \leq -\mathbf{z}_1^T\mathbf{z}_1 - \mathbf{z}_3^T\mathbf{z}_3 + \sigma_1\mathbf{z}_2^T\mathbf{z}_2 + \sigma_2\mathbf{z}_4^T\mathbf{z}_4 + \sigma_3\mathbf{z}_5^T\mathbf{z}_5. \tag{5.39}$$

Considering the termination time of control t_f [66, 80] and taking integration on both sides of (5.39) with respect to time t, we obtain the following H_∞ performance:

$$\frac{\int_0^{t_f}(\mathbf{z}_1^T\mathbf{z}_1 + \mathbf{z}_3^T\mathbf{z}_3) - \mathbf{V}(0)}{\int_0^{t_f}(\sigma_1\mathbf{z}_2^T\mathbf{z}_2 + \sigma_2\mathbf{z}_4^T\mathbf{z}_4 + \sigma_3\mathbf{z}_5^T\mathbf{z}_5)} \leq 1. \tag{5.40}$$

Remark 5.2. *In* (5.40), $\mathbf{z}_1$ *and* $\mathbf{z}_3$ *relate to the values of* $\hat{\mathbf{v}}(t)$ *and* $\hat{\mathbf{v}}(t_\gamma)$*, respectively, which are further related to the tracking error* $\hat{\mathbf{e}}(t)$ *and* $\hat{\mathbf{e}}(t_\gamma)$*. It can be seen that smaller value of* σ_1*,* σ_2 *and* σ_3 *will reduce* $\int_0^{t_f}(\mathbf{z}_1^T\mathbf{z}_1 + \mathbf{z}_3^T\mathbf{z}_3)$*, which leads to an improved* H_∞ *performance. In this chapter, finding the value of* σ_1*,* σ_2 *and* σ_3 *can be formulated as a generalized eigenvalue problem (GEVP), which can be handled through SOSTOOLS [37].*

The above result is based on the satisfaction of $\mathbf{\Theta}(\mathbf{x},\mathbf{x_r}) < 0$. If Schur comple-

ment lemma is applied directly to deal with the last term in (5.38), $\mathbf{R}^{-1}$ will be generated and further leads to a non-convex condition. To circumvent this problem, we use the inequality $2\xi\mathbf{X}(\tilde{\mathbf{x}})-\xi^2\mathbf{R} \leq \mathbf{X}(\tilde{\mathbf{x}})\mathbf{R}^{-1}\mathbf{X}(\tilde{\mathbf{x}})$ [42], where ξ is a scalar chosen by the user, to render it to a convex condition. By adopting the above discussion and Schur complement lemma, $\boldsymbol{\Theta}(\mathbf{x}, \mathbf{x_r}) < 0$ is implied by the following condition:

$$\sum_{i=1}^{p}\sum_{j=1}^{c} \tilde{w}_i(\mathbf{x})\tilde{m}_j(\mathbf{y}(t_\gamma))\boldsymbol{\Xi}_{ij}(\mathbf{x}, \mathbf{x_r}) < 0, \tag{5.41}$$

where

$$\boldsymbol{\Xi}_{ij}(\mathbf{x}, \mathbf{x_r}) = \begin{bmatrix} \boldsymbol{\Delta}_{ij}(\mathbf{x}, \mathbf{x_r}) + \boldsymbol{\Lambda} & * \\ h_s\boldsymbol{\Phi}_{ij}(\mathbf{x}, \mathbf{x_r}) & -h_s(2\xi\mathbf{X}(\tilde{\mathbf{x}}) - \xi^2\mathbf{R}) \end{bmatrix}. \tag{5.42}$$

Consequently, the satisfaction of $\boldsymbol{\Xi}_{ij}(\mathbf{x}, \mathbf{x_r}) < 0$ for all i and j can make sure that $\boldsymbol{\Theta}(\mathbf{x}, \mathbf{x_r}) < 0$.

The results for the stability analysis and H_∞ performance are summarized in the following theorem.

Theorem 5.1. *Considering the IT2 SDOF PFMB control system, which is formed by a nonlinear plant represented by the IT2 polynomial fuzzy model* (2.12) *and the IT2 SDOF polynomial fuzzy controller* (5.11) *connected in a closed loop, its system states are driven to follow those of the reference model* (4.1) *subject to the H_∞ performance* (5.40) *if there exist scalars $\sigma_1 > 0$, $\sigma_2 > 0$, $\sigma_3 > 0$, and polynomial matrices $\mathbf{M}_j(\mathbf{h}(t_\gamma)) \in \Re^{m\times q}$, $\mathbf{N}_j(\mathbf{h}(t_\gamma)) \in \Re^{m\times q}$, $\mathbf{X}(\tilde{\mathbf{x}}) = \mathbf{X}(\tilde{\mathbf{x}})^T \in \Re^{N\times N}$ with the structure given in* (5.20)*, $\mathbf{R} = \mathbf{R}^T \in \Re^{N\times N}$, $j = 1, 2, \ldots, c$, such that the following GEVP is feasible:*

$$\begin{aligned}
&\min \sigma_1 + \sigma_2 + \sigma_3 \text{ subject to} \\
&\sigma_1 > 0; \\
&\sigma_2 > 0; \\
&\sigma_3 > 0; \\
&\nu_1^T(\mathbf{X}(\tilde{\mathbf{x}}) - \varepsilon_1(\tilde{\mathbf{x}})\mathbf{I})\nu_1 \text{ is SOS}; \\
&\nu_1^T(\mathbf{R} - \varepsilon_2\mathbf{I})\nu_1 \text{ is SOS}; \\
&-\nu_2^T(\boldsymbol{\Xi}_{ij}(\mathbf{x}, \mathbf{x_r}) + \varepsilon_3(\mathbf{x}, \mathbf{x_r})\mathbf{I})\nu_2 \text{ is SOS}, \\
&i = 1, 2, \ldots, p; j = 1, 2, \ldots, c,
\end{aligned} \tag{5.43}$$

where $\nu_1 \in \Re^N$ and $\nu_2 \in \Re^{5N+m}$ are arbitrary vectors independent of $\mathbf{x}$ and $\mathbf{x_r}$; ξ is a predefined scalar; $\varepsilon_1(\tilde{\mathbf{x}}) > 0$ and $\varepsilon_3(\mathbf{x}, \mathbf{x_r}) > 0$ are predefined scalar polynomials; $\varepsilon_2 > 0$ is a predefined scalar. The polynomial feedback gains are defined in (5.25) *abd* (5.26).

Remark 5.3. *The stability conditions in Theorem 5.1 are MFI, which do not have any information of membership functions and thus are conservative. In the following, MFD stability analysis will be conducted with the consideration of different levels of the information of lower and upper membership functions to relax the stability conditions.*

5.2.2 MFD Stability Conditions with H_∞ Performance

The idea of bringing the membership functions into the analysis will relax the stability analysis results, i.e., the condition in (5.41). However, it will lead to the stability conditions depending on membership functions and will end up stability conditions of infinite number if the original ones, $\tilde{w}_i(\mathbf{x})\tilde{m}_j(\mathbf{y}(t_\gamma))$, are applied directly, which is impractical to be solved numerically. To circumvent this difficulty, the sub-domain information, approximation of $\tilde{w}_i(\mathbf{x})\tilde{m}_j(\mathbf{y}(t_\gamma))$ and output-state information are used, which are to be detailed in the following.

To obtain the sub-domain information, the operating domain of $\mathbf{x}$ denoted as Φ is divided into L connected sub-domains according to $\mathbf{x}$ denoted as Φ_l, $l = 1, 2, \ldots, L$ such that $\Phi = \bigcup_{l=1}^{L} \Phi_l$ and denote $\tilde{h}_{ij}(\mathbf{x}, \mathbf{y}(t_\gamma)) \equiv \tilde{w}_i(\mathbf{x})\tilde{m}_j(\mathbf{y}(t_\gamma))$. An approximation function $\underline{h}_{ijl}(\mathbf{x})$ of the l-th operating sub-domain for $\mathbf{x} \in \Phi_l$ is chosen to estimate $\tilde{h}_{ij}(\mathbf{x}, \mathbf{y}(t_\gamma))$ that the constant approximation error δ_{ijl} in the l-th operating sub-domain satisfies

$$0 \leq \tilde{h}_{ij}(\mathbf{x}, \mathbf{y}(t_\gamma)) - \underline{h}_{ijl}(\mathbf{x}) \leq \delta_{ijl}, \ \forall\, l, \mathbf{x} \in \Phi_l. \tag{5.44}$$

It should be pointed out that $\underline{h}_{ijl}(\mathbf{x})$ will be used in the stability conditions and the stability conditions are going to be solved by numerical software such as SOSTOOLS, therefore $\underline{h}_{ijl}(\mathbf{x})$ should be in a favorable form such as a constant, a linear function or a polynomial function of $\mathbf{x}$, which can be processed by the numerical software. In general, the originial membership functions $\tilde{h}_{ij}(\mathbf{x}, \mathbf{y}(t_\gamma))$ cannot be processed directly by the numerical software which is the main reason why the approximation function $\underline{h}_{ijl}(\mathbf{x})$ is introduced to facilitate the analysis.

To take the output-state information into account, it is assumed that the system output $\mathbf{y}$ is elementwisely lower bounded by $\underline{\mathbf{y}}_l \in \Re^q$ and upper bounded by $\overline{\mathbf{y}}_l \in \Re^q$ in the l-th sub-operating domain. As a results, we can establish the following inequality:

$$(\mathbf{y} - \underline{\mathbf{y}}_l)^T \mathbf{D}(\overline{\mathbf{y}}_l - \mathbf{y})\mathbf{S}_l(\mathbf{y}) \geq 0, \ \forall\, l, \mathbf{x} \in \Phi_l, \tag{5.45}$$

where $\mathbf{D} = \text{diag}\{d_1, d_2, \ldots, d_q\} \in \Re^{q \times q}$ is a diagonal matrix whose elements are either 0 or 1. When $d_r = 1$, $r = 1, 2, \ldots, q$, the output-state information of y_r is included, otherwise, not included; $0 \leq \mathbf{S}_l(\mathbf{y}) = \mathbf{S}_l^T(\mathbf{y}) \in \Re^{(5N+m)\times(5N+m)}$, $l = 1, 2, \ldots, L$, is a slack polynomial matrix to be determined.

Considering (5.44) and (5.45), and defining slack matrix variable $0 \leq \mathbf{Y}_{ijl}(\mathbf{x}, \mathbf{x_r}) = \mathbf{Y}_{ijl}(\mathbf{x}, \mathbf{x_r})^T \in \Re^{(5N+m)\times(5N+m)}$ which satisfies $\mathbf{Y}_{ijl}(\mathbf{x}, \mathbf{x_r}) \geq \mathbf{\Xi}_{ij}(\mathbf{x}, \mathbf{x_r})$, these information is added to (5.41) such that we have

$$
\begin{aligned}
&\sum_{i=1}^{p}\sum_{j=1}^{c} \tilde{h}_{ij}(\mathbf{x}, \mathbf{y}(t_\gamma))\mathbf{\Xi}_{ij} \\
&= \sum_{i=1}^{p}\sum_{j=1}^{c} (\underline{h}_{ijl}(\mathbf{x}) + \tilde{h}_{ij}(\mathbf{x}, \mathbf{y}(t_\gamma)) - \underline{h}_{ijl}(\mathbf{x}))\mathbf{\Xi}_{ij}(\mathbf{x}, \mathbf{x_r}) \\
&= \sum_{i=1}^{p}\sum_{j=1}^{c} \underline{h}_{ijl}(\mathbf{x})\mathbf{\Xi}_{ij}(\mathbf{x}, \mathbf{x_r}) + \sum_{i=1}^{p}\sum_{j=1}^{c} (\tilde{h}_{ij}(\mathbf{x}, \mathbf{y}(t_\gamma)) - \underline{h}_{ijl}(\mathbf{x}))\mathbf{\Xi}_{ij}(\mathbf{x}, \mathbf{x_r}) \\
&\leq \sum_{i=1}^{p}\sum_{j=1}^{c} \underline{h}_{ijl}(\mathbf{x})\mathbf{\Xi}_{ij}(\mathbf{x}, \mathbf{x_r}) + \sum_{i=1}^{p}\sum_{j=1}^{c} |\tilde{h}_{ij}(\mathbf{x}, \mathbf{y}(t_\gamma)) - \underline{h}_{ijl}(\mathbf{x})|\mathbf{Y}_{ijl}(\mathbf{x}, \mathbf{x_r}) \\
&\leq \sum_{i=1}^{p}\sum_{j=1}^{c} \underline{h}_{ijl}(\mathbf{x})\mathbf{\Xi}_{ij}(\mathbf{x}, \mathbf{x_r}) + \sum_{i=1}^{p}\sum_{j=1}^{c} \delta_{ijl}\mathbf{Y}_{ijl}(\mathbf{x}, \mathbf{x_r}) + (\mathbf{y} - \underline{\mathbf{y}}_l)^T\mathbf{D}(\overline{\mathbf{y}}_l - \mathbf{y})\mathbf{S}_l(\mathbf{y}) \\
&= \sum_{i=1}^{p}\sum_{j=1}^{c} (\underline{h}_{ijl}(\mathbf{x})\mathbf{\Xi}_{ij}(\mathbf{x}, \mathbf{x_r}) + \delta_{ijl}\mathbf{Y}_{ijl}(\mathbf{x}, \mathbf{x_r})) + (\mathbf{y} - \underline{\mathbf{y}}_l)^T\mathbf{D}(\overline{\mathbf{y}}_l - \mathbf{y})\mathbf{S}_l(\mathbf{y}),\ \forall\, l, \mathbf{x} \in \Phi_l.
\end{aligned}
\tag{5.46}
$$

When the right hand side of (5.46) is negative definite, the system states of the IT2 SDOF PFMB control system are driven to follow those of the reference model (4.1) subject to the H_∞ performance (5.40). The above MFD stability analysis results are summarized as in the following theorem.

Theorem 5.2. *Considering the IT2 SDOF PFMB control system, which is formed by a nonlinear plant represented by the IT2 polynomial fuzzy model* (2.12) *and the IT2 SDOF polynomial fuzzy controller* (5.11) *connected in a closed loop, its system states are driven to follow those of the reference model* (4.1) *subject to the H_∞ performance* (5.40) *if there exist polynomial matrices $\mathbf{S}_l(\mathbf{y}) = \mathbf{S}_l(\mathbf{y})^T \in \Re^{(5N+m)\times(5N+m)}$, $\mathbf{M}_j(\mathbf{h}(t_\gamma)) \in \Re^{m\times q}$, $\mathbf{N}_j(\mathbf{h}(t_\gamma)) \in \Re^{m\times q}$, $\mathbf{X}(\tilde{\mathbf{x}}) = \mathbf{X}(\tilde{\mathbf{x}})^T \in \Re^{N\times N}$, $\mathbf{Y}_{ijl}(\mathbf{x}, \mathbf{x_r}) = \mathbf{Y}_{ijl}(\mathbf{x}, \mathbf{x_r})^T \in \Re^{(5N+m)\times(5N+m)}$, $i = 1, 2, \ldots, p$, $j = 1, 2, \ldots, c$, $l = 1, 2, \ldots, L$, such that the following SOS-based GEVP conditions are satisfied:*

$$
\begin{aligned}
&\min \sigma_1 + \sigma_2 + \sigma_3 \text{ subject to} \\
&\sigma_1 > 0; \\
&\sigma_2 > 0; \\
&\sigma_3 > 0; \\
&\rho^T(\mathbf{S}_l(\mathbf{y}) - \varepsilon_1(\mathbf{y})\mathbf{I})\rho \text{ is SOS}, \quad \forall\, l; \\
&\nu^T(\mathbf{X}(\tilde{\mathbf{x}}) - \varepsilon_2(\tilde{\mathbf{x}})\mathbf{I})\nu \text{ is SOS}; \\
&\rho^T(\mathbf{Y}_{ijl}(\mathbf{x}, \mathbf{x_r}) - \varepsilon_3(\mathbf{x}, \mathbf{x_r})\mathbf{I})\rho \text{ is SOS}, \quad \forall\, i, j, l;
\end{aligned}
$$

$$\rho^T(\mathbf{Y}_{ijl}(\mathbf{x},\mathbf{x_r}) - \mathbf{\Xi}_{ij}(\mathbf{x},\mathbf{x_r}) - \varepsilon_4(\mathbf{x},\mathbf{x_r})\mathbf{I})\rho \text{ is SOS}, \forall\, i,j,l;$$
$$-\rho^T\big(\sum_{i=1}^{p}\sum_{j=1}^{c}(\underline{h}_{ijl}(\mathbf{x})\mathbf{\Xi}_{ij}(\mathbf{x},\mathbf{x_r}) + \delta_{ijl}\mathbf{Y}_{ijl}(\mathbf{x},\mathbf{x_r}))+$$
$$(\mathbf{y}-\underline{\mathbf{y}}_l)^T\mathbf{D}(\overline{\mathbf{y}}_l - \mathbf{y})\mathbf{S}_l(\mathbf{y}) + \varepsilon_5(\mathbf{x},\mathbf{x_r})\mathbf{I}\big)\rho \text{ is SOS}, \quad \forall\, l$$

where $\nu \in \Re^N$ *is an arbitrary vector independent of* $\mathbf{x}$, $\mathbf{x_r}$ *and* $\mathbf{y}$, $\rho \in \Re^{5N+m}$ *is an arbitrary vector independent of* $\mathbf{x}$, $\mathbf{x_r}$ *and* $\mathbf{y}$, $\underline{h}_{ijl}(\mathbf{x})$ *and* δ_{ijl} *are determined by the upper and lower bounds of the IT2 membership functions;* $\mathbf{D} = diag\{d_1, d_2, \ldots, d_q\} \in \Re^{q\times q}$ *is a predefined diagonal matrix;* $\varepsilon_1(\mathbf{y}) > 0$, $\varepsilon_2(\tilde{\mathbf{x}}) > 0$, $\varepsilon_3(\mathbf{x},\mathbf{x_r}) > 0$, $\varepsilon_4(\mathbf{x},\mathbf{x_r}) > 0$, $\varepsilon_5(\mathbf{x},\mathbf{x_r}) > 0$ *are predefined scalar polynomials;* $\underline{\mathbf{y}}_l$ *and* $\overline{\mathbf{y}}_l$ *are the predefined lower and upper bounds of the system output vector* $\mathbf{y}$*, respectively, in the* l*-th operating sub-domain. The polynomial feedback gains are defined in* (5.25) *and* (5.26).

Remark 5.4. *Some conditions in Theorem 5.2 contain the output state vector* $\mathbf{y}$*. From* (2.12)*,* $\mathbf{y}$ *is a function of* $\mathbf{x}$*, it is thus all conditions in Theorem 5.2 depending on* $\mathbf{x}$ *(continuous and sampled versions) only.*

In order to obtain the values of $\underline{h}_{ijl}(\mathbf{x})$ and δ_{ijl}, the following analysis steps are adopted:

5.2.2.1 Finding $\dot{\hat{\mathbf{x}}}_{max}$

To apply Theorem 5.2, it needs to determine δ_{ijl} which satisfies the condition (5.44). In order to determine δ_{ijl}, $\dot{\hat{\mathbf{x}}}_{max}$ needs to be determined first. To obtain $\dot{\hat{\mathbf{x}}}_{max}$ used in (5.50) and (5.51), let us recall the definition of $\dot{\hat{\mathbf{x}}}$ in (5.14), which is $\dot{\hat{\mathbf{x}}} = \mathbf{T}(\mathbf{x})\dot{\mathbf{x}}$. Then the $\dot{\hat{\mathbf{x}}}_{max}$ can be calculated by $\mathbf{T}(\mathbf{x})$ and $\dot{\mathbf{x}}$:

$$\dot{\hat{\mathbf{x}}} = \begin{bmatrix} \mathbf{T}_1(\mathbf{x})\dot{\mathbf{x}} \\ \mathbf{T}_2(\mathbf{x})\dot{\mathbf{x}} \\ \vdots \\ \mathbf{T}_N(\mathbf{x})\dot{\mathbf{x}} \end{bmatrix} \tag{5.47}$$

and

$$\dot{\hat{\mathbf{x}}}_{max} = \begin{bmatrix} \max\limits_{\mathbf{x}\in\Phi}(\mathbf{T}_1(\mathbf{x})\dot{\mathbf{x}}) \\ \max\limits_{\mathbf{x}\in\Phi}(\mathbf{T}_2(\mathbf{x})\dot{\mathbf{x}}) \\ \vdots \\ \max\limits_{\mathbf{x}\in\Phi}(\mathbf{T}_N(\mathbf{x})\dot{\mathbf{x}}) \end{bmatrix}, \tag{5.48}$$

where $\mathbf{T}_1(\mathbf{x}), \mathbf{T}_2(\mathbf{x}), \ldots, \mathbf{T}_N(\mathbf{x})$ are the row vectors of $\mathbf{T}(\mathbf{x})$ and Φ denotes the operating domain of $\mathbf{x}$ defined in prior.

5.2.2.2 Finding δ_{ijl}

Recalling that $\tilde{h}_{ij}(\mathbf{x}, \mathbf{y}(t_\gamma)) \equiv \tilde{w}_i(\mathbf{x})\tilde{m}_j(\mathbf{y}(t_\gamma))$, it depends on both $\mathbf{x}(t)$ and $\mathbf{y}(t_\gamma)$. When we treat $\mathbf{y}(t_\gamma)$ as an independent variable with $\mathbf{x}(t)$, the information of membership function may not be captured well by δ_{ijl} as $\mathbf{y}(t_\gamma)$ is somewhat related to $\mathbf{x}$ according to the system output defined in (2.12). If we can estimate $\tilde{m}_j(\mathbf{y}(t_\gamma))$ by $\tilde{m}_j(\mathbf{x})$, then $\tilde{h}_{ij}(\mathbf{x}, \mathbf{y}(t_\gamma))$ can be estimated by $\tilde{w}_i(\mathbf{x})\tilde{m}_j(\mathbf{x})$ which depends on the only variable $\mathbf{x}$. As a result, it could make easy the estimation of δ_{ijl} in (5.44).

To realize the above estimation, we first find the relationship between $\mathbf{y}(t_\gamma)$ and $\mathbf{y}(t)$ during the sampling period by considering the system output. With (2.12) and (5.14), we have

$$\mathbf{y}(t) - \mathbf{y}(t_\gamma) = \int_{t_\gamma}^{t} \dot{\mathbf{y}}(\sigma)d\sigma = \int_{t_\gamma}^{t} \mathbf{C}\dot{\hat{\mathbf{x}}}(\mathbf{x}(\sigma))d\sigma. \tag{5.49}$$

Denoting $\dot{\hat{\mathbf{x}}}_{max} \in \Re^N$ as a vector of constant values which is the maximum value of $|\dot{\hat{\mathbf{x}}}(\mathbf{x}(t))|$ in the operating domain, i.e., $|\dot{\hat{\mathbf{x}}}(\mathbf{x}(t))| \leq \dot{\hat{\mathbf{x}}}_{max}$, from (5.49), we can obtain

$$|\mathbf{y}(t) - \mathbf{y}(t_\gamma)| \leq (t - t_\gamma)\mathbf{C}\dot{\hat{\mathbf{x}}}_{max} \leq h_s\mathbf{C}\dot{\hat{\mathbf{x}}}_{max}. \tag{5.50}$$

From (5.49) and (5.50), it follows that

$$\begin{aligned} \mathbf{y}(t_\gamma) &\in [\mathbf{y}(t) - h_s\mathbf{C}\dot{\hat{\mathbf{x}}}_{max}, \quad \mathbf{y}(t) + h_s\mathbf{C}\dot{\hat{\mathbf{x}}}_{max}] \\ &= [\mathbf{C}\hat{\mathbf{x}}(t) - h_s\mathbf{C}\dot{\hat{\mathbf{x}}}_{max}, \quad \mathbf{C}\hat{\mathbf{x}}(t) + h_s\mathbf{C}\dot{\hat{\mathbf{x}}}_{max}]. \end{aligned} \tag{5.51}$$

The above result is summarized as follows: given any $\mathbf{x}$, assuming that $|\dot{\hat{\mathbf{x}}}(\mathbf{x}(t))| \leq \dot{\hat{\mathbf{x}}}_{max}$ is satisfied, $\mathbf{y}(t_\gamma)$ will be in the range of $[\mathbf{C}\hat{\mathbf{x}}(t) - h_s\mathbf{C}\dot{\hat{\mathbf{x}}}_{max}, \quad \mathbf{C}\hat{\mathbf{x}}(t) + h_s\mathbf{C}\dot{\hat{\mathbf{x}}}_{max}]$. Consequently, from (5.44), δ_{ijl} can be determined numerically by estimating $|\tilde{h}_{ij}(\mathbf{x}, \mathbf{y}(t_\gamma)) - \hat{h}_{ijl}(\mathbf{x})|$ for $\mathbf{x} \in \Phi_l$; $\mathbf{y}(t_\gamma) \in [\mathbf{C}\hat{\mathbf{x}}(t) - h_s\mathbf{C}\dot{\hat{\mathbf{x}}}_{max}, \quad \mathbf{C}\hat{\mathbf{x}}(t) + h_s\mathbf{C}\dot{\hat{\mathbf{x}}}_{max}]$ and all l.

5.3 Simulation Examples

5.3.1 Numerical Example

To demonstrate the effectiveness of the proposed approach, we design a polynomial fuzzy control system equipped with different model and fuzzy control rules to track the states of the reference using only the sampled-data system output.

Let us consider a three-rule polynomial fuzzy model with $\hat{\mathbf{x}}(\mathbf{x}(t)) = \mathbf{x}(t) = [x_1(t) \quad x_2(t)]^T$,

$$\mathbf{A}_1(x_1(t)) = \begin{bmatrix} 0.59 - 0.12x_1(t) & -7.29 - 1.82x_1(t) \\ 0.01 & -2.85 \end{bmatrix},$$

$$\mathbf{A}_2(x_1(t)) = \begin{bmatrix} 0.02 + 2.25x_1(t) & -4.64 + 0.72x_1(t) \\ 0.35 & -8.56 \end{bmatrix},$$

$$\mathbf{A}_3(x_1(t)) = \begin{bmatrix} 0.73 + 0.45x_1(t) & 8.45 + 2.13x_1(t) \\ 0.26 & -15.43 \end{bmatrix},$$

$$\mathbf{B}_1(x_1(t)) = \begin{bmatrix} 1 + 1.35x_1(t) + 2.33x_1(t)^2 \\ 0 \end{bmatrix},$$

$$\mathbf{B}_2(x_1(t)) = \begin{bmatrix} 8 - 0.62x_1(t) \\ 0 \end{bmatrix},$$

$$\mathbf{B}_3(x_1(t)) = \begin{bmatrix} 4 - 0.73x_1(t) + 3.35x_1(t)^2 \\ 0.8 \end{bmatrix},$$

$$\mathbf{C} = [1 \quad 0].$$

Given that $\mathbf{C} = [1 \quad 0]$, we have the output $\mathbf{y}(t) = \mathbf{C}\hat{\mathbf{x}}(\mathbf{x}(t)) = x_1(t)$ in this simulation and we will use $x_1(t)$ in this example instead of using $\mathbf{y}(t)$. The membership functions are chosen as $\underline{w}_1(x_1(t)) = 1 - 1/(1 + e^{(-x_1(t)-3.5)})$, $\underline{w}_3(x_1(t)) = 1/(1 + e^{(-x_1(t)+3.5)})$, $\overline{w}_2(x_1(t)) = 1 - \underline{w}_1(x_1(t)) - \underline{w}_3(x_1(t))$; $\overline{w}_1(x_1(t)) = 1 - 1/(1 + e^{(-x_1(t)-2.5)})$, $\overline{w}_3(x_1(t)) = 1/(1 + e^{(-x_1(t)+2.5)})$, $\underline{w}_2(x_1(t)) = 1 - \overline{w}_1(x_1(t)) - \overline{w}_3(x_1(t))$.

A two-rule IT2 SDOF polynomial fuzzy controller is employed to realise the tracking control where the IT2 membership functions are chosen as follows:

$$\underline{m}_1(x_1(t)) = \begin{cases} 1 & \text{for } x_1(t) < -5.2 \\ \frac{-x_1(t)+4.8}{10} & \text{for } -5.2 \leq x_1(t) \leq 4.8 \\ 0 & \text{for } x_1(t) > 4.8 \end{cases}, \tag{5.52}$$

$$\overline{m}_1(x_1(t)) = \begin{cases} 1 & \text{for } x_1(t) < -4.8 \\ \frac{-x_1(t)+5.2}{10} & \text{for } -4.8 \leq x_1(t) \leq 5.2 \\ 0 & \text{for } x_1(t) > 5.2 \end{cases}, \tag{5.53}$$

$\overline{m}_2(x_1(t)) = 1 - \underline{m}_1(x_1(t))$, $\underline{m}_2(x_1(t)) = 1 - \overline{m}_1(x_1(t))$, and $\tilde{m}_2(x_1(t)) = 1 - \tilde{m}_1(x_1(t))$.

The reference model is chosen as $\mathbf{A_r} = \begin{bmatrix} -1 & -1 \\ 0.25 & -10.5 \end{bmatrix}$, $\mathbf{B_r} = \begin{bmatrix} 0 \\ 1 \end{bmatrix}$ and $r(t) = 0.5\sin(0.2t)$.

It is considered that the system is working in $x_1 \in [-10, 10]$. As $y = x_1$, it suggests that the lower and upper bounds of y is $\underline{y} = -10$ and $\overline{y} = 10$. The sampling period in this simulation is set as $h_s = 0.05$s. Assuming $\dot{x_1}(t) \in [-20 \quad 20]$, the largest variation of x_1 within the sampling period is $\int_t^{t+h_s} \dot{x_1}(t)dt \leq 20 \times h_s$, which is within domain $[-1 \quad 1]$. It should be noted that this assumption should

be verified by simulations. With this information, from Section 5.2.2.2, it can be obtained that $y(t_\gamma) \in [x_1(t) - 1, \quad x_1(t) + 1]$. By dividing the operating domain $x_1(t)$ into 15 uniform sub-domains (i.e., $L = 15$), we have $\underline{y}_l = \underline{x}_{1_l} = -\frac{34}{3} + \frac{4}{3}l$ and $\overline{y}_l = \overline{x}_{1_l} = -10 + \frac{4}{3}l$, $l = 1, 2, \ldots, 15$, which are the lower and upper bounds of the l-th operating sub-domains of the operating domain, respectively. It is chosen that $\mathbf{D} = 1$ is considered. The values of $\underline{h}_{ijl}(x_1(t))$ are chosen as constants denoted as $\underline{h}_{ijl}$ which is shown in Table 5.1. With the consideration of $y(t_\gamma) \in [x_1(t)-1, \quad x_1(t)+1]$, the values of δ_{ijl} can be found numerically which are shown in Table 5.2.

Table 5.1: The coefficients of the approximation of the membership functions in 15 operating sub-domains.

$\underline{h}_{ijl}$	$l = 1$	$l = 2$	$l = 3$	$l = 4$
$\underline{h}_{1,1,l}$	9.9433×10^{-1}	9.7881×10^{-1}	9.2414×10^{-1}	7.3714×10^{-1}
$\underline{h}_{1,2,l}$	0	0	0	0
$\underline{h}_{2,1,l}$	4.4731×10^{-4}	1.6509×10^{-3}	6.2306×10^{-3}	2.3715×10^{-2}
$\underline{h}_{2,2,l}$	0	0	0	0
$\underline{h}_{3,1,l}$	1.1169×10^{-6}	4.1287×10^{-6}	1.5673×10^{-5}	5.9436×10^{-5}
$\underline{h}_{3,2,l}$	0	0	0	0
$\underline{h}_{ijl}$	$l = 5$	$l = 6$	$l = 7$	$l = 8$
$\underline{h}_{1,1,l}$	3.5973×10^{-1}	1.0404×10^{-1}	2.3485×10^{-2}	4.7454×10^{-3}
$\underline{h}_{1,2,l}$	0	5.3618×10^{-2}	2.1706×10^{-2}	7.4807×10^{-3}
$\underline{h}_{2,1,l}$	8.5269×10^{-2}	2.3946×10^{-1}	4.2803×10^{-1}	3.5604×10^{-1}
$\underline{h}_{2,2,l}$	0	3.4327×10^{-2}	1.7644×10^{-1}	3.5604×10^{-1}
$\underline{h}_{3,1,l}$	2.2859×10^{-4}	7.4742×10^{-4}	2.4215×10^{-3}	7.4807×10^{-3}
$\underline{h}_{3,2,l}$	0	1.0220×10^{-4}	8.3787×10^{-4}	4.7454×10^{-3}
$\underline{h}_{ijl}$	$l = 9$	$l = 10$	$l = 11$	$l = 12$
$\underline{h}_{1,1,l}$	8.3787×10^{-4}	1.0220×10^{-4}	0	0
$\underline{h}_{1,2,l}$	2.4215×10^{-3}	7.4742×10^{-4}	2.2859×10^{-4}	5.9436×10^{-5}
$\underline{h}_{2,1,l}$	1.7644×10^{-1}	3.4327×10^{-2}	0	0
$\underline{h}_{2,2,l}$	4.2803×10^{-1}	2.3946×10^{-1}	8.5269×10^{-2}	2.3715×10^{-2}
$\underline{h}_{3,1,l}$	2.1706×10^{-2}	5.3618×10^{-2}	0	0
$\underline{h}_{3,2,l}$	2.3485×10^{-2}	1.0404×10^{-1}	3.5973×10^{-1}	7.3714×10^{-1}
$\underline{h}_{ijl}$	$l = 13$	$l = 14$	$l = 15$	
$\underline{h}_{1,1,l}$	0	0	0	
$\underline{h}_{1,2,l}$	1.5673×10^{-5}	4.1287×10^{-6}	1.1169×10^{-6}	
$\underline{h}_{2,1,l}$	0	0	0	
$\underline{h}_{2,2,l}$	6.2306×10^{-3}	1.6509×10^{-3}	4.4731×10^{-4}	
$\underline{h}_{3,1,l}$	0	0	0	
$\underline{h}_{3,2,l}$	9.2414×10^{-1}	9.7881×10^{-1}	9.9433×10^{-1}	

Table 5.2: The coefficients of $\delta_{i,j,l}$ in 15 operating sub-domains.

δ_{ijl}	$l=1$	$l=2$	$l=3$	$l=4$
$\delta_{1,1,l}$	5.2201×10^{-3}	1.9524×10^{-2}	6.9585×10^{-2}	2.3898×10^{-1}
$\delta_{1,2,l}$	1.3221×10^{-23}	1.3221×10^{-23}	1.3221×10^{-23}	3.6051×10^{-2}
$\delta_{2,1,l}$	5.2179×10^{-3}	1.9515×10^{-2}	6.9553×10^{-2}	2.0554×10^{-1}
$\delta_{2,2,l}$	1.3221×10^{-23}	1.3221×10^{-23}	1.3221×10^{-23}	7.8980×10^{-3}
$\delta_{3,1,l}$	1.3019×10^{-5}	4.9520×10^{-5}	1.8775×10^{-4}	6.8606×10^{-4}
$\delta_{3,2,l}$	1.3221×10^{-23}	1.3221×10^{-23}	1.3221×10^{-23}	2.5682×10^{-5}
δ_{ijl}	$l=5$	$l=6$	$l=7$	$l=8$
$\delta_{1,1,l}$	5.4926×10^{-1}	4.7685×10^{-1}	2.4079×10^{-1}	7.3392×10^{-2}
$\delta_{1,2,l}$	1.2795×10^{-1}	7.4327×10^{-2}	1.0335×10^{-1}	5.2263×10^{-2}
$\delta_{2,1,l}$	3.9108×10^{-1}	3.5027×10^{-1}	1.6170×10^{-1}	1.8119×10^{-1}
$\delta_{2,2,l}$	9.0114×10^{-2}	2.1323×10^{-1}	2.2866×10^{-1}	1.8119×10^{-1}
$\delta_{3,1,l}$	2.2053×10^{-3}	6.9434×10^{-3}	2.0492×10^{-2}	5.2263×10^{-2}
$\delta_{3,2,l}$	4.8688×10^{-4}	3.1939×10^{-3}	1.6683×10^{-2}	7.3392×10^{-2}
δ_{ijl}	$l=9$	$l=10$	$l=11$	$l=12$
$\delta_{1,1,l}$	1.6683×10^{-2}	3.1939×10^{-3}	4.8688×10^{-4}	2.5682×10^{-5}
$\delta_{1,2,l}$	2.0492×10^{-2}	6.9434×10^{-3}	2.2053×10^{-3}	6.8606×10^{-4}
$\delta_{2,1,l}$	2.2866×10^{-1}	2.1323×10^{-1}	9.0114×10^{-2}	7.8980×10^{-3}
$\delta_{2,2,l}$	1.6170×10^{-1}	3.5027×10^{-1}	3.9108×10^{-1}	2.0554×10^{-1}
$\delta_{3,1,l}$	1.0335×10^{-1}	7.4327×10^{-2}	1.2795×10^{-1}	3.6051×10^{-2}
$\delta_{3,2,l}$	2.4079×10^{-1}	4.7685×10^{-1}	5.4926×10^{-1}	2.3898×10^{-1}
δ_{ijl}	$l=13$	$l=14$	$l=15$	
$\delta_{1,1,l}$	1.3221×10^{-23}	1.3221×10^{-23}	1.3221×10^{-23}	
$\delta_{1,2,l}$	1.8775×10^{-4}	4.9520×10^{-5}	1.3019×10^{-5}	
$\delta_{2,1,l}$	1.3221×10^{-23}	1.3221×10^{-23}	1.3221×10^{-23}	
$\delta_{2,2,l}$	6.9553×10^{-2}	1.9515×10^{-2}	5.2179×10^{-3}	
$\delta_{3,1,l}$	1.3221×10^{-23}	1.3221×10^{-23}	1.3221×10^{-23}	
$\delta_{3,2,l}$	6.9585×10^{-2}	1.9524×10^{-2}	5.2201×10^{-3}	

By applying the stability conditions in Theorem 5.2, it is chosen that $\varepsilon_1(\mathbf{y}) = \varepsilon_2(\tilde{\mathbf{x}}) = \varepsilon_3(\mathbf{x},\mathbf{x_r}) = \varepsilon_4(\mathbf{x},\mathbf{x_r}) = \varepsilon_5(\mathbf{x},\mathbf{x_r}) = 0.0001$, $\mathbf{X}(\tilde{\mathbf{x}})$ as a polynomial of degree 0; $\mathbf{M}_j(x_1(t_\gamma))$ and $\mathbf{N}_j(x_1(t_\gamma))$, $j = 1, 2$ are polynomials with monomials in x_1 of degree 0; $\mathbf{S}_l(x_1(t))$ is of degree 0; $\mathbf{X}_{22}(\tilde{\mathbf{x}})$ is of degree 0 which lead to $\mathbf{X}(\tilde{\mathbf{x}})$ a constant matrix with $\tilde{\mathbf{x}}$ as a null vector.

The feedback gains are obtained as $\mathbf{F}_1 = -1.1515$, $\mathbf{F}_2 = -7.0323$, $\mathbf{G}_1 = 1.0067\times10^{-11}$, $\mathbf{G}_2 = 9.3380\times10^{-12}$, and $\mathbf{X} = \begin{bmatrix} 7.7228\times10^{-4} & 1.9405\times10^{-4} \\ 1.9405\times10^{-4} & 1.5048\times10^{-3} \end{bmatrix}$. The minimum values of σ_1, σ_2 and σ_3 are obtained as 1.8368, 0.9796 and 1.5696, respectively.

To perform simulation, it is chosen that $\underline{\lambda}_1(x_1(t)) = (\sin(5x_1(t))+1)/2$, $\overline{\lambda}_1(x_1(t)) = 1-\underline{\lambda}_1(x_1(t))$, $\underline{\lambda}_3(x_1(t)) = (\cos(5x_1(t))+1)/2$, $\overline{\lambda}_3(x_1(t)) = 1-\underline{\lambda}_3(x_1(t))$, which act as the uncertainty of the nonlinear plant embedded in the IT2 membership functions to obtain $\tilde{w}_1(x_1(t))$ and $\tilde{w}_3(x_1(t))$. Since $\tilde{w}_2(x_1(t)) = 1 - \tilde{w}_1(x_1(t)) - \tilde{w}_3(x_1(t))$ by the definition of $\tilde{w}_i(x_1(t))$, there is no need to obtain the explicit form of $\underline{\lambda}_2(x_1(t))$ and $\overline{\lambda}_2(x_1(t))$ once $\tilde{w}_1(x_1(t))$ and $\tilde{w}_3(x_1(t))$ are defined.

On the other hand, the type reduction in (5.7) for the controller are chosen as $\underline{\kappa}_j(x_1(t)) = \overline{\kappa}_j(x_1(t)) = 0.5$, $j = 1, 2$. By applying the IT2 SDOF polynomial fuzzy controller for tracking control with the initial conditions $\mathbf{x}(0) = [0 \quad 0]$ and $\mathbf{x_r}(0) = [0.5 \quad 0]$, the simulation results of state response and control signal are shown in Figs. 5.2 to 5.4, which demonstrate that the tracking errors are sufficiently small.

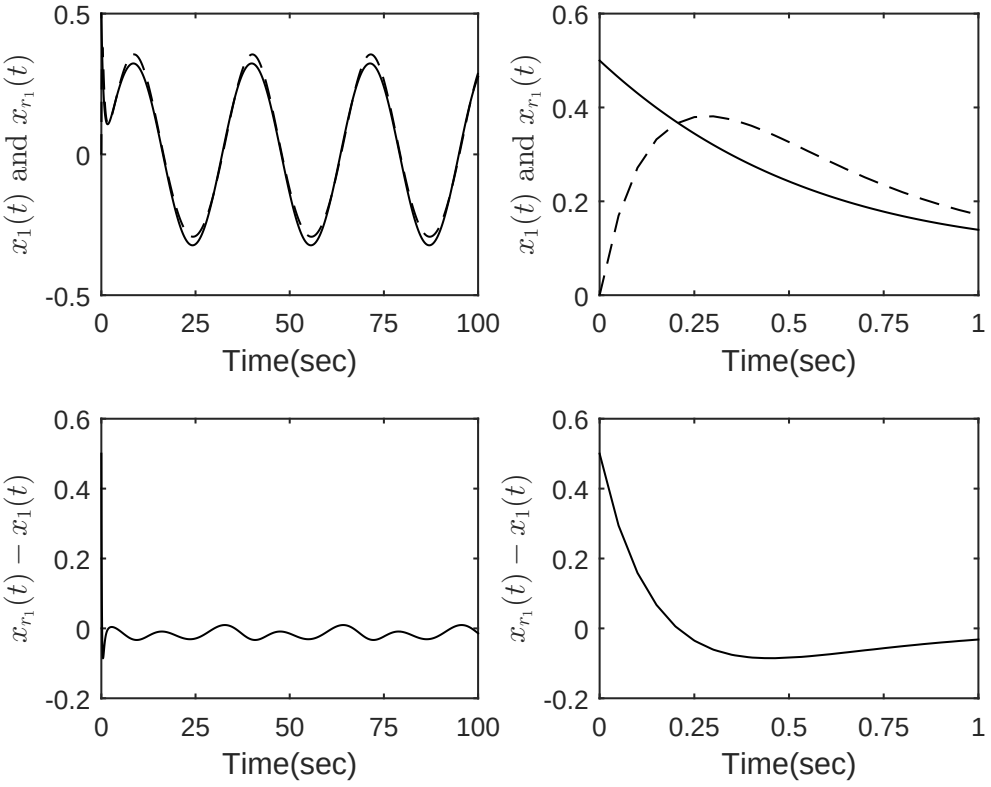

Figure 5.2: Tracking control performance for $x_1(t)$ under 15 sub-domains approach. Top left panel: responses of $x_1(t)$ (Solid line) and $x_{r_1}(t)$ (Dash line) from 0 to 100 seconds. Top right panel: responses of $x_1(t)$ (Solid line) and $x_{r_1}(t)$ (Dash line) from 0 to 1 second. Bottom left panel: response of $x_{r_1}(t) - x_1(t)$ from 0 to 100 seconds. Bottom right panel: response of $x_{r_1}(t) - x_1(t)$ from 0 to 1 second.

For comparison purposes, Theorem 5.1 is applied with $\varepsilon_1(\tilde{\mathbf{x}}) = \varepsilon_2 = \varepsilon_3(\mathbf{x}, \mathbf{x_r}) = 0.001$ and the same degrees of feedback gains and $\tilde{\mathbf{x}}$ used above. However, no feasible solution can be found. It shows that bringing the information of membership functions helps relax the stability analysis results.

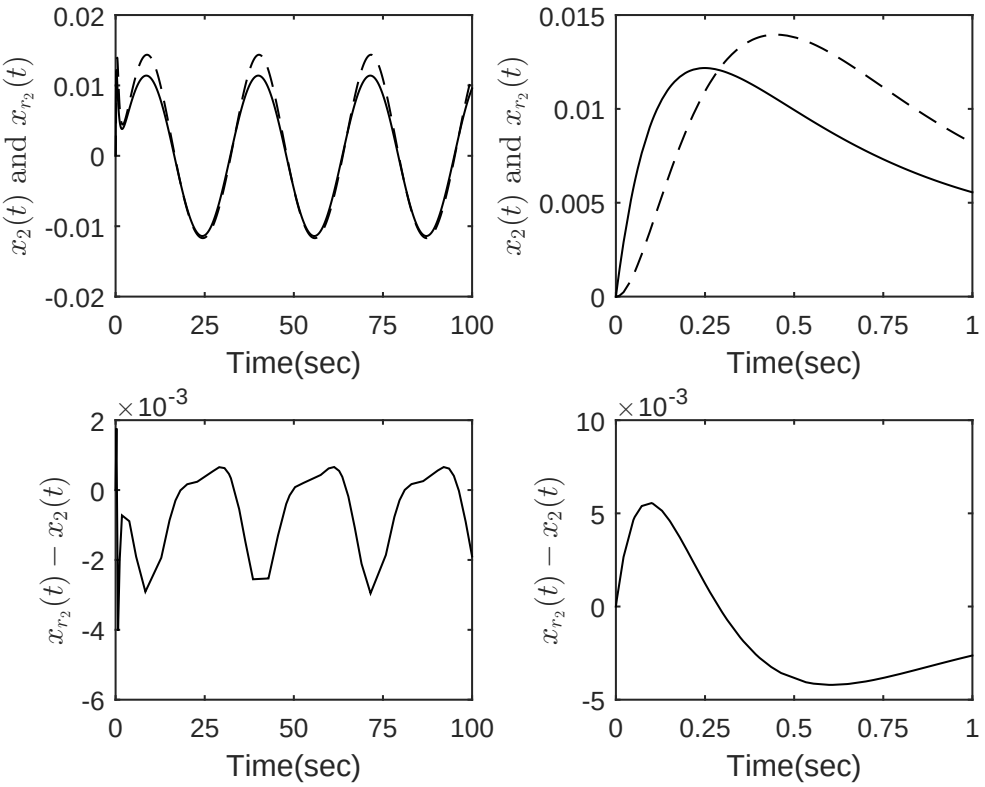

Figure 5.3: Tracking control performance for $x_2(t)$ under 15 sub-domains approach. Top left panel: responses of $x_2(t)$ (Solid line) and $x_{r2}(t)$ (Dash line) from 0 to 100 seconds. Top right panel: responses of $x_2(t)$ (Solid line) and $x_{r_2}(t)$ (Dash line) from 0 to 1 second. Bottom left panel: response of $x_{r_2}(t) - x_2(t)$ from 0 to 100 seconds. Bottom right panel: response of $x_{r_2}(t) - x_2(t)$ from 0 to 1 second.

5.3.2 Inverted Pendulum

An inverted pendulum subject to parameter uncertainty is considered. An IT2 polynomial fuzzy model is first built through Taylor series approach [39] and then an IT2 SDOF polynomial fuzzy controller is designed to perform the tracking control that the system states is driven to follow those of a stable reference model subject to the H_∞ performance (5.40).

The dynamic equation for the inverted pendulum [45] is given by

$$\ddot{\theta}(t) = \frac{g\sin(\theta(t)) - am_pS\dot{\theta}(t)^2\sin(2\theta(t))/2 - a\cos(\theta(t))u(t)}{4S/3 - am_pS\cos^2(\theta(t))}, \tag{5.54}$$

where $\theta(t)$ is the angular displacement of the inverted pendulum, $g = 9.8\ \mathrm{m/s^2}$, $m_p \in [m_{p_{\min}} \quad m_{p_{\max}}] = [0.5 \quad 1]$ kg is the mass of the pendulum, $M_c \in [M_{c_{\min}} \quad M_{c_{\max}}] = [18 \quad 20]$ kg is the mass of the cart, $a = \frac{1}{m_p + M_c}$, $2S = 1$m is the length of the pendulum, and $u(t)$ is the force applied on the cart. m_p and M_c are treated as the parameter uncertainties.

Considering the operating domain $\theta(t) = [\frac{-5\pi}{12}, \frac{5\pi}{12}]$ and $\dot{\theta}(t) = [-4, 4]$, the follow-

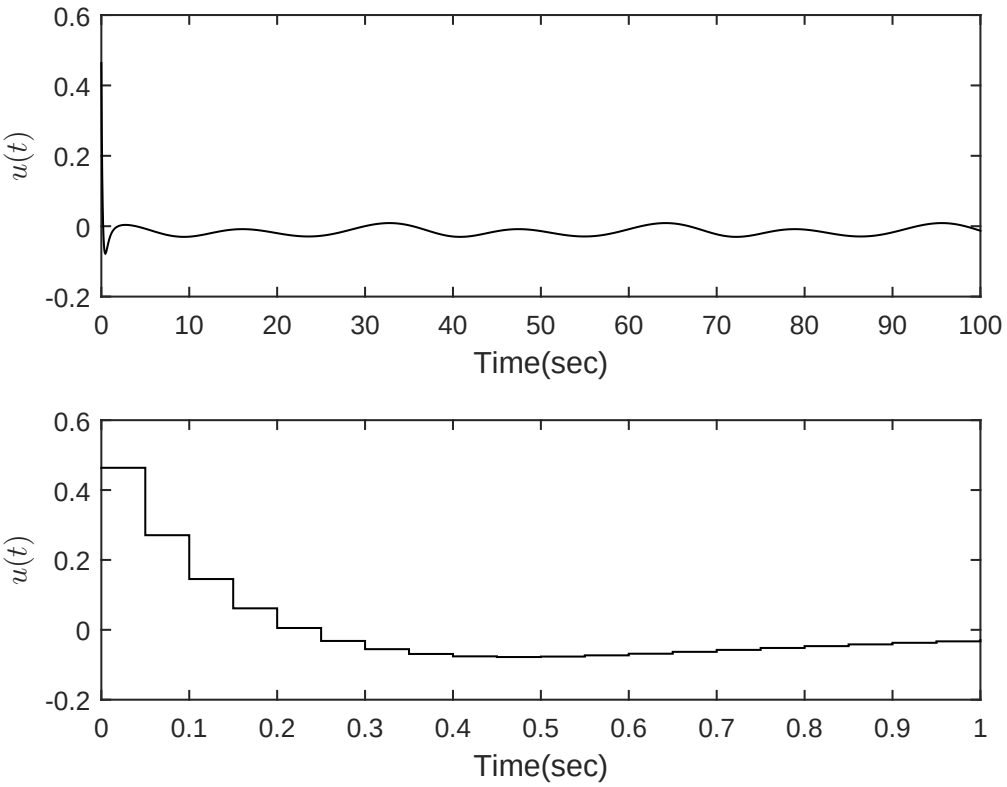

Figure 5.4: The control signal $u(t)$ under 15 sub-domains approach. Top panel: $u(t)$ from 0 to 100 seconds. Bottom panel: $u(t)$ from 0 to 1 second.

ing 4 rules are used to describe the inverted pendulum:

$$\begin{aligned}
&\text{Rule } i: \text{IF } f_1(\mathbf{x}(t)) \text{ is } \tilde{M}_1^i \text{ AND } f_2(\mathbf{x}(t)) \text{ is } \tilde{M}_2^i \\
&\text{THEN } \dot{\mathbf{x}}(t) = \mathbf{A}_i(\mathbf{x}(t))\hat{\mathbf{x}}(\mathbf{x}(t)) + \mathbf{B}_i(\mathbf{x}(t))\mathbf{u}(t), \\
&\qquad \mathbf{y}(t) = \mathbf{C}\mathbf{x}(t), \\
&\qquad i = 1, 2, 3, 4.
\end{aligned} \tag{5.55}$$

The IT2 polynomial fuzzy model is obtained as

$$\dot{\mathbf{x}}(t) = \sum_{i=1}^{4} \tilde{w}_i\big(\mathbf{A}_i(\mathbf{x}(t))\hat{\mathbf{x}}(\mathbf{x}(t)) + \mathbf{B}_i(\mathbf{x}(t))u(t)\big), \tag{5.56}$$

$$\mathbf{y}(t) = \mathbf{C}\mathbf{x}(t), \tag{5.57}$$

where

$$\begin{aligned}
&\hat{\mathbf{x}}(t) = \mathbf{x}(t) = [x_1(t) \quad x_2(t)]^T = [\theta(t) \quad \dot{\theta}(t)]^T, \\
&x_1(t) \in [\frac{-5\pi}{12} \quad \frac{5\pi}{12}], \quad x_2(t) \in [-4 \quad 4],
\end{aligned}$$

$$\mathbf{A}_1(\mathbf{x}(t)) = \mathbf{A}_2(\mathbf{x}(t)) = \begin{bmatrix} 0 & 1 \\ f_{1_{\min}}(\mathbf{x}(t)) & 0 \end{bmatrix},$$

$$\mathbf{A}_3(\mathbf{x}(t)) = \mathbf{A}_4(\mathbf{x}(t)) = \begin{bmatrix} 0 & 1 \\ f_{1_{\max}}(\mathbf{x}(t)) & 0 \end{bmatrix},$$

$$\mathbf{B}_1(\mathbf{x}(t)) = \mathbf{B}_3(\mathbf{x}(t)) = \begin{bmatrix} 0 \\ f_{2_{\min}}(\mathbf{x}(t)) \end{bmatrix},$$

$$\mathbf{B}_2(\mathbf{x}(t)) = \mathbf{B}_4(\mathbf{x}(t)) = \begin{bmatrix} 0 \\ f_{2_{\max}}(\mathbf{x}(t)) \end{bmatrix}, \mathbf{C} = \begin{bmatrix} 1 & 0 \\ 0 & 1 \end{bmatrix}.$$

The lower and upper membership functions are defined in Table 5.3 of which $f_1(\mathbf{x}(t))$ and $f_2(\mathbf{x}(t))$ are defined as follows.

Table 5.3: Lower and Upper Membership Functions for the Interval Type-2 Fuzzy Model of the Inverted Pendulum.

Lower and upper membership functions	
$\underline{\mu}_{\tilde{M}_1^1}(f_1(\mathbf{x}(t))) = \underline{\mu}_{\tilde{M}_1^2}(f_1(\mathbf{x}(t)))$ $= \frac{f_{1_{\max}} - f_1(\mathbf{x}(t))}{f_{1_{\max}} - f_{1_{\min}}}$;	$\underline{\mu}_{\tilde{M}_2^1}(f_2(\mathbf{x}(t))) = \underline{\mu}_{\tilde{M}_2^3}(f_2(\mathbf{x}(t)))$ $= \frac{f_{2_{\max}} - f_2(\mathbf{x}(t))}{f_{2_{\max}} - f_{2_{\min}}}$;
$\overline{\mu}_{\tilde{M}_1^3}(f_1(\mathbf{x}(t))) = \overline{\mu}_{\tilde{M}_1^4}(f_1(\mathbf{x}(t)))$ $= \frac{f_1(\mathbf{x}(t)) - f_{1_{\min}}}{f_{1_{\max}} - f_{1_{\min}}}$;	$\overline{\mu}_{\tilde{M}_2^2}(f_2(\mathbf{x}(t))) = \overline{\mu}_{\tilde{M}_2^4}(f_2(\mathbf{x}(t)))$ $= \frac{f_2(\mathbf{x}(t)) - f_{2_{\min}}}{f_{2_{\max}} - f_{2_{\min}}}$
with $x_2(t) = 0, m_p = m_{p_{\max}}$ $= 1$kg and $M_c = M_{c_{\min}} = 18$kg	with $m_p = m_{p_{\max}}$ $= 1$kg and $M_c = M_{c_{\max}} = 20$kg
$\overline{\mu}_{\tilde{M}_1^1}(f_1(\mathbf{x}(t))) = \overline{\mu}_{\tilde{M}_1^2}(f_1(\mathbf{x}(t)))$ $= \frac{f_{1_{\max}} - f_1(\mathbf{x}(t))}{f_{1_{\max}} - f_{1_{\min}}}$;	$\overline{\mu}_{\tilde{M}_2^1}(f_2(\mathbf{x}(t))) = \overline{\mu}_{\tilde{M}_2^3}(f_2(\mathbf{x}(t)))$ $= \frac{f_{2_{\max}} - f_2(\mathbf{x}(t))}{f_{2_{\max}} - f_{2_{\min}}}$
$\underline{\mu}_{\tilde{M}_1^3}(f_1(\mathbf{x}(t))) = \underline{\mu}_{\tilde{M}_1^4}(f_1(\mathbf{x}(t)))$ $= \frac{f_1(\mathbf{x}(t)) - f_{1_{\min}}}{f_{1_{\max}} - f_{1_{\min}}}$;	$\underline{\mu}_{\tilde{M}_2^2}(f_2(\mathbf{x}(t))) = \underline{\mu}_{\tilde{M}_2^4}(f_2(\mathbf{x}(t)))$ $= \frac{f_2(\mathbf{x}(t)) - f_{2_{\min}}}{f_{2_{\max}} - f_{2_{\min}}}$;
with $x_2(t) = x_{2_{\max}}, m_p = m_{p_{\max}}$ $= 1$kg and $M_c = M_{c_{\min}} = 18$kg	with $m_p = m_{p_{\min}} = 0.5$kg and $M_c = M_{c_{\min}} = 18$kg

$$f_1(\mathbf{x}(t)) = \frac{g - am_pSx_2(t)^2\cos(x_1(t))}{4S/3 - am_pS\cos^2(x_1(t))}\left(\frac{\sin(x_1(t))}{x_1(t)}\right), \tag{5.58}$$

$$f_2(\mathbf{x}(t)) = \frac{-a\cos(x_1(t))}{4S/3 - am_pS\cos^2(x_1(t))}. \tag{5.59}$$

Applying the same procedure in Chapter 3 and 4, the minimum and maximum values of $f_1(\mathbf{x}(t))$ and $f_2(\mathbf{x}(t))$ can be obtained in polynomial functions as follows:

$$f_{1_{\min}}(\mathbf{x}(t)) = 0.12996x_1(t)^2 + 10.5323,$$

$$f_{1_{\max}}(\mathbf{x}(t)) = 0.1299x_1(t)^2 + 15.3041,$$

$$f_{2_{\min}}(\mathbf{x}(t)) = 0.0037x_1(t)^2 - 0.0828,$$
$$f_{2_{\max}}(\mathbf{x}(t)) = 0.0037x_1(t)^2 - 0.0249.$$

The lower and upper grades of membership are respectively defined as:

$$w_i^L(\mathbf{x}(t)) = \underline{\mu}_{\tilde{M}_1^i}(f_1(\mathbf{x}(t))) \times \underline{\mu}_{\tilde{M}_2^i}(f_2(\mathbf{x}(t)),$$
$$w_i^U(\mathbf{x}(t)) = \overline{\mu}_{\tilde{M}_1^i}(f_1(\mathbf{x}(t))) \times \overline{\mu}_{\tilde{M}_2^i}(f_2(\mathbf{x}(t)))$$

for all i.

The reference model is chosen as $\mathbf{A_r} = \begin{bmatrix} 0 & 1 \\ -4 & -4 \end{bmatrix}$, $\mathbf{B_r} = \begin{bmatrix} 0 \\ 1 \end{bmatrix}$ and $r(t) = 4\sin(0.3t)$.

Based on the IT2 polynomial fuzzy model, an IT2 SDOF polynomial fuzzy controller with 2 rules is employed to perform the tracking control:

$$\begin{aligned} &\text{Rule } j : \text{IF } y_1(t_\gamma) \text{ is } \tilde{N}_1^j \\ &\qquad \text{THEN } \mathbf{u}(t) = \mathbf{F}_j(\mathbf{h}(t_\gamma))\mathbf{e_y}(t_\gamma) + \mathbf{G}_j(\mathbf{h}(t_\gamma))\mathbf{y_r}(t_\gamma), \\ &\qquad j = 1, 2. \end{aligned} \tag{5.60}$$

It should be noted that in this case $y_1(t_\gamma) = x_1(t_\gamma)$ due to $\mathbf{C} = \begin{bmatrix} 1 & 0 \\ 0 & 1 \end{bmatrix}$ and $x_1(t_\gamma)$ will be adopted instead of $y_1(t_\gamma)$. The overall IT2 SDOF polynomial fuzzy controller is obtained as follows:

$$\begin{aligned} \mathbf{u}(t) = &\tilde{m}_1(x_1(t_\gamma))(\mathbf{F}_1(\mathbf{h}(t_\gamma))\mathbf{e_y}(t_\gamma) + \mathbf{G}_1(\mathbf{h}(t_\gamma))\mathbf{y_r}(t_\gamma)) \\ &+ \tilde{m}_2(x_1(t_\gamma))(\mathbf{F}_2(\mathbf{h}(t_\gamma))\mathbf{e_y}(t_\gamma) + \mathbf{G}_2(\mathbf{h}(t_\gamma))\mathbf{y_r}(t_\gamma)) \end{aligned} \tag{5.61}$$

where the upper and lower membership functions are chosen as follows:

$$\overline{m}_1(x_1(t)) = \begin{cases} 0 & \text{for } x_1(t) < -\frac{5\pi}{12} \\ \frac{x_1(t)+5\pi/12}{5\pi/12} & \text{for } -\frac{5\pi}{12} \le x_1(t) \le 0 \\ \frac{5\pi/12-x_1(t)}{5\pi/12} & \text{for } 0 \le x_1(t) \le \frac{5\pi}{12} \\ 0 & \text{for } x_1(t) > \frac{5\pi}{12} \end{cases} \tag{5.62}$$

$$\underline{m}_1(x_1(t)) = \begin{cases} 0 & \text{for } x_1(t) < -\frac{5\pi}{12} \\ \frac{0.9(x_1(t)+5\pi/12)}{5\pi/12} & \text{for } -\frac{5\pi}{12} \le x_1(t) \le 0 \\ \frac{0.9(5\pi/12-x_1(t))}{5\pi/12} & \text{for } 0 \le x_1(t) \le \frac{5\pi}{12} \\ 0 & \text{for } x_1(t) > \frac{5\pi}{12} \end{cases} \tag{5.63}$$

$\overline{m}_2(x_1(t)) = 1-\underline{m}_1(x_1(t))$, $\underline{m}_2(x_1(t)) = 1-\overline{m}_1(x_1(t))$, and $\tilde{m}_2(x_1(t)) = 1-\tilde{m}_1(x_1(t))$;

and $\underline{\kappa}_j(x_1(t)) = \overline{\kappa}_j(x_1(t)) = 0.5$, $j = 1, 2$.

It can be found that the membership functions depend on $x_1(t)$ which is used to determine their bounds δ_{ijl}. Recalling that $x_1 \in [\frac{-5\pi}{12}, \frac{5\pi}{12}]$, it suggests that the lower and upper bounds of x_1 is $\underline{x}_1 = \frac{-5\pi}{12}$ and $\overline{x}_1 = \frac{5\pi}{12}$. The sampling period in this simulation is set as $h_s = 0.005$s. From the polynomial fuzzy model, we have $\dot{x_1}(t) = x_2(t) \in [-4 \quad 4]$ that it gives the largest variation of x_1 within the sampling period as $-4 \times h_s \leq \int_t^{t+h_s} \dot{x_1}(\sigma)d\sigma \leq 4 \times h_s$, which is within the domain $[-0.125 \quad 0.125]$. As we did in the first example, this consideration will be verified by simulations. With this information, from Section 5.2.2.2, it can be obtained that $x_1(t_\gamma) \in [x_1(t) - 0.125, \quad x_1(t) + 0.125]$.

By dividing the operating domain $x_1(t)$ into 10 uniform sub-domains (i.e., $L = 10$), it can be obtained that $\underline{y}_{1_l} = \underline{x}_{1_l} = \frac{-6\pi}{12} + \frac{\pi}{12}l$ and $\overline{y}_{1_l} = \overline{x}_{1_l} = \frac{-5\pi}{12} + \frac{\pi}{12}l$, $l = 1$, 2, …, 10, which are the lower and upper bounds of the l-th operating sub-domain, respectively. It is chosen that $\mathbf{D} = \text{diag}\{1, 0\}$, which means only $y_1 = x_1$ of the output vector has been included as the state information to facilitate the stability analysis. The values of $\hat{h}_{ijl}(x_1(t))$ are chosen as constants denoted as $\hat{h}_{ijl}$ which are shown in Table 5.4. With $x_1(t_\gamma) \in [x_1(t) - 0.125, \quad x_1(t) + 0.125]$, the values of δ_{ijl} are found numerically and shown in Table 5.5.

Table 5.4: The coefficients of the approximation of the membership functions in 10 operating sub-domains.

$\underline{h}_{ijl}$	$l=1$	$l=2$	$l=3$	$l=4$
$\underline{h}_{1,1,l}$	0	0	6.0956×10^{-2}	0
$\underline{h}_{1,2,l}$	0	0	1.2517×10^{-2}	0
$\underline{h}_{2,1,l}$	0	0	6.8411×10^{-2}	2.2699×10^{-1}
$\underline{h}_{2,2,l}$	0	0	6.2798×10^{-2}	0
$\underline{h}_{3,1,l}$	-1.1073×10^{-16}	1.0804×10^{-1}	3.9270×10^{-2}	0
$\underline{h}_{3,2,l}$	2.8336×10^{-1}	6.4079×10^{-2}	4.1458×10^{-3}	0
$\underline{h}_{4,1,l}$	-4.2294×10^{-32}	0	1.4042×10^{-1}	0
$\underline{h}_{4,2,l}$	3.3723×10^{-16}	1.1124×10^{-1}	3.9727×10^{-2}	0
$\underline{h}_{ijl}$	$l=5$	$l=6$	$l=7$	$l=8$
$\underline{h}_{1,1,l}$	-2.6927×10^{-16}	-2.6927×10^{-16}	0	6.1547×10^{-2}
$\underline{h}_{1,2,l}$	0	0	0	1.1483×10^{-2}
$\underline{h}_{2,1,l}$	4.4003×10^{-1}	4.4643×10^{-1}	2.3271×10^{-1}	7.2556×10^{-2}
$\underline{h}_{2,2,l}$	0	0	0	6.2221×10^{-2}
$\underline{h}_{3,1,l}$	-2.4241×10^{-19}	-2.4241×10^{-19}	0	3.7154×10^{-2}
$\underline{h}_{3,2,l}$	0	0	0	3.0268×10^{-3}
$\underline{h}_{4,1,l}$	0	0	0	1.4247×10^{-1}
$\underline{h}_{4,2,l}$	0	0	0	3.7569×10^{-2}
$\underline{h}_{ijl}$	$l=9$	$l=10$		
$\underline{h}_{1,1,l}$	0	0		
$\underline{h}_{1,2,l}$	1.1029×10^{-2}	1.3615×10^{-3}		
$\underline{h}_{2,1,l}$	0	0		
$\underline{h}_{2,2,l}$	0	0		
$\underline{h}_{3,1,l}$	1.0619×10^{-1}	7.4838×10^{-3}		
$\underline{h}_{3,2,l}$	6.1020×10^{-2}	2.7358×10^{-1}		
$\underline{h}_{4,1,l}$	5.7193×10^{-3}	7.0534×10^{-5}		
$\underline{h}_{4,2,l}$	1.0928×10^{-1}	8.1019×10^{-3}		

Table 5.5: The coefficients of $\delta_{i,j,l}$ in 10 operating sub-domains.

δ_{ijl}	$l=1$	$l=2$	$l=3$	$l=4$
$\delta_{1,1,l}$	6.3604×10^{-2}	1.3911×10^{-1}	1.0489×10^{-1}	1.6585×10^{-1}
$\delta_{1,2,l}$	1.5383×10^{-1}	1.5383×10^{-1}	9.7547×10^{-2}	6.1688×10^{-2}
$\delta_{2,1,l}$	2.8933×10^{-2}	1.6579×10^{-1}	3.6571×10^{-1}	7.7301×10^{-1}
$\delta_{2,2,l}$	6.2791×10^{-2}	1.4455×10^{-1}	1.1216×10^{-1}	1.7496×10^{-1}
$\delta_{3,1,l}$	2.4459×10^{-1}	1.3655×10^{-1}	1.6713×10^{-1}	1.2494×10^{-1}
$\delta_{3,2,l}$	7.1664×10^{-1}	3.9916×10^{-1}	1.6449×10^{-1}	4.8625×10^{-2}
$\delta_{4,1,l}$	9.9798×10^{-2}	2.6751×10^{-1}	2.1408×10^{-1}	3.5450×10^{-1}
$\delta_{4,2,l}$	2.4448×10^{-1}	1.3324×10^{-1}	1.7524×10^{-1}	1.3218×10^{-1}
δ_{ijl}	$l=5$	$l=6$	$l=7$	$l=8$
$\delta_{1,1,l}$	1.4594×10^{-1}	1.4538×10^{-1}	1.6512×10^{-1}	1.0358×10^{-1}
$\delta_{1,2,l}$	2.9830×10^{-2}	2.9239×10^{-2}	6.0362×10^{-2}	9.7138×10^{-2}
$\delta_{2,1,l}$	5.5997×10^{-1}	5.5357×10^{-1}	7.6729×10^{-1}	3.7132×10^{-1}
$\delta_{2,2,l}$	1.5754×10^{-1}	1.5717×10^{-1}	1.7507×10^{-1}	1.1285×10^{-1}
$\delta_{3,1,l}$	5.7201×10^{-2}	5.5649×10^{-2}	1.2245×10^{-1}	1.6662×10^{-1}
$\delta_{3,2,l}$	1.1717×10^{-2}	1.1214×10^{-2}	4.6629×10^{-2}	1.5987×10^{-1}
$\delta_{4,1,l}$	3.1858×10^{-1}	3.1371×10^{-1}	3.5693×10^{-1}	2.1446×10^{-1}
$\delta_{4,2,l}$	6.1673×10^{-2}	6.0032×10^{-2}	1.2963×10^{-1}	1.7507×10^{-1}
δ_{ijl}	$l=9$	$l=10$		
$\delta_{1,1,l}$	1.4144×10^{-1}	6.5881×10^{-2}		
$\delta_{1,2,l}$	1.4116×10^{-1}	1.5083×10^{-1}		
$\delta_{2,1,l}$	1.7212×10^{-1}	3.1208×10^{-2}		
$\delta_{2,2,l}$	1.4628×10^{-1}	6.5625×10^{-2}		
$\delta_{3,1,l}$	1.4002×10^{-1}	2.3873×10^{-1}		
$\delta_{3,2,l}$	3.8946×10^{-1}	7.0375×10^{-1}		
$\delta_{4,1,l}$	2.6435×10^{-1}	1.0433×10^{-1}		
$\delta_{4,2,l}$	1.3718×10^{-1}	2.3836×10^{-1}		

During the simulation, m_p is set as 1kg and M_c is set as 18kg, which are both within the bounds of the uncertainty and not known by the IT2 SDOF polynomial fuzzy controller. To apply Theorem 5.2, we set $\varepsilon_1(\mathbf{y}) = \varepsilon_2(\tilde{\mathbf{x}}) = \varepsilon_3(\mathbf{x}, \mathbf{x_r}) = \varepsilon_4(\mathbf{x}, \mathbf{x_r}) = \varepsilon_5(\mathbf{x}, \mathbf{x_r}) = 0.001$; $\mathbf{X}(\tilde{\mathbf{x}})$ is a polynomial of degree 0; $\tilde{\mathbf{x}}$ as a null vector; $\mathbf{M}_j(x_1(t_\gamma))$ and $\mathbf{N}_j(x_1(t_\gamma))$, $j = 1, 2$, are polynomials with monomials in x_1 of degree 0, $\mathbf{S}_l(x_1(t))$ is of degree 0.

The feedback gains are obtained as $\mathbf{F}_1 = [3852.7564 \quad 2020.09610]$, $\mathbf{F}_2 = [2822.5654 \quad 1482.4192]$, $\mathbf{G}_1 = [-1.8970\times10^{-11} \quad -8.1558\times10^{-12}]$, $\mathbf{G}_2 = [-4.10707\times10^{-12} \quad -1.5208\times10^{-12}]$, $\mathbf{X} = \begin{bmatrix} 1.3248 & 2.4269 \\ 2.4269 & 5.6270 \end{bmatrix}$. The minimum values of σ_1, σ_2 and σ_3 are obtained as 7.7796, 0.4194 and 0.5508, respectively.

The IT2 SDOF fuzzy controller is employed to control the nonlinear plant subject to the initial conditions $\mathbf{x}(0) = [5\pi/12 \quad 0]^T$ and $\mathbf{x_r}(0) = [0 \quad 0]^T$. Simulation results of state response and control signal are shown in Figs. 5.5 to 5.7. It can be seen that the system states are able to follow those of the the reference model closely.

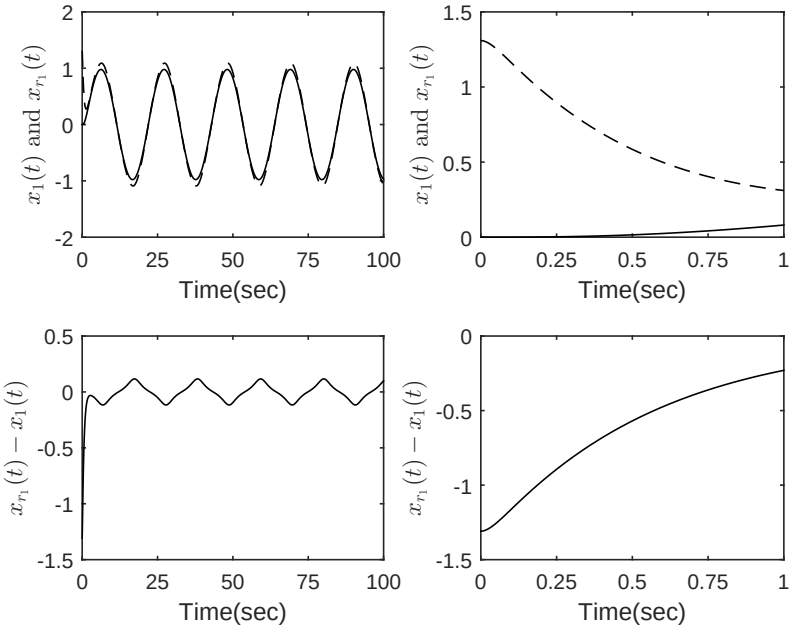

Figure 5.5: Tracking control performance for $x_1(t)$ under 10 sub-domains approach. Top left panel: responses of $x_1(t)$ (Solid line) and $x_{r_1}(t)$ (Dash line) from 0 to 100 seconds. Top right panel: responses of $x_1(t)$ (Solid line) and $x_{r_1}(t)$ (Dash line) from 0 to 1 second. Bottom left panel: response of $x_{r_1}(t) - x_1(t)$ from 0 to 100 seconds. Bottom right panel: response of $x_{r_1}(t) - x_1(t)$ from 0 to 1 second.

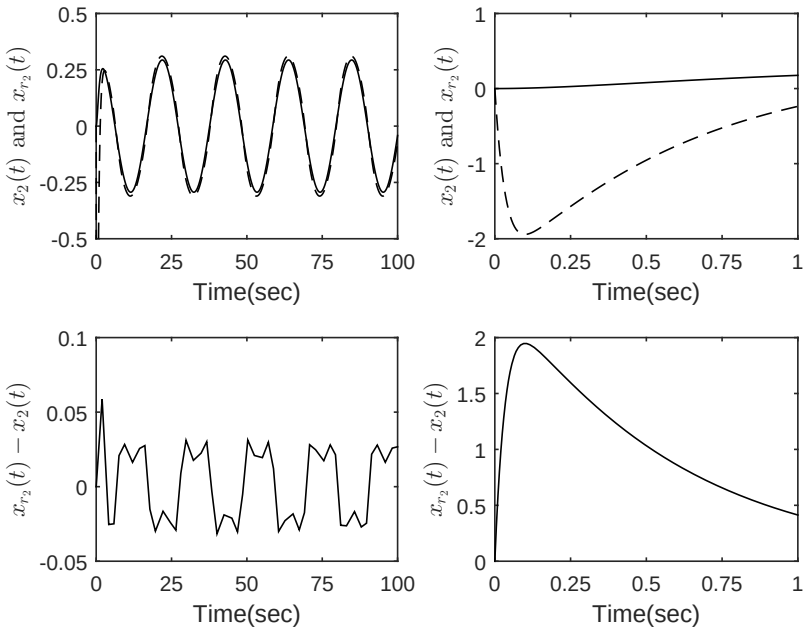

Figure 5.6: Tracking control performance for $x_2(t)$ under 10 sub-domains approach. Top left panel: responses of $x_2(t)$ (Solid line) and $x_{r_2}(t)$ (Dash line) from 0 to 100 seconds. Top right panel: responses of $x_2(t)$ (Solid line) and $x_{r_2}(t)$ (Dash line) from 0 to 1 second. Bottom left panel: response of $x_{r_2}(t) - x_2(t)$ from 0 to 100 seconds. Bottom right panel: response of $x_{r_2}(t) - x_2(t)$ from 0 to 1 second.

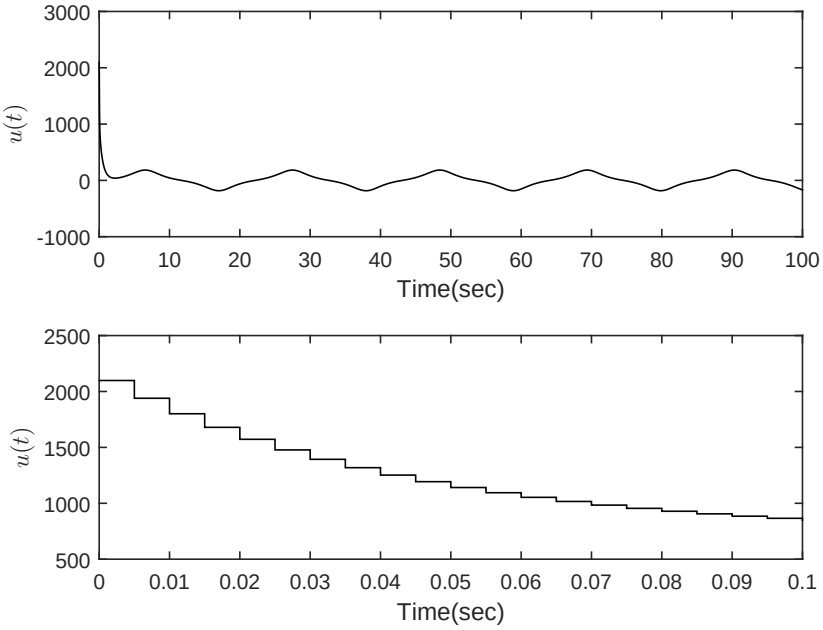

Figure 5.7: The control signal $u(t)$ under 10 sub-domains approach. Top panel: $u(t)$ from 0 to 100 seconds. Bottom panel: $u(t)$ from 0 to 0.1 second.

For comparison purposes, Theorem 5.1 is applied with $\varepsilon_1(\tilde{\mathbf{x}}) = \varepsilon_2 = \varepsilon_3(\mathbf{x}, \mathbf{x_r}) = 0.001$ and the same degrees of feedback gains and $\tilde{\mathbf{x}}$ used above, no feasible solution can be found which suggests that bringing the information of membership functions

can help relax the stability analysis results.

5.4 Conclusion

In this chapter, the SDOF tracking control problem for the IT2 PFMB control system has been investigated using the SOS-based analysis. An IT2 SDOF polynomial fuzzy controller has been employed to perform the tracking control, which is to drive the system states to follow those of a stable reference model characterized by H_∞ performance. Both MFI and MFD approaches are employed to conduct stability analysis. Under the MFD approach, the information of membership functions, system states and sampling process are utilized for the relaxation of stability analysis results. From the simulation examples, it can be shown that the MFD analysis approach helps relax the stability conditions.

Chapter 6

Conclusion and Future Work

In this thesis, the stability analysis and the performance improvement of the IT2 PFMB control systems have been investigated. In Chapter 3, the stabilization issues of the IT2 PFMB control systems have been investigated and three methods are provided to relax the stability conditions by considering the information of the membership functions into the stability analysis. The simulation results demonstrate that all the three methods help to reduce the conservativeness lying in the stability conditions. Also, it verifies that the MFD approach has its own contribution to the relaxation of the stability conditions. In Chapter 4, the output feedback tracking control design of the IT2 PFMB control systems is studied. Through the MFD approach, the stability conditions for the tracking control system are easier to obtain and the tracking control performance can also be improved subject to minimizing an H_∞ performance index. In Chapter 5, the tracking control design based on the sampled output is investigated for digital implementation of fuzzy controllers. In the stability analysis, by including the uncertainty due to the sample-and-hold process and the uncertainty in the system in the IT2 membership functions, the MFD approach is also applied to relax the stability conditions. As the results show, the MFD approach is able to find the solutions of the tracking control design and it also improves the tracking performance judged by the H_∞ performance.

Although considerable tasks have been completed in the thesis, there are still many issues related with the IT2 PFMB control system remain untouched. The future research will continue on other topics in the control theory. Time-delay, which generally considered as the source of poor system performance, appears commonly in various practical systems such as chemical processes, networked systems and communication systems [31–34] and instability. Given that there exist many complex nonlinear systems with time delay in practical situations and FMB control approaches are effective to represent the dynamics of nonlinear systems, it is natural to investigate nonlinear systems with time delay via the corresponding FMB control approaches [19]. Therefore, the research on the FMB control system with time-delay is of great importance and researchers have dedicated considerable effects to

the problems of analysis and synthesis for time-delay FMB control systems. There are two main approaches to handle the time-delay problems in the literature, namely the delay-independent [19–21] and the delay-dependent [22–35] approaches. For the delay-independent approach, the stability conditions include no information of the delay, which means that the stability conditions are valid for arbitrary time delay. On the contrary, the delay-dependent approach contains the information of the delay, which is able to achieve less conservative results than the delay-independent approach, especially when the delay time is small. Within the delay-dependent approach, there are works on the constant time delay problems [22–24, 26] and time-varying delay problems [27, 29, 30, 32–35]. The advantage of the time-varying approach is that the constant time-delay case can be regarded as a special case of time-varying delay FMB control systems. It is also noticed that in the works in [146, 147], the time delay issues based on IT2 fuzzy sets were investigated. From the literature, it can be found that the time-varying delay effects on the IT2 PFMB control has not been investigated, therefore, it can be a possible future research topic to make the contribution.

Bibliography

[1] H. K. Lam and S.-H. Tsai, "Stability analysis of polynomial-fuzzy-model-based control systems with mismatched premise membership functions," *IEEE Trans. Fuzzy Syst.*, vol. 22, no. 1, pp. 223–229, 2014.

[2] L. A. Zadeh, *The concept of a linguistic variable and its application to approximate reasoning.* Springer, 1974.

[3] ——, "Outline of a new approach to the analysis of complex systems and decision processes," *IEEE Trans. Syst., Man, Cybern.*, no. 1, pp. 28–44, 1973.

[4] A. Sala, T. M. Guerra, and R. Babuška, "Perspectives of fuzzy systems and control," *Fuzzy Sets Syst.*, vol. 156, no. 3, pp. 432–444, 2005.

[5] G. Feng, "A survey on analysis and design of model-based fuzzy control systems," *IEEE Trans. Fuzzy Syst.*, vol. 14, no. 5, pp. 676–697, 2006.

[6] T. M. Guerra, A. Sala, and K. Tanaka, "Fuzzy control turns 50: 10 years later," *Fuzzy Sets Syst.*, vol. 281, pp. 168–182, 2015.

[7] K. Tanaka, T. Ikeda, and H. O. Wang, "Fuzzy regulators and fuzzy observers: relaxed stability conditions and LMI-based designs," *IEEE Trans. Fuzzy Syst.*, vol. 6, no. 2, pp. 250–265, 1998.

[8] E. Kim and H. Lee, "New approaches to relaxed quadratic stability condition of fuzzy control systems," *IEEE Trans. Fuzzy Syst.*, vol. 8, no. 5, pp. 523–534, Oct. 2000.

[9] L. Xiaodong and Z. Qingling, "New approaches to H_∞ controller designs based on fuzzy observers for Takagi-Sugeno fuzzy systems via LMI," *Automatica*, vol. 39, no. 9, pp. 1571–1582, 2003.

[10] K. Tanaka and H. O. Wang, *Fuzzy control systems design and analysis: a linear matrix inequality approach.* John Wiley & Sons, 2004.

[11] H. O. Wang, K. Tanaka, and M. F. Griffin, "An approach to fuzzy control of nonlinear systems: stability and design issues," *IEEE Trans. Fuzzy Syst.*, vol. 4, no. 1, pp. 14–23, Feb. 1996.

[12] M. C. M. Teixeira, E. Assuncao, and R. G. Avellar, "On relaxed LMI-based designs for fuzzy regulators and fuzzy observers," *IEEE Trans. Fuzzy Syst.*, vol. 11, no. 5, pp. 613–623, Oct. 2003.

[13] C. H. Fang, Y. S. Liu, S. W. Kau, L. Hong, and C. H. Lee, "A new LMI-based approach to relaxed quadratic stabilization of Takagi-Sugeno fuzzy control systems," *IEEE Trans. Fuzzy Syst.*, vol. 14, no. 3, pp. 386–397, Jun. 2006.

[14] A. Sala and C. Ariño, "Asymptotically necessary and sufficient conditions for stability and performance in fuzzy control: Applications of Polya's theorem," *Fuzzy Sets Syst.*, vol. 158, no. 24, pp. 2671–2686, Jul. 2007.

[15] S. K. Nguang and P. Shi, "H_∞ fuzzy output feedback control design for nonlinear systems: An LMI approach," *IEEE Trans. Fuzzy Syst.*, vol. 11, no. 3, pp. 331–340, Jun. 2003.

[16] S. Xu and J. Lam, "Robust H_∞ control for uncertain discrete-time-delay fuzzy systems via output feedback controllers," *IEEE Trans. Fuzzy Syst.*, vol. 13, no. 1, pp. 82–93, 2005.

[17] C. Lin, Q.-G. Wang, and T. H. Lee, "Improvement on observer-based H_∞ control for T-S fuzzy systems," *Automatica*, vol. 41, no. 9, pp. 1651–1656, 2005.

[18] S. Zhou, G. Feng, J. Lam, and S. Xu, "Robust H_∞ control for discrete-time fuzzy systems via basis-dependent Lyapunov functions," *Inf. Sci.*, vol. 174, no. 3, pp. 197–217, 2005.

[19] Y.-Y. Cao and P. M. Frank, "Analysis and synthesis of nonlinear time-delay systems via fuzzy control approach," *IEEE Trans. Fuzzy Syst.*, vol. 8, no. 2, pp. 200–211, 2000.

[20] ——, "Stability analysis and synthesis of nonlinear time-delay systems via linear Takagi-Sugeno fuzzy models," *Fuzzy Sets Syst.*, vol. 124, no. 2, pp. 213–229, 2001.

[21] R.-J. Wang, W.-W. Lin, and W.-J. Wang, "Stabilizability of linear quadratic state feedback for uncertain fuzzy time-delay systems," *IEEE Trans. Syst. Man, Cybern. B, Cybern.*, vol. 34, no. 2, pp. 1288–1292, 2004.

[22] X. Guan and C. Chen, "Delay-dependent guaranteed cost control for ts fuzzy systems with time delays," *IEEE Trans. Fuzzy Syst.*, vol. 12, no. 2, pp. 236–249, 2004.

[23] C. Chen, G. Feng, and X. Guan, "Delay-dependent stability analysis and controller synthesis for discrete-time T-S fuzzy systems with time delays," *IEEE Trans. Fuzzy Syst.*, vol. 13, no. 5, pp. 630–643, 2005.

[24] S. Zhou and T. Li, "Robust stabilization for delayed discrete-time fuzzy systems via basis-dependent Lyapunov-Krasovskii function," *Fuzzy Sets Syst.*, vol. 151, no. 1, pp. 139–153, 2005.

[25] B. Chen, X. Liu, and S. Tong, "Delay-dependent stability analysis and control synthesis of fuzzy dynamic systems with time delay," *Fuzzy Sets Syst.*, vol. 157, no. 16, pp. 2224–2240, 2006.

[26] H.-N. Wu, "Delay-dependent stability analysis and stabilization for discrete-time fuzzy systems with state delay: A fuzzy Lyapunov-Krasovskii functional approach," *IEEE Trans. Syst. Man, Cybern. B, Cybern.*, vol. 36, no. 4, pp. 954–962, 2006.

[27] H.-N. Wu and H.-X. Li, "New approach to delay-dependent stability analysis and stabilization for continuous-time fuzzy systems with time-varying delay," *IEEE Trans. Fuzzy Syst.*, vol. 15, no. 3, pp. 482–493, 2007.

[28] H. K. Lam and F. H. Leung, "Sampled-data fuzzy controller for time-delay nonlinear systems: fuzzy-model-based LMI approach," *IEEE Trans. Syst. Man, Cybern. B, Cybern.*, vol. 37, no. 3, pp. 617–629, 2007.

[29] H. Gao, X. Liu, and J. Lam, "Stability analysis and stabilization for discrete-time fuzzy systems with time-varying delay," *IEEE Trans. Syst. Man, Cybern. B, Cybern.*, vol. 39, no. 2, pp. 306–317, 2009.

[30] B. Zhang and S. Xu, "Delay-dependent robust H_∞ control for uncertain discrete-time fuzzy systems with time-varying delays," *IEEE Trans. on Fuzzy syst.*, vol. 17, no. 4, pp. 809–823, 2009.

[31] Y. Zhao, H. Gao, J. Lam, and B. Du, "Stability and stabilization of delayed T-S fuzzy systems: A delay partitioning approach," *IEEE Trans. Fuzzy Syst.*, vol. 17, no. 4, pp. 750–762, 2009.

[32] L. Wu, X. Su, P. Shi, and J. Qiu, "A new approach to stability analysis and stabilization of discrete-time T-S fuzzy time-varying delay systems," *IEEE Trans. Syst. Man, Cybern. B, Cybern.*, vol. 41, no. 1, pp. 273–286, 2011.

[33] X. Su, P. Shi, L. Wu, and Y.-D. Song, "A novel control design on discrete-time takagi-sugeno fuzzy systems with time-varying delays," *IEEE Trans. Fuzzy Syst.*, vol. 21, no. 4, pp. 655–671, 2013.

[34] X. Yang, L. Wu, H. K. Lam, and X. Su, "Stability and stabilization of discrete-time T-S fuzzy systems with stochastic perturbation and time-varying delay," *IEEE Trans. Fuzzy Syst.*, vol. 22, no. 1, pp. 124–138, 2014.

[35] L. Wu, X. Yang, and H. K. Lam, "Dissipativity analysis and synthesis for discrete-time t–s fuzzy stochastic systemswith time-varying delay," *IEEE Trans. Fuzzy Syst.*, vol. 22, no. 2, pp. 380–394, 2014.

[36] K. Tanaka, H. Yoshida, H. Ohtake, and H. O. Wang, "A sum-of-squares approach to modeling and control of nonlinear dynamical systems with polynomial fuzzy systems," *IEEE Trans. Fuzzy Syst.*, vol. 17, no. 4, pp. 911–922, 2009.

[37] S. Prajna, A. Papachristodoulou, and P. A. Parrilo, "SOSTOOLS: sum of squares optimization toolbox for Matlab," *Control and Dynamical Systems, California Institute of Technology, Pasadena, CA*, vol. 91125, 2004.

[38] K. Tanaka, H. Ohtake, and H. O. Wang, "Guaranteed cost control of polynomial fuzzy systems via a sum of squares approach," *IEEE Trans. Syst, Man, Cybern. B, Cybern.*, vol. 39, no. 2, pp. 561–567, 2009.

[39] A. Sala and C. Ario, "Polynomial fuzzy models for nonlinear control: A Taylor series approach," *IEEE Trans. Fuzzy Syst.*, vol. 17, no. 6, pp. 1284–1295, 2009.

[40] M. Narimani and H. K. Lam, "SOS-based stability analysis of polynomial fuzzy-model-based control systems via polynomial membership functions," *IEEE Trans. Fuzzy Syst.*, vol. 18, no. 5, pp. 862–871, 2010.

[41] H. K. Lam, "Polynomial fuzzy-model-based control systems: stability analysis via piecewise-linear membership functions," *IEEE Trans. Fuzzy Syst.*, vol. 19, no. 3, pp. 588–593, 2011.

[42] ——, "Stabilization of nonlinear systems using sampled-data output-feedback fuzzy controller based on polynomial-fuzzy-model-based control approach," *IEEE Trans. Syst, Man, Cybern. B, Cybern.*, vol. 42, no. 1, pp. 258–267, 2012.

[43] C. Liu, H. K. Lam, X. Zhang, H. Li, and S. H. Ling, "Relaxed stability conditions based on taylor series membership functions for polynomial fuzzy-model-based control systems," in *Proc. IEEE Int. Conf. Fuzzy Syst.*, 2014, pp. 2111–2118.

[44] J. M. Mendel, "Type-2 fuzzy sets and systems: an overview," *IEEE Comput. Intell. Mag.*, vol. 2, no. 1, pp. 20–29, 2007.

[45] H. K. Lam and L. D. Seneviratne, "Stability analysis of interval type-2 fuzzy-model-based control systems," *IEEE Trans. Syst, Man, Cybern. B, Cybern.*, vol. 38, no. 3, pp. 617–628, 2008.

[46] W. Pedrycz and F. Gomide, *Fuzzy systems engineering: toward human-centric computing.* John Wiley & Sons, 2007.

[47] H. Bustince, J. Fernandez, H. Hagras, F. Herrera, M. Pagola, and E. Barrenechea, "Interval type-2 fuzzy sets are generalization of interval-valued fuzzy sets: toward a wider view on their relationship," *IEEE Trans. Fuzzy Syst.*, vol. 23, no. 5, pp. 1876–1882, 2015.

[48] N. N. Karnik, J. M. Mendel, and Q. Liang, "Type-2 fuzzy logic systems," *IEEE Trans. Fuzzy Syst.*, vol. 7, no. 6, pp. 643–658, 1999.

[49] Q. Liang and J. M. Mendel, "Interval type-2 fuzzy logic systems: theory and design," *IEEE Trans. Fuzzy Syst.*, vol. 8, no. 5, pp. 535–550, 2000.

[50] O. Castillo and P. Melin, "A review on the design and optimization of interval type-2 fuzzy controllers," *Appl. Soft Comput.*, vol. 12, no. 4, pp. 1267–1278, 2012.

[51] C. F. Juang and C. H. Hsu, "Reinforcement interval type-2 fuzzy controller design by online rule generation and Q-value-aided ant colony optimization," *IEEE Trans. Syst., Man, Cybern. B, Cybern.*, vol. 39, no. 6, pp. 1528–1542, 2009.

[52] M. Biglarbegian, W. W. Melek, and J. M. Mendel, "On the stability of interval type-2 TSK fuzzy logic control systems," *IEEE Trans. Syst., Man, Cybern. B, Cybern.*, vol. 40, no. 3, pp. 798–818, 2010.

[53] S. Jafarzadeh, M. S. Fadali, and A. H. Sonbol, "Stability analysis and control of discrete type-1 and type-2 TSK fuzzy systems: Part I. stability analysis," *IEEE Trans. Fuzzy Syst.*, vol. 19, no. 6, pp. 989–1000, 2011.

[54] ——, "Stability analysis and control of discrete type-1 and type-2 TSK fuzzy systems: Part II. control design," *IEEE Trans. Fuzzy Syst.*, vol. 19, no. 6, pp. 1001–1013, 2011.

[55] H. K. Lam, H. Li, C. Deters, E. Secco, H. A. Wurdemann, and K. Althoefer, "Control design for interval type-2 fuzzy systems under imperfect premise matching," *IEEE Trans. Ind. Electron.*, vol. 61, no. 2, pp. 956–968, 2014.

[56] H. Li, C. Wu, S. Yin, and H. K. Lam, "Observer-based fuzzy control for nonlinear networked systems under unmeasurable premise variables," *IEEE Trans. Fuzzy Syst.*, vol. 24, no. 5, pp. 1233–1245, 2016.

[57] G. Feng, C. L. Chen, D. Sun, and Y. Zhu, "H_∞ controller synthesis of fuzzy dynamic systems based on piecewise Lyapunov functions and bilinear matrix inequalities," *IEEE Trans. Fuzzy Syst.*, vol. 13, no. 1, pp. 94–103, Feb. 2005.

[58] J. Qiu, H. Tian, Q. Lu, and H. Gao, "Nonsynchronized robust filtering design for continuous-time T-S fuzzy affine dynamic systems based on piecewise Lyapunov functions," *IEEE Trans. Cybern.*, vol. 43, no. 6, pp. 1755–1766, Dec. 2013.

[59] H. K. Lam, M. Narimani, H. Li, and H. Liu, "Stability analysis of polynomial-fuzzy-model-based control systems using switching polynomial Lyapunov function," *IEEE Trans. Fuzzy Syst.*, vol. 21, no. 5, pp. 800–813, Oct. 2013.

[60] L. A. Mozelli, R. M. Palhares, and G. S. C. Avellar, "A systematic approach to improve multiple Lyapunov function stability and stabilization conditions for fuzzy systems," *Inf. Sci.*, vol. 179, no. 8, pp. 1149–1162, Mar. 2009.

[61] M. Bernal and T. Guerra, "Generalized nonquadratic stability of continuous-time Takagi-Sugeno models," *IEEE Trans. Fuzzy Syst.*, vol. 18, no. 4, pp. 815–822, Aug. 2010.

[62] J.-T. Pan, T. M. Guerra, S.-M. Fei, and A. Jaadari, "Nonquadratic stabilization of continuous T-S fuzzy models: LMI solution for a local approach," *IEEE Trans. Fuzzy Syst.*, vol. 20, no. 3, pp. 594–602, Jun. 2012.

[63] H. K. Lam and F. H. F. Leung, "Stability analysis of fuzzy control systems subject to uncertain grades of membership," *IEEE Trans. Syst, Man and Cybern. B, Cybern.*, vol. 35, no. 6, pp. 1322–1325, Dec. 2005.

[64] H. K. Lam and M. Narimani, "Stability analysis and performance deign for fuzzy-model-based control system under imperfect premise matching," *IEEE Trans. Fuzzy Syst.*, vol. 17, no. 4, pp. 949–961, Aug 2009.

[65] ——, "Quadratic-stability analysis of fuzzy-model-based control systems using staircase membership functions," *IEEE Trans. Fuzzy Syst.*, vol. 18, no. 1, pp. 125–137, 2010.

[66] C.-S. Tseng, B.-S. Chen, and H.-J. Uang, "Fuzzy tracking control design for nonlinear dynamic systems via ts fuzzy model," *IEEE Trans. Fuzzy Syst.*, vol. 9, no. 3, pp. 381–392, 2001.

[67] X. Liu and Q. Zhang, "Approaches to quadratic stability conditions and H_∞ control designs for Takagi-Sugeno fuzzy systems," *IEEE Trans. Fuzzy Syst.*, vol. 11, no. 6, pp. 830–839, Dec. 2003.

[68] S. Tong, T. Wang, and H. X. Li, "Fuzzy robust tracking control for uncertain nonlinear systems," *Int. J. Approx. Reason.*, vol. 30, no. 2, pp. 73–90, Jun. 2002.

[69] B. S. Chen, B. K. Lee, and L. B. Guo, "Optimal tracking design for stochastic fuzzy systems," *IEEE Trans. Fuzzy Syst.*, vol. 11, no. 6, pp. 796–813, Dec. 2003.

[70] W. Chang, J. B. Park, Y. H. Joo, and G. Chen, "Static output-feedback fuzzy controller for Chen's chaotic system with uncertainties," *Inf. Sci.*, vol. 151, pp. 227–244, May 2003.

[71] J.-C. Lo and M.-L. Lin, "Robust H_∞ nonlinear control via fuzzy static output feedback," *IEEE Trans. Circuits Syst. I, Fundam. Theory Appl.*, vol. 50, no. 11, pp. 1494–1502, 2003.

[72] S. K. Nguang and P. Shi, "Fuzzy output feedback control of nonlinear systems under sampled measurements," *Automatica*, vol. 39, no. 12, pp. 2169–2174, Dec. 2003.

[73] D. Huang and S. K. Nguang, "Robust H_∞ static output feedback control of fuzzy systems: An LMI approach," *IEEE Trans. Syst., Man and Cybern. B, Cybern.*, vol. 36, no. 1, pp. 216–222, Feb. 2006.

[74] Z. X. Han, G. Feng, B. L. Walcott, and J. Ma, "Dynamic output feedback controller design for fuzzy systems," *IEEE Trans. Syst., Man and Cybern. B, Cybern.*, vol. 30, no. 1, pp. 204–210, Feb. 2000.

[75] W. Assawinchaichote and S. K. Nguang, "Fuzzy H_∞ output feedback control design for singularly perturbed systems with pole placement constraints: an LMI approach," *IEEE Trans. Fuzzy Syst.*, vol. 14, no. 3, pp. 361–371, Jun. 2006.

[76] K. Y. Lian and J. J. Liou, "Output tracking control for fuzzy systems via output feedback design," *IEEE Trans. Fuzzy Syst.*, vol. 14, no. 5, pp. 628–639, Oct. 2006.

[77] K. Guelton, T. Bouarar, and N. Manamanni, "Robust dynamic output feedback fuzzy Lyapunov stabilization of Takagi-Sugeno systems - A descriptor redundancy approach," *Fuzzy Sets Syst.*, vol. 160, no. 19, pp. 2796–2811, Oct. 2009.

[78] B. Mansouri, N. Manamanni, K. Guelton, A. Kruszewski, and T. M. Guerra, "Output feedback LMI tracking control conditions with H_∞ criterion for uncertain and disturbed T-S models," *Inf. Sci.*, vol. 179, no. 4, pp. 446–457, Feb. 2009.

[79] H. K. Lam and L. D. Seneviratne, "Tracking control of sampled-data fuzzy-model-based control systems," *IET Control Theory Appl.*, vol. 3, no. 1, pp. 56–67, Jan. 2009.

[80] H. K. Lam and H. Li, "Output-feedback tracking control for polynomial fuzzy-model-based control systems," *IEEE Trans. Ind. Electron.*, vol. 60, no. 12, pp. 5830–5840, 2013.

[81] H. K. Lam and F. H. Leung, "Design and stabilization of sampled-data neural-network-based control systems," *IEEE Trans. Syst. Man Cybern. B, Cybern.*, vol. 36, no. 5, pp. 995–1005, 2006.

[82] H. Gao and T. Chen, "Stabilization of nonlinear systems under variable sampling: A fuzzy control approach," *IEEE Trans. Fuzzy Syst.*, vol. 15, no. 5, pp. 972–983, Dec. 2007.

[83] H. K. Lam and W. Ling, "Sampled-data fuzzy controller for continuous nonlinear systems," *IET Control Theory Appl.*, vol. 2, no. 1, pp. 32–39, 2008.

[84] X.-L. Zhu, B. Chen, D. Yue, and Y. Wang, "An improved input delay approach to stabilization of fuzzy systems under variable sampling," *IEEE Trans. Fuzzy Syst.*, vol. 20, no. 2, pp. 330–341, Apr. 2012.

[85] F. Yang, H. Zhang, and Y. Wang, "An enhanced input-delay approach to sampled-data stabilization of T-S fuzzy systems via mixed convex combination," *Nonlinear Dyn.*, vol. 75, no. 3, pp. 501–512, Feb. 2014.

[86] H. Li, X. Sun, P. Shi, and H. K. Lam, "Control design of interval type-2 fuzzy systems with actuator fault: Sampled-data control approach," *Inf. Sci.*, vol. 32, pp. 1–13, May 2015.

[87] C. Liu and H. K. Lam, "Design of polynomial fuzzy observer-controller with sampled-output measurements for nonlinear systems considering unmeasurable premise variables," *IEEE Trans.Fuzzy Syst.*, vol. 23, no. 6, pp. 2067–2079, 2015.

[88] H. Katayama and A. Ichikawa, "H_∞ control for sampled-data nonlinear systems described by Takagi-Sugeno fuzzy systems," *Fuzzy Sets Syst.*, vol. 148, no. 3, pp. 431–452, 2004.

[89] X. Jiang, "On sampled-data fuzzy control design approach for T-S model-based fuzzy systems by using discretization approach," *Inf. Sci.*, vol. 296, pp. 307–314, Mar. 2015.

[90] W. Chang, J. B. Park, and Y. H. Joo, "GA-based intelligent digital redesign of fuzzy-model-based controllers," *IEEE Trans. Fuzzy Syst.*, vol. 11, no. 1, pp. 35–44, Feb. 2003.

[91] H. J. Lee, H. Kim, Y. H. Joo, W. Chang, and J. B. Park, "A new intelligent digital redesign for T-S fuzzy systems: global approach," *IEEE Trans. Fuzzy Syst.*, vol. 12, no. 2, pp. 274–284, April 2004.

[92] H. J. Lee, J. B. Park, and Y. H. Joo, "Digitalizing a fuzzy observer-based output-feedback control: intelligent digital redesign approach," *IEEE Trans. Fuzzy Syst.*, vol. 13, no. 5, pp. 701–716, Oct. 2005.

[93] H. J. Lee and D. Wan Kim, "Intelligent digital redesign revisited: Approximate discretization and stability limitation," *Fuzzy Sets Syst.*, vol. 159, no. 23, pp. 3221–3231, Dec. 2008.

[94] H. C. Sung, D. W. Kim, J. B. Park, and Y. H. Joo, "Robust digital control of fuzzy systems with parametric uncertainties: LMI-based digital redesign approach," *Fuzzy Sets Syst.*, vol. 161, no. 6, pp. 919–933, Mar. 2010.

[95] D. W. Kim and H. J. Lee, "Sampled-data observer-based output-feedback fuzzy stabilization of nonlinear systems: Exact discrete-time design approach," *Fuzzy Sets Syst.*, vol. 201, pp. 20–39, Aug. 2012.

[96] H. K. Lam, "Sampled-data fuzzy-model-based control systems: stability analysis with consideration of analogue-to-digital converter and digital-to-analogue converter," *IET Control Theory Applicat.*, vol. 4, no. 7, pp. 1131–1144, Jul. 2010.

[97] S. K. Nguang and P. Shi, "Fuzzy H_∞ output feedback control of nonlinear systems under sampled measurements," *Automatica*, vol. 39, no. 12, pp. 2169–2174, 2003.

[98] H. Zhang, H. Yan, Q. Chen, and T. Liu, "Quantised H_∞ control for sampled fuzzy systems," *IET Control Theory Applicat.*, vol. 6, no. 17, pp. 2686–2695, Nov. 2012.

[99] C. P. G. Flores, B. C. Toledo, J. P. G. Sandoval, S. D. Gennaro, and V. G. lvarez, "A reset observer with discrete/continuous measurements for a class of fuzzy nonlinear systems," *J. Franklin Inst.*, vol. 350, no. 8, pp. 1974–1991, 2013.

[100] H. Li, X. Sun, H. R. Karimi, and B. Niu, "Dynamic output-feedback passivity control for fuzzy systems under variable sampling," *Math. Problems Eng.*, vol. 2013, art. no. 767093 (10 pages), 2013.

[101] H. Li, X. Jing, H. K. Lam, and P. Shi, "Fuzzy sampled-data control for uncertain vehicle suspension systems," *IEEE Trans. Cybern.*, vol. 44, no. 7, pp. 1111–1126, Sept. 2013.

[102] K. Tanaka, T. Ikeda, and H. Wang, "Design of fuzzy control systems based on relaxed LMI stability conditions," in *Proc. IEEE 35th Conf. Decision Control*, vol. 1, 1996, pp. 598–603.

[103] K. Tanaka, T. Taniguchi, and H. O. Wang, "Model-based fuzzy control of tora system: fuzzy regulator and fuzzy observer design via lmis that represent decay rate, disturbance rejection, robustness, optimality," in *Proc. Int. IEEE Conf. Fuzzy Syst., Anchorage, AK*, vol. 1, 1998, pp. 313–318.

[104] S. P. Boyd, *Linear Matrix Inequalities in System and Control Theory.* Society for Industrial and Applied Mathematics (SIAM), 1994.

[105] K. Tanaka, T. Ikeda, and H. O. Wang, "Fuzzy regulators and fuzzy observers: relaxed stability conditions and LMI-based designs," *IEEE Trans. Fuzzy Syst.*, vol. 6, no. 2, pp. 250–265, May 1998.

[106] X. Liu and Q. Zhang, "New approaches to H_∞ controller designs based on fuzzy observers for Takagi-Sugeno fuzzy systems via LMI," *Automatica*, vol. 39, no. 9, pp. 1571–1582, Sep. 2003.

[107] J. C. Lo and J. R. Wan, "Studies on linear matrix inequality relaxations for fuzzy control systems via homogeneous polynomials," *IET Control Theory & Applications,*, vol. 4, no. 11, pp. 2293–2302, Nov. 2010.

[108] H. K. Lam and F. H. F. Leung, "LMI-based stability and performance design of fuzzy control systems: fuzzy models and controllers with different premises," in *Proc. IEEE Int. Conf. Fuzzy Syst.*, Vancouver, BC, Canada, 2006, pp. 9499–9506.

[109] A. Sala and C. Ariño, "Relaxed stability and performance conditions for Takagi-Sugeno fuzzy systems with knowledge on membership function overlap," *IEEE Trans. Syst. Man, Cybern. B, Cybern.*, vol. 37, no. 3, pp. 727–732, Jun. 2007.

[110] C. Ariño and A. Sala, "Extensions to "stability analysis of fuzzy control systems subject to uncertain grades of membership"," *IEEE Trans. Syst. Man, Cybern. B, Cybern.*, vol. 38, no. 2, pp. 558 –563, Apr. 2008.

[111] A. Sala and C. Ariño, "Relaxed stability and performance LMI conditions for Takagi-Sugeno fuzzy systems with polynomial constraints on membership function shapes," *IEEE Trans. Fuzzy Syst.*, vol. 16, no. 5, pp. 1328–1336, Oct. 2008.

[112] A. Kruszewski, A. Sala, T. Guerra, and C. Arino, "A triangulation approach to asymptotically exact conditions for fuzzy summations," *IEEE Trans. Fuzzy Syst.*, vol. 17, no. 5, pp. 985–994, Oct. 2009.

[113] M. Narimani and H. K. Lam, "Relaxed LMI-based stability conditions for Takagi-Sugeno fuzzy control systems using regional-membership-function-shape-dependent analysis approach," *IEEE Trans. Fuzzy Syst.*, vol. 17, no. 5, pp. 1221–1228, Oct. 2009.

[114] H. K. Lam, "LMI-based stability analysis for fuzzy-model-based control systems using artificial T-S fuzzy model," *IEEE Trans. Fuzzy Syst.*, vol. 19, no. 3, pp. 505–513, Jun. 2011.

[115] M. Johansson, A. Rantzer, and K. E. Arzen, "Piecewise quadratic stability of fuzzy systems," *IEEE Trans. Fuzzy Syst.*, vol. 7, no. 6, pp. 713–722, Dec. 1999.

[116] M. Feng and C. J. Harris, "Piecewise Lyapunov stability conditions of fuzzy systems," *IEEE Trans. Syst. Man, Cybern. B, Cybern.*, vol. 31, no. 2, pp. 259–262, Apr. 2001.

[117] G. Feng, "Controller synthesis of fuzzy dynamic systems based on piecewise Lyapunov functions," *IEEE Trans. Fuzzy Systems*, vol. 11, no. 5, pp. 605–612, Oct. 2003.

[118] ——, "H_∞ controller design of fuzzy dynamic systems based on piecewise Lyapunov functions," *IEEE Trans. Syst. Man, Cybern. B, Cybern.*, vol. 34, no. 1, pp. 283–292, Feb. 2004.

[119] H. Ohtake, K. Tanaka, and H. O. Wang, "Switching fuzzy controller design based on switching Lyapunov function for a class of nonlinear systems," *IEEE Trans. Syst. Man, Cybern. B, Cybern.*, vol. 36, no. 1, pp. 13–23, Feb. 2006.

[120] W. J. Wang, Y. J. Chen, and C. H. Sun, "Relaxed stabilization criteria for discrete-time T-S fuzzy control systems based on a switching fuzzy model and piecewise Lyapunov function," *IEEE Trans. Syst. Man, Cybern. B, Cybern.*, vol. 37, no. 3, pp. 551–559, Jun. 2007.

[121] J. Dong and G. H. Yang, "Dynamic output feedback control synthesis for continuous-time T-S fuzzy systems via a switched fuzzy control scheme," *IEEE Trans. Syst. Man, Cybern. B, Cybern.*, vol. 38, no. 4, pp. 1166–1175, Aug. 2008.

[122] K. Tanaka, T. Hori, and H. O. Wang, "A multiple Lyapunov function approach to stabilization of fuzzy control systems," *IEEE Trans. Fuzzy Syst.*, vol. 11, no. 4, pp. 582–589, Oct. 2003.

[123] T. M. Guerra and L. Vermeiren, "LMI-based relaxed nonquadratic stabilization conditions for nonlinear systems in the Takagi-Sugeno's form," *Automatica*, vol. 40, no. 5, pp. 823–829, May 2004.

[124] B. J. Rhee and S. Won, "A new fuzzy Lyapunov function approach for a Takagi-Sugeno fuzzy control system design," *Fuzzy Sets Syst.*, vol. 157, no. 9, pp. 1211–1228, May 2006.

[125] K. Tanaka, H. Ohtake, and H. O. Wang, "A descriptor system approach to fuzzy control system design via fuzzy Lyapunov functions," *IEEE Trans. Fuzzy Syst.*, vol. 15, no. 3, pp. 333–341, 2007.

[126] H. K. Lam and F. H. F. Leung, "LMI-based stability and performance conditions for continuous-time nonlinear systems in Takagi-Sugeno's form," *IEEE Trans. Syst. Man, Cybern. B, Cybern.*, vol. 37, no. 5, pp. 1396–1406, Oct. 2007.

[127] J. Li, S. Zhou, and S. Xu, "Fuzzy control system design via fuzzy Lyapunov functions," *IEEE Trans. Syst. Man, Cybern. B, Cybern.*, vol. 38, no. 6, pp. 1657–1661, Dec. 2008.

[128] X. H. Chang and G. H. Yang, "Relaxed stabilization conditions for continuous-time Takagi-Sugeno fuzzy control systems," *Inf. Sci.*, vol. 180, no. 17, pp. 3273–3287, Sep. 2010.

[129] D. H. Lee, J. B. Park, and Y. H. Joo, "A fuzzy Lyapunov function approach to estimating the domain of attraction for continuous-time Takagi-Sugeno fuzzy systems," *Inf. Sci.*, vol. 185, no. 1, pp. 230–248, Feb. 2012.

[130] B. C. Ding, H. X. Sun, and P. Yang, "Further studies on LMI-based relaxed stabilization conditions for nonlinear systems in Takagi-Sugeno's form," *Automatica*, vol. 42, no. 3, pp. 503–508, Mar. 2006.

[131] M. Bernal and P. Husek, "Non-quadratic performance design for Takagi-Sugeno fuzzy systems," *Int. J. Appl. Math. Comput. Sci.*, vol. 15, no. 3, pp. 383–391, Sep. 2005.

[132] B. C. Ding, "Stabilization of Takagi-Sugeno model via nonparallel distributed compensation law," *IEEE Trans. Fuzzy Syst.*, vol. 18, no. 1, pp. 188–194, Feb. 2010.

[133] B. Ding, "Quadratic boundedness via dynamic output feedback for constrained nonlinear systems in Takagi-Sugeno's form," *Automatica*, vol. 45, no. 9, pp. 2093–2098, Sep. 2009.

[134] ——, "Homogeneous polynomially nonquadratic stabilization of discrete-time TakagiSugeno systems via nonparallel distributed compensation law," *IEEE Trans. Fuzzy Syst.*, vol. 18, no. 5, pp. 994–1000, Oct. 2010.

[135] T. M. Guerra, H. Kerkeni, J. Lauber, and L. Vermeiren, "An efficient Lyapunov function for discrete T-S models: observer design," *IEEE Trans. Fuzzy Syst.*, vol. 1, no. 20, pp. 187–192, Feb. 2012.

[136] T. Bouarar, K. Guelton, and N. Manamanni, "Robust fuzzy Lyapunov stabilization for uncertain and disturbed Takagi-Sugeno descriptors," *ISA Transactions*, vol. 49, no. 4, pp. 447–461, Oct. 2010.

[137] T. M. Guerra, M. Bernal, K. Guelton, and S. Labiod, "Non-quadratic local stabilization for continuous-time Takagi-Sugeno models," *Fuzzy Sets Syst.*, vol. 201, pp. 40–54, Aug. 2012.

[138] H. K. Lam and J. Lauber, "Membership-function-dependent stability analysis of fuzzy-model-based control systems using fuzzy Lyapunov functions," *Inf. Sci.*, vol. 232, pp. 253–266, May 2013.

[139] H. K. Lam, L. Wu, and J. Lam, "Two-step stability analysis for general polynomial-fuzzy-model-based control systems," *IEEE Trans. Fuzzy Syst.*, vol. 23, no. 3, pp. 511–524, 2015.

[140] S. S. Chang and T. Peng, "Adaptive guaranteed cost control of systems with uncertain parameters," *IEEE Trans. Autom. Control*, vol. 17, no. 4, pp. 474–483, 1972.

[141] J. C. Doyle, K. Glover, P. P. Khargonekar, and B. A. Francis, "State-space solutions to standard H_2 and H_∞ control problems," *IEEE Trans. Autom. Control*, vol. 34, no. 8, pp. 831–847, 1989.

[142] P. Gahinet and P. Apkarian, "A linear matrix inequality approach to H_∞ control," *Int. J. Robust Nonlinear Control*, vol. 4, no. 4, pp. 421–448, 1994.

[143] C.-S. Tseng, "Model reference output feedback fuzzy tracking control design for nonlinear discrete-time systems with time-delay," *IEEE Trans. Fuzzy Syst.*, vol. 14, no. 1, pp. 58–70, 2006.

[144] C. Lin, Q.-G. Wang, and T. H. Lee, "H_∞ output tracking control for nonlinear systems via TS fuzzy model approach," *IEEE Trans. Syst. Man, Cybern. B, Cybern.*, vol. 36, no. 2, pp. 450–457, 2006.

[145] K. Gu, "An integral inequality in the stability problem of time-delay systems," in *Proc. IEEE 39th Conf. Decision Control*, vol. 3, 2000, pp. 2805–2810.

[146] Q. Zhou, D. Liu, Y. Gao, H. K. Lam, and R. Sakthivel, "Interval type-2 fuzzy control for nonlinear discrete-time systems with time-varying delays," *Neurocomputing*, vol. 157, pp. 22–32, 2015.

[147] H. Li, J. Wang, L. Wu, H. K. Lam, and Y. Gao, "Optimal guaranteed cost sliding mode control of interval type-2 fuzzy time-delay systems," *IEEE Trans. Fuzzy Syst.*, 2017.